Superfluidity in Coherently Driven Microcavity-Polaritons

Richard Juggins

I, Richard Juggins, confirm that the work presented in this thesis is my own. Where information has been derived from other sources, I confirm that this has been indicated in the work.

Parts of this thesis have been published in:

Juggins, R., Keeling, J., Szymańska, M. Coherently driven microcavity-polaritons and the question of superfluidity. *Nat. Commun.* **9**, 4062 (2018).

When you are a Bear of Very Little Brain, and you Think of Things, you find sometimes that a Thing which seemed very Thingish inside you is quite different when it gets out into the open and has other people looking at it.

The House at Pooh Corner, A. A. Milne

Abstract

Superfluidity is a spectacular emergent effect in quantum mechanics where fluids flow without friction, cannot rotate except in quantised vortices, and can form metastable currents that persist for astronomical timescales. First discovered in liquid helium, superfluidity has been extensively studied in thermal equilibrium. Microcavity-polaritons however, which are two-dimensional quasiparticles formed by the strong coupling of cavity photons and quantum well excitons, do not usually equilibrate due to photons leaking from the cavity, and must be pumped with a laser to maintain a steady state. Polaritons are bosonic and have been shown to condense on experimental scales, yet their driven-dissipative nature poses questions regarding whether they may become superfluids. Some associated effects have been observed, and notably the report of nearly dissipationless flow for coherently driven polaritons was taken as evidence of superflow. Here, we use a Keldysh path integral technique to show the superfluid response, given by the difference between the currents induced by longitudinal and transverse forces, is zero for coherently driven polaritons that are continuously and homogeneously pumped, and find this a consequence of the gapped excitation spectrum caused by external phase locking. Furthermore, at zero pump momentum the system forms a rigid state that does not respond to either type of perturbation. It does however exhibit a normal response at finite momenta, due to a coupling between the perturbation and the amplitude of the state rather than a change in its momentum. This response almost vanishes when the real part of the spectrum is linear at low frequency, which was the regime investigated experimentally. These results suggest the observed suppression of scattering should be interpreted as a sign of this new rigid state and not a superfluid, and that driven-dissipative systems exhibit a richer collection of macroscopic quantum phenomena than those in equilibrium.

Impact statement

This work is concerned with fundamental ideas regarding the phenomenon of superfluidity, with particular emphasis on how it is affected by drive and decay. The core findings of this thesis were published in *Nature Communications*[1] and featured in *New Scientist*[2]. During peer review for the former a referee suggested these results 'can be a milestone' in understanding superfluidity in open systems. This is significant: superfluidity is amongst the most substantial and intriguing manifestations of quantum mechanics on a macroscopic scale, with direct relevance to at least four Nobel prizes.

Microcavity-polaritons, which are quasiparticles of light, are driven-dissipative systems that must be pumped with a laser to maintain a steady state. By investigating the nature of macroscopic states in coherently driven systems pumped continuously and homogeneously below the optical parametric oscillation threshold, and finding that they are not, as previously thought, superfluids, but instead a new rigid macroscopic quantum state, this work deepens understanding both of superfluidity and of the rich tapestry of quantum effects that occur in open systems.

Polaritons are now being used in the field of quantum technologies. It is hoped that a lattice of polaritons will soon be used to build a fully quantum simulator. Any insights we have into synthetic states of light may prove invaluable in this pursuit. The present work interrogates the behaviour of coherently driven macroscopic states and elucidates what kind of effects one can expect to see in them and is therefore directly relevant to any applications for which such a system could be put to use.

Acknowledgements

While I have of course had help and support from many places while I have been working for this degree, there are a few special people to whom I am particularly thankful.

My supervisor, Marzena Szymańska, for all her ideas, assistance, and positivity. Jonathan Keeling for his support and consistent patience. All my research group, with special mention to Alejandro Zamora, Themistoklis Mavrogordatos, Kirsty Dunnett, and Alexander Ferrier for putting up with my many and varied questions down the years. Iacopo Carusotto for useful discussions about my paper. And Andrew Maxwell for all those hours spent in front of the whiteboard.

Of course, my very best is saved for Mum, Dad, Peter, and Mark, who have been there for me for literally a lifetime (well, almost). And to Katarina, who more than anyone saw my ups and downs, and gave me love, support, and encouragement.

Contents

III   General Conclusions   119

8   Conclusions   121

Appendices   125

A   Response function coefficients   125

B   A note on dimensional factors   139

C   Integration of the response function   143

List of Figures

List of Tables

Part I

Introduction and Background

Chapter 1

General introduction

Emergent phenomena are amongst the most extraordinary to be found in nature. Far from it being possible to construct a complete understanding of the universe by looking only at its smallest constituent parts, many spectacular effects only occur when the number of those parts becomes very large[3], such as air molecules forming hurricanes, water crystallising into snowflakes, or particle spins aligning into magnets. Superfluidity is a striking example of emergence in quantum physics[4], where a macroscopic state forms characterised by a series of peculiar flow properties, such as vanishingly small viscosity, the inability to rotate except in tiny quantised vortices, and the flow of metastable currents that persist for astronomical timescales. First discovered in 1938 in liquid helium-4 when cooled below 2.17K[5], superfluidity has been widely studied, and found to occur in a variety of other systems, including helium-3, ultra-cold bosonic atoms, and charged Cooper pairs in superconductors[6,7].

While historical research on superfluidity has concentrated on examples in thermal equilibrium, in recent years driven-dissipative systems, which never thermalise due to constant decay and must be pumped to maintain a steady state, have begun to generate substantial interest. Examples of such systems are numerous, including Bose-Einstein condensates (BEC) of photons[8,9], cold atoms coupled to photonic modes in optical cavities[10], and cavity arrays[11,12,13]. Of particular note are microcavity-polaritons[14,15,16], which are two-dimensional bosonic quasiparticles made of photons trapped in a cavity strongly coupled to excitons in a quantum well. Polariton experiments have observed a number of effects usually associated with superfluidity, such as the suppression of scattering for flow past a defect[17,18,19], metastable persistent currents[20], and quantised vortices[21], and the question of how superfluidity may occur in these out-of-equilibrium systems has proved contentious[21,22,23,24,25,26,27]. Indeed, it is unclear whether all the effects seen in equilibrium will continue to apply[14,28,29].

Of particular importance when classifying these systems is the fact that superfluidity is a 'complex of phenomena'[5]. While flow without viscosity is perhaps the most famous of these, irrotationality of superflow is crucial for characterising a superfluid state. Unlike the

former property, which is only approximately true at finite temperature and provides no clear distinction between true superfluids and generic low viscosity systems, the definition of a superfluid as a macroscopic quantum state in which the bulk does not rotate provides a precise description. This property is encoded in the response of a system to longitudinal and transverse perturbations. Given that superfluids exhibit the former but not the latter, if there exists a difference between the two the system in question must contain a superfluid component. Indeed, this has become a standard definition of superfluidity [23,30,31,32,33,34,35]. Furthermore, the fraction of a system that behaves this way can be used to quantify how much of it is 'superfluid' and how much is 'normal'.

The properties of microcavity-polaritons are heavily dependent on how the system is pumped – that is, on how photons are injected into the cavity. When this occurs incoherently, i.e. when photons are injected far off-resonance, then relaxation processes involving excitons and phonons will under the right conditions lead to the 'condensation' of polaritons into a low energy state of the system [36]. This process involves the spontaneous breaking of symmetry of the phase of the macroscopic wavefunction leading to a Goldstone mode in the excitation spectrum of the system [37,38]. In a theoretical study of the longitudinal and transverse response functions of an incoherently driven system using a Keldysh path integral technique [23], it was found that the gapless excitation spectrum allowed superfluidity to survive despite the driven-dissipative nature of the system. Alternatively, polaritons may be pumped coherently, i.e. they are injected at a specific energy and momentum, and can form a macroscopic state with a phase fixed to that of the external pump [39]. Because of this phase fixing, the excitation spectrum in such a system is gapped. However, experiments have observed that coherently pumped polaritons can flow past a defect with vanishing dissipation – a result claimed as evidence of superfluidity [17]. If the strength of the coherent pump is large enough and its momentum near the inflection point of the lower polariton dispersion, the macroscopic state becomes unstable to parametric scattering in a process called optical parametric oscillation (OPO) [40,41]. In this case, two new macroscopic 'signal' and 'idler' states form with opposite phases, where this phase is chosen spontaneously and there is a Goldstone mode. Experiments and theoretical analysis have also found reduced dissipation for flow past a defect in this regime [19].

1.1 Overview

This thesis is concerned with whether coherently driven polaritons below the OPO threshold, where the pumping is continuous and homogeneous, can be a superfluid, or whether experimental observations of dissipationless flow [17] are of a different phenomenon. This is investigated by using Keldysh field theory to calculate the longitudinal and transverse static current-current response functions, which are found to be identical, indicating that the sys-

tem is not a superfluid. Furthermore, we find that at zero pump momentum the system forms a rigid state that does not respond to either type of perturbation.

In Part 1, we motivate the physics of the problem. Chapter 2 describes superfluidity in detail, its relationship to BEC and two-dimensional systems, and its definition in terms of response functions is developed; Chapter 3 introduces the specifics of microcavity-polaritons, as well as previous research into condensation and superfluidity in such systems; and in Chapter 4, we motivate Keldysh field theory and derive the Green's functions of a coherently driven system of polaritons.

In Part 2, we calculate the difference between the longitudinal and transverse response functions of our system and analyse the results. In Chapter 5, we use the Green's functions to calculate the excitation spectrum and probe its relevance towards superfluidity; in Chapter 6, we use a Keldysh path integral method to calculate the static current-current response function; and in Chapter 7, we find the difference between the longitudinal and transverse components is zero and describe the existence of a new rigid state, as well as other consequences of the calculation.

Part 3 offers a general conclusion and some technical details are dealt with in the appendices.

Chapter 2

Superfluidity

In 1928, Keesom and Wolfke, working in Leiden, concluded that liquid helium-4 exists in two distinct phases separated by a transition at $T_c = 2.17\text{K}$, which they christened helium-I above T_c and helium-II below[42]. Experiments into their thermodynamic properties over the following years identified a now-famous lambda shaped peak in the specific heat at the critical temperature, but more astonishing were the hydrodynamic properties of the low temperature phase. In 1938, Kapitsa in Moscow and Allen and Misener in Cambridge independently observed a sharp drop in the viscosity of the fluid at the phase transition. Kapitsa named this discovery superfluidity after its similarity with superconductivity, which had been found in Leiden by Onnes in 1911[7]. Further investigation identified other peculiar flow properties of helium-II: it did not rotate except in the form of tiny vortices, it could support extremely long-lived metastable currents, and, perhaps most bizarrely, its lack of viscosity meant it could spontaneously climb up the walls of its container and empty itself onto the floor.

To explain this extraordinary phenomenon, London and Tisza suggested that the observations were caused by Bose-Einstein condensation (BEC), where a macroscopic number of particles occupy the ground state of the system, which was at the time unobserved and controversial. Dissipationless flow could then result from the system moving as a single macroscopic quantum state. By contrast, in the early 1940s, Landau developed a full hydrodynamic theory of superfluid helium-4 without referencing BEC at all (in which he did not believe)[43]. Starting from the ground state of a fluid and calculating the circumstances in which viscosity could dissipate energy through excitations, he derived a criterion in which superflow can occur below a critical velocity set by the excitation spectrum. Both Landau and Tisza postulated a two-fluid model where the system consists of two components, one 'superfluid' and the other the 'normal'. The normal component, which is viscous and rotates like an ordinary fluid, gradually disappears as the temperature tends to absolute zero. While the postulated two fluids do not represent literal separations of particles, they provide

a useful basis for understanding the dynamics of the system. Landau and Tisza discovered that there should be a type of 'second sound' wave where entropy fluctuations are carried by out-of-phase oscillations of the superfluid and normal components[44].

Later theoretical work, notably that of Bogoliubov[45], Beliaev[46], and Feynman[47], established that the microscopic basis of superfluid helium is indeed BEC and calculated its excitation spectrum. Eventually, neutron scattering experiments in helium became sophisticated enough to lend support to this[48], and in 1995 BEC was observed in an ultracold atomic gas[49,50] allowing the connection between the two phenomena to be studied more explicitly[51]. Additionally, it was found in 1972 that helium-3, a fermionic system, can become a superfluid through the condensation of pairs of atoms, similar to Cooper pairing in superconductors, and this process has been observed in ultracold Fermi gases as well[6].

Despite the link between superfluidity and Bose-Einstein condensation, it is crucial to note that they are not equivalent. Superfluidity is defined by flow properties and BEC by the macroscopic occupation of a single state, and it is significant that thermal fluctuations prevent the formation of BECs in two-dimensions yet superfluidity can still exist[52,53]. Two-dimensional bosonic systems can undergo the Berezinskii-Kosterlitz-Thouless (BKT) transition[54] to a low temperature phase that possesses algebraic order, as opposed to true long-range order in BECs, which is seemingly enough for superfluidity to occur. Crucially, these systems are sufficiently ordered for a 'local' macroscopic wavefunction to be defined[55]. Microcavity-polaritons, which are the subject of this thesis, are an example of a two-dimensional bosonic system[14], and the history of their relationship with superfluidity is explored in Chapter 3.

In this chapter, we examine the causes of superfluidity and how it is defined. Section 2.1 is concerned with off-diagonal long-range order and Section 2.2 on how it leads to flow properties such as bulk irrotationality, quantised vortices, and metastable persistent currents; Sections 2.3 and 2.4 look at the Landau criterion and the two-fluid model, respectively; Section 2.5 describes Bose-Einstein condensation and spontaneous symmetry breaking and their relationship to superfluidity, including how this changes in two-dimensional systems; and Section 2.6 defines superfluidity in terms of the current-current response function.

2.1 Off-diagonal long-range order

Fundamentally, superfluidity is a macroscopic quantum phenomenon. While fluids are ordinarily highly disordered, the particles in a superfluid behave collectively and form a single quantum state the size of the entire system. Mathematically, we can describe this in terms of off-diagonal long-range order[5,6,7]. The single particle density matrix is given by

$$\rho(\boldsymbol{x}, \boldsymbol{x}') = \langle \hat{\psi}^{\dagger}(\boldsymbol{x}) \hat{\psi}(\boldsymbol{x}') \rangle, \qquad (2.1)$$
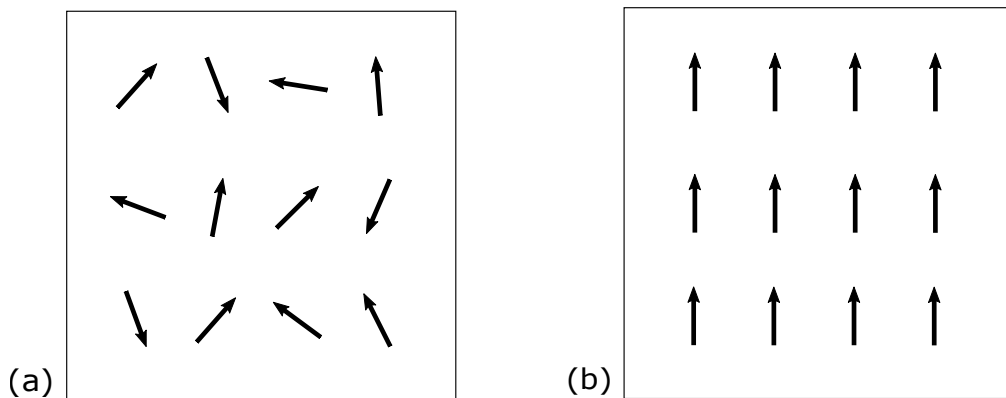
Figure 2.1: **(a)** At high temperatures, spins on a lattice form a disordered state where there is an exponential decay of correlations. **(b)** In some circumstances, lattice spins may line up in an ordered state with constant correlations and finite magnetism.

showing the overlap between a field at $\boldsymbol{x}$ and another at $\boldsymbol{x}'$, averaged over the rest of the system. This can be thought of as a measure of how correlated different points of the system are. If a system is disordered, then these correlations will decay exponentially, and the density matrix is given by

$$\rho(\boldsymbol{x}, \boldsymbol{x}') \sim e^{-|\boldsymbol{x} - \boldsymbol{x}'|/\xi(T)}, \tag{2.2}$$

where the length scale of correlations is set by the temperature dependent quantity $\xi(T)$, known as the correlation length. In this case the density matrix is almost diagonal. To visualise this, consider the case of magnetism, where the complex field describes the amplitudes and angles of orientation of magnetic moments on a lattice. In the disordered state (shown in Fig. 2.1(a)), the directions of the individual spins are uncorrelated, and their magnetic moments cancel out leading to zero overall magnetisation.

By contrast, suppose we have a density matrix that is constant as the distance between the two points tends to infinity, $|\boldsymbol{x} - \boldsymbol{x}'| \to \infty$,

$$\lim_{|\boldsymbol{x} - \boldsymbol{x}'| \to \infty} \rho(\boldsymbol{x}, \boldsymbol{x}') = \langle \hat{\psi}^{\dagger}(\boldsymbol{x})\hat{\psi}(\boldsymbol{x}') \rangle \sim \text{constant}. \tag{2.3}$$

This roughly corresponds to all the spins in the magnet being aligned (see Fig. 2.1(b)) leading to finite overall magnetisation. In this case, the density matrix is approximately the same at all values of $\boldsymbol{x}$ and $\boldsymbol{x}'$, i.e. the system has off-diagonal long-range order (ODLRO). As the values as $\boldsymbol{x}$ and $\boldsymbol{x}'$ are independent, we have that

$$\langle \hat{\psi}^{\dagger}(\boldsymbol{x})\hat{\psi}(\boldsymbol{x}') \rangle \simeq \langle \hat{\psi}^{\dagger}(\boldsymbol{x}) \rangle \langle \hat{\psi}(\boldsymbol{x}') \rangle \sim \text{constant}, \tag{2.4}$$

and the order in the system can be defined by a complex order parameter,

$$\langle \hat{\psi}(\boldsymbol{x}) \rangle = \psi(\boldsymbol{x}) = |\psi(\boldsymbol{x})| \, \mathrm{e}^{i\phi(\boldsymbol{x})}, \tag{2.5}$$

which we may interpret as the wavefunction of a macroscopic quantum state. As the order parameter is an average over the system of the value of the field, the mean-field approximation will yield a finite value.

2.2   Superfluid flow properties

Amongst the defining flow properties of superfluids, bulk irrotationality, quantised vortices, and metastable persistent currents follow quite straightforwardly from the macroscopic wavefunction. As quantum fluctuations are small on macroscopic scales, we may find the current associated with this wavefunction by substituting Eq. (2.5) into the expression for the current in quantum mechanics:

$$\boldsymbol{j}(\boldsymbol{x}) = -\frac{i\hbar}{2m} \left[\psi^*(\boldsymbol{x}) \nabla \psi(\boldsymbol{x}) - [\nabla \psi^*(\boldsymbol{x})] \psi(\boldsymbol{x}) \right] = |\psi(\boldsymbol{x})|^2 \, \frac{\hbar}{m} \nabla \phi(\boldsymbol{x}). \tag{2.6}$$

As the current is given by a density times a velocity, we see that the velocity of the macroscopic state, which we call the superfluid velocity $\boldsymbol{v}_s(\boldsymbol{x})$, is proportional to the gradient of the wavefunction phase:

$$\boldsymbol{v}_s(\boldsymbol{x}) = \frac{\hbar}{m} \nabla \phi(\boldsymbol{x}). \tag{2.7}$$

It follows that the curl of this is zero,

$$\boldsymbol{\omega}_s = \nabla \times \boldsymbol{v}_s(\boldsymbol{x}) = \boldsymbol{0}, \tag{2.8}$$

and superfluid flow is irrotational. However, looking instead at the circulation,

$$\Gamma = \iint \boldsymbol{\omega}_s . d\boldsymbol{S} = \oint \boldsymbol{v}_s(\boldsymbol{x}) . d\boldsymbol{l}, \tag{2.9}$$

we see that the superfluid velocity gives

$$\Gamma = \oint \frac{\hbar}{m} \nabla \phi(\boldsymbol{x}) . d\boldsymbol{l} = \frac{\hbar}{m} \Delta \phi(\boldsymbol{x}), \tag{2.10}$$

which, due to the compact nature of the phase, admits some finite solutions. For the wavefunction to be single valued, the change in phase around a closed loop must be an integer multiple of 2π, and so the circulation is quantised:

$$\Gamma = \frac{h}{m} n. \tag{2.11}$$
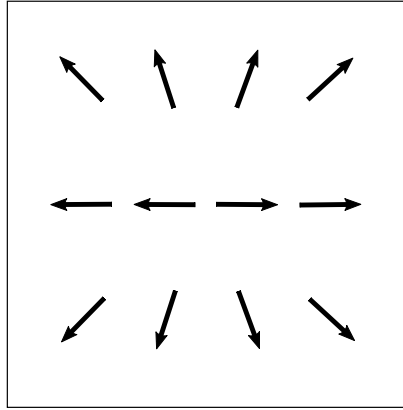
Figure 2.2: A vortex results from an integer number of rotations of the phase around a loop. This is easiest to visualise in the case of spins on a lattice. In a superfluid there is no lattice and it is the phase of the macroscopic wavefunction that leads to vortices.

This effect manifests itself as the appearance of quantised vortices, which are infinitesimal defects that allow the superfluid to carry angular momentum (see Fig. 2.2) despite the bulk being irrotational. The integer n, the number of rotations of the phase around the loop, is known as the winding number, and can be negative as well as positive, corresponding to antivortices that can combine with positive vortex configurations and annihilate. The loops in phase that lead to vortices cannot be smoothly deformed away and consequently vortices are often described as topological defects[7].

2.2.1 The Hess-Fairbank effect

A spectacular experimental demonstration of bulk irrotationality and quantised vortices is known as the Hess-Fairbank effect. In this experiment, a bucket of radius R full of liquid helium above the superfluid transition temperature is rotated with angular velocity ω, and the fluid allowed to come into equilibrium with the container walls. The temperature is then cooled below T_c, at which point it is found that the superfluid component ceases to rotate (giving its angular momentum back to the bucket). However, if the angular velocity is above one half of a quantum of vorticity,

$$\omega > \frac{\omega_c}{2} = \frac{1}{2}\frac{\hbar}{mR^2}, \tag{2.12}$$

then a vortex will form in the superfluid to carry the angular momentum. In the case where $\omega \gg \omega_c$ then lots of vortices will form and arrange themselves into a lattice (see Figs. 2.3 and 2.4).

The Meissner effect in superconductors, where magnetic fields are expelled from the bulk of the material, is analogous to the Hess-Fairbank effect. To see this, consider changing to the frame of the bucket. When cooled below T_c, the absence of rotation in the lab frame
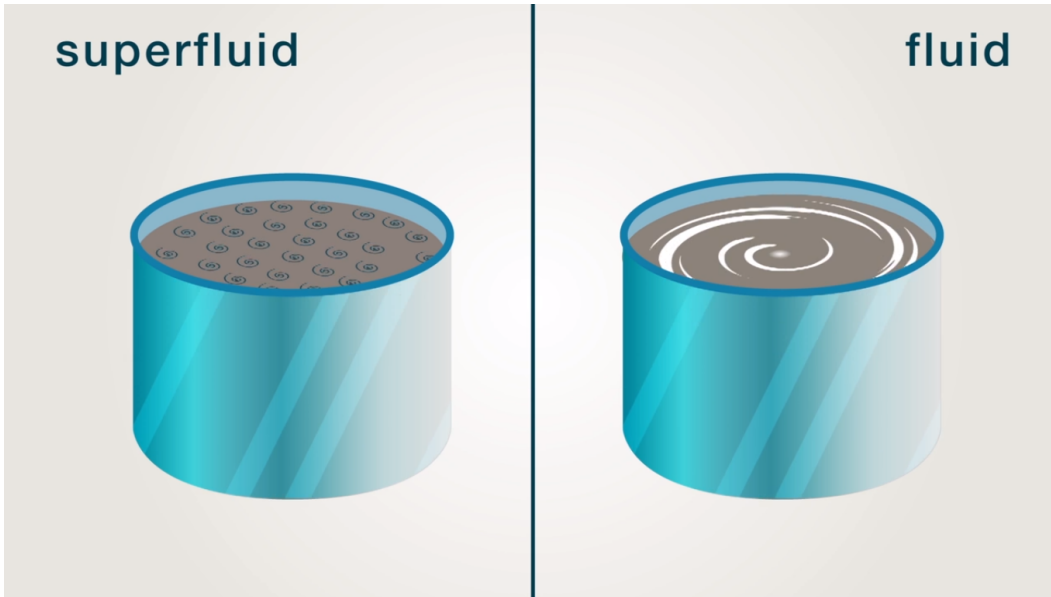
Figure 2.3: An ordinary fluid (right) in a spinning bucket will rotate along with the container. By contrast, a superfluid (left), can only rotate in the form of quantised vortices.

is equivalent to a flow of current in the converse direction, rendering the system perfectly diamagnetic[6].

2.2.2   Metastable persistent currents

Another remarkable property of superfluids is that they can host metastable states in which a current flows for extremely long timescales. This can be shown experimentally with a torus of radius R and cross-sectional width a, where $R \gg a$, filled with liquid helium. Starting above T_c, the torus is rotated at an angular velocity $\omega > \omega_c$ and allowed to equilibrate with the container. The system is then cooled through the transition and, unlike in the
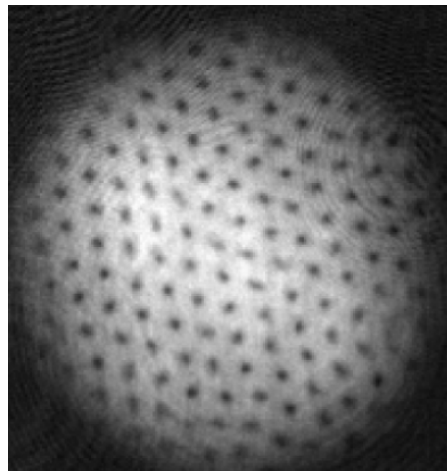
Figure 2.4: Vortices arranged in a lattice on the surface of a macroscopic state of sodium atoms stirred by a laser beam[56].

Hess-Fairbank effect, the current in the fluid will continue to flow as the geometry allows a winding of the phase around the torus to support it, much like a macroscopically sized vortex. Remarkably, if the rotation of the container is then stopped, this current will carry on flowing in a metastable state unlikely to decay for astronomical timescales[6]. In contrast to a normal current, the flow around the torus cannot continuously slow down – it is topologically protected – and it can be shown that the toroidal geometry is an essential requirement for this[14]. Notably, this effect is only possible in the presence of repulsive interactions between particles[5], and it cannot be considered a generic consequence of BEC as it breaks down for order parameters more complicated than a complex number.

2.3   The Landau criterion

Dissipationless flow (see Fig. 2.5) can be qualitatively understood as a result of the unified motion of the particles in the macroscopic quantum state. A more precise description of this behaviour was provided by Landau, who constructed an explanation based on energetic arguments around the appearance of excitations above the ground state of a flowing fluid at absolute zero[43]. In fact, while consistent with them, his arguments do not reference BEC or long-range order at all.

Landau reasoned that a viscous fluid requires available excitation states through which to dissipate energy[30]. Indeed, if arbitrarily small transfers of momentum and energy are impossible, then there will be a regime in which the fluid flows without friction[57]. To examine this, we consider a fluid flowing with energy E and momentum $\boldsymbol{P}$ between the
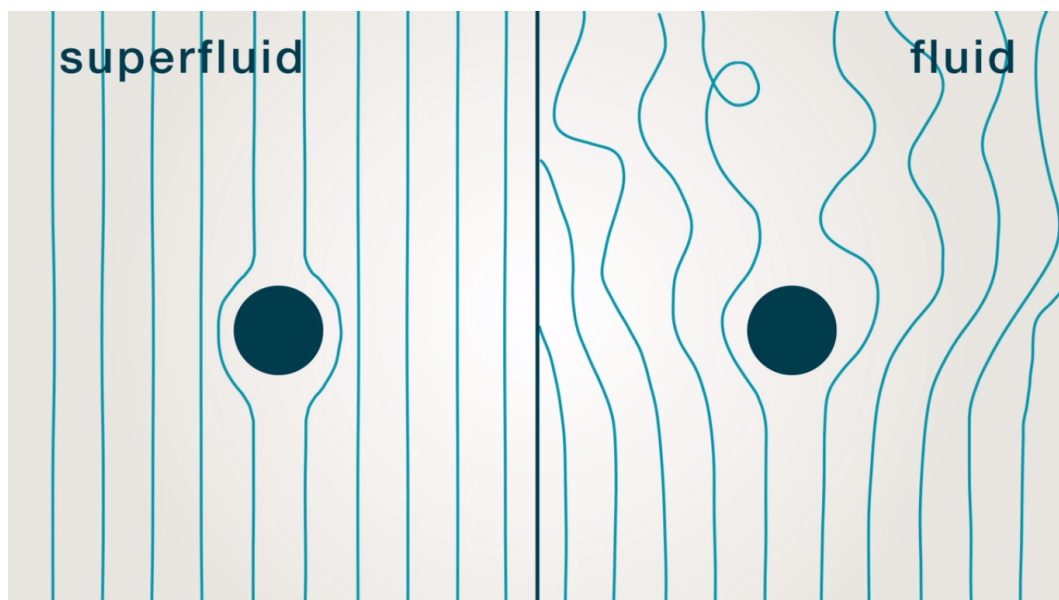
Figure 2.5: When an ordinary fluid (right) flows against an obstacle, excitations may form which scatter off the object and dissipate energy. In a superfluid (left), excitations cannot form, and the fluid passes the obstacle without dissipation.
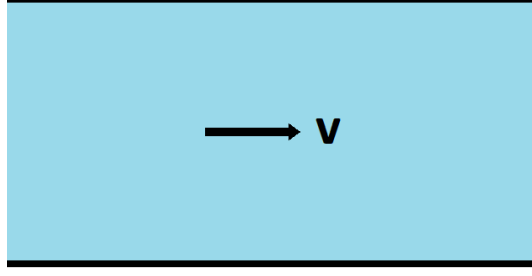
Figure 2.6: A fluid flows between the walls of a container with velocity $\boldsymbol{v}$. It is in the ground state and at absolute zero.

walls of a container (see Fig. 2.6). In a new frame, K', moving with velocity $\boldsymbol{V}$ compared to the original frame K, we have that

$$\boldsymbol{P'} = \boldsymbol{P} - M\boldsymbol{V}, \tag{2.13}$$

$$E' = \frac{1}{2M}\left|\boldsymbol{P} - M\boldsymbol{V}\right|^2 = E - \boldsymbol{P}.\boldsymbol{V} + \frac{1}{2}M\left|\boldsymbol{V}\right|^2. \tag{2.14}$$

Now, taking K to be the rest frame of the fluid and considering the case where $T = 0$ so it is in its ground state, we can see that if a single excitation with momentum $\boldsymbol{p}$ and energy $\epsilon(\boldsymbol{p})$ were to exist (see Fig. 2.7), the total energy and momentum would be

$$\boldsymbol{P} = \boldsymbol{p}, \tag{2.15}$$

$$E = E_0 + \epsilon(\boldsymbol{p}), \tag{2.16}$$

where E_0 is the ground state energy of the fluid at rest. Changing to frame K', where $\boldsymbol{V} = -\boldsymbol{v}$, so the fluid flows at velocity $+\boldsymbol{v}$, our total energy and momentum are now

$$\boldsymbol{P'} = \boldsymbol{p} + M\boldsymbol{v} \tag{2.17}$$

$$E' = E_0 + \epsilon(\boldsymbol{p}) + \boldsymbol{p}.\boldsymbol{v} + \frac{1}{2}M\left|\boldsymbol{v}\right|^2. \tag{2.18}$$
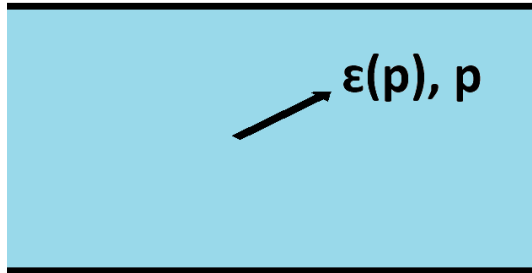
Figure 2.7: An excitation with energy $\epsilon(\boldsymbol{p})$ and momentum $\boldsymbol{p}$ forms in the rest frame of the fluid.

Therefore, it will be energetically favourable for excitations to form if

$$\epsilon(\boldsymbol{p}) + \boldsymbol{p}.\boldsymbol{v} < 0. \tag{2.19}$$

This is only true if the flow velocity is larger than a critical velocity given by

$$v_c = \min_p \frac{\epsilon(\boldsymbol{p})}{p}, \tag{2.20}$$

where by $\min_p$ we mean the value of p which minimises the expression. In a fluid flowing above v_c, excitations will proliferate and allow the system to dissipate energy through viscosity, destroying the superfluid state. This condition is known as the Landau criterion for superfluidity. Crucially, it can only be fulfilled if the critical velocity is finite, which depends on the excitation spectrum. For a linear excitation spectrum, $\epsilon(\boldsymbol{p}) = cp$ (Fig. 2.8(a)), we have that

$$v_c = \min_p \frac{cp}{p} = c. \tag{2.21}$$

That is, the critical velocity is equal to the speed of sound, c. The Landau criterion is also fulfilled by gapped spectra, for example $\epsilon(\boldsymbol{p}) = \Delta + Ap^2$ where Δ and A are constants (Fig. 2.8(b)), with a critical velocity given by $v_c = 2\sqrt{\Delta A}$. By contrast, for a gapless quadratic spectrum, which characterises massive free particles, the critical velocity is zero:

$$v_c = \min_p \frac{Ap^2}{p} = 0. \tag{2.22}$$

Such a system can never be a superfluid because excitations can form at any flow velocity. Another notable system that fulfils the criterion is that of a weakly interacting Bose
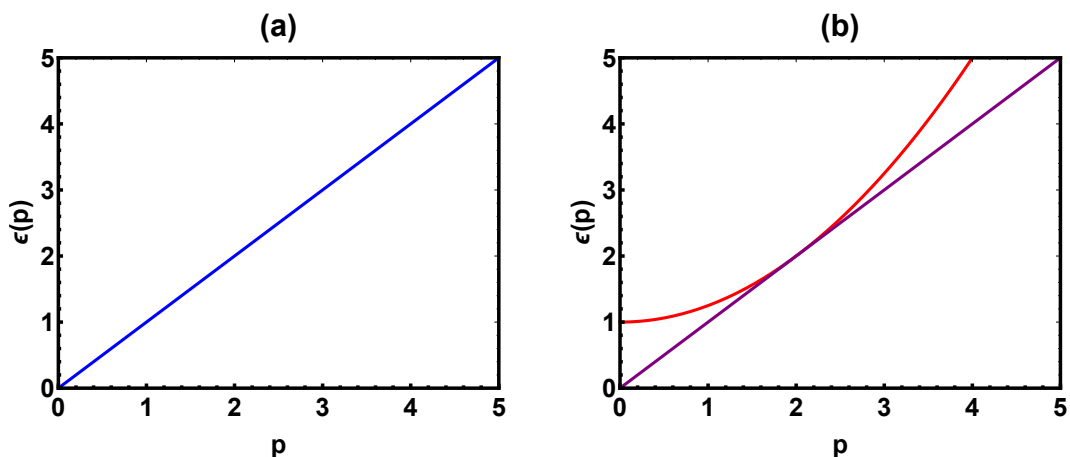
Figure 2.8: **(a)** For a linear excitation spectrum the critical velocity is the slope of the line. **(b)** For a gapped spectrum (red), the critical velocity is the slope of the shallowest line that both goes through the origin and touches the spectrum (purple). For a gapless quadratic spectrum this line has zero gradient and thus the critical velocity is zero.
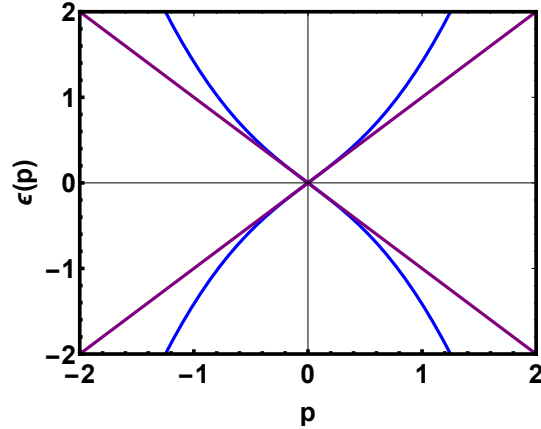
Figure 2.9: The Bogoliubov spectrum (blue) is the excitation spectrum of a weakly interacting Bose gas that has undergone BEC. In the limit of small momenta this tends to a linear spectrum and thus has a finite critical velocity (given by the slope of the purple lines).

gas that has undergone BEC, where the excitations are given by the Bogoliubov spectrum (Fig. 2.9)[33]:

$$\epsilon_B(\boldsymbol{p}) = \pm\sqrt{\frac{p^2}{2m}\left(\frac{p^2}{2m} + 2n_0 V\right)}. \tag{2.23}$$

This system has a critical velocity given by $v_c = \sqrt{n_0 V/m}$, where n_0 is the particle number density in the condensed state and V is the interaction strength.

By considering the Bogoliubov spectrum in the laboratory frame for a condensate flowing with velocity v_0, we can visualise how excitation states become energetically available only above the critical velocity. Eqs. (2.17) and (2.18) show how in this frame, as well as there being a shift in condensate energy and momentum (which here plays the role of
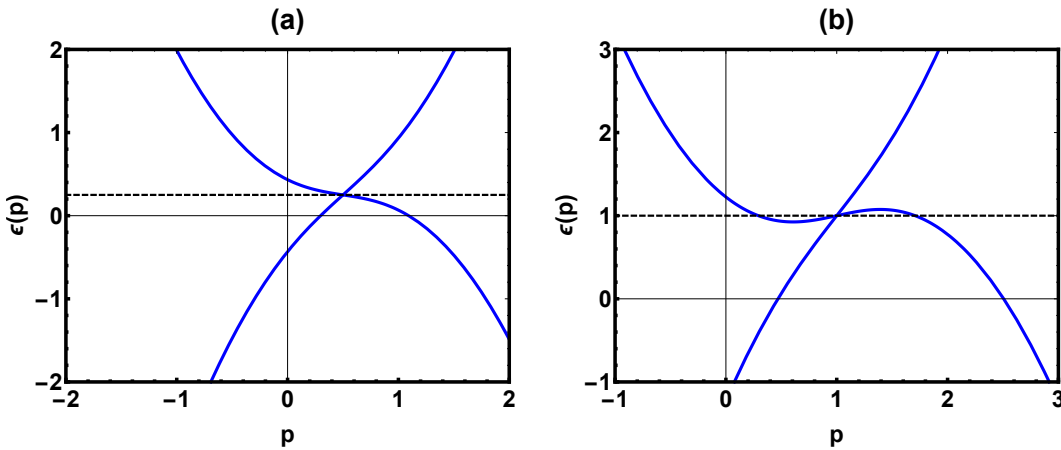
Figure 2.10: **(a)** In the laboratory frame for a condensate travelling with velocity v_0, the excitation spectrum is tilted and shifted in energy and momentum. However, below the critical velocity v_c there are no excitation energies at the same energy as the condensate (indicated by the dashed line) into which scattering may occur. **(b)** When $v_0 > v_c$, the tilt in the excitation spectrum becomes more pronounced leading to available states into which there may be scattering.

Landau's ground state fluid), there is a term pv_0 added to the spectrum (Eq. (2.23)) which causes it to be tilted. Fig. 2.10(a) shows this for where $v_0 < v_c$, and it can be seen that in this case there are no excitation states at the condensate energy, indicated by the dashed line, into which there may be scattering. However, as shown in Fig. 2.10(b), this changes when $v_0 > v_c$ as the tilt in the spectrum becomes so pronounced that there are available excitation states into which the system may dissipate energy.

2.4 The two-fluid model

Landau's argument for dissipationless flow assumes the fluid is at $T = 0$, which is not true of any real system. Consequently, there will always be a finite number of thermal excitations that will behave like a 'normal' fluid and dissipate energy viscously, irrespective of the flow velocity. To incorporate this, Landau proposed the two-fluid model (also suggested by Tisza[44]): a superfluid system contains two fractions, 'superfluid' and 'normal', where only the former possesses superfluid flow properties. It is important to note that these fractions do not correspond literally to particles in the system but are rather a way of quantifying the system's behaviour (indeed, the excitations here are quasiparticles, not simply excited helium atoms). We can write the current in terms of the densities of these components as

$$\boldsymbol{j} = \rho_s \boldsymbol{v}_s + \rho_n \boldsymbol{v}_n, \tag{2.24}$$

where the total density is $\rho = \rho_s + \rho_n$. Landau used this idea to formulate a complete series of hydrodynamic equations describing the motion of helium-II[43], and experimental results have confirmed the two-fluid picture as accurate[58].

The existence of a normal fraction shows that the intuitively satisfying interpretation of defining superfluids as simply fluids without viscosity is incorrect. All real superfluids will be at finite temperature and will possess a viscous normal component. Additionally, such a definition makes no distinction between a fluid with merely low viscosity and one possessing the collection of properties described in Section 2.2. By contrast, the two-fluid model allows us to classify superfluids quantitatively by defining the superfluid fraction. Putting this explicitly, the proportion of the fluid that is 'superfluid' rather than 'normal' is given by[34]

$$f_s(T) = \frac{\rho_s(T)}{\rho}, \tag{2.25}$$

which is zero at $T = T_c$ and unity at $T = 0$. To measure this experimentally we note that a superfluid will display a reduced, nonclassical moment of inertia. Therefore, if we rotate a container of our fluid below the critical temperature, we will find that the superfluid fraction

is given by

$$f_s(T) = 1 - \lim_{\omega \to 0} \frac{\langle L \rangle}{I_{cl}\omega}, \tag{2.26}$$

where $\langle L \rangle$ is the expectation value of the angular momentum and I_{cl} is the classical moment of inertia. Other common formulations of this idea are that of the superfluid stiffness, $\rho_s = m^2 K_s$, which is related to the energy required to twist the macroscopic phase [27] (and thus induce a current), $E(\phi(\boldsymbol{x})) = (K_s/2) \int d\boldsymbol{x} (\nabla \phi(\boldsymbol{x}))^2$, and also a description in terms of the static current-current response function, where the superfluid density is equal to the difference between the longitudinal and transverse responses of the system to perturbations. The latter idea will be developed in Section 2.6 and forms the basis of the calculations in Chapters 6 and 7.

2.5 Bose-Einstein condensation

Bose-Einstein condensation, while distinct from superfluidity, has been closely associated with it ever since London offered it as an explanation of Kapitsa, Allen, and Misener's observations in 1938. Significantly, BEC is a mechanism by which a three-dimensional bosonic system may acquire off-diagonal long-range order. To see this, consider the Bose-Einstein distribution, which governs the occupation of states in bosonic systems:

$$n_B(\epsilon, T) = \frac{1}{e^{(\epsilon - \mu)/k_B T} - 1}. \tag{2.27}$$

This function diverges at positive energies unless the chemical potential μ is less than zero. If we approximate the energy levels as continuous, we get a condition for the Bose-Einstein distribution to hold,

$$\int_0^\infty \frac{\rho(\epsilon) d\epsilon}{e^{\beta\epsilon} - 1} \geq N, \tag{2.28}$$

where $\rho(\epsilon)$ is the density of states and N is the total number of particles in the system. In one- and two-dimensions, $\rho(\epsilon)$ is proportional to $\epsilon^{-1/2}$ and a constant, respectively, and Eq. (2.28) holds for all T. However, in three-dimensions, the density of states is given by

$$\rho(\epsilon) = V \frac{g_s}{4\pi^2} \frac{(2m)^{3/2}}{\hbar^3} \epsilon^{1/2}, \tag{2.29}$$

where V is the volume and g_s the number of spin projections, and Eq. (2.28) fails at a critical temperature given by

$$k_B T_c \simeq 3.31 \left(\frac{N}{V g_s} \right)^{2/3} \frac{\hbar^2}{m}. \tag{2.30}$$

At temperatures lower than T_c, the distribution becomes infinite at the lowest energies and Bose-Einstein condensation occurs where a macroscopic number of particles occupy the

ground state of the system. By 'macroscopic', we mean that the occupation of the ground state N_0 is of the same order of magnitude as N. Notably, the transition occurs when the de Broglie wavelength $\lambda = h/p$ is roughly the same as the average separation between the particles, highlighting that this is a quantum effect dependent on them having a wave-like nature.

To relate this back to long-range order, we may write the one particle density matrix as

$$\rho(\boldsymbol{x}, \boldsymbol{x}') = \langle \hat{\psi}^\dagger(\boldsymbol{x})\hat{\psi}(\boldsymbol{x}')\rangle = \frac{1}{V}\sum_{\boldsymbol{p}} e^{-i\boldsymbol{p}.(\boldsymbol{x}-\boldsymbol{x}')}\langle \hat{\psi}_{\boldsymbol{p}}^\dagger \hat{\psi}_{\boldsymbol{p}}\rangle = \frac{1}{V}\sum_{\boldsymbol{p}} e^{-i\boldsymbol{p}.(\boldsymbol{x}-\boldsymbol{x}')}N_{\boldsymbol{p}}, \qquad (2.31)$$

where we have Fourier transformed the field operators into momentum space and assumed that the system is homogeneous and isotropic. For a condensate, the momentum distribution is:

$$N_{\boldsymbol{p}} = N_0 \delta_{\boldsymbol{p},\boldsymbol{0}} + N'_{\boldsymbol{p}}, \qquad (2.32)$$

where the first term gives the ground state and the second the Bose-Einstein distribution with $\epsilon = p^2/2m$ and $\mu = 0$. Substituting this into the one particle density matrix, we get

$$\rho(\boldsymbol{x}, \boldsymbol{x}') = n_0 + \rho'(\boldsymbol{x}, \boldsymbol{x}'), \qquad (2.33)$$

where $n_0 = N_0/V$. The density matrix for the excited states, $\rho'(\boldsymbol{x}, \boldsymbol{x}')$, will follow the usual exponential decay of correlations, and so in the limit $|\boldsymbol{x} - \boldsymbol{x}'| \to \infty$ we have that

$$\lim_{|\boldsymbol{x}-\boldsymbol{x}'|\to\infty} \rho(\boldsymbol{x}, \boldsymbol{x}') = n_0 = \text{constant.} \qquad (2.34)$$

That is, Bose-Einstein condensation causes off-diagonal long-range order.

While the above derivation is for non-interacting systems, statistical arguments can be made suggesting it is likely that all liquid bosonic systems condense at $T = 0$[6]. Given that the one-particle density matrix is Hermitian, we may diagonalise it into a complete set of orthonormal eigenfunctions $\chi_i(\boldsymbol{x})$,

$$\rho(\boldsymbol{x}, \boldsymbol{x}') = \sum_i N_i \chi_i(\boldsymbol{x})\chi_i(\boldsymbol{x}'). \qquad (2.35)$$

A general definition of BEC is a system in which one of the eigenvalues N_i is roughly equal to the total number of particles N.

Interestingly, in systems that are both a BEC and a superfluid, the condensate fraction, N_0/N, may be different to the superfluid fraction, ρ_s/ρ, which is true in liquid helium-4 at $T = 0$, where $N_0/N \sim 9\%$[48] and yet $\rho_s/\rho = 100\%$. This is remarkable, as it shows that the
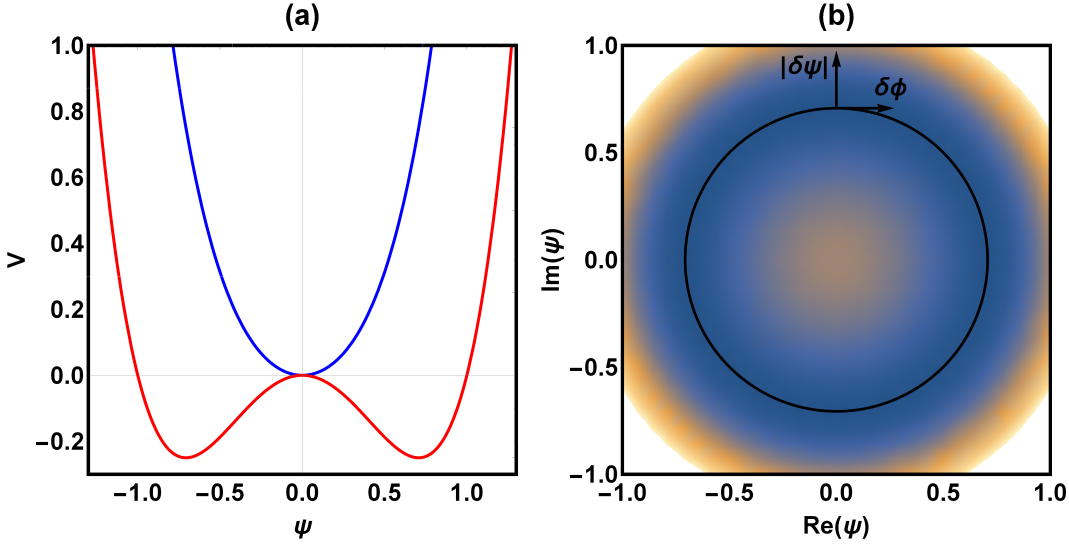
Figure 2.11: **(a)** The minima in potential energy depend on the sign of α, the coefficient of the quadratic term in Eq. (2.37). When $\alpha > 0$, the minimum is where the order parameter $\psi = 0$ and the state is unordered. However, when $\alpha < 0$, ψ is finite and the state is ordered. **(b)** In the ordered state the degenerate minima of potential energy form a circle in the Argand diagram of complex ψ. Amplitude fluctuations away from the minima cost energy and contribute a mass term to the action. By contrast, fluctuations in phase cost no potential energy, resulting in a massless mode around the bottom of the potential that is known as a Goldstone mode.

order in the system due to 9% condensation is sufficient for 100% to flow like a superfluid, and it can be explained by the strong interactions between particles in helium, leading to a finite probability for non-condensate particles to participate in the superflow[31]. By contrast, in three-dimensional ultracold Bose gases, where interactions are much weaker, the condensate and superfluid fractions are the same[42].

2.5.1   Spontaneous symmetry breaking

Applying Landau's theory of phase transitions, the free energy in a system of neutral, interacting bosons with order parameter $\psi = \langle \hat{\psi}(\boldsymbol{x}) \rangle$ is given by[57]

$$F[\psi] = \int d\boldsymbol{x} \left(\frac{\hbar^2}{2m} |\nabla \psi|^2 + \alpha |\psi|^2 + \lambda |\psi|^4 ... \right), \tag{2.36}$$

where we neglect higher order terms as we are interested in small ψ around the transition point. Thus, the potential energy density in the system is

$$V[\psi] = \alpha |\psi|^2 + \lambda |\psi|^4, \tag{2.37}$$

where for the energy to be bounded from below we have that $\lambda > 0$. The shape of the potential energy curve, and consequently the behaviour of the system, depends on the sign of α. As shown in Fig. 2.11(a), when $\alpha > 0$ the minimum of energy is at $\psi = 0$ and the

state is unordered. By contrast, when $\alpha < 0$ the order parameter is finite, $\psi \neq 0$, and there is a degenerate energy minimum around a circle in the Argand diagram of complex ψ (Fig. 2.11(b)). The transition between the unordered and ordered states occurs when $\alpha = 0$, so an appropriate form for α to describe a system in which the phase transition is temperature dependent is where the sign changes at the critical temperature T_c,

$$\alpha(T) = a(T_c - T), \tag{2.38}$$

for some constant a. While the phase of the order parameter is a continuous symmetry of the action, during the transition to the ordered state one particular phase must be picked out in a process known as spontaneous symmetry breaking. E.g., in the case of magnetism, this corresponds to the fact that the magnetisation may in theory point in any direction, but during the transition one in particular will be chosen.

To see how a real system might behave we must go beyond the mean-field and look at fluctuations. We can decompose these into those of amplitude and phase: $\psi = (|\psi_0| + |\delta\psi|)\exp(i\phi + i\delta\phi)$ (see Fig. 2.11(b)). Amplitude fluctuations involve increases in potential energy and thus contribute a mass term to the action. By contrast, fluctuations in phase cost no potential energy at all, leading to a massless branch of excitations known as a Goldstone mode. Typically, a Goldstone mode will have a gapless spectrum that goes to zero linearly in the long-range limit, $\boldsymbol{p} \to \boldsymbol{0}$[59]. For instance, consider a system described by the Lagrangian

$$L = \int dx \left(\frac{1}{2}|\partial_t \psi|^2 - \frac{1}{2}|\nabla\psi|^2 - V(|\psi|) \right), \tag{2.39}$$

where $x = (t, \boldsymbol{x})$ and $\psi = \psi(x)$. If we take fluctuations in the phase around the bottom of the potential, that is, we write $\psi(x) = \psi_0 e^{i(\phi_0 + \delta\psi(x))}$, then the Lagrangian becomes

$$L = \int dx \left(\frac{|\psi_0|^2}{2}(\partial_t \delta\phi)^2 - \frac{|\psi_0|^2}{2}(\nabla\delta\phi)^2 - V(|\psi_0|) \right), \tag{2.40}$$

Substituting this into the Euler-Lagrange equation to find the equation of motion for the fluctuations $\delta\phi$, we see that it is a wave equation with linear dispersion relation. That is, for this particular kind of fluctuation there are no potential terms that contribute in the long-range limit, so the spectrum is gapless.

It stands to reason that low energy excitations will dictate the behaviour of a system at extremely low temperatures. In superfluid helium-4, the excitation spectrum is given by gapless phonons and gapped rotons (see Fig. 2.12), where both parts of the excitation spectrum fulfil the Landau criterion for dissipationless flow.
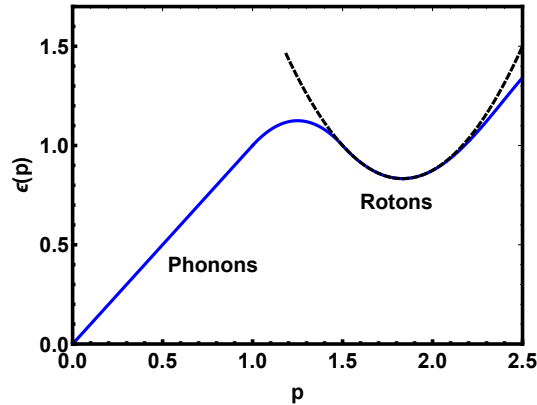
Figure 2.12: The excitation spectrum of the low temperature phase of helium-4. At lower tem-
peratures the behaviour of the system is dominated by gapless, linearly dispersed
phonons. As the temperature rises the gapped, approximately quadratic rotons
become more important. Both parts of the spectrum corresponding to these quasi-
particles fulfil the Landau criterion.

2.5.2   Two-dimensional systems

When moving beyond a mean-field analysis we must consider whether the ordered state is
stable in the presence of fluctuations. Specifically, the free energy is a function of entropy,
$F = E - TS$, and so to minimise F there will be competition between the potential min-
imum and temperature fluctuations towards higher entropy states, where the outcome will
depend on the system dimension. When the dimension is two or lower, the Mermin-Wagner
theorem[60] states that there cannot be spontaneous breaking of a continuous symmetry, and
so a finite complex order parameter cannot exist.

For instance, we may describe the phase of a complex order parameter in a two-
dimensional system by using the continuum XY-model for spins in a plane[61]:

$$H_{XY} = J \int d^2\boldsymbol{x} (\nabla \phi(\boldsymbol{x}))^2. \tag{2.41}$$

In agreement with the Mermin-Wagner theorem, in the presence of fluctuations the single
particle density matrix for this Hamiltonian shows an algebraic decay of correlations at all
temperatures[57]

$$\rho(\boldsymbol{x}, \boldsymbol{x}') = \langle \hat{\psi}^\dagger(\boldsymbol{x}) \hat{\psi}(\boldsymbol{x}') \rangle = a \, |\boldsymbol{x} - \boldsymbol{x}'|^{-\eta(T)} \,, \tag{2.42}$$

for some constant a and temperature-dependent exponent $\eta(T)$. If we extend the model
to include vortices, an argument given by Berezinskii, Kosterlitz, and Thouless (BKT)[54]
shows that above a critical temperature vortex-antivortex pairs in the system will find it
energetically favourable to unbind, on account of the associated increase in entropy. The
proliferation of individual vortices destroys the algebraic order leading to a high-temperature
phase with exponentially decaying correlations (Eq. (2.2)).
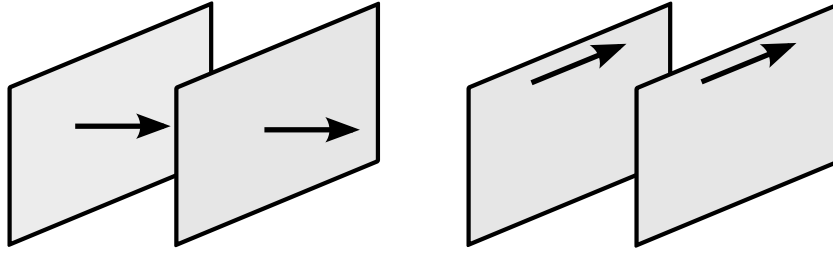
Figure 2.13: A current flowing in response to a perturbing force may originate through longitudinal or transverse actions, corresponding to pushing and shearing, respectively. A superfluid responds to longitudinal but not transverse perturbations[30,31,32,33,57].

While not true long-range order, the algebraic decay of correlations is much slower than exponential decay and we may consider this system to be quasiordered. Indeed, the decay is slow enough that we may assume the existence of a local BEC and a local condensate wavefunction[55]. This local order is sufficient for the existence of superfluidity, which has been shown to survive in two-dimensional systems such as thin films of helium-4[52] and ultracold atomic gases confined by a potential[53].

2.6 Response functions

As referenced in Section 2.4, the fact that superfluids do not respond to slow rotations provides a mechanism to clearly define superfluidity and the superfluid fraction[30,31,32,33,57]. This property can be formulated in terms of the linear response of the system to perturbations.

For a perturbation $\boldsymbol{f}$ coupled to a current, $\delta\hat{H} = \sum_{\boldsymbol{q}} \hat{\boldsymbol{j}}(\boldsymbol{q}).\boldsymbol{f}(\boldsymbol{q})$, the static current-current response function $\chi_{ij}(\boldsymbol{q})$ is defined as the generalised susceptibility for a current to flow in response to the perturbation,

$$j_i(\boldsymbol{q}) = \chi_{ij}(\boldsymbol{q})f_j(\boldsymbol{q}), \tag{2.43}$$

where χ_{ij} is given by the correlator of two current operators, with the average taken over the perturbed system[59,62],

$$\chi_{ij}(\boldsymbol{q}) = -i\langle\hat{j}_i(\boldsymbol{q})\hat{j}_j(-\boldsymbol{q})\rangle. \tag{2.44}$$

The superfluid fraction responds to longitudinal perturbations (potential forces or pushes) but not transverse ones (to shears) (see Fig. 2.13), whereas the normal fraction will respond equally to both. Consequently, if the difference between the longitudinal and transverse parts of the current-current response function is finite, this shows that there is a superfluid component in the system.

Mathematically, the longitudinal and transverse response functions (χ^L and χ^T) can be found by taking the long-range limit of a diagonal component of the full response function,

$\chi_{ii}(\boldsymbol{q} \to \boldsymbol{0})$, and varying the order in which the longitudinal and transverse components of $\boldsymbol{q}$ (those parallel to and perpendicular to i, respectively) are taken to zero. For example, consider a two-dimensional system which is perturbed in the x-direction. If we wish to find the current that flows in the x-direction in response to this, we want to calculate χ_{xx}. To find the component of this response that is longitudinal, we take the transverse momentum q_y to zero, effectively ignoring it, and find the limiting behaviour of the system as $q_x \to 0$. That is to say, the momentum in the longitudinal direction is the physically relevant limit, so the result is χ^L. By contrast, if we take $q_x \to 0$ first then the limit of the transverse momentum, $q_y \to 0$, will be the physically relevant one and we will get χ^T. In an isotropic system, we may use rotational symmetry to write this decomposition as

$$\chi_{ij}(\boldsymbol{q}) = \frac{q_i q_j}{q^2} \chi^L(\boldsymbol{q}) + \left(\delta_{ij} - \frac{q_i q_j}{q^2}\right) \chi^T(\boldsymbol{q}). \tag{2.45}$$

Note that if the longitudinal and transverse responses are the same in the long-range limit, i.e. $\chi^L(\boldsymbol{q} \to \boldsymbol{0}) = \chi^T(\boldsymbol{q} \to \boldsymbol{0}) = \chi'$, then $\chi_{ij}(\boldsymbol{q} \to \boldsymbol{0}) = \delta_{ij}\chi'$.

2.6.1 Sum rules

While the difference between the longitudinal and transverse response functions can show us whether there is a superfluid component in a system, to relate this to the superfluid fraction (Eq. (2.25)), we need a relationship between the response functions and the densities, $\rho = \rho_n + \rho_s$. For an isotropic system that conserves particle number, this relationship is given by what is known as the f-sum rule [30], where the 'sum' refers to the fact that it involves an integral over frequency [63]. Linear response theory gives an expression for the response function in terms of the current as [64]

$$\chi_{ij}(\boldsymbol{q}) = \frac{2}{\mathcal{Z}} \sum_{n,m} \frac{\mathrm{e}^{\beta E_n}}{E_n - E_m} \langle n|\hat{j}_i^\dagger(\boldsymbol{q})|m\rangle \langle m|\hat{j}_j(\boldsymbol{q})|n\rangle, \tag{2.46}$$

which, combined with Eq. (2.45), gives for the longitudinal response function,

$$\chi^L(\boldsymbol{q}) = \frac{q_i q_j}{q^2} \chi_{ij}(\boldsymbol{q}) = \frac{2}{q^2 \mathcal{Z}} \sum_{n,m} \frac{\mathrm{e}^{-\beta E_n}}{E_n - E_m} \left|\langle n|\boldsymbol{q}.\hat{\boldsymbol{j}}(\boldsymbol{q})|m\rangle\right|^2. \tag{2.47}$$

If particle number is conserved in our system, the continuity equation will be valid. In momentum space this is given by

$$[\hat{H}, \hat{\rho}(\boldsymbol{q})] = -\hbar\boldsymbol{q}.\hat{\boldsymbol{j}}(\boldsymbol{q}), \tag{2.48}$$

which substituted into the longitudinal response function leads to

$$\chi^L(\boldsymbol{q}) = \frac{1}{\hbar^2 q^2 \mathcal{Z}} \sum_n e^{-\beta E_n} \langle n | [\hat{\rho}(\boldsymbol{q}), [\hat{H}, \hat{\rho}^\dagger(\boldsymbol{q})]] | n \rangle. \tag{2.49}$$

The f-sum rule is the energy weighted moment of the structure factor and is given by

$$\hbar^2 \int d\omega \, \omega \, S(\omega, \boldsymbol{q}) = \frac{1}{2} \langle [\hat{\rho}(\boldsymbol{q}), [\hat{H}, \hat{\rho}^\dagger(\boldsymbol{q})]] \rangle = N \frac{\hbar^2 q^2}{2m}. \tag{2.50}$$

Substituting this into the above expression for $\chi^L(\boldsymbol{q})$ leads to an expression for the total density of the system:

$$\rho = m\chi^L(\boldsymbol{q})/A. \tag{2.51}$$

Similarly, the normal density is given by the transverse response function in the long-range limit [30,33]:

$$\rho_n = m\chi^T(\boldsymbol{q} \to \boldsymbol{0})/A, \tag{2.52}$$

and thus, the superfluid fraction can be found by taking the difference between the longitudinal and transverse response functions in this limit:

$$f_s = \frac{\rho_s}{\rho} = \lim_{\boldsymbol{q} \to \boldsymbol{0}} \left(\frac{\chi^L(\boldsymbol{q}) - \chi^T(\boldsymbol{q})}{\chi^L(\boldsymbol{q})} \right). \tag{2.53}$$

Chapter 3

Microcavity-polaritons

Unlike ordinary matter, photons may not form stable fluids as they are massless and interact only very weakly [14]. However, experiments using semiconductor microcavities [65] have established a technique which rectifies this. Photons can acquire a mass when they are trapped in a two-dimensional plane between two mirrors. They may then be brought into resonance with excitons in quantum wells in the cavity, to which they couple strongly, leading to anticrossing and the formation of quasiparticle states called microcavity-polaritons. Due to their excitonic component, polaritons exhibit significant interparticle interactions and may form stable fluids of light.

These cavities cannot trap photons perfectly however, and so polaritonic systems must be pumped continuously with a laser to maintain a steady state. Because of this, they are known as driven-dissipative systems and often polariton decay is fast enough that it prevents thermalisation. As a composite of photons and excitons, polaritons have bosonic exchange symmetry and much research has concentrated on their relationship with Bose-Einstein condensation [15], particularly with respect to how it is affected by their two-dimensional and nonequilibrium nature. Additionally, the topic of polariton superfluids has attracted substantial interest in recent years.

In this chapter, we introduce microcavity-polaritons and their properties. Section 3.1 describes the system and the coupling between cavity-photons and quantum well excitons; Section 3.2 deals with the decay of photons from the cavity and the laser driving required to maintain a steady state; and Sections 3.3 and 3.4 review previous work on condensation and superfluidity in microcavity-polaritons, respectively.

3.1   Strong coupling of photons and excitons

Semiconductor microcavities (see Fig. 3.1) consist of two micron-scale distributed Bragg reflectors (DBRs) which may be used to trap photons in one direction [15]. DBRs, which are typically constructed from cadmium telluride or gallium arsenide, consist of layers of alternating refractive index leading to high quality reflection for wavelengths close to four
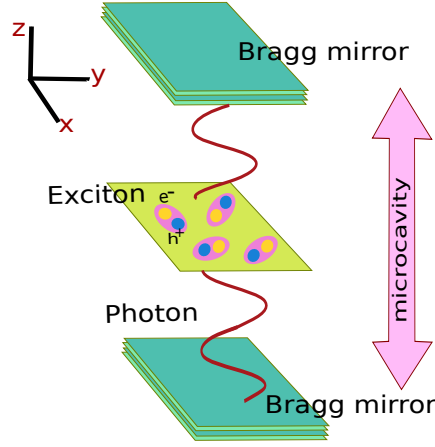
Figure 3.1: Microcavity-polaritons are quasiparticles formed by the strong coupling of photons trapped between two distributed Bragg reflectors and excitons trapped in quantum wells. Polaritons are free to move in the two-dimensional plane perpendicular to their confinement.

times the layer widths. Photons trapped in the cavity are free to move in the two-dimensional plane perpendicular to their confinement, with a dispersion relation given by [16] (from now on we take $\hbar = 1$)

$$\omega_c(\boldsymbol{k}) = \frac{c}{n}\sqrt{q_z^2 + k^2} = \frac{c}{n}\sqrt{\left(\frac{2\pi N}{L_w}\right)^2 + k^2}, \tag{3.1}$$

where c is the speed of light, n the refractive index, k the in-plane momentum, and q_z the momentum in the cavity direction, which is given by the cavity mode N (we will always take $N = 1$) and the cavity size L_w. For small wavevectors, this can be expanded,

$$\omega_c(\boldsymbol{k}) \simeq \omega_c^0 + \frac{k^2}{2m_c}, \tag{3.2}$$

and we see that trapping photons in two-dimensions causes them to acquire a mass, given by $m_c = (n/c)(2\pi N/L_w)$, which is very small compared to that of an electron, $m_c \sim 10^{-4} m_e$, and may be tuned by changing the cavity parameters.

Cavity-photons can be brought in to resonance with Wannier-Mott excitons trapped in two-dimensions in quantum wells in the centre of the cavity. This leads to a coupling between them where, roughly speaking, photons create excitons and vice versa. The coupling is strongest when the quantum wells are located at an antinode of the light mode. The system can be described by a Jaynes-Cummings interaction:

$$\hat{H}_0 = \sum_{\boldsymbol{k}} \omega_c(\boldsymbol{k})\hat{c}_{\boldsymbol{k}}^\dagger \hat{c}_{\boldsymbol{k}} + \sum_{\boldsymbol{k}} \omega_x(\boldsymbol{k})\hat{x}_{\boldsymbol{k}}^\dagger \hat{x}_{\boldsymbol{k}} + \frac{\Omega_R}{2}\sum_{\boldsymbol{k}}\left(\hat{c}_{\boldsymbol{k}}^\dagger \hat{x}_{\boldsymbol{k}} + \hat{x}_{\boldsymbol{k}}^\dagger \hat{c}_{\boldsymbol{k}}\right), \tag{3.3}$$

where $\hat{c}_{\boldsymbol{k}}$ and $\hat{x}_{\boldsymbol{k}}$ are photonic and excitonic operators, respectively, and Ω_R is the Rabi frequency. Here we have made the rotating wave approximation, i.e. there are no antireso-
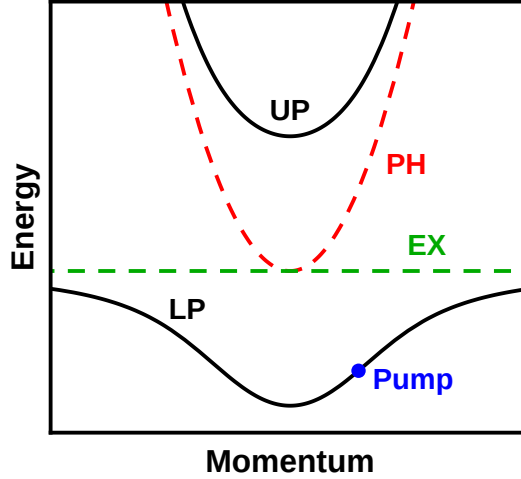
Figure 3.2: The excitonic dispersion (dashed green) is approximately constant compared to the photonic (dashed red) due to the much larger exciton mass. Strong coupling leads to anticrossing and the formation of upper and lower polariton branches (solid black). Polaritons interact because of their excitonic component, while their photonic part causes decay and the need for an external drive. A coherent laser pump resonantly tuned to the polariton dispersion is marked by a blue dot (see Section 3.2). The minimum energy difference between the lower and upper polariton dispersions is given by the Rabi energy.

nant terms like $\hat{c}_{\boldsymbol{k}}\hat{x}_{\boldsymbol{k}}$, which is valid when Ω_R is small compared to the photon and exciton energies[14]. The photonic dispersion (Eq. (3.2)) is parabolic, while the excitonic dispersion, $\omega_x(\boldsymbol{k}) = \omega_x + k^2/2m_x$, can be considered flat by comparison due to excitons having a much higher mass, so we take it to be constant, $\omega_x(\boldsymbol{k}) \simeq \omega_x$.

In the limit of 'strong coupling', where the coupling strength exceeds the damping and lifetime of the particles[66], there is anticrossing (see Fig. 3.2) and we may diagonalise the Hamiltonian in terms of quasiparticle operators $\hat{a}_{UP/LP,\boldsymbol{k}}$, known as upper and lower polaritons:

$$\hat{H}_0 = \sum_{\boldsymbol{k}} \omega_{LP}(\boldsymbol{k})\hat{a}^{\dagger}_{LP,\boldsymbol{k}}\hat{a}_{LP,\boldsymbol{k}} + \sum_{\boldsymbol{k}} \omega_{UP}(\boldsymbol{k})\hat{a}^{\dagger}_{UP,\boldsymbol{k}}\hat{a}_{UP,\boldsymbol{k}}. \tag{3.4}$$

This is not possible for weak coupling strengths as the eigenmodes of the system remain photons and excitons. The diagonalisation is given by the transformation[15,67,68]

$$\begin{pmatrix} \hat{a}_{LP,\boldsymbol{k}} \\ \hat{a}_{UP,\boldsymbol{k}} \end{pmatrix} = \begin{pmatrix} X_{\boldsymbol{k}} & C_{\boldsymbol{k}} \\ -C_{\boldsymbol{k}} & X_{\boldsymbol{k}} \end{pmatrix} \begin{pmatrix} \hat{x}_{\boldsymbol{k}} \\ \hat{c}_{\boldsymbol{k}} \end{pmatrix}, \tag{3.5}$$

where $X_{\boldsymbol{k}}$ and $C_{\boldsymbol{k}}$ are known as the excitonic and photonic Hopfield coefficients, respectively,

$$X_{\boldsymbol{k}} = \frac{\omega_{LP}(\boldsymbol{k}) - \omega_c(\boldsymbol{k})}{\sqrt{(\omega_{LP}(\boldsymbol{k}) - \omega_c(\boldsymbol{k}))^2 + \Omega_R^2/4}}, \tag{3.6}$$

$$C_{\boldsymbol{k}} = -\frac{\Omega_R}{2\sqrt{(\omega_{LP}(\boldsymbol{k}) - \omega_c(\boldsymbol{k}))^2 + \Omega_R^2/4}}, \qquad (3.7)$$

which obey the relation $|C_{\boldsymbol{k}}|^2 + |X_{\boldsymbol{k}}|^2 = 1$. The upper and lower polaritons have distinct dispersion relations given by

$$\omega_{UP/LP}(\boldsymbol{k}) = \frac{1}{2}\left(\omega_x - \omega_c(\boldsymbol{k}) \pm \sqrt{(\omega_x - \omega_c(\boldsymbol{k})^2 + \Omega_R^2}\right). \qquad (3.8)$$

In what follows we recognise that the energies we are interested in are all much smaller than Ω_R, and therefore we neglect the upper polaritons (we will now write $\hat{a}_{LP,\boldsymbol{k}} = \hat{a}_{\boldsymbol{k}}$).

Excitonic interactions in the system, which at low momenta are dominated by the short-range exchange of electrons between excitons[16], can be modelled as a weak contact interaction between polaritons:

$$\hat{H}_{int} = \frac{V}{2}\sum_{\boldsymbol{k},\boldsymbol{k}',\boldsymbol{q}} \hat{a}_{\boldsymbol{k}-\boldsymbol{q}}^{\dagger}\hat{a}_{\boldsymbol{k}'+\boldsymbol{q}}^{\dagger}\hat{a}_{\boldsymbol{k}}\hat{a}_{\boldsymbol{k}'}, \qquad (3.9)$$

where V is the interaction strength. We see also that combining the Hamiltonians $\hat{H}_0 + \hat{H}_{int}$ from Eqs. (3.4) and (3.9) gives the Hamiltonian for a weakly interacting Bose gas.

3.2   Drive and decay

Due to photons leaking from the microcavity, polaritons decay on a timescale of around 5ps[69]. This process can be described in the Hamiltonian by a coupling to a decay bath[68,70]:

$$\hat{H}_{bath} = \sum_{\boldsymbol{p}} \omega_A(\boldsymbol{p})\hat{A}_{\boldsymbol{p}}^{\dagger}\hat{A}_{\boldsymbol{p}} + \sum_{\boldsymbol{k},\boldsymbol{p}} \zeta_{\boldsymbol{k},\boldsymbol{p}}(\hat{a}_{\boldsymbol{k}}^{\dagger}\hat{A}_{\boldsymbol{p}} + \hat{A}_{\boldsymbol{p}}^{\dagger}\hat{a}_{\boldsymbol{k}}), \qquad (3.10)$$

where $\zeta_{\boldsymbol{k},\boldsymbol{p}}$ is the coupling between the polaritons and the bath modes $\hat{A}_{\boldsymbol{p}}$, and $\omega_A(\boldsymbol{p})$ is the dispersion of these modes. Energy and momentum are conserved during polariton decay, allowing the polariton dispersion, lineshape, and coherence properties to be inferred from measurements of the emitted photons. As the rate of decay is often faster than thermalisation, these systems tend to be out-of-equilibrium and have no clearly defined temperature or chemical potential.

To maintain a steady state given this decay, polaritons must be pumped with a laser. Broadly speaking, there are two different ways of achieving this. Incoherent, or non-resonant, pumping, involves the driving laser being tuned to high energies far from the lower polariton dispersion. The injected particles create high energy excitons which relax via phonon emission and absorption, as well as recombining into photons, eventually forming lower polaritons[71]. Alternatively, the system may be pumped coherently, i.e. resonantly or near-resonantly with the lower polariton dispersion, directly creating polaritons that inherit the

coherence of the laser pump. The momentum k_p of the coherently generated polaritons is set by the angle θ at which the laser is incident on the system through the equation, $k_p = (\omega_p/c)\sin\theta$, where ω_p is the pump frequency and c the speed of light. We can describe coherent pumping by introducing a term to the Hamiltonian[68],

$$\hat{H}_{pump} = \frac{1}{\sqrt{2}}(F_p(t)\hat{a}_{\boldsymbol{k}_p}^\dagger + F_p^*(t)\hat{a}_{\boldsymbol{k}_p}), \qquad (3.11)$$

where $F_p(t)$, the amplitude of the pump, is given by $F_p(t) = F_p\mathrm{e}^{-i\omega_p t}$, and without loss of generality we may select the pump momentum to be in the x-direction, $\boldsymbol{k}_p = (k_p, 0)$. Combining Eqs (3.4), (3.9), (3.10), and (3.11), and performing a gauge transformation to remove the time-dependence,

$$\hat{a} \to \hat{a}\mathrm{e}^{-i\omega_p t}, \qquad\qquad \hat{A} \to \hat{A}\mathrm{e}^{-i\omega_p t}, \qquad (3.12)$$

we can write the full Hamiltonian for coherently pumped polaritons as

$$\begin{aligned}
\hat{H} &= \sum_{\boldsymbol{k}} \omega_{LP}(\boldsymbol{k} + \boldsymbol{k}_p)\hat{a}_{\boldsymbol{k}}^\dagger \hat{a}_{\boldsymbol{k}} + \frac{V}{2}\sum_{\boldsymbol{k},\boldsymbol{k}',\boldsymbol{q}} \hat{a}_{\boldsymbol{k}-\boldsymbol{q}}^\dagger \hat{a}_{\boldsymbol{k}'+\boldsymbol{q}}^\dagger \hat{a}_{\boldsymbol{k}} \hat{a}_{\boldsymbol{k}'} + \frac{F_p}{\sqrt{2}}(\hat{a}_{\boldsymbol{0}}^\dagger + \hat{a}_{\boldsymbol{0}}) \\
&\quad + \sum_{\boldsymbol{p}} \omega_A(\boldsymbol{p} + \boldsymbol{k}_p)\hat{A}_{\boldsymbol{p}}^\dagger \hat{A}_{\boldsymbol{p}} + \sum_{\boldsymbol{k},\boldsymbol{p}} \zeta_{\boldsymbol{k},\boldsymbol{p}}(\hat{a}_{\boldsymbol{k}}^\dagger \hat{A}_{\boldsymbol{p}} + \hat{A}_{\boldsymbol{p}}^\dagger \hat{a}_{\boldsymbol{k}}),
\end{aligned} \qquad (3.13)$$

where the momenta have been resummed to be with respect to the pump, $\boldsymbol{k} \to \boldsymbol{k} + \boldsymbol{k}_p$, and we write $\hat{a}_{\boldsymbol{k}}$ to mean $\hat{a}_{\boldsymbol{k}+\boldsymbol{k}_p}$ for brevity.

One advantage of polaritonic systems is their versatility. For instance, it is possible to tune the interaction strength by changing the detuning between the photons and excitons and the density by changing the pump power[69].

3.3 Polariton condensation

Bose-Einstein condensation was first definitively observed 70 years after it was originally predicted[49], with part of the difficultly stemming from achieving extremely cold transition temperatures ($\sim$ 170nK in rubidium-87). The critical temperature for BEC is inversely proportional the particle mass, $T_c \sim 1/m$ (Eq. (2.30)), so due to their extremely low mass polaritons, which have bosonic exchange symmetry, should permit the study of condensation at relatively high temperatures. That being said, BEC was originally proposed for infinite three-dimensional systems in thermal equilibrium, whereas polaritons are two-dimensional with finite lifetime and size. How these complications affect condensation in polaritonic systems has been the subject of much experimental and theoretical work, which we review here.

3.3.1   Incoherent pumping

Early experiments on incoherently pumped polaritons saw stimulated scattering effects [66] and eventually observations of a massively occupied ground state and increased spatial and temporal coherence were made at 19K and high densities [36]. Interestingly, these results were taken to be evidence of Bose-Einstein condensation despite the two-dimensional nature of the system, because the finite size of the pump spot was sufficiently small for complete coherence across the cloud of polaritons. In this case, density rather than temperature was used as the tuning parameter of the phase transition.

While coherent states of light naturally draw comparisons with lasing, a polariton condensate has stronger interactions and does not require population inversion. Further experiments elucidated this difference by confining polaritons in a harmonic trap [72]. Previous observations of condensation had occurred inside the region excited by the laser, whereas here the polaritons were created outside the centre of the trap before moving into it and condensing away from the excitation area.

The first-order correlation function of an incoherently pumped condensate was measured and found to follow the power law distribution expected of a two-dimensional system [73]. This was in contrast to previous claims of full BEC, and the discrepancy was explained as being a result of a highly disordered sample in the earlier experiment. However, a theoretical analysis [74] found that true algebraic order is impossible in the long-range limit as the nonequilibrium nature of polaritonic systems leads to a nonlinearity in the Kardar-Parisi-Zhang (KPZ) equation for the polariton phase. Above a certain length scale, too large to be seen in current experiments, the decay becomes a stretched exponential instead. Further studies [26,75], which included vortices by using a duality mapping between the KPZ equation and a theory of nonlinear electrodynamics coupled to charges, identified a further, astronomically large, length scale above which vortex-antivortex pairs unbind and all remaining order in the system is destroyed. It was noted that this transition is distinct to the BKT transition.

Remarkably, observations have been made of polariton condensation at room temperature in microcavities containing organic molecules [76]. This occurs because organic semiconductors host Frenkel excitons with high binding energies compared to the Wannier-Mott excitons in conventional semiconductors.

3.3.2   Coherent pumping

In contrast to incoherently driven systems, pumping coherently, by which we mean resonantly or near-resonantly with the lower polariton dispersion, can create a macroscopically occupied state directly at the pump energy and momentum [39,40]. This state is not a condensate in the usual sense because there is no phase transition and no spontaneous symmetry

breaking – the macroscopic state inherits its phase directly from the external pump. Additionally, the complications arising from the KPZ nonlinearity in the incoherently pumped case[74] do not apply here as, due to the fixed phase, there is a gapped excitation spectrum and a mass term in the KPZ equation which dominates over the nonlinear term in the long-range limit. The lack of phase freedom also inhibits the formation of vortices[14], which cannot therefore destroy the macroscopic state either.

There are two significant circumstances where the macroscopic state created by the pump becomes unstable. First, if the pump is sufficiently blue-detuned away from the polariton dispersion, there is a Kerr instability and the system becomes bistable[16]. In this regime, there are two metastable solutions to the mean-field equations, referred to as bright and dark states on account of their occupations, $n_p = \left| \langle \hat{\psi} \rangle \right|^2$, which are related by a hysteresis curve on which there is also a third, unstable solution (see Section 5.4).

Secondly, if the macroscopic pump state is created at the inflection point of the lower polariton dispersion (sometimes referred to as the 'magic' angle[77]), then above a certain driving strength threshold the pump state becomes unstable to parametric scattering into two new states, a 'signal' at low momentum and an 'idler' at high momentum, which both become macroscopically occupied[78] (see Fig. 3.3). This process is called optical parametric oscillation (OPO). Not only are these new states related by their momenta, $\boldsymbol{k}_s = 2\boldsymbol{k}_p - \boldsymbol{k}_i$, but they also share an equal and opposite phase shift from the pump state[68]. Significantly, this phase shift is free to be chosen and the system undergoes spontaneous symmetry breaking as it goes through the OPO phase transition. Simulations have shown that this
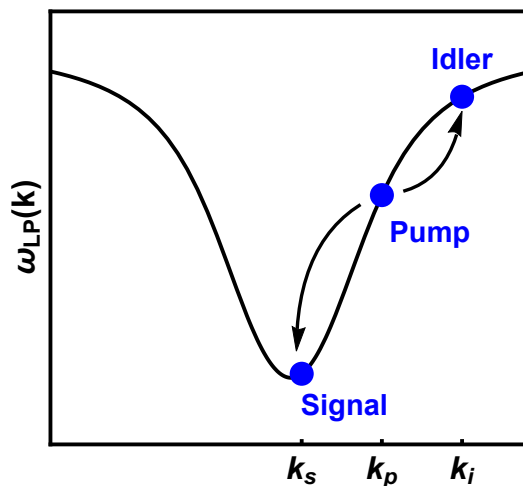
Figure 3.3: If polaritons are injected coherently at the inflection point ('magic' angle) of the lower polariton dispersion and above a certain power threshold, parametric scattering occurs out of the pump state and into two new macroscopically occupied 'signal' and 'idler' states in a process known as optical parametric oscillation (OPO). The new states have momenta related by $\boldsymbol{k}_s = 2\boldsymbol{k}_p - \boldsymbol{k}_i$ and share an equal and opposite phase shift from the pump state which, significantly, is chosen spontaneously leading to a gapless Goldstone mode in the excitation spectrum[68].

transition involves a vortex binding-unbinding mechanism that resembles the equilibrium BKT transition, albeit where the quasiordered phase can have a larger power law decay exponent[79].

While the aforementioned theoretical analysis of vortex pair unbinding using the KPZ equation[26] identified a length scale above which order is destroyed that is far too big to apply to real systems, it has been suggested that this length scale may be much smaller for polaritons in the OPO regime[80].

3.4   Polariton superfluidity

Of central importance to the question of whether polaritons can form superfluids is the effect on the system of driving and decay. Notably, these processes lead to excitation spectra which are complex and heavily dependent on the pumping scheme. Incoherently pumped condensates and the 'signal' state in coherently pumped systems above the OPO threshold exhibit spontaneous symmetry breaking and have gapless excitation spectra containing Goldstone modes[38,81,82]. However, these spectra are diffusive, i.e. they are flat, and do not fulfil the Landau criterion. In coherently pumped systems below the OPO threshold, the condensate phase is locked to the pump and the excitation spectrum is gapped[83], suggesting that the low energy behaviour of the system may be different to a conventional superfluid with a gapless spectrum. While for a particular detuning the real part of the complex spectrum fulfils the Landau criterion[84], it is not clear how this condition, which was formulated for equilibrium systems with entirely real excitation spectra, applies in the case of imaginary excitation energies. Here, we review experimental and theoretical studies into these questions. Tables 3.1 and 3.2 provide summaries of these findings.

3.4.1   Incoherent pumping

Theoretical studies of the excitation spectrum in incoherently pumped systems using Keldysh field theory[37] and the Gross-Pitaevskii equation (GPE)[38] found that it is complex and diffusive, with a Goldstone mode present as a signature of spontaneous breaking of phase symmetry. While this spectrum does not fulfil the Landau criterion, a separate study at the mean-field level using the GPE[22] found a sharp onset of fringes in the density profile associated with a critical flow velocity and developed a generalised Landau criterion in terms of the complex wavevector to explain this finding. At present, flow without friction is experimentally uninvestigated in incoherently pumped systems.

A calculation of the superfluid density of incoherently pumped polaritons was made using a Keldysh path integral technique to find the longitudinal and transverse static current-current response functions[23]. It was found that superfluidity can survive in driven-

dissipative systems, but that the superfluid fraction can never be 100% as there is always a normal component due to driving and decay. Crucial to this analysis was the fact that the response functions have the same poles as the Green's functions of the system [27], which are given by the excitation spectrum. Despite not fulfilling the Landau criterion, the gapless excitation spectrum causes singular behaviour in these functions in the long-range limit, which in turn leads to a difference between the longitudinal and transverse responses. The superfluid density was found to survive even in the context of a stretched exponential decay of correlations [85], although it may be destroyed by vortex-antivortex unbinding in very large systems [26].

The effect of disorder on superfluidity was analysed using the GPE in a calculation of the superfluid stiffness [24], where this was defined as the change in energy due to a phase twist imposed across the system. It was concluded that, even for weak disorder, superfluidity is destroyed in the thermodynamic limit. Further investigations into the effects of disorder using the GPE [25] found that the superfluid and normal fractions, as defined by the response to a vector potential, are physically meaningless in disordered non-equilibrium systems. Indeed, it was shown that at the mean-field level these fractions no longer add up to one and may even be negative.

The formation of pinned quantised vortices has been experimentally observed [21] where, unlike in atomic condensates, they appeared spontaneously without stirring. However, this observation was not taken in and of itself to be evidence of 'conventional' superfluidity. Simulations of an incoherently pumped system using a stochastic classical field model [86] discovered that vortices seeded by an additional coherent laser persist for longer than the lifetime of the excess density introduced by that laser. This suggests that vortices present in the condensate are metastable, a feature characteristic of topological defects in superfluids.

3.4.2 Optical parametric oscillation (OPO)

In a coherently pumped system above the threshold of optical parametric oscillation, where the pump state is unstable to parametric scattering into 'signal' and 'idler' states, an experimental investigation [20] discovered that it was possible to create metastable persistent superflows by injecting vortices into the signal state. This was taken as evidence of superfluidity as, unlike a classical flow that dies away after it ceases to be stirred, the observed vorticity persisted for as long as it could be measured. Another experimental study [87] found that imprinting a vortex on the signal state leads to the formation of an antivortex in the idler as a result of angular momentum conservation in the parametric scattering process. Simulations using the GPE with weak noise [88] found that stable vortices form spontaneously in the signal and, additionally, that metastable vortex states could be created by the application of an external laser pulse.

It is possible to select the in-plane momentum of the signal state by triggering OPO with a pulsed laser at the desired idler momentum. An experimental investigation of the signal state in a triggered OPO system[18] observed dissipationless flow against defects present in the microcavity when the signal travels below a critical velocity. Another investigation, in this case without a trigger pulse, involving experiments, simulations, and theoretical calculations[19] also showed the signal state flowing past defects without dissipation, in contrast to the pump and idler states.

3.4.3 Coherent pumping (below the OPO threshold)

A consequence of external phase fixing in coherently pumped systems below the OPO threshold is that topological features such as solitons and vortices cannot occur spontaneously[14]. However, if the pump is finite in space or time, then the phase of the macroscopic state will be free to evolve outside of it. For instance, it has been shown experimentally and theoretically that a defect outside the pump spot may generate vortices and solitons[89,90], as can a defect in a system pumped with a pulsed laser[91], or one in a system where a support field is used alongside the main drive[92].

Theoretical studies[83,84] have analysed the gapped excitation spectrum and shown that it changes depending on the detuning. Notably, when the system is blue-detuned away from the bare polariton dispersion but in resonance with the interactions-renormalised dispersion,
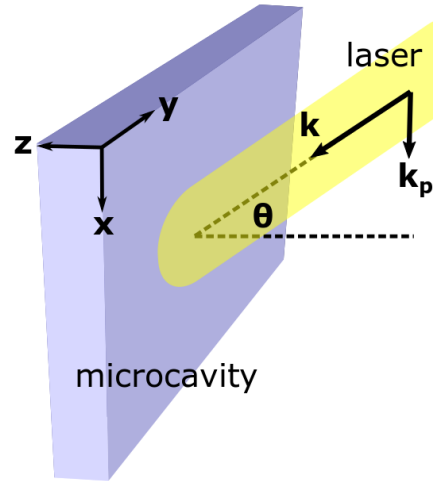
Figure 3.4: The microcavity can be pumped coherently with an incident beam of momentum k at an angle θ to the direction of confinement (z-direction), leading to a macroscopic state with in-plane momentum $k_p = k \sin \theta$ (taken generally in the x-direction). This set-up is naturally suited to measuring flow against a defect, as the condensate has finite velocity and the pump spot can be trained onto a natural defect formed during the construction of the cavity. A notable experiment[17] employing this procedure observed the suppression of scattering when the detuning was at the shifted resonance point, where the real part of the spectrum is linear, and saw scattering return in the form of Cherenkov waves when k_p/m exceeded the speed of sound (i.e. the gradient of the real part of the spectrum).

$\Delta_p = \omega_p - \omega_{LP}(\boldsymbol{k}_p) - V|\psi_0| = 0$, which we call the shifted resonance point, the real part of
the dispersion becomes linear at small momenta, resembling the Bogoliubov dispersion (see
Chapter 5). Unlike the diffusive spectra in the incoherently pumped and OPO cases, the
real part of this spectrum fulfils the Landau criterion for dissipationless flow.

Because coherently pumped polaritons can be created with a finite momentum k_p (see
Fig. 3.4), it is possible to train the pump spot onto a defect in the semiconductor and observe
whether the polaritons scatter as they flow past. This idea was tested experimentally for a
continuous and homogeneous pump[17], where for a given detuning the real and momentum
space images of the condensate were measured as the pump power was increased. It was
found that for detuning above the shifted resonance point (i.e. low powers) there were density
modulations past the defect and a scattering ring in momentum space, yet as the power was
tuned into the shifted resonance, where the real part of the excitation spectrum becomes
linear, these disappeared and the flow was seen to be dissipationless. These findings, which
agreed with theoretical calculations of the photon emission made by taking linear fluctuations
on top of the GPE[84], were taken as evidence of superfluidity. Furthermore, for flows faster
than the speed of sound, given by the slope of the real part of the excitation spectrum,
scattering returned in the form of Cherenkov radiation, as would be expected for a system
fulfilling the Landau criterion. However, given the fixed phase and gapped imaginary part of
the spectrum, questions remain about whether this is simply evidence of a very low viscosity
fluid rather than a superfluid. Suppression of scattering past a defect has also been shown in
an organic microcavity at room temperature[93], albeit in this case for a pulsed drive allowing
the phase of the system to subsequently evolve freely.

Theoretical studies of the drag force for polaritons flowing past a defect[29,94] found that
the crossover in drag between the suppressed scattering regime and the viscous regime above
the speed of sound is smoother than in equilibrium superfluids. Additionally, there is always
a residual drag component dependent on the polariton lifetime, suggesting that observations
of drastically reduced scattering were of nearly, rather than perfect, dissipationless flow.

This thesis investigates superfluidity in coherently driven polaritons, where the pump is
continuous and homogeneous and below the OPO threshold, by calculating the longitudinal
and transverse static current-current response functions and taking the difference. We find
in Chapter 7 that these response functions are equal, so the system is not a superfluid, and
that at zero pump momentum it forms a rigid state that does not respond to either type of
perturbation.

Table 3.1: Theoretical superfluid properties in different systems

System	No viscosity	Landau criterion	SSB	No transverse response	Quantised vortices	Persistent flow
Helium/ Cold atoms	Yes	Yes	Yes	Yes	Yes	Yes
Polaritons (incoherent)	Yes	No	Yes	Yes	Yes	Yes
Polaritons (OPO)	Yes	No	Yes	?	Yes	Yes
Polaritons (coherent)	Yes	Real part	No	?*	Injected	n/a

Table 3.2: Experimental observations of superfluid properties in different systems

System	No viscosity	No transverse response	Quantised vortices	Persistent flow
Helium/ Cold atoms	Yes	Yes	Yes	Yes
Polaritons (incoherent)	?	?	Yes	?
Polaritons (OPO)	Yes	?	Yes	Yes
Polaritons (coherent)	Yes	?	Injected	n/a

Superfluidity refers to a set of flow properties occurring in conjunction[6], and macroscopic states in polaritonic systems do not necessarily share all of those exhibited by equilibrium superfluids like helium or cold atoms. Furthermore, the properties of polaritons depend on the way they are pumped, which is indicated here in the system columns in parentheses. Not all these properties have yet had their presence or absence established theoretically and/or experimentally, which we denote with question marks. Here, 'coherent' refers to a continuous and homogenous pump below the OPO threshold, and we note that for these rows: 'Real part' refers to complex excitation spectrum and the fact that the real, but not imaginary, part fulfils the Landau criterion; 'Injected' refers to the fact that vortices can be injected via the pump, but cannot form spontaneously; and 'n/a' refers to the fact that if the phase of the macroscopic state is fixed by the pump the concept of persistent flow is ill-defined. SSB is an abbreviation of spontaneous symmetry breaking.

*The calculation of the longitudinal and transverse responses of coherently pumped polaritons is the topic of this thesis. Unlike in superfluids, these are found to be equal and, at $k_p = 0$, they are both zero suggesting the formation of a rigid state that does not respond to either type of perturbation. For more details, see Chapter 7.

Chapter 4

Keldysh Green's functions

For a differential equation of the form, $\hat{L}\phi(x) = J(x)$, where $\hat{L}$ is a linear differential operator and $J(x)$ is a source term, the solution can be written as

$$\phi(x) = \int dx' \, D(x - x')J(x'). \tag{4.1}$$

Here, the function $D(x - x')$ is called a propagator: it weights the contribution of the source at all points x' to the solution at x. For this to be a solution, the propagator must obey the relation

$$\hat{L} \, D(x - x') = \delta(x - x'), \tag{4.2}$$

which is the mathematical definition of a Green's function[95]. In many-body physics, the term Green's function is used to refer to the 2-point correlation function[59,63], for example,

$$D(x, x') = -i\langle T[\hat{\phi}(x)\hat{\phi}^\dagger(x')]\rangle, \tag{4.3}$$

where $x = (t, \boldsymbol{x})$ and T is the time-ordering operator. A number of different types of Green's function can be defined and we should note that the terminology is still widely used even when the system is not linear and the original mathematical definition does not apply.

Green's functions give the spectrum of excitations of the system through their poles[96], and we can use this to study superfluidity. The excitation spectrum of a system can be used to explain dissipationless flow in equilibrium superfluids via the Landau criterion (Section 2.3), and we have seen how this picture becomes more complicated in driven-dissipative systems due to the complex nature of the spectrum (Section 3.4). Additionally, the poles of the finite frequency response function, $\chi_{ij}(\omega, \boldsymbol{q})$, are the same as for the single particle Green's function[27], which may affect the calculation of the longitudinal and transverse responses in the static, long-range limit (Section 2.6).

Green's functions can be calculated using path integral techniques. However, for non-equilibrium systems such as microcavity-polaritons that have a distribution set by the drive

and decay, equilibrium methods such as an imaginary time approach are insufficient. Keldysh field theory can be used to get around this problem and treat systems with arbitrary distributions [97].

In this chapter, we explain and apply concepts for calculating non-equilibrium Green's functions which will be used to find the excitation spectrum and static current-current response function of coherently driven polaritons in Chapters 5 and 6, respectively. Section 4.1 shows how to derive the Green's functions of a system through an equilibrium path integral technique; Section 4.2 extends this to non-equilibrium systems using Keldysh field theory; and Sections 4.3 and 4.4 derive the retarded, advanced, and Keldysh Green's functions for coherently pumped polaritons.

4.1   Path integrals

The correlation function $\langle \hat{\phi}(t)\hat{\phi}^\dagger(t') \rangle$, which we refer to as a Green's function, gives the overlap between the fields at t and t' averaged over the rest of the system. In thermal equilibrium, this is given by a trace over the quantum Gibbs distribution [59]:

$$\langle \hat{\phi}(t)\hat{\phi}^\dagger(t') \rangle = \frac{\mathrm{Tr}\left\{ e^{-\beta(\hat{H}-\mu\hat{N})}\hat{\phi}(t)\hat{\phi}^\dagger(t') \right\}}{\mathrm{Tr}\left\{ e^{-\beta(\hat{H}-\mu\hat{N})} \right\}}. \tag{4.4}$$

To calculate this, we wish to reformulate the above expression in terms of path integrals, i.e.,

$$\langle \hat{\phi}(t)\hat{\phi}^\dagger(t') \rangle = \frac{\int \mathcal{D}(\bar{\phi},\phi)\, \phi(t)\bar{\phi}(t') e^{iS[\bar{\phi},\phi]}}{\int \mathcal{D}(\bar{\phi},\phi) e^{iS[\bar{\phi},\phi]}}. \tag{4.5}$$

We start by writing the partition function as a trace over states of definite particle number, $|n\rangle$:

$$\mathcal{Z} = \mathrm{Tr}\left\{ e^{-\beta\hat{H}} \right\} = \sum_n \langle n| e^{-\beta\hat{H}} |n\rangle, \tag{4.6}$$

where for brevity we have written $\hat{H} - \mu\hat{N} \to \hat{H}$. Here, the Hamiltonian $\hat{H} = \hat{H}(\hat{a}^\dagger, \hat{a})$ is a function of bosonic creation and annihilation operators. The eigenstates of these operators are known as coherent states, and are defined by

$$|\phi\rangle = |0\rangle + \phi|1\rangle + \phi^2|2\rangle + ... = e^{\phi\hat{a}^\dagger}|0\rangle. \tag{4.7}$$

In this basis, the resolution of the identity is

$$|\phi\rangle = \int d(\bar{\phi},\phi) e^{-|\phi|^2} |\phi\rangle\langle\phi|, \tag{4.8}$$

and we can use this to rewrite the partition function as

$$\mathcal{Z} = \sum_n \int d(\bar{\phi}, \phi) e^{-|\phi|^2} \langle n|\phi\rangle \langle \phi| e^{-\beta \hat{H}} |n\rangle = \int d(\bar{\phi}, \phi) e^{-|\phi|^2} \langle \phi| e^{-\beta \hat{H}} |\phi\rangle. \quad (4.9)$$

Noting the similarity between the exponent $e^{-\beta \hat{H}}$ and the operator for unitary time evolution, $e^{-i\hat{H}t}$, we can define an imaginary time variable $\tau = it$ as $\tau = \beta$. To build a path integral, we discretise τ into N steps $\delta\tau$,

$$\mathcal{Z} = \int d(\bar{\phi}, \phi) e^{-|\phi|^2} \langle \phi| e^{-\delta\tau \hat{H}} e^{-\delta\tau \hat{H}} ... e^{-\delta\tau \hat{H}} |\phi\rangle, \quad (4.10)$$

and insert a resolution of the identity in-between each factor of $e^{-\delta\tau \hat{H}}$. Using numbered subscripts to denote the discrete timesteps and periodic boundary conditions $\phi_0 = \phi_N$, we get

$$\mathcal{Z} = \prod_{i=1}^{N} \int d(\bar{\phi}_i, \phi_i) e^{-|\phi_i|^2} \langle \phi_N| e^{-\delta\tau \hat{H}} |\phi_{N-1}\rangle \langle \phi_{N-1}| e^{-\delta\tau \hat{H}} ... |\phi_1\rangle \langle \phi_1| e^{-\delta\tau \hat{H}} |\phi_0\rangle. \quad (4.11)$$

Resolving for the eigenvalues, $\langle \phi_j| \hat{H}(\hat{a}^\dagger, \hat{a}) |\phi_i\rangle = \langle \phi_j| H(\bar{\phi}_j, \phi_i) |\phi_i\rangle$, and noting that the overlap between coherent states is given by

$$\langle \phi_i|\phi_j\rangle = e^{\bar{\phi}_i \phi_j}, \quad (4.12)$$

the partition function becomes

$$\mathcal{Z} = \prod_{i=1}^{N} \int d(\bar{\phi}_i, \phi_i) \exp\left[-\delta\tau \sum_{i=0}^{N} \left(\phi_i \frac{\bar{\phi}_i - \bar{\phi}_{i+1}}{\delta\tau} + H(\bar{\phi}_{i+1}, \phi_i) \right) \right]. \quad (4.13)$$

If we take $\delta\tau \to 0$ and $N \to \infty$, this expression tends to a path integral:

$$\mathcal{Z} = \int \mathcal{D}(\bar{\phi}, \phi) \exp\left[-\int d\tau \left(\bar{\phi} \partial_\tau \phi + H(\bar{\phi}, \phi) \right) \right] \quad (4.14)$$

$$= \int \mathcal{D}(\bar{\phi}, \phi) \exp\left[-S_E[\bar{\phi}, \phi] \right], \quad (4.15)$$

where $\phi = \phi(\tau)$, $\int \mathcal{D}(\bar{\phi}, \phi) = \lim_{N \to \infty} \prod_{i=1}^{N} \int d(\bar{\phi}_i, \phi_i)$, and $S_E[\bar{\phi}, \phi]$ is the Euclidean action.

4.1.1 Gaussian integrals

To relate the path integral to the Green's functions of the system, we note that we may write it as a complex Gaussian functional integral:

$$\mathcal{Z} = \int \mathcal{D}(\bar{\phi}, \phi) \exp\left[-\int \int d\tau d\tau' \bar{\phi}(\tau) \hat{A}^{-1}(\tau, \tau') \phi(\tau') \right], \quad (4.16)$$

where $\hat{A}^{-1}$ is the inverse of some differential operator. The general form of this kind of integral is given by[59]

$$
\begin{aligned}
I[\bar{J}, J'] \quad = \quad & \int \mathcal{D}[\bar{\phi}, \phi] \exp\left[-\int\int d\tau d\tau' \bar{\phi}(\tau)\hat{A}^{-1}(\tau, \tau')\phi(\tau') \right. \\
& \left. + \int d\tau (\bar{J}(\tau)\phi(\tau) + \bar{\phi}(\tau)J'(\tau)) \right] \\
& \propto (\det[\hat{A}^{-1}])^{-1} \exp\left[\int d\tau d\tau' \bar{J}(\tau)\hat{A}(\tau, \tau')J'(\tau') \right] .
\end{aligned}
\tag{4.17}
$$

where we include fields $J(\tau)$ and $J'(\tau)$, generally known as source fields. By differentiating with respect to the source fields, we can calculate correlation functions:

$$
D(\tau, \tau') = \langle \phi(\tau)\bar{\phi}(\tau') \rangle = \frac{1}{I[0,0]} \frac{d^2 I[\bar{J}, J']}{d\bar{J}(\tau)dJ'(\tau')}\bigg|_{\bar{J}=J'=0} = A(\tau, \tau'),
\tag{4.18}
$$

and we see that the Green's function of a system represented by the path integral in Eq. (4.16) is $A(\tau, \tau')$. Indeed, for this integral to be valid, $\hat{A}^{-1}$ must be a linear operator, so its inverse will be a Green's function.

4.2 Keldysh field theory

The imaginary time path integral derived in Section (4.1) requires that the system is in thermodynamic equilibrium, which can be seen from the Gibbs distribution in Eq. (4.6). Coherently pumped microcavity-polaritons are in general out-of-equilibrium, and so we must modify our approach. One technique for dealing with arbitrary distributions is called Keldysh field theory[59,97]. Given the time evolution operator,

$$
\hat{U}_{t,t'} = \exp\left(-i\hat{H}(t - t') \right),
\tag{4.19}
$$

we define the partition function in terms of some initial density matrix $\hat{\rho}_0$ as

$$
\mathcal{Z} = \frac{\text{Tr}\{\hat{U}_{\mathcal{C}}\hat{\rho}_0\}}{\text{Tr}\{\hat{\rho}_0\}},
\tag{4.20}
$$

where

$$
\hat{U}_{\mathcal{C}} = \hat{U}_{-\infty,+\infty}\hat{U}_{+\infty,-\infty} = \exp\left(-i\oint_{\mathcal{C}} \hat{H} dt \right).
\tag{4.21}
$$

Here, the contour $\mathcal{C}$ starts at $t = -\infty$ and runs out to $t = +\infty$ before running back to $t = -\infty$ again (see Fig. 4.1). Assuming the fields are the same on both branches of the contour, we have that $\mathcal{Z} = 1$.

To construct a path integral, we follow the prescription from the previous section and
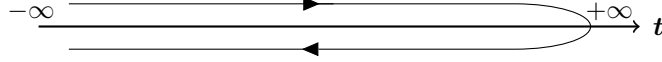
Figure 4.1: The forwards branch of the Keldysh time contour starts at $t = -\infty$ and evolves to $t = +\infty$, before the backwards branch evolves from there back to $t = -\infty$.

rewrite the partition function in terms of states of definite particle number, $|n\rangle$:

$$\mathcal{Z} = \mathcal{Z}_0^{-1} \sum_n \langle n|\hat{U}_\mathcal{C}\hat{\rho}_0|n\rangle, \tag{4.22}$$

where $\mathcal{Z}_0 = \text{Tr}\{\hat{\rho}_0\}$, and partition the time contour into positive and negative real time slices $\pm\delta t$:

$$\mathcal{Z} = \mathcal{Z}_0^{-1} \sum_n \langle n|e^{i\hat{H}\delta t}...e^{i\hat{H}\delta t}\mathbb{1}e^{-i\hat{H}\delta t}...e^{-i\hat{H}\delta t}\hat{\rho}_0|n\rangle. \tag{4.23}$$

Inserting resolutions of the identity over coherent states $|\phi_i\rangle$, where i runs from $t = 0$ to $t = 2N$ and $\phi_0 = \phi_{2N}$, leads to the expression:

$$
\begin{aligned}
\mathcal{Z} &= \mathcal{Z}_0^{-1} \sum_{i=1}^{2N} \int d(\bar{\phi}_i, \phi_i)e^{-|\phi_i|^2} \langle\phi_{2N}|e^{i\hat{H}\delta t}|\phi_{2N-1}\rangle...\langle\phi_{N+2}|e^{i\hat{H}\delta t}|\phi_{N+1}\rangle \\
&\quad \times \langle\phi_{N+1}|\mathbb{1}|\phi_N\rangle\langle\phi_N|e^{-i\hat{H}\delta t}|\phi_{N-1}\rangle...\langle\phi_2|e^{-i\hat{H}\delta t}|\phi_1\rangle\langle\phi_1|\hat{\rho}_0|\phi_0\rangle.
\end{aligned} \tag{4.24}
$$

To illustrate this, consider the simple case of bosons occupying a single energy level, $\hat{H} = \omega_0\hat{a}^\dagger\hat{a}$, and where the initial distribution is thermal. Collecting terms together, the action is given by

$$S[\bar{\phi}, \phi] = \sum_{j=2}^{2N} \delta t_j \left(i\bar{\phi}_j \frac{\phi_j - \phi_{j-1}}{\delta t_j} - \omega_0\bar{\phi}_j\phi_{j-1}\right) + i\bar{\phi}_1\left(\phi_1 - i\rho(\omega_0)\phi_{2N}\right), \tag{4.25}$$

where $\delta t_j = \pm\delta t$ depending on the branch, and $\rho(\omega_0) = e^{-\beta\omega_0}$. We must be careful however not to immediately take the continuum limit, $\delta t \to 0$ and $N \to \infty$, as this removes the term dependent on $\rho(\omega_0)$. Instead, we examine the discrete Green's function given by

$$\langle\phi_j\bar{\phi}_{j'}\rangle = \int \mathcal{D}(\bar{\phi}, \phi)\phi_j\bar{\phi}_{j'} \exp\left(i\sum_{l,l'}^{2N} \bar{\phi}_l D_{ll'}^{-1}\phi_{l'}\right), \tag{4.26}$$

where $\int \mathcal{D}(\bar{\phi}, \phi) = \mathcal{Z}_0^{-1} \prod_{j=1}^{2N} d(\bar{\phi}_j, \phi_j)$. Bosonic Green's functions are defined on the Keldysh contour by[63]

$$D(s, s') = -i\langle T_s[\hat{\phi}(s)\hat{\phi}^\dagger(s')]\rangle, \tag{4.27}$$

where s and s' refer to positions on the contour and T_s is a contour-ordering operator. Rewriting the fields to make it explicit which branch they are on, where those on the

forwards branch, i.e. time slices 0 to N, are denoted by ϕ^+ and those on the backwards branch (time slices $N+1$ to $2N$) by ϕ^-, and inverting the matrix $D^{-1}_{jj'}$, we get four different Green's functions:

$$
iD_{jj'} = \begin{pmatrix} \langle \phi_j^+ \bar{\phi}_{j'}^+ \rangle & \langle \phi_j^+ \bar{\phi}_{j'}^- \rangle \\ \langle \phi_j^- \bar{\phi}_{j'}^+ \rangle & \langle \phi_j^- \bar{\phi}_{j'}^- \rangle \end{pmatrix} = i \begin{pmatrix} D_{jj'}^T & D_{jj'}^< \\ D_{jj'}^> & D_{jj'}^{\tilde{T}} \end{pmatrix}. \tag{4.28}
$$

Here, D^T and $D^{\tilde{T}}$ are the time-ordered and anti-time-ordered Green's functions and $D^<$ and $D^>$ give correlations between the branches of the Keldysh contour. Taking the continuum limit, the distribution $\rho(\omega_0)$ is now properly accounted for. In the simple case investigated above where $\hat{H} = \omega_0 \hat{a}^\dagger \hat{a}$, these Green's functions are given by

$$
iD^<(t,t') \;=\; n_B(\omega_0)\mathrm{e}^{-i\omega_0(t-t')} \tag{4.29}
$$

$$
iD^>(t,t') \;=\; (n_B(\omega_0)+1)\mathrm{e}^{-i\omega_0(t-t')} \tag{4.30}
$$

$$
iD^T(t,t') \;=\; \theta(t-t')iD^<(t,t') + \theta(t'-t)iD^<(t,t') \tag{4.31}
$$

$$
iD^{\tilde{T}}(t,t') \;=\; \theta(t'-t)iD^<(t,t') + \theta(t-t')iD^<(t,t') \tag{4.32}
$$

where we have introduced the bosonic occupation number $n_B(\omega_0)$:

$$
n_B(\omega_0) = \frac{\rho(\omega_0)}{1-\rho(\omega_0)}. \tag{4.33}
$$

A continuum formulation, then, can be developed if the Green's functions above are taken to be the propagators of the theory[59]. Indeed, unlike the continuum version of Eq. (4.25) we see that there are correlations between the ϕ^+ and ϕ^- components that are dependent on the distribution $\rho(\omega_0)$. We may utilise the relationship $D^T(t,t') + D^{\tilde{T}}(t,t') - D^>(t,t') - D^<(t,t') = 0$ and define a rotation to new fields that reduces the number of Green's functions to three, where the distribution is contained in one of these. The new fields, $\phi^{c/q}$, are called 'classical' and 'quantum' and are given by:

$$
\phi^c(t) = \frac{1}{\sqrt{2}}(\phi^+(t) + \phi^-(t)), \qquad \phi^q(t) = \frac{1}{\sqrt{2}}(\phi^+(t) - \phi^-(t)). \tag{4.34}
$$

The Green's functions in this basis are the retarded, advanced, and Keldysh Green's functions:

$$D^R(t,t') \quad = \quad -i\langle\phi^c(t)\bar{\phi}^q(t')\rangle \tag{4.35}$$

$$= \quad \theta(t-t')[D^>(t,t') - D^<(t,t')] \tag{4.36}$$

$$D^A(t,t') \quad = \quad -i\langle\phi^q(t)\bar{\phi}^c(t')\rangle \tag{4.37}$$

$$= \quad \theta(t'-t)[D^<(t,t') - D^>(t,t')] \tag{4.38}$$

$$D^K(t,t') \quad = \quad -i\langle\phi^c(t)\bar{\phi}^c(t')\rangle \tag{4.39}$$

$$= \quad D^>(t,t') + D^<(t,t'). \tag{4.40}$$

For our simple model, $\hat{H} = \omega_0 \hat{a}^\dagger \hat{a}$, these are given in frequency space by

$$D^R(\omega) \quad = \quad \frac{1}{\omega - \omega_0 + i\delta}, \tag{4.41}$$

$$D^A(\omega) \quad = \quad \frac{1}{\omega - \omega_0 - i\delta}, \tag{4.42}$$

$$D^K(\omega) \quad = \quad -2\pi i[2n_B(\omega) + 1]\delta(\omega - \omega_0), \tag{4.43}$$

where we see that the distribution is contained in the Keldysh Green's function. In thermal equilibrium, the occupation function is given by $n_B(\omega) = 1/(e^{(\omega-\mu)/2T} - 1)$ and D^K can be written as

$$D^K(\omega) = \coth\left(\frac{\omega - \mu}{2T}\right)(D^R(\omega) - D^A(\omega)). \tag{4.44}$$

More generally, the Keldysh Green's function can be written in terms of a Hermitian distribution matrix F as $D^K = D^R F - F D^A$, where this is a statement of the fluctuation-dissipation theorem. The full inverse Green's function in the rotated basis is given by

$$\mathcal{D}^{-1} = \left[\begin{pmatrix} D^K & D^R \\ D^A & 0 \end{pmatrix}\right]^{-1} = \begin{pmatrix} 0 & [D^{-1}]^A \\ [D^{-1}]^R & [D^{-1}]^K \end{pmatrix}, \tag{4.45}$$

and thus, a full continuum action can be written as

$$S[\phi^c, \phi^q] = \iint_{-\infty}^{+\infty} dt\, dt'\, (\bar{\phi}^c, \bar{\phi}^q)_t \begin{pmatrix} 0 & [D^{-1}]^A \\ [D^{-1}]^R & [D^{-1}]^K \end{pmatrix}_{t,t'} \begin{pmatrix} \phi^c \\ \phi^q \end{pmatrix}_{t'}, \tag{4.46}$$

where $[D^{-1}]^{R/A} = [D^{R/A}]^{-1}$ and

$$[D^{-1}]^K = -[D^R]^{-1}D^K[D^A]^{-1} = [D^R]^{-1}F - F[D^A]^{-1}. \tag{4.47}$$

4.3   Coherently driven polariton action

The distribution of polaritons is set by the decay bath. To find this, we may use the Hamiltonian in Eq. (3.13) with coherent states, $|\psi^\pm\rangle$ and $|\chi^\pm\rangle$, for the polaritons and the bath, respectively, to construct a Keldysh path integral. We distinguish between fields on the forwards and backwards branches of the time contour [68],

$$S[\psi^\pm, \chi^\pm] = \int dt\, S^+[\psi^+, \chi^+] - \int dt\, S^-[\psi^-, \chi^-], \tag{4.48}$$

and perform the Keldysh rotation to an action in terms of fields $\mathbf{\Psi} = (\psi^c, \psi^q)$ and $\boldsymbol{\chi} = (\chi^c, \chi^q)$:

$$
\begin{aligned}
S[\mathbf{\Psi}, \boldsymbol{\chi}] \;=\; & \int dt \Big[\sum_{\boldsymbol{k}} \bar{\mathbf{\Psi}}(t, \boldsymbol{k})(i\partial_t - \omega_{LP}(\boldsymbol{k} + \boldsymbol{k}_p))\sigma_1^K \mathbf{\Psi}(t, \boldsymbol{k}) \\
& - F_p(\bar{\psi}^q(t, \mathbf{0}) + \psi^q(t, \mathbf{0})) + \sum_{\boldsymbol{p}} \bar{\boldsymbol{\chi}}(t, \boldsymbol{p})(i\partial_t - \omega_\chi(\boldsymbol{p}))\sigma_1^K \boldsymbol{\chi}(t, \boldsymbol{p}) \\
& - \sum_{\boldsymbol{k}, \boldsymbol{p}} \zeta_{\boldsymbol{k}, \boldsymbol{p}}(\bar{\boldsymbol{\chi}}(t, \boldsymbol{p})\sigma_1^K \mathbf{\Psi}(t, \boldsymbol{k}) + \bar{\mathbf{\Psi}}(t, \boldsymbol{k})\sigma_1^K \boldsymbol{\chi}(t, \boldsymbol{p})) \\
& - \sum_{\boldsymbol{k}, \boldsymbol{k}', \boldsymbol{q}} \frac{V}{2}\Big(\bar{\psi}^c(t, \boldsymbol{k} - \boldsymbol{q})\bar{\psi}^q(t, \boldsymbol{k}' + \boldsymbol{q}) \\
& \qquad\qquad \times \big[\psi^c(t, \boldsymbol{k})\psi^c(t, \boldsymbol{k}') + \psi^q(t, \boldsymbol{k})\psi^q(t, \boldsymbol{k}')\big] + \text{c.c.}\Big)\Big],
\end{aligned}
\tag{4.49}
$$

where σ_1^K is the first Pauli matrix in Keldysh space. Specifically, the decay bath action is given by

$$
\begin{aligned}
S_{bath}[\mathbf{\Psi}, \boldsymbol{\chi}] \;=\; & \int dt \Big[\sum_{\boldsymbol{p}} \bar{\boldsymbol{\chi}}(t, \boldsymbol{p})(i\partial_t - \omega_\chi(\boldsymbol{p}))\sigma_1^K \boldsymbol{\chi}(t, \boldsymbol{p}) \\
& - \sum_{\boldsymbol{k}, \boldsymbol{p}} \zeta_{\boldsymbol{k}, \boldsymbol{p}}(\bar{\boldsymbol{\chi}}(t, \boldsymbol{p})\sigma_1^K \mathbf{\Psi}(t, \boldsymbol{k}) + \bar{\mathbf{\Psi}}(t, \boldsymbol{k})\sigma_1^K \boldsymbol{\chi}(t, \boldsymbol{p})) \Big].
\end{aligned}
\tag{4.50}
$$

The bath fields here are quadratic and can thus be integrated out. Comparing this to the expression for a complex Gaussian functional integral in Eq. (4.17), we see that

$$\phi(x) \quad \to \quad \boldsymbol{\chi}(t, \boldsymbol{p}) \tag{4.51}$$

$$A^{-1}(x, x') \quad \to \quad -(i\partial_t - \omega_\chi(\boldsymbol{p}))\sigma_1^K \tag{4.52}$$

$$J(x) \quad \to \quad -\zeta_{\boldsymbol{k}, \boldsymbol{p}}\bar{\mathbf{\Psi}}(t, \boldsymbol{k})\sigma_1^K \tag{4.53}$$

$$J'(x) \quad \to \quad -\zeta_{\boldsymbol{k}, \boldsymbol{p}}\sigma_1^K \mathbf{\Psi}(t, \boldsymbol{k}), \tag{4.54}$$

and the bath action becomes

$$S_{bath}[\bar{\boldsymbol{\Psi}}, \boldsymbol{\Psi}] = -\int dt \sum_{\boldsymbol{k}, \boldsymbol{k}', \boldsymbol{p}} \bar{\boldsymbol{\Psi}}(t, \boldsymbol{k}) \sigma_1^K \zeta_{\boldsymbol{k}, \boldsymbol{p}} \zeta_{\boldsymbol{k}', \boldsymbol{p}} [(i\partial_t - \omega_\chi(\boldsymbol{p}))\sigma_1^K]^{-1} \sigma_1^K \boldsymbol{\Psi}(t, \boldsymbol{k}'). \quad (4.55)$$

This manifests itself as a self-energy term for the polariton fields, and noting that the result of the integral is a Green's function rather than an inverse Green's function, it can be written in terms of the bath Green's functions in Keldysh space:

$$[(i\partial_t - \omega_\chi(\boldsymbol{p}))\sigma_1^K]^{-1} = \begin{pmatrix} \hat{D}_{\omega_\chi}^K(t - t', \boldsymbol{p}) & \hat{D}_{\omega_\chi}^R(t - t', \boldsymbol{p}) \\ \hat{D}_{\omega_\chi}^A(t - t', \boldsymbol{p}) & 0 \end{pmatrix}. \quad (4.56)$$

We can simplify this by assuming the coupling between the bath and the system is independent of the polariton momentum, $\zeta_{\boldsymbol{k}, \boldsymbol{p}} \zeta_{\boldsymbol{k}', \boldsymbol{p}} = \zeta_{\boldsymbol{p}}^2$, and by suggesting that, if the bath frequencies $\omega_\chi(\boldsymbol{p})$ form a dense spectrum and the coupling constants $\zeta_{\boldsymbol{p}} = \zeta(\omega_\chi)$ are smooth functions of these, we can replace the sum over bath modes with the integral [37],

$$\sum_{\boldsymbol{p}} \zeta_{\boldsymbol{p}}^2 \to \int d\omega_\chi \zeta(\omega_\chi)^2 N_\chi(\omega_\chi), \quad (4.57)$$

where $N_\chi(\omega_\chi)$ is the bath density of states. As the bath is assumed to be much larger than the system, the Green's functions in Eq. (4.56) are of free bosons. These are given in frequency space by Eqs. (4.41-4.43) modified for a general distribution, $F(\omega_\chi)$:

$$D_{\omega_\chi}^{R/A}(\omega) = \frac{1}{\omega - \omega_\chi \pm i\delta}, \quad (4.58)$$

$$D_{\omega_\chi}^K(\omega) = -2\pi i F(\omega_\chi)\delta(\omega - \omega_\chi). \quad (4.59)$$

Fourier transforming the action, substituting in Eqs. (4.58) and (4.59), and integrating over ω_χ gives

$$S_{bath}[\bar{\boldsymbol{\Psi}}, \boldsymbol{\Psi}] = -\int d\omega \sum_{\boldsymbol{k}} \bar{\boldsymbol{\Psi}}(\omega, \boldsymbol{k}) \begin{pmatrix} 0 & d^A(\omega) \\ d^R(\omega) & d^K(\omega) \end{pmatrix} \boldsymbol{\Psi}(\omega, \boldsymbol{k}). \quad (4.60)$$

The bath self-energies $d^{R/A/K}$ are found using the identity [59],

$$\int d\omega \frac{1}{\omega - \omega_\chi \pm i\delta} = \int d\omega \left(\mathcal{P} \frac{1}{\omega - \omega_\chi} \mp i\pi \delta(\omega - \omega_\chi) \right), \quad (4.61)$$

where $\mathcal{P}$ refers to the Cauchy principal value of the integral, giving

$$d^{R/A}(\omega) \;=\; \mathcal{P}\int d\omega_\chi \frac{\zeta(\omega_\chi)^2 N_\chi(\omega_\chi)}{\omega - \omega_\chi} \mp i\pi\zeta(\omega)^2 N_\chi(\omega), \tag{4.62}$$

$$d^K(\omega) \;=\; -2\pi i\zeta(\omega)^2 N_\chi(\omega)F(\omega). \tag{4.63}$$

We can separate $d^{R/A}(\omega)$ into real and imaginary parts, $d^{R/A}(\omega) = R(\omega) \mp i\kappa(\omega)$, where

$$R(\omega) \;=\; \mathcal{P}\int d\omega_\chi \frac{\zeta(\omega_\chi)^2 N_\chi(\omega_\chi)}{\omega - \omega_\chi}, \tag{4.64}$$

$$\kappa(\omega) \;=\; \pi\zeta(\omega)^2 N_\chi(\omega), \tag{4.65}$$

leading to $d^K(\omega) = -2i\kappa(\omega)F(\omega)$. Thus, the bath action is given by:

$$S_{bath} = -\int d\omega \sum_{\boldsymbol{k}} \bar{\boldsymbol{\Psi}}(\omega,\boldsymbol{k}) \begin{pmatrix} 0 & R(\omega)+i\kappa(\omega) \\ R(\omega)-i\kappa(\omega) & -2i\kappa(\omega)F(\omega) \end{pmatrix} \boldsymbol{\Psi}(\omega,\boldsymbol{k}). \tag{4.66}$$

The energies of the polaritons are much larger than those of photons outside of the cavity, i.e. their characteristic timescale is much faster, so we may take the bath to be frequency-independent (Markovian), where $\kappa(\omega) = \kappa$ and $R(\omega) = 0$. Thus, the action for coherently pumped polaritons becomes

$$\begin{aligned}
S[\bar{\boldsymbol{\Psi}}, \boldsymbol{\Psi}] \;=\;& \sum_k (\bar{\psi}^c(k), \bar{\psi}^q(k)) \begin{pmatrix} 0 & g^{-1}(k) \\ (g^{-1})^*(k) & 2i\kappa F(\omega) \end{pmatrix} \begin{pmatrix} \psi^c(k) \\ \psi^q(k) \end{pmatrix} \\
& - \sum_{k,k',q} \frac{V}{2}\Big(\bar{\psi}^c(k-q)\bar{\psi}^q(k'+q)\big[\psi^c(k)\psi^c(k') \\
& +\psi^q(k)\psi^q(k')\big] + \text{c.c.}\Big) - F_p\big(\bar{\psi}^q(0) + \psi^q(0)\big),
\end{aligned} \tag{4.67}$$

where $k = (\omega, \boldsymbol{k})$, the frequency arguments are with respect to the pump frequency, ω_p, and the free inverse Green's functions are $g^{-1}(k) = \omega + \omega_p - \omega_{LP}(\boldsymbol{k} + \boldsymbol{k}_p) - i\kappa$.

4.4   Polariton Green's functions

To calculate the Green's functions of coherently pumped polaritons, we perform a semi-classical approximation on the action (Eq. (4.67)), which is necessary in order to treat the interaction term. Formally, we note that the action can be rewritten in terms of a Nambu vector, $\boldsymbol{\Psi}(k) = (\psi^c(k), \bar{\psi}^c(-k), \psi^q(k), \bar{\psi}^q(-k))$, where $k = (\omega, \boldsymbol{k})$, and we perform a Taylor

expansion around the mean-field $\mathbf{\Psi}_0 = (\sqrt{2}\psi_0, \sqrt{2}\bar{\psi}_0, 0, 0)$,

$$S[\mathbf{\Psi}_0 + \delta\mathbf{\Psi}] = S[\mathbf{\Psi}_0] + \sum_k \frac{dS[\mathbf{\Psi}]}{d\mathbf{\Psi}(k)}\mid_{\mathbf{\Psi}=\mathbf{\Psi}_0} \delta\mathbf{\Psi}(k) \tag{4.68}$$

$$+\frac{1}{2}\sum_{k,k'} \delta\mathbf{\Psi}^\dagger(k) \frac{d^2 S[\mathbf{\Psi}]}{d\mathbf{\Psi}(k)d\mathbf{\Psi}^\dagger(k')}\mid_{\mathbf{\Psi}=\mathbf{\Psi}_0} \delta\mathbf{\Psi}(k') + ...,$$

where by the definition of the saddle point the first order term is zero. We note here that the mean-field of the quantum component is zero because $\langle\hat{\psi}^q\rangle \sim \langle\hat{\psi}^+\rangle - \langle\hat{\psi}^-\rangle = 0$. This expansion modifies the path integral to

$$\mathcal{Z} = \int \mathcal{D}(\delta\bar{\mathbf{\Psi}}, \delta\mathbf{\Psi}) \exp[iS_0 + i\sum \delta\bar{\mathbf{\Psi}}\mathcal{D}^{-1}\delta\mathbf{\Psi}], \tag{4.69}$$

where $\mathcal{D}^{-1}$ is the inverse matrix of Green's functions:

$$\mathcal{D}^{-1}(k,k') = \begin{pmatrix} 0 & [D^{-1}]^A(k,k') \\ [D^{-1}]^R(k,k') & [D^{-1}]^K(k,k') \end{pmatrix}. \tag{4.70}$$

We see from Eq. (4.68) that $\mathcal{D}^{-1}$ is given by the matrix of second order derivatives,

$$\mathcal{D}^{-1}(k,k') = \begin{pmatrix} d/d\bar{\psi}^c(k) \\ d/d\psi^c(-k) \\ d/d\bar{\psi}^q(k) \\ d/d\psi^q(-k) \end{pmatrix} \begin{pmatrix} d/d\psi^c(k') \\ d/d\bar{\psi}^c(-k') \\ d/d\psi^q(k') \\ d/d\bar{\psi}^q(-k') \end{pmatrix}^T S[\mathbf{\Psi}]. \tag{4.71}$$

Calculating this, we have for the inverse matrix of Green's functions:

$$\mathcal{D}^{-1}(k,k') = \begin{pmatrix} 0 & 0 & J^*(\omega,\boldsymbol{k}) & -V\psi_0^2 \\ 0 & 0 & -V\bar{\psi}_0^2 & J(-\omega,-\boldsymbol{k}) \\ J(\omega,\boldsymbol{k}) & -V\psi_0^2 & 2i\kappa F(\omega) & 0 \\ -V\bar{\psi}_0^2 & J^*(-\omega,-\boldsymbol{k}) & 0 & 2i\kappa F(-\omega) \end{pmatrix} \delta_{k,k'}, \tag{4.72}$$

where $J(\pm\omega, \pm\boldsymbol{k}) \equiv \pm\omega + \omega_p - \omega_{LP}(\boldsymbol{k}_p \pm \boldsymbol{k}) + i\kappa - 2V|\psi_0|^2$. The retarded and advanced Green's functions obey the relations, $[D^{-1}]^{R/A} = [D^{R/A}]^{-1}$, so inverting the retarded and advanced components of Eq. (4.72) gives

$$D^R(\omega, \boldsymbol{k}) = \frac{1}{J(\omega,\boldsymbol{k})J^*(-\omega,-\boldsymbol{k}) - V^2\bar{\psi}_0^2\psi_0^2} \begin{pmatrix} J^*(-\omega,-\boldsymbol{k}) & V\psi_0^2 \\ V\bar{\psi}_0^2 & J(\omega,\boldsymbol{k}) \end{pmatrix}, \tag{4.73}$$

$$D^A(\omega, \boldsymbol{k}) = \frac{1}{J(-\omega, -\boldsymbol{k})J^*(\omega, \boldsymbol{k}) - V^2\bar{\psi}_0^2\psi_0^2} \begin{pmatrix} J(-\omega, -\boldsymbol{k}) & V\psi_0^2 \\ V\bar{\psi}_0^2 & J^*(\omega, \boldsymbol{k}) \end{pmatrix}. \tag{4.74}$$

The relation $[D^{-1}]^K = [D^K]^{-1}$ does not hold for the Keldysh Green's function, which is instead given by $D^K = -D^R[D^{-1}]^K D^A$:

$$D^K(\omega, \boldsymbol{k}) = -\frac{2i\kappa}{\left| J(\omega, \boldsymbol{k})J^*(-\omega, -\boldsymbol{k}) - V^2\bar{\psi}_0^2\psi_0^2 \right|^2} \tag{4.75}$$

$$\times \begin{pmatrix} d_1^K(-\omega, -\boldsymbol{k}) & d_2^K(\omega, \boldsymbol{k})^* \\ d_2^K(\omega, \boldsymbol{k}) & d_1^K(\omega, \boldsymbol{k}) \end{pmatrix}, \tag{4.76}$$

where

$$d_1^K(\omega, \boldsymbol{k}) = J^*(\omega, \boldsymbol{k})J(\omega, \boldsymbol{k})F(-\omega) + V^2\bar{\psi}_0^2\psi_0^2 F(\omega), \tag{4.77}$$

$$d_2^K(\omega, \boldsymbol{k}) = [J(-\omega, -\boldsymbol{k})F(\omega) + J(\omega, \boldsymbol{k})F(-\omega)]V\bar{\psi}_0^2. \tag{4.78}$$

Another consequence of the polariton energies being much larger than the energy of the thermal photons outside of the cavity is that the decay bath occupation, given by $F(\omega) = n_B(\omega) + 1$, is effectively zero and we can set $F \simeq 1$[98], leading to

$$D^K(\omega, \boldsymbol{k}) = -\frac{2i\kappa}{\left| J(\omega, \boldsymbol{k})J^*(-\omega, -\boldsymbol{k}) - V^2\bar{\psi}_0^2\psi_0^2 \right|^2} \tag{4.79}$$

$$\times \begin{pmatrix} J^*(-\omega, -\boldsymbol{k})J(-\omega, -\boldsymbol{k}) + V^2\bar{\psi}_0^2\psi_0^2 & [J^*(-\omega, -\boldsymbol{k}) + J^*(\omega, \boldsymbol{k})]V\psi_0^2 \\ [J(-\omega, -\boldsymbol{k}) + J(\omega, \boldsymbol{k})]V\bar{\psi}_0^2 & J^*(\omega, \boldsymbol{k})J(\omega, \boldsymbol{k}) + V^2\bar{\psi}_0^2\psi_0^2 \end{pmatrix}.$$

Combining the retarded, advanced, and Keldysh Green's functions above in the form

$$\mathcal{D}(\omega, \boldsymbol{k}) = \begin{pmatrix} D^K(\omega, \boldsymbol{k}) & D^R(\omega, \boldsymbol{k}) \\ D^A(\omega, \boldsymbol{k}) & 0 \end{pmatrix}, \tag{4.80}$$

gives the full matrix of Green's function of our system.

Part II

Superfluid Response of Coherently Driven Polaritons

Chapter 5

Excitation spectrum

If a system possesses a gapless mode in its excitation spectrum, then this will dominate its low energy properties[59], which can be seen in the context of superfluidity from the Landau criterion (Section 2.3), where the form of the excitation spectrum determines a critical velocity below which dissipationless flow is possible. For microcavity-polaritons, the way the system is pumped has a large effect on the form of the spectrum. Incoherently driven systems, as well as the 'signal' state in those pumped coherently above the optical parametric oscillation (OPO) threshold, possess a diffusive (i.e. flat) Goldstone mode in their excitation spectrum[37,38], which has been linked in theoretical studies to the existence of superfluidity in such systems[22,23]. Previous work on the spectrum of coherently pumped systems below the OPO threshold has remarked on how blue-detuning can lead to the real part of the spectrum fulfilling the Landau criterion[83,84], and experimental observations of nearly-dissipationless flow have been made in this regime[17]. However, this work has largely neglected the fact that in these systems the phase of the macroscopic state is fixed by the external pump, meaning that, in contrast to other pumping schemes and superfluid systems such as helium-4, the excitation spectrum is gapped.

In this chapter, we calculate the excitation spectrum of coherently pumped polaritons using the retarded Green's function and investigate its low energy properties. In Section 5.1, we derive the form of the excitation spectrum from the poles of the retarded Green's function; in Section 5.2, we calculate the mean-field ψ_0 in the system from the saddle points of the action; in Section 5.3, we calculate the spectrum and examine its properties in different parameter regimes; and in Section 5.4, we examine the onset of optical bistability and how it can lead to exceptional cases where the spectrum becomes gapless.

5.1   Poles of the retarded Green's function

The excitation spectrum is given by the poles of the retarded Green's function (Eq. (4.73))[96].
From Eqs. (4.70) and (4.72), we see that the inverse retarded Green's function is

$$[D^{-1}]^R(\omega, \boldsymbol{k}) = \frac{1}{2}\begin{pmatrix} \omega - \alpha(\boldsymbol{k}) + i\kappa & -V\psi_0^2 \\ -V\bar{\psi}_0^2 & -\omega - \alpha(-\boldsymbol{k}) - i\kappa \end{pmatrix}, \tag{5.1}$$

where for ease of calculation we write $\alpha(\pm\boldsymbol{k}) \equiv -\omega_p + \epsilon(\pm\boldsymbol{k}) + 2V|\psi_0|^2$, and, given we
are interested in low values of k, we have approximated the lower polariton dispersion as
quadratic:

$$\omega_{LP}(\boldsymbol{k}_p \pm \boldsymbol{k}) \to \epsilon(\pm\boldsymbol{k}) = \frac{(\boldsymbol{k}_p \pm \boldsymbol{k})^2}{2m} = \frac{(k_p \pm k_x)^2 + k_y^2}{2m}. \tag{5.2}$$

Here, m is the effective mass and, without loss of generality, we take the pump to be in the
x-direction, $\boldsymbol{k}_p = (k_p, 0)$. The poles of D^R are given by the determinant of Eq. (5.1) set to
zero[68]:

$$(\omega - \alpha(\boldsymbol{k}) + i\kappa)(-\omega - \alpha(-\boldsymbol{k}) - i\kappa) - V^2|\psi_0|^4 = 0. \tag{5.3}$$

Solving this equation for ω, we find that the excitation spectrum, $\omega = \omega^\pm(\boldsymbol{k})$, is

$$\omega^\pm(\boldsymbol{k}) = \frac{\alpha(\boldsymbol{k}) - \alpha(-\boldsymbol{k})}{2} - i\kappa \pm \sqrt{\left(\frac{\alpha(\boldsymbol{k}) + \alpha(-\boldsymbol{k})}{2}\right)^2 - V^2|\psi_0|^4}, \tag{5.4}$$

where we note that this spectrum involves an ordinary positive energy branch as well as a
negative energy branch due to holes, sometimes referred to as a 'ghost' branch[30,99].

5.2   Mean-field equations

To calculate the spectrum in Eq. (5.4), we first need to find the mean-field ψ_0. This
is the solution to the saddle point equations, which are found by differentiating the
coherently pumped action (Eq. (4.67)) with respect to the Nambu vector $\boldsymbol{\Psi}(k) =$
$(\psi^c(k), \bar{\psi}^c(-k), \psi^q(k), \bar{\psi}^q(-k))$, where $k = (\omega, \boldsymbol{k})$, and setting the results to zero:

$$\frac{dS}{d\boldsymbol{\Psi}^\dagger(k)} \equiv \left(\frac{d}{d\bar{\psi}^c(k)}, \frac{d}{d\psi^c(-k)}, \frac{d}{d\bar{\psi}^q(k)}, \frac{d}{d\psi^q(-k)}\right) S = 0. \tag{5.5}$$

Taking $F(\omega) \simeq 1$ as in Section 4.4, this gives

$$\frac{dS}{d\bar{\psi}^c(k)} = (\omega + \omega_p - \epsilon(\boldsymbol{k}) - i\kappa)\psi^q(k)$$

$$- \frac{V}{2}\sum_{k',q}\left(\bar{\psi}^q(k'+q)[\psi^c(k+q)\psi^c(k') + \psi^q(k+q)\psi^q(k')]\right.$$

$$\left. + 2\bar{\psi}^c(k'+q)\psi^q(k+q)\psi^c(k')\right) = 0,$$

$$\frac{dS}{d\psi^c(-k)} = (-\omega + \omega_p - \epsilon(-\boldsymbol{k}) + i\kappa)\bar{\psi}^q(-k)$$

$$-\frac{V}{2}\sum_{k',q}\Big(\psi^q(k'+q)[\bar{\psi}^c(-k+q)\bar{\psi}^c(k') + \bar{\psi}^q(-k+q)\bar{\psi}^q(k')]$$

$$+2\psi^c(k'+q)\bar{\psi}^q(-k+q)\bar{\psi}^c(k')\Big) = 0,$$

$$\frac{dS}{d\bar{\psi}^q(k)} = (\omega + \omega_p - \epsilon(\boldsymbol{k}) + i\kappa)\psi^c(k) + 2i\kappa\psi^q(k) - \sqrt{2}F_p\delta_{k,0}$$

$$-\frac{V}{2}\sum_{k',q}\Big(\bar{\psi}^c(k'+q)[\psi^c(k+q)\psi^c(k') + \psi^q(k+q)\psi^q(k')]$$

$$+2\bar{\psi}^q(k'+q)\psi^q(k+q)\psi^c(k')\Big) = 0,$$

$$\frac{dS}{d\psi^q(-k)} = (-\omega + \omega_p - \epsilon(-\boldsymbol{k}) - i\kappa)\bar{\psi}^c(-k) + 2i\kappa\bar{\psi}^q(-k) - \sqrt{2}F_p\delta_{-k,0}$$

$$-\frac{V}{2}\sum_{k',q}\Big(\psi^c(k'+q)[\bar{\psi}^c(-k+q)\bar{\psi}^c(k') + \bar{\psi}^q(-k+q)\bar{\psi}^q(k')]$$

$$+2\psi^q(k'+q)\bar{\psi}^q(-k+q)\bar{\psi}^c(k')\Big) = 0.$$

Now, making the mean-field approximation, $(\psi^c(k), \psi^q(k)) \rightarrow (\sqrt{2}\psi_0, 0)\delta_{k,0}$, the saddle point equations become

$$(\omega_p - \epsilon(\boldsymbol{0}) + i\kappa)\psi_0 - F_p = V|\psi_0|^2\psi_0, \tag{5.6}$$

$$(\omega_p - \epsilon(\boldsymbol{0}) - i\kappa)\bar{\psi}_0 - F_p = V|\psi_0|^2\bar{\psi}_0. \tag{5.7}$$

Mod-squaring these allows us to solve for the occupancy of the pump mode, $n_p = |\psi_0|^2$, with respect to the pump intensity, F_p^2:

$$V^2n_p^3 - 2\delta_p V n_p^2 + (\delta_p^2 + \kappa^2)n_p - F_p^2 = 0, \tag{5.8}$$

where $\delta_p = \omega_p - \epsilon(\boldsymbol{0})$ is the detuning, i.e. we take the general case where the coherent pump is slightly off-resonance with the bare lower polariton dispersion. For small detuning, the only real solution of Eq. (5.8) is

$$n_p = |\psi_0|^2 = \frac{2\delta_p}{3V} - \frac{2^{1/3}(3V^2\kappa^2 - V^2\delta_p^2)}{3V^2\beta} + \frac{\beta}{2^{1/3}3V^2}, \tag{5.9}$$

where

$$\begin{aligned}
\beta &= \Big[27F_p^2 V^4 - 2V^3\delta_p^3 - 18V^3\delta_p\kappa^2 \tag{5.10}\\
&\quad + \sqrt{4(3V^2\kappa^2 - V^2\delta_p^2)^3 + (27F_p^2 V^4 - 2V^3\delta_p^3 - 18V^3\delta_p\kappa^2)^2}\,\Big]^{1/3}.
\end{aligned}$$

The mean-field can then be calculated by rearranging Eq. (5.6) to get

$$\psi_0 = -\frac{F_p}{Vn_p - \delta_p - i\kappa}. \tag{5.11}$$

5.3   Coherently driven excitation spectrum

For a given detuning, δ_p, we may identify that different pump powers, F_p^2, lead to different excitation spectra. Fig. 5.1 shows the values of Eq. (5.4) for a range of pump powers where these are measured in terms of the mean-field density, $n_p = |\psi_0|^2$. The values of the other parameters are $m = 5 \times 10^{-5} m_e$, where m_e is the electron mass, $V = 0.0025\,\text{meV}\,\mu\text{m}^2$, $\kappa = 0.05\,\text{meV}$, $k_p = 0.1\,\mu\text{m}^{-1}$, and $\delta_p = 0.05\,\text{meV}$.

It is important to check whether the solution to the saddle point equations calculated above is stable to fluctuations. This can be done by expanding the Gross-Pitaevskii equation to linear order in fluctuations, leading to an equation of the form[84],

$$i\frac{d}{dt}\delta\psi = \mathcal{L}\delta\psi, \tag{5.12}$$

where the eigenvalues of the operator $\mathcal{L}$ give the excitation spectrum (Eq. (5.4)). The crucial point is that the state is stable if all the eigenvalues have negative imaginary parts[83], i.e. if the imaginary components of both branches of the excitation spectrum are negative. As can be seen in Fig. 5.1, this is true for the range of parameters we are considering.

We note that the real part of the spectrum takes a Bogoliubov form (Eq. (2.23)) that is linear at small ω, k when $|\psi_0|^2 = 20.0\,\mu\text{m}^{-2}$ (Fig. 5.1(c)), which is the density where the pump is in resonance with the interactions renormalised dispersion, which we refer to as the shifted resonance point. We define the detuning relative to this as

$$\Delta_p = \delta_p - V|\psi_0|^2 = \omega_p - \epsilon(\mathbf{0}) - V|\psi_0|^2. \tag{5.13}$$

Thus, we can say that when $\Delta_p = 0$ the real part of the excitation spectrum fulfils the Landau criterion. Usefully, for a given pump power we can calculate the density at which
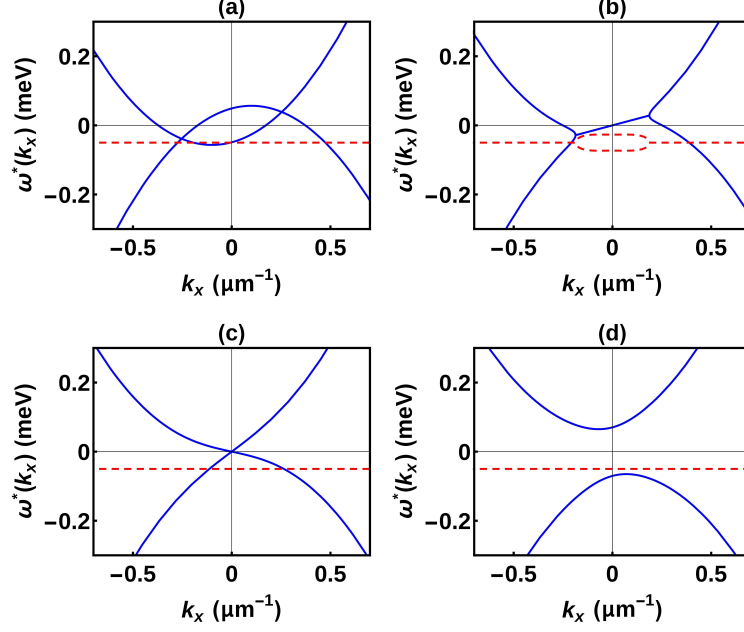
Figure 5.1: The real (solid blue) and the imaginary (dashed red) parts of the spectrum in the frame of the pump momentum, which is $k_p = 0.1\mu m^{-1}$ in the x-direction, for $k_y = 0$ and blue-detuning $\delta_p = 0.05$meV. In **(a)** and **(b)** the densities are $|\psi_0|^2 = 0.2\mu m^{-2}$ and $|\psi_0|^2 = 9.3\mu m^{-2}$ respectively. In **(c)** the density is $|\psi_0|^2 = 20.0\mu m^{-2}$ and the pump comes into resonance with the interactions renormalised lower polariton dispersion, $\Delta_p = \delta_p - V|\psi_0|^2 = 0$, at which point the real part takes the linear form of the Bogoliubov spectrum. Here, and in **(d)** where $|\psi_0|^2 = 30.9\mu m^{-2}$, the Landau criterion is fulfilled in the real part. However, it is significant that the imaginary part is always gapped.

this occurs by substituting $\delta_p = V n_p$ into Eq. (5.8), giving

$$F_p^2 = \kappa^2 |\psi_0|^2 . \tag{5.14}$$

However, because the phase of the macroscopic state is fixed externally by a laser, the full excitation spectrum is always gapped. In coherently pumped polaritons, we see from Fig. 5.1 that the gap in the spectrum is generally, but not exclusively, in the imaginary part. The gapped spectrum in Fig. 5.1(d), when $|\psi_0|^2 = 30.9\mu m^{-2}$, also fulfils the Landau criterion in the real part. However, it is not clear what the Landau criterion means when the spectrum is complex. Indeed, it has been shown that in driven-dissipative systems scattering past an obstacle can only be reduced, not eliminated[29], and furthermore in the case of incoherently pumped polaritons superfluidity can exist when the criterion is not fulfilled at all[27]. The survival of superfluidity in this system was found instead to depend on the gaplessness of the excitation spectrum as $\omega \to 0$, $\boldsymbol{k} \to \boldsymbol{0}$, because this led to a difference between the response of the system to longitudinal and transverse perturbations. Therefore, while the observation of nearly-dissipationless flow in coherently pumped systems[17] may be explained by the real part of the spectrum fulfilling the Landau criterion, we have reason

to believe the gapped nature of the complex spectrum could be a barrier to such a system being a superfluid.

5.4   Optical bistability

If the pump is blue-detuned sufficiently away from the bare lower polariton dispersion, there is a Kerr instability and the system becomes bistable[100]. This corresponds to the situation where the imaginary part of the excitation spectrum becomes positive, the condition for which is

$$\delta_p > \sqrt{3}\kappa. \tag{5.15}$$

In this regime, the polariton density at a given pump intensity is described by a curve of the form shown in Fig. 5.2(a), in which $\delta_p = 3\kappa = 0.15\text{meV}$, where at low and high intensity there is a single stable state, separated by a bistable region in which there are three real solutions of Eq. (5.8), two stable (solid red and blue) and one unstable (dashed green). By contrast, Fig. 5.2(b) shows the density below the bistability threshold (in this case $\delta_p = \kappa = 0.05\text{meV}$, the same parameters as in Fig. 5.1), which is known as the optical limiter regime. Here, Eq. (5.9) is the only real solution to Eq. (5.8).

The excitation spectra on the stable (solid red and blue) branches are given in Figs. 5.3 and 5.4. Here we see that, contrary to its usual behaviour, the spectrum becomes gapless at exactly the boundary between the stable and unstable regions. Notably, these gapless spectra do not fulfil the Landau criterion. When $k_p = 0$, the spectra at these points are diffusive and similar to the incoherently pumped case[38], with a flat real part (see Fig. 5.5). Otherwise, for finite k_p there are real energy states available at the condensate energy into which there may be scattering.
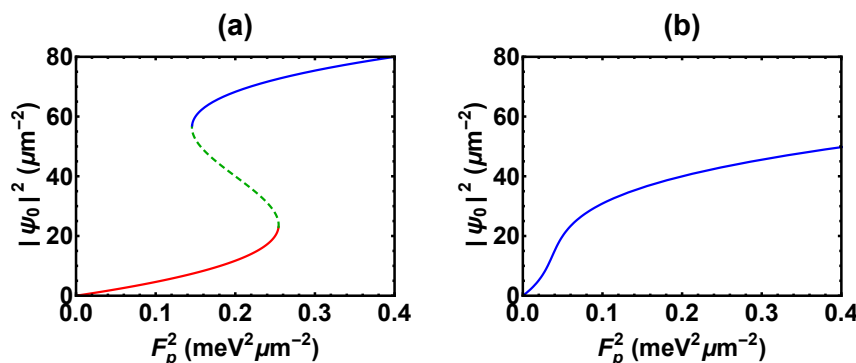
Figure 5.2: Polariton mean-field density at different values of pump intensity. In **(a)**, $\delta_p = 3\kappa = 0.15\text{meV}$ and we are in the bistable regime. There are two stable states (solid red and blue at low and high density, respectively) and an unstable state (dashed green), where the former can be physically observed and the latter exists only mathematically. In **(b)**, $\delta_p = \kappa = 0.05\text{meV}$ and we are below the bistability threshold in the optical limiter regime. Here, there is one stable state which monotonically increases in density with pump intensity.
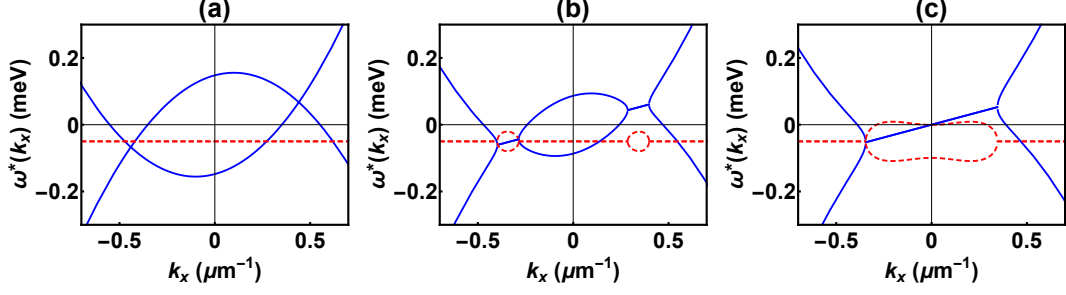
Figure 5.3: Excitation spectra on the lower branch of the bistability curve in Fig. 5.2(a) where $k_p = 0.1\mu m^{-1}$ in the x-direction. In **(a)**, $F_p^2 = 0.01 meV^2 \mu m^{-2}$, outside the bistable region in the low density 'dim' state. In **(b)**, $F_p^2 = 0.2 meV^2 \mu m^{-2}$, inside the bistable region. In **(c)**, $F_p^2 = 0.25443 meV^2 \mu m^{-2}$, at the turning point on the bistability curve precisely between the stable and unstable states (solid red and dashed green, respectively, in Fig. 5.2(a)) where the spectrum becomes gapless.
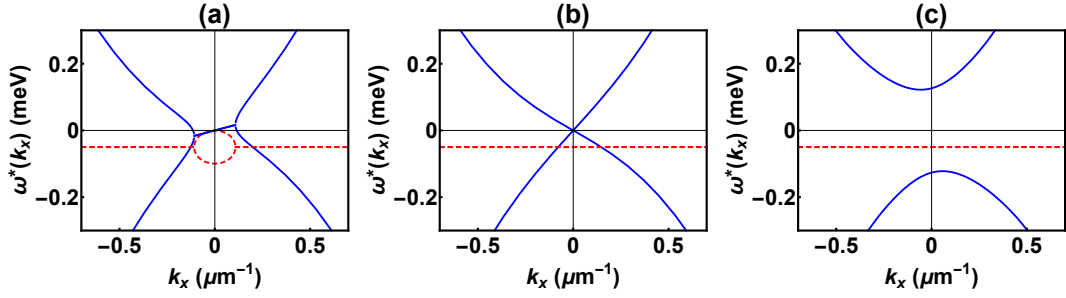
Figure 5.4: Excitation spectra on the upper branch of the bistability curve in Fig. 5.2(a) where $k_p = 0.1\mu m^{-1}$ in the x-direction. In **(a)**, $F_p^2 = 0.14557 meV^2 \mu m^{-2}$, at the turning point on the bistability curve precisely between the stable and unstable states (solid blue and dashed green, respectively, in Fig. 5.2(a)) where the spectrum becomes gapless. In **(b)**, $F_p^2 = 0.15 meV^2 \mu m^{-2}$, inside the bistable region at the shifted resonance point where the real part of the spectrum takes a Bogoliubov form. In **(c)**, $F_p^2 = 0.3 meV^2 \mu m^{-2}$, outside the bistable region in the high density 'bright' state.

By substituting $\omega^\pm = 0$, $\boldsymbol{k} = \boldsymbol{0}$ into Eq. (5.4), we find the condition for a coherently pumped system below the OPO threshold to have a gapless spectrum is

$$3V^2 n_p^2 - 4\delta_p V n_p + \delta_p^2 + \kappa^2 = 0. \tag{5.16}$$

Solving for $n_p = |\psi_0|^2$ gives

$$|\psi_0|^2 = \frac{1}{3V} \left(2\delta_p \pm \sqrt{\delta_p^2 - 3\kappa^2} \right), \tag{5.17}$$

and we see that there are only real solutions when $\delta_p > \sqrt{3}\kappa$, precisely the bistability condition in Eq. (5.15). Interestingly, if we rearrange Eq. (5.8) to be in terms of the pump strength, F_p^2, and solve for $dF_p^2/dn_p = 0$, i.e. we find the equation for the turning points of the bistability curve in Fig. 5.2(a), we get precisely Eq. (5.16). That is, there can be a gapless spectrum only at the points where the imaginary component crosses from negative to positive and the system becomes unstable. The response function at these points is
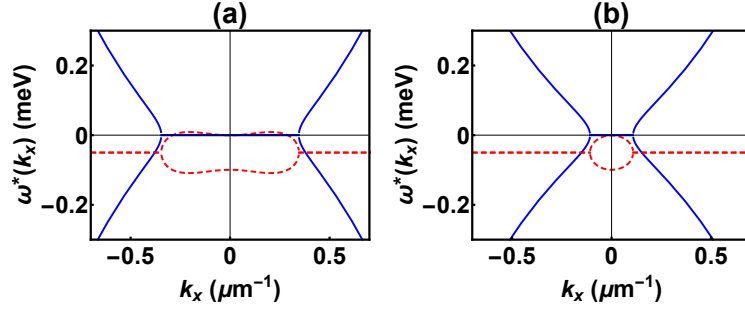
Figure 5.5: Diffusive excitation spectra at the turning points of the bistability curve at zero pump momentum. **(a)** The spectrum at the turning point on the lower branch in Fig. 5.2(a) where $F_p^2 = 0.25443 \text{meV}^2 \mu\text{m}^{-2}$. **(b)** The spectrum at the turning point on the upper branch where $F_p^2 = 0.14557 \text{meV}^2 \mu\text{m}^{-2}$. These values of F_p^2 can be found by substituting Eq. (5.17) into Eq. (5.8).

investigated at the mean-field level in Section 7.5.

Chapter 6

Calculation of the response function

The current-current response function is the generalised susceptibility for a current to flow due to a perturbing force and is given by the correlation function of two current operators (Section 2.6). In the long-range limit, this function can be used to find the response of a system to longitudinal and transverse perturbations. While normal fluids respond to both types of perturbations equally, superfluids respond longitudinally but not transversely. Therefore, by calculating the difference between the two types of response, it is possible to find whether a system has a superfluid component.

In this chapter, we use a Keldysh path integral technique[23] to calculate the static current-current response function for coherently driven microcavity-polaritons, where the pump is homogeneous, continuous, and below the OPO threshold. This involves adding a term to the action containing source fields coupled to currents and differentiating the partition function with respect to the sources, which gives the correlation function of two current operators as the source fields are taken to zero. For a system described in terms of the semiclassical approximation, i.e. where the action is written in terms of a mean-field and quadratic fluctuations, the result is given by a Gaussian integral over the fluctuations. It is important to note that the mean-field will be a function of the source fields.

In Section 6.1, we define the current in the system, introduce the momentum vertex, and calculate the source term to be added to the action; in Section 6.2, we perform the semiclassical approximation, differentiate the path integral with respect to the source fields, and integrate over the field fluctuations, finding that the response function is made up of three terms: one from the mean-field and two from fluctuations; in Section 6.3, we define the mean-field in terms of the source fields, find the saddle point equations including the sources, and calculate the mean-field term in the response function; in Section 6.4, we calculate the two fluctuations terms; and in Section 6.5, we present the full response function resulting from the calculation. More details of some of the steps we take can be found in Appendix A.

6.1   Keldysh currents and source fields

In driven-dissipative systems, two kinds of current can be distinguished: one internal to the system and another exchanging particles with the bath[85]. We are interested in the internal response of the system to perturbations, and so the relevant current is the standard quantum mechanical current in the limit that pumping and decay go to zero. This current, given by the left-hand side of Eq. (2.6), will obey the continuity equation, which for interacting bosons with dispersion relation $\epsilon(\boldsymbol{k})$ can be written in momentum space as

$$[\hat{H}, \hat{\rho}(\boldsymbol{q})] = -\sum_{\boldsymbol{k}}[\epsilon(\boldsymbol{k}+\boldsymbol{q}) - \epsilon(\boldsymbol{k})]\hat{\psi}^{\dagger}(\boldsymbol{k})\hat{\psi}(\boldsymbol{k}+\boldsymbol{q}) = -\boldsymbol{q}.\hat{\boldsymbol{j}}(\boldsymbol{q}). \tag{6.1}$$

Thus, the current for a general dispersion is

$$\hat{\boldsymbol{j}}(\boldsymbol{q}) = \sum_{\boldsymbol{k}}\boldsymbol{\gamma}(\boldsymbol{k}+\boldsymbol{q},\boldsymbol{k})\hat{\psi}^{\dagger}(\boldsymbol{k})\hat{\psi}(\boldsymbol{k}+\boldsymbol{q}), \tag{6.2}$$

where $\boldsymbol{\gamma}(\boldsymbol{k}+\boldsymbol{q},\boldsymbol{k})$ is the momentum vertex, defined by

$$\boldsymbol{q}.\boldsymbol{\gamma}(\boldsymbol{k}+\boldsymbol{q},\boldsymbol{k}) = \epsilon(\boldsymbol{k}+\boldsymbol{q}) - \epsilon(\boldsymbol{k}). \tag{6.3}$$

For the quadratic dispersion given in Eq. (5.2), we have that

$$\boldsymbol{q}.\boldsymbol{\gamma}(\boldsymbol{k}+\boldsymbol{q},\boldsymbol{k}) = \frac{1}{2m}(2(k_p+k_x)q_x + q_x^2 + 2k_yq_y + q_y^2), \tag{6.4}$$

so the momentum vertex is given by

$$\boldsymbol{\gamma}(\boldsymbol{k}+\boldsymbol{q},\boldsymbol{k}) = \frac{1}{2m}\begin{pmatrix} 2k_p+2k_x+q_x \\ \\ 2k_y+q_y \end{pmatrix}. \tag{6.5}$$

We note that $\gamma_i(\boldsymbol{k}+\boldsymbol{q},\boldsymbol{k}) = \gamma_i(\boldsymbol{k},\boldsymbol{k}+\boldsymbol{q})$, and in the rest of this thesis, any time one of the arguments is equal to zero, e.g. $\gamma_i(\boldsymbol{k},0)$ or $\gamma_i(0,\boldsymbol{k})$, it will be written with one argument only: i.e., $\gamma_i(\boldsymbol{k})$.

Generalising to Keldysh field theory, the current we wish to measure in response to a perturbation is the normal-ordered particle current:[27]

$$\begin{aligned} \boldsymbol{j}(\boldsymbol{q}) &= \sum_{\boldsymbol{k}}\boldsymbol{\gamma}(\boldsymbol{k}+\boldsymbol{q},\boldsymbol{k})\big[\psi^+(\boldsymbol{k}+\boldsymbol{q})\bar{\psi}^-(\boldsymbol{k})\big], &&(6.6) \\[2mm] &= \frac{1}{2}\sum_{\boldsymbol{k}}\boldsymbol{\gamma}(\boldsymbol{k}+\boldsymbol{q},\boldsymbol{k})\big[\psi^c(\boldsymbol{k}+\boldsymbol{q})\bar{\psi}^c(\boldsymbol{k}) - \psi^c(\boldsymbol{k}+\boldsymbol{q})\bar{\psi}^q(\boldsymbol{k}) &&(6.7) \\[2mm] &\qquad +\psi^q(\boldsymbol{k}+\boldsymbol{q})\bar{\psi}^c(\boldsymbol{k}) - \psi^q(\boldsymbol{k}+\boldsymbol{q})\bar{\psi}^q(\boldsymbol{k})\big], \end{aligned}$$

where we are working now in the functional integral, rather than operator, picture. However, this current couples to an unphysical field[85], which we call $\boldsymbol{\theta}$. By contrast, the 'quantum' current,

$$\boldsymbol{j}^q(\boldsymbol{q}) = \sum_{\boldsymbol{k}} \boldsymbol{\gamma}(\boldsymbol{k}+\boldsymbol{q},\boldsymbol{k})\big[\psi^q(\boldsymbol{k}+\boldsymbol{q})\bar{\psi}^c(\boldsymbol{k}) + \psi^c(\boldsymbol{k}+\boldsymbol{q})\bar{\psi}^q(\boldsymbol{k})\big], \tag{6.8}$$

which is itself unphysical, couples to a field $\boldsymbol{f}$ that is physical. Therefore, the correlator of these two currents gives the physical current that flows in response to a physical perturbation, i.e., it is the current-current response function:

$$\chi_{ij}(\boldsymbol{q}) = \frac{i}{2}\langle j_i(\boldsymbol{q})j_j^q(-\boldsymbol{q})\rangle. \tag{6.9}$$

Treating $\boldsymbol{f}$ and $\boldsymbol{\theta}$ as source fields, we may add an extra term to the action where they are coupled to the relevant currents. Given that for an arbitrary source $S(x)$ coupled to a current $J(x)$, the Fourier transform to momentum space is

$$\int dx S(x)J(x) \rightarrow \sum_{k} S(k)J(-k), \tag{6.10}$$

then the extra term in the action is given by

$$\delta S[\boldsymbol{f},\boldsymbol{\theta}] = \sum_{\omega,\boldsymbol{q},\boldsymbol{k}} \gamma_i(\boldsymbol{k}+\boldsymbol{q},\boldsymbol{k})(\bar{\psi}^c,\bar{\psi}^q)_{\omega,\boldsymbol{k}+\boldsymbol{q}} \begin{pmatrix} \theta_i & f_i+\theta_i \\ f_i-\theta_i & -\theta_i \end{pmatrix}_{\boldsymbol{q}} \begin{pmatrix} \psi^c \\ \psi^q \end{pmatrix}_{\omega,\boldsymbol{k}}, \tag{6.11}$$

where we have utilised the fact that $\boldsymbol{j}(-\boldsymbol{q}) = \boldsymbol{j}^*(\boldsymbol{q})$ and taken $\boldsymbol{k} \to \boldsymbol{k}+\boldsymbol{q}$. We see here that the momentum vertex $\boldsymbol{\gamma}$ gives the bare coupling between excitations of momentum $\boldsymbol{q}$ and the source fields. Combining this term with the action for coherently pumped polaritons coupled to a Markovian bath in Eq. (4.67) (and setting $F(\omega) \simeq 1$), we get the full action for our system with an applied perturbation:

$$\begin{aligned} S \;=\; & \sum_{\omega,\boldsymbol{k}}(\bar{\psi}^c(\omega,\boldsymbol{k}),\bar{\psi}^q(\omega,\boldsymbol{k})) \begin{pmatrix} 0 & g^{-1}(\omega,\boldsymbol{k}) \\ (g^{-1})^*(\omega,\boldsymbol{k}) & 2i\kappa \end{pmatrix} \begin{pmatrix} \psi^c(\omega,\boldsymbol{k}) \\ \psi^q(\omega,\boldsymbol{k}) \end{pmatrix} \\ & - \sum_{\omega,\omega',\nu}\sum_{\boldsymbol{k},\boldsymbol{k}',\boldsymbol{q}} \frac{V}{2}\Big(\bar{\psi}^c(\omega-\nu,\boldsymbol{k}-\boldsymbol{q})\bar{\psi}^q(\omega'+\nu,\boldsymbol{k}'+\boldsymbol{q})\big[\psi^c(\omega,\boldsymbol{k})\psi^c(\omega',\boldsymbol{k}') \\ & +\psi^q(\omega,\boldsymbol{k})\psi^q(\omega',\boldsymbol{k}')\big] + \text{c.c.}\Big) - F_p\left(\bar{\psi}^q(0,\boldsymbol{0}) + \psi^q(0,\boldsymbol{0})\right) \\ & + \sum_{\omega,\boldsymbol{q},\boldsymbol{k}} \gamma_i(\boldsymbol{k}+\boldsymbol{q},\boldsymbol{k})(\bar{\psi}^c,\bar{\psi}^q)_{\omega,\boldsymbol{k}+\boldsymbol{q}} \begin{pmatrix} \theta_i & f_i+\theta_i \\ f_i-\theta_i & -\theta_i \end{pmatrix}_{\boldsymbol{q}} \begin{pmatrix} \psi^c \\ \psi^q \end{pmatrix}_{\omega,\boldsymbol{k}}, \end{aligned} \tag{6.12}$$

where the free inverse Green's function $g^{-1}(\omega,\boldsymbol{k}) = \omega + \omega_p - \epsilon(\boldsymbol{k}) - i\kappa$, and all the coordinates

are defined relative to the pump mode $(\omega_p, \boldsymbol{k}_p)$.

6.2   Functional differentiation of the action

To calculate the current-current response function we construct a path integral,

$$\mathcal{Z} = \int \mathcal{D}(\bar{\Psi}, \Psi) \exp\left(iS[\bar{\Psi}, \Psi, \boldsymbol{f}, \boldsymbol{\theta}]\right), \tag{6.13}$$

where the action $S[\bar{\Psi}, \Psi, \boldsymbol{f}, \boldsymbol{\theta}]$ is given by Eq. (6.12) and $\Psi(k) = (\psi^c(k), \bar{\psi}^c(-k), \psi^q(k), \bar{\psi}^q(-k))$ is a Nambu vector of the fields with $k = (\omega, \boldsymbol{k})$, and we differentiate it with respect to the source fields,

$$\chi_{ij}(\boldsymbol{q}) = -\frac{i}{2} \frac{1}{\mathcal{Z}[\boldsymbol{0}, \boldsymbol{0}]} \frac{d^2 \mathcal{Z}[\boldsymbol{f}, \boldsymbol{\theta}]}{df_i(\boldsymbol{q}) d\theta_j(-\boldsymbol{q})}\bigg|_{\boldsymbol{f}=\boldsymbol{\theta}=\boldsymbol{0}}, \tag{6.14}$$

which are then set to zero. To calculate this we must perform a Gaussian integral which, due to the quartic interaction term in the Hamiltonian, requires us first to make the semiclassical approximation (Eq. (4.68)), which is equivalent to making the substitution $\Psi = \Psi_0 + \delta\Psi$, where Ψ_0 is the mean-field and $\delta\Psi$ are fluctuations, where we keep the latter to quadratic order. This modifies the path integral to

$$\mathcal{Z} = \int \mathcal{D}(\delta\bar{\Psi}, \delta\Psi) \exp\left(iS_0[\boldsymbol{f}, \boldsymbol{\theta}] + i\sum \delta\bar{\Psi}(\mathcal{D}^{-1} + A[\boldsymbol{f}, \boldsymbol{\theta}])\delta\Psi\right), \tag{6.15}$$

where the mean-field action S_0 is a function of the source fields, $\mathcal{D}^{-1}$ is the inverse matrix of Green's functions (Eq. (4.72)), and A is a matrix containing the fluctuation terms that are dependent on the sources. Performing the Gaussian integration gives

$$
\begin{aligned}
\mathcal{Z}[\boldsymbol{f}, \boldsymbol{\theta}] &= \exp(iS_0[\boldsymbol{f}, \boldsymbol{\theta}]) \\
&\quad \times \int \mathcal{D}(\delta\bar{\Psi}, \delta\Psi) \exp\left[i\sum \delta\bar{\Psi}\mathcal{D}^{-1}(\mathbb{1} + \mathcal{D}A[\boldsymbol{f}, \boldsymbol{\theta}])\delta\Psi\right] \\
&= \exp(iS_0[\boldsymbol{f}, \boldsymbol{\theta}]) \det\left[\mathcal{D}^{-1}(\mathbb{1} + \mathcal{D}A[\boldsymbol{f}, \boldsymbol{\theta}])\right]^{-1/2} \\
&= \mathcal{N} \exp\left(iS_0[\boldsymbol{f}, \boldsymbol{\theta}] - \frac{1}{2}\operatorname{Tr}\ln(\mathbb{1} + \mathcal{D}A[\boldsymbol{f}, \boldsymbol{\theta}])\right),
\end{aligned}
$$

$$\tag{6.16}$$
$$\tag{6.17}$$
$$\tag{6.18}$$

where $\mathcal{N} = \det\left[\mathcal{D}^{-1}\right]^{-1/2}$. Because the Nambu vector contains each field twice, we introduce a square root on the second line to prevent double counting. Expanding the logarithm,

$$\mathcal{Z} = \mathcal{N} \exp\left[iS_0 - \frac{1}{2}\operatorname{Tr}\left(\mathcal{D}A - \frac{1}{2}\mathcal{D}A\mathcal{D}A + ...\right)\right], \tag{6.19}$$

and differentiating with respect to $\boldsymbol{f}(\boldsymbol{q})$ and $\boldsymbol{\theta}(-\boldsymbol{q})$, gives

$$\frac{d^2\mathcal{Z}[\boldsymbol{f},\boldsymbol{\theta}]}{df_i(\boldsymbol{q})d\theta_j(-\boldsymbol{q})} = \left[i\frac{d^2S_0[\boldsymbol{f},\boldsymbol{\theta}]}{df_i(\boldsymbol{q})d\theta_j(-\boldsymbol{q})} + \frac{1}{2}\operatorname{Tr}\left(\mathcal{D}\frac{dA[\boldsymbol{f},\boldsymbol{\theta}]}{df_i(\boldsymbol{q})}\mathcal{D}\frac{dA[\boldsymbol{f},\boldsymbol{\theta}]}{d\theta_j(-\boldsymbol{q})}\right)\right.$$

$$\left. -\frac{1}{2}\operatorname{Tr}\left(\mathcal{D}\frac{d^2A[\boldsymbol{f},\boldsymbol{\theta}]}{df_i(\boldsymbol{q})d\theta_j(-\boldsymbol{q})}\right) + ...\right]\mathcal{Z}[\boldsymbol{f},\boldsymbol{\theta}]$$

$$+\left[i\frac{dS_0[\boldsymbol{f},\boldsymbol{\theta}]}{d\theta_j(-\boldsymbol{q})} - \frac{1}{2}\operatorname{Tr}\left(\mathcal{D}\frac{dA[\boldsymbol{f},\boldsymbol{\theta}]}{d\theta_j(-\boldsymbol{q})}\right) + ...\right]\frac{d\mathcal{Z}[\boldsymbol{f},\boldsymbol{\theta}]}{df_i(\boldsymbol{q})}, \tag{6.20}$$

where the higher order terms will vanish when the source fields are taken to zero. Furthermore, when $\boldsymbol{\theta} \to \boldsymbol{0}$, the action (Eq. (6.12)) becomes a proper Keldysh action in the sense that the $\bar{\psi}^q\psi^q$ term is zero. This means that $\mathcal{Z} = 1$ (see Section 4.2), so we have that $d\mathcal{Z}[\boldsymbol{f},\boldsymbol{0}]/df_i(\boldsymbol{q}) = 0$ and the bottom line vanishes. Therefore, from Eq. (6.14) we get for the static current-current response function the expression

$$\chi_{ij}(\boldsymbol{q}) = -\frac{i}{2}\left[i\frac{d^2S_0}{df_i(\boldsymbol{q})d\theta_j(-\boldsymbol{q})} + \frac{1}{2}\operatorname{Tr}\left(\mathcal{D}\frac{dA^{(1)}}{df_i(\boldsymbol{q})}\mathcal{D}\frac{dA^{(1)}}{d\theta_j(-\boldsymbol{q})}\right) - \frac{1}{2}\operatorname{Tr}\left(\mathcal{D}\frac{d^2A^{(2)}}{df_i(\boldsymbol{q})d\theta_j(-\boldsymbol{q})}\right)\right], \tag{6.21}$$

where $A^{(1)}$ and $A^{(2)}$ are first and second order in the source fields and all higher order terms disappear when the sources are set to zero. It is because the mean-field is a function of the source fields that S_0 and $A^{(2)}$ can be second order in the sources.

6.2.1 Definitions of terms

In what follows, we shall describe the various terms in Eq. (6.21) as:

- The mean-field response function:

$$\chi_{ij}^{mf}(\boldsymbol{q}) = \frac{1}{2}\frac{d^2S_0[\boldsymbol{f},\boldsymbol{\theta}]}{df_i(\boldsymbol{q})d\theta_j(-\boldsymbol{q})}, \tag{6.22}$$

  where we shall refer to the source-dependent mean-field action, $S_0[\boldsymbol{f},\boldsymbol{\theta}]$, as simply the mean-field action. By contrast, the source-free mean-field action will be called as such.

- The fluctuations response function:

$$\chi_{ij}^{fl}(\boldsymbol{q}) = \chi_{ij}^{A^{(1)}}(\boldsymbol{q}) + \chi_{ij}^{A^{(2)}}(\boldsymbol{q}), \tag{6.23}$$

$$= -\frac{i}{4}\operatorname{Tr}\left(\mathcal{D}\frac{dA^{(1)}[\boldsymbol{f},\boldsymbol{\theta}]}{df_i(\boldsymbol{q})}\mathcal{D}\frac{dA^{(1)}[\boldsymbol{f},\boldsymbol{\theta}]}{d\theta_j(-\boldsymbol{q})}\right) + \frac{i}{4}\operatorname{Tr}\left(\mathcal{D}\frac{d^2A^{(2)}[\boldsymbol{f},\boldsymbol{\theta}]}{df_i(\boldsymbol{q})d\theta_j(-\boldsymbol{q})}\right),$$

  where the matrices $A^{(1)}$ and $A^{(2)}$ will be referred to as the first and second order matrices. Because of this, the term $\chi_{ij}^{A^{(1)}}(\boldsymbol{q})$ containing factors of $A^{(1)}$ will be referred to as the first order response function and the term $\chi_{ij}^{A^{(2)}}(\boldsymbol{q})$ containing $A^{(2)}$ as the

second order response function. Note that this is just a naming convention based on the order in the source fields of the matrices that they contain, and that overall both $\chi_{ij}^{A^{(1)}}$ and $\chi_{ij}^{A^{(2)}}$ are independent of the source fields due to the differentiation.

Given that we already know the Green's functions $\mathcal{D}$ (Eq. (4.80)), to calculate the current-current response function we must find expressions for the mean-field action S_0 and the first and second order matrices $A^{(1)}$ and $A^{(2)}$.

6.3   Mean-field response function

To calculate the mean-field action we must first find an expression for the mean-field itself using the source-dependent action (Eq. (6.12)). To do this we follow the same procedure as in Section 5.2 and calculate the saddle point equations by differentiating the action by each field (where $k = (\omega, \boldsymbol{k})$) and setting them to zero:

$$
\begin{aligned}
\frac{dS}{d\bar{\psi}^c(k)} = {} & (\omega + \omega_p - \epsilon(\boldsymbol{k}) - i\kappa)\psi^q(k) \\
& -\frac{V}{2}\sum_{k',q}\Big(\bar{\psi}^q(k'+q)[\psi^c(k+q)\psi^c(k') + \psi^q(k+q)\psi^q(k')] \\
& \quad + 2\bar{\psi}^c(k'+q)\psi^q(k+q)\psi^c(k')\Big) \\
& + \sum_q \gamma_i(\boldsymbol{k}, \boldsymbol{k}-\boldsymbol{q})\left[\theta_i(\boldsymbol{q})\psi_\omega^c(\boldsymbol{k}-\boldsymbol{q}) + (f_i(\boldsymbol{q})+\theta_i(\boldsymbol{q}))\psi_\omega^q(\boldsymbol{k}-\boldsymbol{q})\right] = 0
\end{aligned}
\tag{6.24}
$$

$$
\begin{aligned}
\frac{dS}{d\psi^c(-k)} = {} & (-\omega + \omega_p - \epsilon(-\boldsymbol{k}) + i\kappa)\bar{\psi}^q(-k) \\
& -\frac{V}{2}\sum_{k',q}\Big(\psi^q(k'+q)[\bar{\psi}^c(-k+q)\bar{\psi}^c(k') + \bar{\psi}^q(-k+q)\bar{\psi}^q(k')] \\
& \quad + 2\psi^c(k'+q)\bar{\psi}^q(-k+q)\bar{\psi}^c(k')\Big) \\
& + \sum_q \gamma_i(-\boldsymbol{k}+\boldsymbol{q}, -\boldsymbol{k})\left[\theta_i(\boldsymbol{q})\bar{\psi}_{-\omega}^c(-\boldsymbol{k}+\boldsymbol{q}) + (f_i(\boldsymbol{q})-\theta_i(\boldsymbol{q}))\bar{\psi}_{-\omega}^q(-\boldsymbol{k}+\boldsymbol{q})\right] = 0
\end{aligned}
\tag{6.25}
$$

$$
\begin{aligned}
\frac{dS}{d\bar{\psi}^q(k)} = {} & (\omega + \omega_p - \epsilon(\boldsymbol{k}) + i\kappa)\psi^c(k) + 2i\kappa\psi^q(k) - \sqrt{2}F_p\delta_{k,0} \\
& -\frac{V}{2}\sum_{k',q}\Big(\bar{\psi}^c(k'+q)[\psi^c(k+q)\psi^c(k') + \psi^q(k+q)\psi^q(k')] \\
& \quad + 2\bar{\psi}^q(k'+q)\psi^q(k+q)\psi^c(k')\Big) \\
& + \sum_q \gamma_i(\boldsymbol{k}, \boldsymbol{k}-\boldsymbol{q})\left[(f_i(\boldsymbol{q})-\theta_i(\boldsymbol{q}))\psi_\omega^c(\boldsymbol{k}-\boldsymbol{q}) - \theta_i(\boldsymbol{q})\psi_\omega^q(\boldsymbol{k}-\boldsymbol{q})\right] = 0
\end{aligned}
\tag{6.26}
$$

$$\frac{dS}{d\psi^q(-k)} = (-\omega + \omega_p - \epsilon(-\boldsymbol{k}) - i\kappa)\bar{\psi}^c(-k) + 2i\kappa\bar{\psi}^q(-k) - \sqrt{2}F_p\delta_{-k,0} \qquad (6.27)$$

$$-\frac{V}{2}\sum_{k',q}\left(\psi^c(k'+q)[\bar{\psi}^c(-k+q)\bar{\psi}^c(k') + \bar{\psi}^q(-k+q)\bar{\psi}^q(k')]\right.$$

$$+2\psi^q(k'+q)\bar{\psi}^q(-k+q)\bar{\psi}^c(k')\Big)$$

$$+\sum_{q}\gamma_i(-\boldsymbol{k}+\boldsymbol{q},-\boldsymbol{k})\left[(f_i(\boldsymbol{q}) + \theta_i(\boldsymbol{q}))\bar{\psi}^c_{-\omega}(-\boldsymbol{k}+\boldsymbol{q}) - \theta_i(\boldsymbol{q})\bar{\psi}^q_{-\omega}(-\boldsymbol{k}+\boldsymbol{q})\right] = 0$$

The solution to these will be a function of the source fields $\boldsymbol{f}(\boldsymbol{q})$ and $\boldsymbol{\theta}(\boldsymbol{q})$. That is, our mean-field ansatz will take the form

$$\Psi(k) = \begin{pmatrix} \bar{\psi}^c(k) \\ \psi^c(-k) \\ \bar{\psi}^q(k) \\ \psi^q(-k) \end{pmatrix} \to \Psi_0(k) = \delta_{\omega,0}\left[\begin{pmatrix} \sqrt{2}\bar{\psi}_0 \\ \sqrt{2}\psi_0 \\ 0 \\ 0 \end{pmatrix}\delta_{\boldsymbol{k},\boldsymbol{0}} + \begin{pmatrix} \bar{X}^{(1)}_{\boldsymbol{k}} \\ X^{(1)}_{-\boldsymbol{k}} \\ \bar{Y}^{(1)}_{\boldsymbol{k}} \\ Y^{(1)}_{-\boldsymbol{k}} \end{pmatrix} + \begin{pmatrix} \bar{X}^{(2)}_{\boldsymbol{k}} \\ X^{(2)}_{-\boldsymbol{k}} \\ \bar{Y}^{(2)}_{\boldsymbol{k}} \\ Y^{(2)}_{-\boldsymbol{k}} \end{pmatrix}\right], \qquad (6.28)$$

where $X^{(1)}/Y^{(1)}$ and $X^{(2)}/Y^{(2)}$ are first and second order in the source fields, respectively, and due to the existence of finite quantum saddle points do not necessarily respect conjugacy relations. We shall refer to them as the first and second order mean-fields (as opposed to the zeroth order mean-field, ψ_0). Higher order terms are not relevant to the response function as they are set to zero after the differentiation in Eq. (6.14). Given this ansatz, the mean-field action is

$$S_0 = S[\Psi_0 = \Psi_{00} + \delta\Psi_0^{(1)} + \delta\Psi_0^{(2)}], \qquad (6.29)$$

where Ψ_{00}, $\delta\Psi^{(1)}$, and $\delta\Psi^{(2)}$ are the three vectors on the right-hand side of Eq. (6.28). To calculate this, we expand around the zeroth order term Ψ_{00}:

$$S_0[\Psi_{00} + \delta\Psi_0^{(1)}] = S_{00} + \delta S_0^{(1)} + \delta S_0^{(2)} \qquad (6.30)$$

$$= S_0[\Psi_{00}] + \sum_{k}\frac{dS_0}{d\Psi_0(k)}\bigg|_{\Psi_0=\Psi_{00}}\delta\Psi_0^{(1)}(k) \qquad (6.31)$$

$$+ \frac{1}{2}\sum_{k,k'}\delta\bar{\Psi}_0^{(1)}(k)\frac{d^2S_0}{d\bar{\Psi}_0(k)d\Psi_0(k')}\bigg|_{\Psi_0=\Psi_{00}}\delta\Psi_0^{(1)}(k').$$

Because the derivative of the source-free action at the source-free saddle point is zero (by definition), the only terms in $dS_0/d\Psi_0|_{\Psi_0=\Psi_{00}}$ that survive are those containing source fields. This means that no second order $X^{(2)}$ and $Y^{(2)}$ terms can contribute to the mean-field response function as they would lead to terms at least third order in the sources.

6.3.1 First order equations

Substituting the mean-field ansatz into the saddle point equations, we may equate terms that are first order in the source fields and use them to find expressions for $X^{(1)}$ and $Y^{(1)}$. Combined with the expression for the zeroth order mean field, ψ_0, which was calculated in Section 5.2, we can use these to find the mean-field action through the expansion in Eq. (6.31). In line with the definition beneath Eq. (4.72), we introduce the shorthand

$$J(\pm\boldsymbol{k}) \equiv \omega_p - \epsilon(\pm\boldsymbol{k}) + i\kappa - 2V\bar{\psi}_0\psi_0, \tag{6.32}$$

and equate the terms in the saddle point equations that are first order in the source fields:

$$J(\boldsymbol{k})X_{\boldsymbol{k}}^{(1)} - V\psi_0^2\bar{X}_{-\boldsymbol{k}}^{(1)} = -2i\kappa Y_{\boldsymbol{k}}^{(1)} - \sqrt{2}\psi_0\gamma_i(\boldsymbol{k})[f_i(\boldsymbol{k}) - \theta_i(\boldsymbol{k})], \tag{6.33}$$

$$J^*(-\boldsymbol{k})\bar{X}_{-\boldsymbol{k}}^{(1)} - V\bar{\psi}_0^2 X_{\boldsymbol{k}}^{(1)} = -2i\kappa\bar{Y}_{-\boldsymbol{k}}^{(1)} - \sqrt{2}\bar{\psi}_0\gamma_i(-\boldsymbol{k})[f_i(\boldsymbol{k}) + \theta_i(\boldsymbol{k})], \tag{6.34}$$

$$J^*(\boldsymbol{k})Y_{\boldsymbol{k}}^{(1)} - V\psi_0^2\bar{Y}_{-\boldsymbol{k}}^{(1)} = -\sqrt{2}\psi_0\gamma_i(\boldsymbol{k})\theta_i(\boldsymbol{k}), \tag{6.35}$$

$$J(-\boldsymbol{k})\bar{Y}_{-\boldsymbol{k}}^{(1)} - V\bar{\psi}_0^2 Y_{\boldsymbol{k}}^{(1)} = -\sqrt{2}\bar{\psi}_0\gamma_i(-\boldsymbol{k})\theta_i(\boldsymbol{k}). \tag{6.36}$$

Arranging these as two matrix equations,

$$M_X^{(1)}\boldsymbol{X}^{(1)} = C_X^{(1)}, \qquad\qquad M_Y^{(1)}\boldsymbol{Y}^{(1)} = C_Y^{(1)}, \tag{6.37}$$

where $\boldsymbol{X}^{(1)} = (X_{\boldsymbol{k}}^{(1)}, \bar{X}_{-\boldsymbol{k}}^{(1)})^T$ and $\boldsymbol{Y}^{(1)} = (Y_{\boldsymbol{k}}^{(1)}, \bar{Y}_{-\boldsymbol{k}}^{(1)})^T$, we can invert $M_X^{(1)}$ and $M_Y^{(1)}$ and solve for $\boldsymbol{X}^{(1)}$ and $\boldsymbol{Y}^{(1)}$:

$$\begin{pmatrix} X_{\boldsymbol{k}}^{(1)} \\ \bar{X}_{-\boldsymbol{k}}^{(1)} \end{pmatrix} = \frac{\sqrt{2}}{V^2\bar{\psi}_0^2\psi_0^2 - J(\boldsymbol{k})J^*(-\boldsymbol{k})} \tag{6.38}$$

$$\times \begin{pmatrix} J^*(-\boldsymbol{k})\psi_0\gamma_i(\boldsymbol{k})\left[f_i(\boldsymbol{k}) - \theta_i(\boldsymbol{k})\right] + V\bar{\psi}_0\psi_0^2\gamma_i(-\boldsymbol{k})\left[f_i(\boldsymbol{k}) + \theta_i(\boldsymbol{k})\right] \\ J(\boldsymbol{k})\bar{\psi}_0\gamma_i(-\boldsymbol{k})\left[f_i(\boldsymbol{k}) + \theta_i(\boldsymbol{k})\right] + V\bar{\psi}_0^2\psi_0\gamma_i(\boldsymbol{k})\left[f_i(\boldsymbol{k}) - \theta_i(\boldsymbol{k})\right] \end{pmatrix}$$

$$+ \frac{2\sqrt{2}i\kappa}{\left[V^2\bar{\psi}_0^2\psi_0^2 - J(\boldsymbol{k})J^*(-\boldsymbol{k})\right]\left[V^2\bar{\psi}_0^2\psi_0^2 - J^*(\boldsymbol{k})J(-\boldsymbol{k})\right]}\theta_i(\boldsymbol{k})$$

$$\times \begin{pmatrix} [J(-\boldsymbol{k})J^*(-\boldsymbol{k})\psi_0 + V^2\bar{\psi}_0^2\psi_0^3]\gamma_i(\boldsymbol{k}) + [J^*(-\boldsymbol{k}) + J^*(\boldsymbol{k})]V\bar{\psi}_0\psi_0^2\gamma_i(-\boldsymbol{k}) \\ [J(\boldsymbol{k})J^*(\boldsymbol{k})\bar{\psi}_0 + V^2\bar{\psi}_0^3\psi_0^2]\gamma_i(-\boldsymbol{k}) + [J(\boldsymbol{k}) + J(-\boldsymbol{k})]V\bar{\psi}_0^2\psi_0\gamma_i(\boldsymbol{k}) \end{pmatrix},$$

$$\begin{pmatrix} Y_{\boldsymbol{k}}^{(1)} \\ \bar{Y}_{-\boldsymbol{k}}^{(1)} \end{pmatrix} = \frac{\sqrt{2}\,\theta_i(\boldsymbol{k})}{V^2\bar{\psi}_0^2\psi_0^2 - J^*(\boldsymbol{k})J(-\boldsymbol{k})} \begin{pmatrix} J(-\boldsymbol{k})\psi_0\gamma_i(\boldsymbol{k}) + V\bar{\psi}_0\psi_0^2\gamma_i(-\boldsymbol{k}) \\ J^*(\boldsymbol{k})\bar{\psi}_0\gamma_i(-\boldsymbol{k}) + V\bar{\psi}_0^2\psi_0\gamma_i(\boldsymbol{k}) \end{pmatrix}. \tag{6.39}$$

6.3.2   First order correction to the mean-field action

From Eq. (6.31), we see that to find the first order correction to the mean-field action, $\delta S_0^{(1)}$, we must calculate $dS_0/d\Psi_0(k)|_{\Psi_0=\Psi_{00}}$. This can be done by evaluating the saddle point equations (Eqs. (6.24-6.27)) at Ψ_{00}:

$$\left.\frac{dS}{d\bar{\psi}^c(k)}\right|_{\Psi=\Psi_{00}} = \sqrt{2}\psi_0\gamma_i(\boldsymbol{k})\theta_i(\boldsymbol{k})\delta_{\omega,0}, \tag{6.40}$$

$$\left.\frac{dS}{d\psi^c(-k)}\right|_{\Psi=\Psi_{00}} = \sqrt{2}\bar{\psi}_0\gamma_i(-\boldsymbol{k})\theta_i(\boldsymbol{k})\delta_{-\omega,0}, \tag{6.41}$$

$$\left.\frac{dS}{d\bar{\psi}^q(k)}\right|_{\Psi=\Psi_{00}} = \sqrt{2}\psi_0\gamma_i(\boldsymbol{k})(f_i(\boldsymbol{k}) - \theta_i(\boldsymbol{k}))\delta_{\omega,0}, \tag{6.42}$$

$$\left.\frac{dS}{d\psi^q(-k)}\right|_{\Psi=\Psi_{00}} = \sqrt{2}\bar{\psi}_0\gamma_i(-\boldsymbol{k})(f_i(\boldsymbol{k}) + \theta_i(\boldsymbol{k}))\delta_{-\omega,0}, \tag{6.43}$$

where the zeroth order terms disappear due to the definition of the source-free saddle point. The first order correction is thus given by

$$\delta S_0^{(1)} = \sum_k \left.\frac{dS_0}{d\Psi_0(k)}\right|_{\Psi_0=\Psi_{00}} \delta\Psi_0^{(1)}(k), \tag{6.44}$$

$$= \sqrt{2}\sum_k \begin{pmatrix} \psi_0\gamma_i(\boldsymbol{k})\theta_i(\boldsymbol{k}) \\ \bar{\psi}_0\gamma_i(-\boldsymbol{k})\theta_i(\boldsymbol{k}) \\ \psi_0\gamma_i(\boldsymbol{k})(f_i(\boldsymbol{k}) - \theta_i(\boldsymbol{k})) \\ \bar{\psi}_0\gamma_i(-\boldsymbol{k})(f_i(\boldsymbol{k}) + \theta_i(\boldsymbol{k})) \end{pmatrix}^T \begin{pmatrix} \bar{X}_{\boldsymbol{k}}^{(1)} \\ X_{-\boldsymbol{k}}^{(1)} \\ \bar{Y}_{\boldsymbol{k}}^{(1)} \\ Y_{-\boldsymbol{k}}^{(1)} \end{pmatrix}, \tag{6.45}$$

where it should be borne in mind that only first order mixed terms, e.g. those proportional to $f_i\theta_j$, survive the eventual differentiation. Thus, the relevant component of the first order correction is

$$\delta S_0^{(1)} = \sum_k \frac{4\bar{\psi}_0\psi_0 f_i(\boldsymbol{k})\theta_j(-\boldsymbol{k})}{V^2\bar{\psi}_0^2\psi_0^2 - J(\boldsymbol{k})J^*(-\boldsymbol{k})} \Big(J(\boldsymbol{k})\gamma_i(-\boldsymbol{k})\gamma_j(-\boldsymbol{k}) \tag{6.46}$$

$$+ V\bar{\psi}_0\psi_0\gamma_i(\boldsymbol{k})\gamma_j(-\boldsymbol{k}) + J^*(-\boldsymbol{k})\gamma_i(\boldsymbol{k})\gamma_j(\boldsymbol{k}) + V\bar{\psi}_0\psi_0\gamma_i(-\boldsymbol{k})\gamma_j(\boldsymbol{k}) \Big).$$

6.3.3   Second order correction to the mean-field action

To calculate the second order correction, $\delta S_0^{(2)}$, in Eq. (6.31), we must find $d^2 S_0/d\bar{\Psi}_0(k)d\Psi_0(k')|_{\Psi_0=\Psi_{00}}$. We can do so by evaluating the second derivative matrix of the action,

$$S'' \equiv \begin{pmatrix} d/d\bar{\psi}^c(k) \\ d/d\psi^c(-k) \\ d/d\bar{\psi}^q(k) \\ d/d\psi^q(-k) \end{pmatrix} \begin{pmatrix} d/d\psi^c(k') \\ d/d\bar{\psi}^c(-k') \\ d/d\psi^q(k') \\ d/d\bar{\psi}^q(-k') \end{pmatrix}^T S, \tag{6.47}$$

at $\Psi = \Psi_{00}$, where due to the differentiation in Eq. (6.22) only terms that do not depend on the source fields will contribute. Consequently, the only relevant terms in S'' are those in the inverse matrix of Green's functions (Eq. 4.72) with $\omega = 0$, and so we have that

$$\delta S_0^{(2)} = \frac{1}{2}\sum_{k,k'}\delta\bar{\Psi}_0^{(1)}(k)\left.\frac{d^2 S_0}{d\bar{\Psi}_0(k)d\Psi_0(k')}\right|_{\Psi_0=\Psi_{00}}\delta\Psi_0^{(1)}(k'), \tag{6.48}$$

$$= \frac{1}{2}\sum_k \begin{pmatrix} \bar{X}_{k'}^{(1)} \\ X_{-k'}^{(1)} \\ \bar{Y}_{k'}^{(1)} \\ Y_{-k'}^{(1)} \end{pmatrix}^T \begin{pmatrix} 0 & 0 & J^*(\boldsymbol{k}) & -V\psi_0^2 \\ 0 & 0 & -V\bar{\psi}_0^2 & J(-\boldsymbol{k}) \\ J(\boldsymbol{k}) & -V\psi_0^2 & 2i\kappa & 0 \\ -V\bar{\psi}_0^2 & J^*(-\boldsymbol{k}) & 0 & 2i\kappa \end{pmatrix} \begin{pmatrix} X_{\boldsymbol{k}}^{(1)} \\ \bar{X}_{-\boldsymbol{k}}^{(1)} \\ Y_{\boldsymbol{k}}^{(1)} \\ \bar{Y}_{-\boldsymbol{k}}^{(1)} \end{pmatrix}, \tag{6.49}$$

Recognising again that only terms containing both source fields contribute to the response function (and therefore $Y^{(1)}Y^{(1)}$ terms do not), the second order correction to the mean-field action is

$$\delta S_0^{(2)} = -\sum_{\boldsymbol{k}}\frac{2\bar{\psi}_0\psi_0 f_i(\boldsymbol{k})\theta_j(-\boldsymbol{k})}{V^2\bar{\psi}_0^2\psi_0^2 - J(\boldsymbol{k})J^*(-\boldsymbol{k})}\Big(J(\boldsymbol{k})\gamma_i(-\boldsymbol{k})\gamma_j(-\boldsymbol{k}) \tag{6.50}$$

$$+V\bar{\psi}_0\psi_0\gamma_i(\boldsymbol{k})\gamma_j(-\boldsymbol{k}) + J^*(-\boldsymbol{k})\gamma_i(\boldsymbol{k})\gamma_j(\boldsymbol{k}) + V\bar{\psi}_0\psi_0\gamma_i(-\boldsymbol{k})\gamma_j(\boldsymbol{k})\Big).$$

6.3.4   Combined mean-field response function

The zeroth order term in Eq. (6.31) disappears when differentiated, so the mean-field response function (Eq. (6.22)) is given by

$$\chi_{ij}^{mf}(\boldsymbol{q}) = \frac{1}{2}\frac{d^2(\delta S^{(1)} + \delta S^{(2)})}{df_i(\boldsymbol{q})d\theta_j(-\boldsymbol{q})} \tag{6.51}$$

$$= -\frac{\bar{\psi}_0\psi_0}{J(\boldsymbol{q})J^*(-\boldsymbol{q}) - V^2\bar{\psi}_0^2\psi_0^2}\Big(J(\boldsymbol{q})\gamma_i(-\boldsymbol{q})\gamma_j(-\boldsymbol{q}) \tag{6.52}$$

$$+V\bar{\psi}_0\psi_0\gamma_i(-\boldsymbol{q})\gamma_j(\boldsymbol{q}) + V\bar{\psi}_0\psi_0\gamma_i(\boldsymbol{q})\gamma_j(-\boldsymbol{q}) + J^*(-\boldsymbol{q})\gamma_i(\boldsymbol{q})\gamma_j(\boldsymbol{q})\Big).$$

We note that the denominator here is equal to the determinant of the inverse retarded Green's function (Eq. (5.1)) at $\omega = 0$, i.e. $J(\boldsymbol{q})J^*(-\boldsymbol{q}) - V^2 |\psi_0|^4 = \det[(D^R)^{-1}(\omega = 0, \boldsymbol{q})]$. Using the shorthand

$$K(\boldsymbol{q}) \equiv -\frac{2}{J(\boldsymbol{q})J^*(-\boldsymbol{q}) - V^2 |\psi_0|^4}, \tag{6.53}$$

we may rewrite the mean-field response function as

$$\chi_{ij}^{mf}(\boldsymbol{q}) = \sum_{\sigma,\sigma' \in \pm} c_{\sigma,\sigma'}^{mf}(\boldsymbol{q}) \gamma_i(\sigma\boldsymbol{q}) \gamma_j(\sigma'\boldsymbol{q}), \tag{6.54}$$

where the coefficients $c_{\sigma,\sigma'}^{mf}(\boldsymbol{q})$ are

$$c_{+,+}^{mf}(\boldsymbol{q}) = \frac{1}{2} |\psi_0|^2 K(\boldsymbol{q}) J^*(-\boldsymbol{q}), \tag{6.55}$$

$$c_{+,-}^{mf}(\boldsymbol{q}) = c_{-,+}^{mf}(\boldsymbol{q}) = \frac{1}{2} |\psi_0|^2 K(\boldsymbol{q}) V |\psi_0|^2, \tag{6.56}$$

$$c_{-,-}^{mf}(\boldsymbol{q}) = \frac{1}{2} |\psi_0|^2 K(\boldsymbol{q}) J(\boldsymbol{q}). \tag{6.57}$$

6.4 Fluctuations response function

To calculate the fluctuations response function (Eq. (6.23)), we note from the expression for the partition function given in Eq. (6.15) that the second derivative matrix (Eq. (6.47)) evaluated at the mean-field gives the first and second order matrices $A^{(1)}$ and $A^{(2)}$ via the expression

$$S''|_{\Psi=\Psi_0} = \mathcal{D}^{-1} + A^{(1)} + A^{(2)}. \tag{6.58}$$

Full calculations of $S''|_{\Psi=\Psi_0}$, $A^{(1)}$, and $A^{(2)}$, as well as the derivatives of the latter with respect to the source fields, are given in Appendix A.

6.4.1 First order term

To calculate the first order response function, $\chi_{ij}^{A^{(1)}}(\boldsymbol{q})$, we have from Appendix A.2 that

$$\frac{dA^{(1)}(k, k')}{df_i(\boldsymbol{q})} = \begin{pmatrix} 0 & a_i(\boldsymbol{k}, \boldsymbol{k}') \\ a_i(\boldsymbol{k}, \boldsymbol{k}') & 0 \end{pmatrix} \delta_{\boldsymbol{k}, \boldsymbol{k}'+\boldsymbol{q}} \delta_{\omega, \omega'}, \tag{6.59}$$

$$\frac{dA^{(1)}(k, k')}{d\theta_j(-\boldsymbol{q})} = \begin{pmatrix} b_{11j}(\boldsymbol{k}, \boldsymbol{k}') & b_{12j}(\boldsymbol{k}, \boldsymbol{k}') \\ b_{21j}(\boldsymbol{k}, \boldsymbol{k}') & b_{22j}(\boldsymbol{k}, \boldsymbol{k}') \end{pmatrix} \delta_{\boldsymbol{k}+\boldsymbol{q}, \boldsymbol{k}'} \delta_{\omega, \omega'}, \tag{6.60}$$

with a and b_{XX} given by Eqs. (A.36), (A.38), and (A.39). For a finite volume, filling in the momentum and frequency arguments explicitly gives

$$\chi_{ij}^{A^{(1)}}(\boldsymbol{q}) = -\frac{i}{4} \sum_{\omega,\omega',\nu,\nu'} \sum_{\boldsymbol{k},\boldsymbol{k}',\boldsymbol{p},\boldsymbol{p}'} \mathrm{Tr} \left(\mathcal{D}_{\omega\nu,\boldsymbol{kp}} \frac{dA_{\nu\omega',\boldsymbol{pk}'}^{(1)}}{df_i(\boldsymbol{q})} \mathcal{D}_{\omega'\nu',\boldsymbol{k}'\boldsymbol{p}'} \frac{dA_{\nu'\omega,\boldsymbol{p}'\boldsymbol{k}}^{(1)}}{d\theta_j(-\boldsymbol{q})} \right). \tag{6.61}$$

Now, $\mathcal{D}_{\omega\omega',\boldsymbol{kk}'} \sim \delta_{\omega,\omega'}\delta_{\boldsymbol{k},\boldsymbol{k}'}$ (Eq. (4.72)) and $A^{(1)} \sim \delta_{\omega,\omega'}$, so this expression becomes

$$\chi_{ij}^{A^{(1)}}(\boldsymbol{q}) = -\frac{i}{4} \sum_{\omega,\boldsymbol{k},\boldsymbol{k}'} \mathrm{Tr} \left(\mathcal{D}_{\omega,\boldsymbol{k}} \frac{dA_{\boldsymbol{kk}'}^{(1)}}{df_i(\boldsymbol{q})} \mathcal{D}_{\omega,\boldsymbol{k}'} \frac{dA_{\boldsymbol{k}'\boldsymbol{k}}^{(1)}}{d\theta_j(-\boldsymbol{q})} \right). \tag{6.62}$$

Substituting in the Green's functions and Eqs. (6.59) and (6.60) (and swapping $\boldsymbol{k}$ and $\boldsymbol{k}'$ in the latter) gives

$$
\begin{aligned}
\chi_{ij}^{A^{(1)}}(\boldsymbol{q}) &= -\frac{i}{4} \sum_{\omega,\boldsymbol{k},\boldsymbol{k}'} \mathrm{Tr} \left[\begin{pmatrix} D^K(\omega,\boldsymbol{k}) & D^R(\omega,\boldsymbol{k}) \\ D^A(\omega,\boldsymbol{k}) & 0 \end{pmatrix} \begin{pmatrix} 0 & a_i(\boldsymbol{k},\boldsymbol{k}') \\ a_i(\boldsymbol{k},\boldsymbol{k}') & 0 \end{pmatrix} \delta_{\boldsymbol{k},\boldsymbol{k}'+\boldsymbol{q}} \right. \\
&\quad \left. \times \begin{pmatrix} D^K(\omega,\boldsymbol{k}') & D^R(\omega,\boldsymbol{k}') \\ D^A(\omega,\boldsymbol{k}') & 0 \end{pmatrix} \begin{pmatrix} b_{11j}(\boldsymbol{k}',\boldsymbol{k}) & b_{12j}(\boldsymbol{k}',\boldsymbol{k}) \\ b_{21j}(\boldsymbol{k}',\boldsymbol{k}) & b_{22j}(\boldsymbol{k}',\boldsymbol{k}) \end{pmatrix} \delta_{\boldsymbol{k},\boldsymbol{k}'+\boldsymbol{q}} \right].
\end{aligned}
$$

The two Kronecker deltas in momentum are identical, so summing over one sets the other to 1. Performing this and taking the continuum limit gives

$$
\begin{aligned}
\chi_{ij}^{A^{(1)}}(\boldsymbol{q}) &= -\frac{i}{4} \int \frac{dk_x}{2\pi} \frac{dk_y}{2\pi} \frac{d\omega}{2\pi} \mathrm{Tr} \left[\begin{pmatrix} D^K(\omega,\boldsymbol{k}+\boldsymbol{q}) & D^R(\omega,\boldsymbol{k}+\boldsymbol{q}) \\ D^A(\omega,\boldsymbol{k}+\boldsymbol{q}) & 0 \end{pmatrix} \right. \\
&\quad \times \begin{pmatrix} 0 & a_i(\boldsymbol{k}+\boldsymbol{q},\boldsymbol{k}) \\ a_i(\boldsymbol{k}+\boldsymbol{q},\boldsymbol{k}) & 0 \end{pmatrix} \\
&\quad \left. \times \begin{pmatrix} D^K(\omega,\boldsymbol{k}) & D^R(\omega,\boldsymbol{k}) \\ D^A(\omega,\boldsymbol{k}) & 0 \end{pmatrix} \begin{pmatrix} b_{11j}(\boldsymbol{k},\boldsymbol{k}+\boldsymbol{q}) & b_{12j}(\boldsymbol{k},\boldsymbol{k}+\boldsymbol{q}) \\ b_{21j}(\boldsymbol{k},\boldsymbol{k}+\boldsymbol{q}) & b_{22j}(\boldsymbol{k},\boldsymbol{k}+\boldsymbol{q}) \end{pmatrix} \right], \tag{6.63}
\end{aligned}
$$

$$
\begin{aligned}
&= -\frac{i}{4} \int \frac{dk_x}{2\pi} \frac{dk_y}{2\pi} \frac{d\omega}{2\pi} \mathrm{Tr} \left[D^R(\omega,\boldsymbol{k}+\boldsymbol{q})a_i(\boldsymbol{k}+\boldsymbol{q},\boldsymbol{k})D^K(\omega,\boldsymbol{k})b_{11j}(\boldsymbol{k},\boldsymbol{k}+\boldsymbol{q}) \right. \\
&\quad + D^K(\omega,\boldsymbol{k}+\boldsymbol{q})a_i(\boldsymbol{k}+\boldsymbol{q},\boldsymbol{k})D^A(\omega,\boldsymbol{k})b_{11j}(\boldsymbol{k},\boldsymbol{k}+\boldsymbol{q}) \tag{6.64} \\
&\quad + D^R(\omega,\boldsymbol{k}+\boldsymbol{q})a_i(\boldsymbol{k}+\boldsymbol{q},\boldsymbol{k})D^R(\omega,\boldsymbol{k})b_{21j}(\boldsymbol{k},\boldsymbol{k}+\boldsymbol{q}) \\
&\quad \left. + D^A(\omega,\boldsymbol{k}+\boldsymbol{q})a_i(\boldsymbol{k}+\boldsymbol{q},\boldsymbol{k})D^A(\omega,\boldsymbol{k})b_{12j}(\boldsymbol{k},\boldsymbol{k}+\boldsymbol{q}) \right].
\end{aligned}
$$

For an explanation of how length and time factors in a finite volume relate to this limit, see Appendix B.

The retarded and advanced Green's functions are defined by causality as having all their poles in the lower and upper half planes, respectively[59]. As the frequency integral may be performed using complex contour integration, then by Cauchy's theorem the last two terms in Eq. (6.64), which are products of $D^R D^R$ and $D^A D^A$, will be zero[95]. This leaves b_{11} as the only relevant 'b' term, which we relabel as simply b. The first order response function is thus given by

$$
\chi_{ij}^{A^{(1)}}(\boldsymbol{q}) = -\frac{i}{4} \int \frac{dk_x}{2\pi} \frac{dk_y}{2\pi} \frac{d\omega}{2\pi} \operatorname{Tr}\left[D^R(\omega, \boldsymbol{k}+\boldsymbol{q}) a_i(\boldsymbol{k}+\boldsymbol{q}, \boldsymbol{k}) D^K(\omega, \boldsymbol{k}) b_j(\boldsymbol{k}, \boldsymbol{k}+\boldsymbol{q}) \right.
$$
$$
\left. + D^K(\omega, \boldsymbol{k}+\boldsymbol{q}) a_i(\boldsymbol{k}+\boldsymbol{q}, \boldsymbol{k}) D^A(\omega, \boldsymbol{k}) b_j(\boldsymbol{k}, \boldsymbol{k}+\boldsymbol{q}) \right], \tag{6.65}
$$

where the matrices $a_i(\boldsymbol{k}+\boldsymbol{q}, \boldsymbol{k})$ and $b_j(\boldsymbol{k}, \boldsymbol{k}+\boldsymbol{q})$ are given in Appendix A.3.

6.4.2 Second order term

To calculate the second order response function, $\chi_{ij}^{A^{(2)}}(\boldsymbol{q})$, we need to find the second order matrix $A^{(2)}$. By examining the terms in $S''|_{\Psi=\Psi_0}$ (Eqs. (A.2-A.17)) that are second order in the source fields, we see there are only six distinct elements in $A^{(2)}$:

$$
A^{(2)} = \begin{pmatrix} A_1^{(2)} & A_2^{(2)} \\ A_2^{(2)} & A_1^{(2)} \end{pmatrix} \delta_{\omega,\omega'} = \begin{pmatrix} A_A^{(2)} & A_B^{(2)} & A_D^{(2)} & A_E^{(2)} \\ A_C^{(2)} & A_A^{(2)} & A_F^{(2)} & A_D^{(2)} \\ A_D^{(2)} & A_E^{(2)} & A_A^{(2)} & A_B^{(2)} \\ A_F^{(2)} & A_D^{(2)} & A_C^{(2)} & A_A^{(2)} \end{pmatrix} \delta_{\omega,\omega'}. \tag{6.66}
$$

Starting with the expression for $\chi_{ij}^{A^{(2)}}$ on the second line of Eq. (6.23) and holding off on the differentiation for now, we may multiply it out using Eq. (6.66) above to get

$$
\operatorname{Tr}\left[\mathcal{D} A^{(2)} \right] = \operatorname{Tr}\left[\begin{pmatrix} D^K & D^R \\ D^A & 0 \end{pmatrix} \begin{pmatrix} A_1^{(2)} & A_2^{(2)} \\ A_2^{(2)} & A_1^{(2)} \end{pmatrix} \right] \tag{6.67}
$$

$$
= \operatorname{Tr}\left[D^K A_1^{(2)} + (D^R + D^A) A_2^{(2)} \right]. \tag{6.68}
$$

The retarded and advanced Green's functions, Eqs. (4.73) and (4.74), can be written as

$$
D^R = \frac{1}{d(\omega)} \begin{pmatrix} J^*(-\omega) & V\psi_0^2 \\ V\bar{\psi}_0^2 & J(\omega) \end{pmatrix}, \qquad D^A = \frac{1}{d^*(\omega)} \begin{pmatrix} J(-\omega) & V\psi_0^2 \\ V\bar{\psi}_0^2 & J^*(\omega) \end{pmatrix}, \tag{6.69}
$$

where we have relabelled $d(\omega) = J(\omega)J^*(-\omega) - V^2 |\psi_0|^4$ and ignored the momentum dependence. Eq. (6.67) then becomes

$$
\begin{aligned}
\text{Tr}\left[\mathcal{D}A^{(2)}\right] &= \text{Tr}\left[D^K A_1^{(2)} + \left(\frac{1}{d(\omega)}\begin{pmatrix} J^*(-\omega) & V\psi_0^2 \\ V\bar{\psi}_0^2 & J(\omega) \end{pmatrix}\right.\right. \\
&\qquad\left.\left. + \frac{1}{d^*(\omega)}\begin{pmatrix} J(-\omega) & V\psi_0^2 \\ V\bar{\psi}_0^2 & J^*(\omega) \end{pmatrix}\right)\begin{pmatrix} A_D^{(2)} & A_E^{(2)} \\ A_F^{(2)} & A_D^{(2)} \end{pmatrix}\right] \\
&= \text{Tr}\left[D^K A_1^{(2)}\right] + A_D\left[\frac{J^*(-\omega)+J(\omega)}{d(\omega)} + \frac{J(-\omega)+J^*(\omega)}{d^*(\omega)}\right] \\
&\quad + V\left(\bar{\psi}_0^2 A_E + \psi_0^2 A_F\right)\left[\frac{1}{d(\omega)} + \frac{1}{d^*(\omega)}\right].
\end{aligned}
$$

(6.70)

Given that all the zeros of $d(\omega)$ are in one half plane, that $d(\omega) \sim \omega^2$ at large ω, and that the factors of frequency cancel in $J(-\omega) + J^*(\omega)$, both the second two terms disappear due to Cauchy's theorem upon integration over frequency. Consequently, $A_1^{(2)}$ is the only term in Eq. (6.66) relevant to the calculation of the response function.

Collecting terms second order in the source fields in the matrix of second derivatives (Eqs. (A.2-A.17)), we see that the relevant three terms in the second order matrix are:

$$
A_A^{(2)} = -V\left[\sum_{\boldsymbol{q}'}(\bar{X}_{\boldsymbol{q}'}^{(1)} Y_{\boldsymbol{q}'}^{(1)} + \bar{Y}_{\boldsymbol{q}'}^{(1)} X_{\boldsymbol{q}'}^{(1)}) + \sqrt{2}\bar{\psi}_0 Y_{\boldsymbol{0}}^{(2)} + \sqrt{2}\psi_0 \bar{Y}_{\boldsymbol{0}}^{(2)}\right],
$$

(6.71)

$$
A_B^{(2)} = -V\left[\sum_{\boldsymbol{q}'} X_{\boldsymbol{q}'}^{(1)} Y_{-\boldsymbol{q}'}^{(1)} + \sqrt{2}\psi_0 Y_{\boldsymbol{0}}^{(2)}\right],
$$

(6.72)

$$
A_C^{(2)} = -V\left[\sum_{\boldsymbol{q}'} \bar{X}_{-\boldsymbol{q}'}^{(1)} \bar{Y}_{\boldsymbol{q}'}^{(1)} + \sqrt{2}\bar{\psi}_0 \bar{Y}_{\boldsymbol{0}}^{(2)}\right].
$$

(6.73)

Note here that the momentum $\boldsymbol{q}$ in Eqs. (A.2-A.17) is not the same as in the calculation of the response function (Eq. (6.14)), so it has been relabelled in the above as $\boldsymbol{q}'$. Additionally, we have shifted $\boldsymbol{q}' \to \boldsymbol{q}' - \boldsymbol{k}$ and, anticipating taking the trace, set $\boldsymbol{k} = \boldsymbol{k}'$.

6.4.3 Second order equations

From Eqs. (6.71-6.73), we see that to calculate the second order matrix we need to find the second order mean-field $Y^{(2)}$. Equating the terms in the saddle point equations that are

second order in the source fields gives:

$$
\begin{aligned}
J(\boldsymbol{k})X_{\boldsymbol{k}}^{(2)} - V\psi_0^2 \bar{X}_{-\boldsymbol{k}}^{(2)} = & -\sum_{\boldsymbol{q}}\Big[\gamma_i(\boldsymbol{k},\boldsymbol{k}-\boldsymbol{q})\Big([f_i(\boldsymbol{q})-\theta_i(\boldsymbol{q})]X_{\boldsymbol{k}-\boldsymbol{q}}^{(1)} - \theta_i(\boldsymbol{q})Y_{\boldsymbol{k}-\boldsymbol{q}}^{(1)}\Big) \\
& -\sqrt{2}V\Big(\psi_0 \bar{X}_{-\boldsymbol{q}}^{(1)} X_{\boldsymbol{k}-\boldsymbol{q}}^{(1)} + \tfrac{1}{2}\bar{\psi}_0 X_{\boldsymbol{q}}^{(1)} X_{\boldsymbol{k}-\boldsymbol{q}}^{(1)} + \tfrac{1}{2}\bar{\psi}_0 Y_{\boldsymbol{q}}^{(1)} Y_{\boldsymbol{k}-\boldsymbol{q}}^{(1)} \\
& +\psi_0 \bar{Y}_{-\boldsymbol{q}}^{(1)} Y_{\boldsymbol{k}-\boldsymbol{q}}^{(1)}\Big)\Big] - 2i\kappa Y_{\boldsymbol{k}}^{(2)},
\end{aligned}
$$

$$
\begin{aligned}
J^*(-\boldsymbol{k})\bar{X}_{-\boldsymbol{k}}^{(2)} - V\bar{\psi}_0^2 X_{\boldsymbol{k}}^{(2)} = & -\sum_{\boldsymbol{q}}\Big[\gamma_i(-\boldsymbol{k}+\boldsymbol{q},-\boldsymbol{k})\Big([f_i(\boldsymbol{q})+\theta_i(\boldsymbol{q})]\bar{X}_{-\boldsymbol{k}+\boldsymbol{q}}^{(1)} - \theta_i(\boldsymbol{q})\bar{Y}_{-\boldsymbol{k}+\boldsymbol{q}}^{(1)}\Big) \\
& -\sqrt{2}V\Big(\bar{\psi}_0 \bar{X}_{-\boldsymbol{q}}^{(1)} X_{\boldsymbol{k}-\boldsymbol{q}}^{(1)} + \tfrac{1}{2}\psi_0 \bar{X}_{-\boldsymbol{q}}^{(1)} \bar{X}_{-\boldsymbol{k}+\boldsymbol{q}}^{(1)} + \tfrac{1}{2}\psi_0 \bar{Y}_{-\boldsymbol{q}}^{(1)} \bar{Y}_{-\boldsymbol{k}+\boldsymbol{q}}^{(1)} \\
& +\bar{\psi}_0 \bar{Y}_{-\boldsymbol{q}}^{(1)} Y_{\boldsymbol{k}-\boldsymbol{q}}^{(1)}\Big)\Big] - 2i\kappa \bar{Y}_{-\boldsymbol{k}}^{(2)},
\end{aligned}
$$

$$
\begin{aligned}
J^*(\boldsymbol{k})Y_{\boldsymbol{k}}^{(2)} - V\psi_0^2 \bar{Y}_{-\boldsymbol{k}}^{(2)} = & -\sum_{\boldsymbol{q}}\Big[\gamma_i(\boldsymbol{k},\boldsymbol{k}-\boldsymbol{q})\Big(\theta_i(\boldsymbol{q})X_{\boldsymbol{k}-\boldsymbol{q}}^{(1)} + [f_i(\boldsymbol{q})+\theta_i(\boldsymbol{q})]Y_{\boldsymbol{k}-\boldsymbol{q}}^{(1)}\Big) \\
& -\sqrt{2}V\Big(\psi_0 \bar{Y}_{-\boldsymbol{q}}^{(1)} X_{\boldsymbol{k}-\boldsymbol{q}}^{(1)} + \psi_0 \bar{X}_{-\boldsymbol{q}}^{(1)} Y_{\boldsymbol{k}-\boldsymbol{q}}^{(1)} + \bar{\psi}_0 X_{\boldsymbol{q}}^{(1)} Y_{\boldsymbol{k}-\boldsymbol{q}}^{(1)}\Big)\Big],
\end{aligned}
$$

$$
\begin{aligned}
J(-\boldsymbol{k})\bar{Y}_{-\boldsymbol{k}}^{(2)} - V\bar{\psi}_0^2 Y_{\boldsymbol{k}}^{(2)} = & -\sum_{\boldsymbol{q}}\Big[\gamma_i(-\boldsymbol{k}+\boldsymbol{q},-\boldsymbol{k})\Big(\theta_i(\boldsymbol{q})\bar{X}_{-\boldsymbol{k}+\boldsymbol{q}}^{(1)} + [f_i(\boldsymbol{q})-\theta_i(\boldsymbol{q})]\bar{Y}_{-\boldsymbol{k}+\boldsymbol{q}}^{(1)}\Big) \\
& -\sqrt{2}V\Big(\bar{\psi}_0 \bar{X}_{-\boldsymbol{q}}^{(1)} Y_{\boldsymbol{k}-\boldsymbol{q}}^{(1)} + \bar{\psi}_0 \bar{Y}_{-\boldsymbol{q}}^{(1)} X_{\boldsymbol{k}-\boldsymbol{q}}^{(1)} + \psi_0 \bar{X}_{-\boldsymbol{q}}^{(1)} \bar{Y}_{-\boldsymbol{k}+\boldsymbol{q}}^{(1)}\Big)\Big].
\end{aligned}
$$

Similar to the first order case, arranging these as two matrix equations,

$$
M_X^{(2)} \boldsymbol{X}^{(2)} = C_X^{(2)}, \qquad\qquad M_Y^{(2)} \boldsymbol{Y}^{(2)} = C_Y^{(2)}, \qquad (6.74)
$$

where $\boldsymbol{X}^{(2)} = (X_{\boldsymbol{k}}^{(2)}, \bar{X}_{-\boldsymbol{k}}^{(2)})^T$ and $\boldsymbol{Y}^{(2)} = (Y_{\boldsymbol{k}}^{(2)}, \bar{Y}_{-\boldsymbol{k}}^{(2)})^T$, we can invert $M_X^{(2)}$ and $M_Y^{(2)}$ and solve for $\boldsymbol{X}^{(2)}$ and $\boldsymbol{Y}^{(2)}$, where we also eliminate any terms of the form $Y^{(1)}Y^{(1)}$ as they do not contain any factors of $\boldsymbol{f}$. The results are given in Appendix A.4.

Substituting the first and second order mean-fields into Eqs. (6.71-6.73), we may then differentiate the second order matrix with respect to the source fields (see Appendix A.5),

$$
\frac{d^2 A_1^{(2)}}{df_i(\boldsymbol{q})d\theta_j(-\boldsymbol{q})} = \frac{d^2}{df_i(\boldsymbol{q})d\theta_j(-\boldsymbol{q})}\begin{pmatrix} A_A^{(2)} & A_B^{(2)} \\ A_C^{(2)} & A_A^{(2)} \end{pmatrix}, \qquad (6.75)
$$

to give

$$
\partial^2 A_{1,ij}^{(2)}(\boldsymbol{q}) = \sum_{\sigma,\sigma'\in\pm} \mathcal{C}_{\sigma,\sigma'}^{(2)}(\boldsymbol{q})\gamma_i(\sigma\boldsymbol{q})\gamma_j(\sigma'\boldsymbol{q}), \qquad (6.76)
$$

where $\partial^2 A_{1,ij}^{(2)}(\boldsymbol{q})$ is shorthand for $d^2 A_1^{(2)}/df_i(\boldsymbol{q})d\theta_j(-\boldsymbol{q})$ and the coefficients $\mathcal{C}_{\sigma,\sigma'}^{(2)}(\boldsymbol{q})$ are given in Appendix A.6.

6.4.4   Correction in the continuum limit

From Eq. (6.23) and the line of reasoning around Eq. (6.70), we have that the second order response function is

$$\chi_{ij}^{A^{(2)}}(\boldsymbol{q}) = \frac{i}{4} \sum_{\omega,\omega',\boldsymbol{k},\boldsymbol{k}'} \mathrm{Tr}\left(D_{\omega\omega',\boldsymbol{k}\boldsymbol{k}'}^K \frac{d^2 A_{1,\,\omega'\omega,\boldsymbol{k}'\boldsymbol{k}}^{(2)}}{df_i(\boldsymbol{q})d\theta_j(-\boldsymbol{q})} \right). \tag{6.77}$$

Noting that $D_{\omega\omega',\boldsymbol{k}\boldsymbol{k}'}^K \sim \delta_{\omega,\omega'}\delta_{\boldsymbol{k},\boldsymbol{k}'}$ and $A_1^{(2)} \sim \delta_{\omega,\omega'}$, this reduces to

$$\chi_{ij}^{A^{(2)}}(\boldsymbol{q}) = \frac{i}{4} \sum_{\omega,\boldsymbol{k}} \mathrm{Tr}\left(D_{\omega,\boldsymbol{k}}^K \frac{d^2 A_{1,\,\boldsymbol{k}}^{(2)}}{df_i(\boldsymbol{q})d\theta_j(-\boldsymbol{q})} \right), \tag{6.78}$$

However, taking the continuum limit of this expression is not straightforward. To see why, consider an action defined on the Keldysh contour before the continuum limit has been taken (see Eq. (4.25))[101]:

$$S = \sum_j^N \delta t \left(i\bar{\psi}_j^+ \frac{\psi_j^+ - \psi_{j-1}^+}{\delta t} - H(\bar{\psi}_j^+, \psi_{j-1}^+) - i\bar{\psi}_{j-1}^- \frac{\psi_{j-1}^- - \psi_j^-}{\delta t} + H(\bar{\psi}_{j-1}^-, \psi_j^-) \right), \tag{6.79}$$

where we ignore the distribution term. Fourier transforming this into the space of Matsubara frequencies, $\omega_n = 2\pi n/N\delta t$,

$$\psi_j = \sum_n^N \psi_n \mathrm{e}^{-i2\pi nj/N}, \qquad\qquad \psi_n = \frac{1}{N} \sum_j^N \psi_n \mathrm{e}^{i2\pi nj/N}, \tag{6.80}$$

we see that there are infinitesimal phase factors $\mathrm{e}^{i\omega_n\delta t}$ and $\mathrm{e}^{-i\omega_n\delta t}$ associated with pairs of the form $\bar{\psi}_j^+\psi_{j-1}^+$ and $\bar{\psi}_{j-1}^-\psi_j^-$, respectively[59]. These can be factored out to give

$$S = N\delta t \sum_n^N \left[\bar{\psi}_n^+\psi_n^+ \left(-i\frac{1 - \mathrm{e}^{-i\omega_n\delta t}}{\delta t} - H_0 \right) \mathrm{e}^{i\omega_n\delta t} \right. \tag{6.81}$$

$$\left. -\bar{\psi}_n^-\psi_n^- \left(i\frac{1 - \mathrm{e}^{i\omega_n\delta t}}{\delta t} - H_0 \right) \mathrm{e}^{-i\omega_n\delta t} + ... \right],$$

where H_0 represents the diagonal contribution from the Hamiltonian, which in the semiclassical approximation has the same pattern of field timesteps for all terms. There are extra, off-diagonal, terms due to interactions, but these do not have mismatched timesteps. If we perform a Gaussian integral over these fields, such as in Eq. (6.17), then the factored out $\mathrm{e}^{\pm i\omega_n\delta t}$ terms cancel in the determinant, so we can drop them. However, phase factors

remain in the non-Hamiltonian parts of the action, which after the Keldysh rotation can be written in Matsubara space as

$$S = N\delta t \sum_n^N \big(-i\alpha(\omega_n)[\bar{\psi}^c(\omega_n)\psi^c(\omega_n) + \bar{\psi}^q(\omega_n)\psi^q(\omega_n)]$$

$$+(\beta(\omega_n) - H_0)[\bar{\psi}^c(\omega_n)\psi^q(\omega_n) + \bar{\psi}^q(\omega_n)\psi^c(\omega_n)] + ...\big),$$

(6.82)

where

$$\alpha(\omega_n) = \frac{1 - \cos(\omega_n\delta t)}{\delta t}, \qquad\qquad \beta(\omega_n) = \frac{\sin(\omega_n\delta t)}{\delta t}.$$

(6.83)

The contribution to the inverse Green's function from the non-Hamiltonian terms is

$$\mathcal{D}^{-1}(\omega_n) = \begin{pmatrix} -i\alpha(\omega_n) & 0 & \beta(\omega_n) & 0 \\ 0 & -i\alpha(\omega_n) & 0 & -\beta(\omega_n) \\ \beta(\omega_n) & 0 & -i\alpha(\omega_n) & 0 \\ 0 & -\beta(\omega_n) & 0 & -i\alpha(\omega_n) \end{pmatrix} + ...,$$

(6.84)

and we see that if the continuum limit were to mean taking $\delta t \to 0$ in isolation, then we would reproduce the non-Hamiltonian contribution to the inverse Green's functions in Eq. (4.72), i.e. $\alpha(\omega) \to 0$ and $\beta(\omega) \to \omega$. However, recalling that $\omega_n\delta t = 2\pi n/N$, at large values of n, i.e. $n \simeq N$, this does not work as $\omega_n\delta t$ is not small (i.e. $\cos(\omega_n\delta t) \not\simeq 1$ and $\sin(\omega_n\delta t) \not\simeq \omega_n\delta t$). There will in fact be an extra contribution to the Green's functions due to the large-n part of frequency space. When n is large, the non-Hamiltonian terms are of order $1/\delta t$, whereas the Hamiltonian terms are of order 1. Therefore, the former will dominate as $\delta t \to 0$ and we may approximate the extra contribution to the Green's functions as the inverse of Eq. (6.84):

$$\mathcal{D}(\omega_n) \simeq \frac{\delta t}{2\alpha(\omega_n)} \begin{pmatrix} i\alpha(\omega_n) & 0 & \beta(\omega_n) & 0 \\ 0 & i\alpha(\omega_n) & 0 & -\beta(\omega_n) \\ \beta(\omega_n) & 0 & i\alpha(\omega_n) & 0 \\ 0 & -\beta(\omega_n) & 0 & i\alpha(\omega_n) \end{pmatrix},$$

(6.85)

where $\alpha^2 + \beta^2 = 2\alpha/\delta t$.

The purpose of this analysis is to correctly take the continuum limit of the sum over frequency in Eq. (6.78). Therefore, consider the frequency sum over the Green's functions, $(1/N\delta t)\sum_n^N \mathcal{D}(\omega_n)$, where we have included the normalising inverse factor of time, $1/T = 1/N\delta t$ (see Appendix B for an explanation of how finite factors of length and time are

included in this calculation). Substituting Eq. (6.85) into this sum, we get

$$
\frac{1}{N\delta t}\sum_n \mathcal{D}(\omega_n) = \frac{1}{2}\frac{1}{N}\sum_n
\begin{pmatrix}
i & 0 & \beta/\alpha & 0 \\
0 & i & 0 & -\beta/\alpha \\
\beta/\alpha & 0 & i & 0 \\
0 & -\beta/\alpha & 0 & i
\end{pmatrix}.
\tag{6.86}
$$

The full summation over β/α is zero,

$$
\sum_n^N \frac{\beta(\omega_n)}{\alpha(\omega_n)} = \sum_n^N \frac{\sin(\omega_n\delta t)}{1-\cos(\omega_n\delta t)} = 0,
\tag{6.87}
$$

and so we have that the extra contribution is

$$
\frac{1}{N\delta t}\sum_n^N \mathcal{D}(\omega_n) = \frac{i}{2}\mathbb{1}.
\tag{6.88}
$$

We see also from Eq. (6.85) that this does not apply to any terms in the response function containing two Green's functions (e.g. Eq. (6.62)), as these will pick up an extra factor of δt and so will disappear when $\delta t \to 0$.

Returning to Eq. (6.78), we now include the contribution from Eq. (6.88) (noting that this applies to the full Green's function, $\mathcal{D}$, not just D_K):

$$
\begin{aligned}
\chi_{ij}^{A^{(2)}}(\boldsymbol{q}) &= \frac{i}{4}\sum_{\boldsymbol{k}}\mathrm{Tr}\left(\left[\frac{i}{2}\mathbb{1}\right]\frac{d^2 A_{\boldsymbol{k}}^{(2)}}{df_i(\boldsymbol{q})d\theta_j(-\boldsymbol{q})}\right) + \frac{i}{4}\sum_{\omega,\boldsymbol{k}}\mathrm{Tr}\left(D_{\omega,\boldsymbol{k}}^K\frac{d^2 A_{1,\boldsymbol{k}}^{(2)}}{df_i(\boldsymbol{q})d\theta_j(-\boldsymbol{q})}\right), \\
&= \frac{i}{4}\sum_{\boldsymbol{k}}\mathrm{Tr}\left(i\frac{d^2 A_{1,\boldsymbol{k}}^{(2)}}{df_i(\boldsymbol{q})d\theta_j(-\boldsymbol{q})}\right) + \frac{i}{4}\sum_{\omega,\boldsymbol{k}}\mathrm{Tr}\left(D_{\omega,\boldsymbol{k}}^K\frac{d^2 A_{1,\boldsymbol{k}}^{(2)}}{df_i(\boldsymbol{q})d\theta_j(-\boldsymbol{q})}\right),
\end{aligned}
$$

where on the second line the new term has picked up a factor of two on account of the two $A_1^{(2)}$ terms in Eq. (6.66) being summing together under the trace. Taking the continuum limit, we have then that the second order response function is given by

$$
\chi_{ij}^{A^{(2)}}(\boldsymbol{q}) = \frac{i}{4}\int\frac{dk_x}{2\pi}\frac{dk_y}{2\pi}\left[i\,\mathrm{Tr}\left(\frac{d^2 A_1^{(2)}(\boldsymbol{k})}{df_i(\boldsymbol{q})d\theta_j(-\boldsymbol{q})}\right) + \int\frac{d\omega}{2\pi}\,\mathrm{Tr}\left(D^K(\omega,\boldsymbol{k})\frac{d^2 A_1^{(2)}(\boldsymbol{k})}{df_i(\boldsymbol{q})d\theta_j(-\boldsymbol{q})}\right)\right].
\tag{6.89}
$$

6.5   Full response function

Combining the mean-field response function with the first and second order response functions in Eqs. (6.65) and (6.89), the full static current-current response function can be

written as

$$
\begin{aligned}
\chi_{ij}(\boldsymbol{q}) \;=\;& \chi_{ij}^{mf}(\boldsymbol{q}) + \frac{i}{4}\int \frac{dk_x}{2\pi}\frac{dk_y}{2\pi}\left(i\,\mathrm{Tr}[\partial^2 A_{1,ij}^{(2)}(\boldsymbol{q})] + \int\frac{d\omega}{2\pi}\,\mathrm{Tr}[D^K(\omega,\boldsymbol{k})\partial^2 A_{1,ij}^{(2)}(\boldsymbol{q})]\right) \\
& -\frac{i}{4}\int \frac{dk_x}{2\pi}\frac{dk_y}{2\pi}\frac{d\omega}{2\pi}\,\mathrm{Tr}\Big[D^R(\omega,\boldsymbol{k}+\boldsymbol{q})a_i(\boldsymbol{k}+\boldsymbol{q},\boldsymbol{k})D^K(\omega,\boldsymbol{k})b_j(\boldsymbol{k},\boldsymbol{k}+\boldsymbol{q}) \\
& \quad +D^K(\omega,\boldsymbol{k}+\boldsymbol{q})a_i(\boldsymbol{k}+\boldsymbol{q},\boldsymbol{k})D^A(\omega,\boldsymbol{k})b_j(\boldsymbol{k},\boldsymbol{k}+\boldsymbol{q})\Big],
\end{aligned}
\tag{6.90}
$$

where the mean-field response function is given in Eq. (6.54), the matrices a_i and b_i in Eqs. (A.40) and (A.41), the matrix $\partial^2 A_{1,ij}^{(2)}$ in Eq. (6.76), and the coefficients $\mathcal{C}_{\sigma,\sigma'}^{(2)}$ in the latter in Eqs. (A.58-A.62).

Chapter 7

Superfluid response

In systems that are isotropic and conserve particle number, the superfluid fraction, i.e. the proportion of the system density that is superfluid, is given by the difference between the longitudinal and the transverse response functions in the long-range limit (Eq. (2.53)). The relationship between the response functions and the densities that leads to this formulation is provided by the f-sum rule, which is dependent on particle conservation (Section 2.6.1). For incoherently pumped microcavity-polaritons, the sum rule holds despite their driven-dissipative nature[23]. However, this is not necessarily true for coherently driven polaritons. Additionally, for finite pump wavevector k_p, coherently pumped systems are anisotropic and will not have scalar longitudinal and transverse responses, implying that they may be more superfluid in some directions than others. While it is not guaranteed that we can associate responses with densities, it is still possible to quantify the behaviour of the system by recognising that a superfluid will exhibit what we may term a *superfluid response*, i.e. if there is a superfluid component in the system, then the longitudinal response function will be larger in the long-range limit than the transverse response function, where this effect may be direction-dependent.

In this chapter, we use the static current-current response function for coherently driven microcavity-polaritons calculated in Chapter 6 (Eq. (6.90)) to find the longitudinal and transverse responses of the system and analyse the results. In Section 7.1, we examine how a lack of Galilean invariance implies that the f-sum rule will not hold and how anisotropy causes the longitudinal and transverse responses to be tensors; in Section 7.2, we take the long-range limit of the response function and find that the longitudinal and transverse responses are equal, so the system is not a superfluid; In Section 7.3, we discover that at $k_p = 0$, the system responds to neither type of perturbation, forming a new kind of rigid macroscopic quantum state. However, at $k_p \neq 0$, perturbations can couple to the amplitude of this state allowing a type of 'normal' response; in Section 7.4, we analyse how this response is dependent on detuning the coherent drive away from the bare polariton dispersion; in Section 7.5, we look at how the response function behaves in the exceptional

case detailed in Section 5.4 where a Kerr instability leads to a gapless excitation spectrum; and in Section 7.6 we outline how the superfluid response of a system of polaritons may be measured.

7.1   Sum rules and anisotropy

In a system in which the f-sum rule holds, we have that $\rho = m\chi^L(\boldsymbol{q} \to \boldsymbol{0})$ and $\rho_n = m\chi^T(\boldsymbol{q} \to \boldsymbol{0})$ (see Section 2.6.1). Hence from Eq. (2.45) for the response function in an isotropic system, we see that using the f-sum rule allows us to write the full static current-current response function in terms of the total and normal densities:

$$m\chi_{ij}(\boldsymbol{q} \to \boldsymbol{0}) = \lim_{\boldsymbol{q} \to \boldsymbol{0}} \frac{q_i q_j}{q^2}(\rho - \rho_n) + \delta_{ij}\rho_n. \tag{7.1}$$

Defining the part of the system that responds longitudinally but not transversely as the superfluid density, $\rho_s = m(\chi^L(\boldsymbol{q} \to \boldsymbol{0}) - \chi^T(\boldsymbol{q} \to \boldsymbol{0}))$, gives us the relation

$$\rho = \rho_s + \rho_n. \tag{7.2}$$

That is, the f-sum rule implies that the 'normal' and 'superfluid' densities add up to the total density of the system. Eq. (7.2) also assumes that the system is Galilean invariant, i.e. that changing from one inertial frame to another does not affect the physics of the system. To see why, we consider the two-fluid model of superfluidity (Section 2.4), in which the current is given by Eq. (2.24). Changing to a new frame moving at velocity $-\boldsymbol{u}$ with respect to the first, we have that the wavefunction of the macroscopic state will be modified according to[6]

$$\psi(\boldsymbol{x}) \to \psi'(\boldsymbol{x}) = \psi(\boldsymbol{x})\mathrm{e}^{im\boldsymbol{u}.\boldsymbol{x}}, \tag{7.3}$$

and consequently, the superfluid velocity (Eq. (2.7)) will shift by

$$\boldsymbol{v}_s(\boldsymbol{x}) \to \boldsymbol{v}_s(\boldsymbol{x}) + \boldsymbol{u}. \tag{7.4}$$

Additionally, given that in a system with long-range order we can diagonalise the density matrix into a complete set of eigenfunctions, $\chi_i(\boldsymbol{x}) = |\chi_i(\boldsymbol{x})|\,\mathrm{e}^{i\phi_i(\boldsymbol{x})}$, with eigenvalues N_i (Eq. (2.35)), we have that the full current is

$$\boldsymbol{j}(\boldsymbol{x}) = \frac{1}{m}\sum_i N_i\,|\chi_i(\boldsymbol{x})|^2\,\nabla\phi_i(\boldsymbol{x}), \tag{7.5}$$

which transforms with the change of frame as

$$\boldsymbol{j}(\boldsymbol{x}) \to \boldsymbol{j}(\boldsymbol{x}) + \rho(\boldsymbol{x})\boldsymbol{u}, \tag{7.6}$$

where $\rho(\boldsymbol{x}) = \sum_i N_i |\chi_i(\boldsymbol{x})|^2$. Finally, the normal velocity transforms straightforwardly as $\boldsymbol{v}_n(\boldsymbol{x}) \to \boldsymbol{v}_n(\boldsymbol{x}) + \boldsymbol{u}$, and thus, under a Galilean transformation, Eq. (2.24) becomes

$$\boldsymbol{j}(\boldsymbol{x}) + \rho(\boldsymbol{x})\boldsymbol{u} = \rho_s(\boldsymbol{x})(\boldsymbol{v}_s(\boldsymbol{x}) + \boldsymbol{u}) + \rho_n(\boldsymbol{x})(\boldsymbol{v}_n(\boldsymbol{x}) + \boldsymbol{u}). \tag{7.7}$$

If the physics of the system is invariant to the transformation, this equation implies the validity of Eq. (7.2).

Coherently pumped polaritons are not Galilean invariant because the pump picks out a special velocity. Consider the pumping term in the Hamiltonian,

$$\hat{H}_{pump} = F_p(\hat{a}_{\boldsymbol{0}}^\dagger + \hat{a}_{\boldsymbol{0}}), \tag{7.8}$$

where momentum arguments are with reference to k_p. Fourier transforming Eq. (7.3), we see that a Galilean transformation of the fields is given in momentum space by

$$\psi'_{\boldsymbol{k}} = \int d\boldsymbol{x}\,\psi'(\boldsymbol{x})\mathrm{e}^{i\boldsymbol{k}.\boldsymbol{x}} = \int d\boldsymbol{x} \sum_{\boldsymbol{q}} \psi_{\boldsymbol{q}}\mathrm{e}^{-i(\boldsymbol{q}-\boldsymbol{k}-m\boldsymbol{u}).\boldsymbol{x}} = \psi_{\boldsymbol{k}+m\boldsymbol{u}}. \tag{7.9}$$

Thus, a Galilean transformation on a coherently pumped system is equivalent to shifting the polariton operators $\hat{a}$ by some momentum $\boldsymbol{k}'$, i.e.

$$\hat{a}_{\boldsymbol{0}} \to \hat{a}_{\boldsymbol{k}'}. \tag{7.10}$$

In the new frame, the pump Hamiltonian will be

$$\hat{H}'_{pump} = F_p(\hat{a}_{\boldsymbol{k}'}^\dagger + \hat{a}_{\boldsymbol{k}'}), \tag{7.11}$$

and the coherently created macroscopic state will now be at momentum $\boldsymbol{k}' + \boldsymbol{k}_p$. That is, the system will have changed physically.

Both Galilean invariance and the f-sum rule imply Eq. (7.2), that the total density is the sum of the normal and superfluid densities. Given that the system is neither Galilean invariant nor conserving of particle number, we should not expect the f-sum rule to hold and we will not use the response function to calculate the superfluid fraction as in Eq. (2.53).

Additionally, when the pump wavevector k_p is finite, coherently driven polaritons are anisotropic. In Eq. (2.45), the isotropic response function contains two tensors, $q_i q_j/q^2$ and $(\delta_{ij} - q_i q_j/q^2)$, which in the long-range limit are associated with unique scalars, $\chi^L(\boldsymbol{q} \to \boldsymbol{0})$ and $\chi^T(\boldsymbol{q} \to \boldsymbol{0})$, corresponding to each kind of response. That these must be scalar follows from the fact that the response is identical in all directions. In anisotropic systems however, this will no longer be the case. The response function will contain more complex tensors

than Eq. (2.45) and will be dependent on direction, i.e.,

$$\chi(\boldsymbol{q}) = \begin{pmatrix} \chi_{xx}(\boldsymbol{q}) & \chi_{xy}(\boldsymbol{q}) \\ \chi_{yx}(\boldsymbol{q}) & \chi_{yy}(\boldsymbol{q}) \end{pmatrix}, \tag{7.12}$$

where these components need not be the same. This implies that in the long-range limit the longitudinal and transverse responses will also be anisotropic: i.e. they too will be tensors, $\chi_{ij}^{L}(\boldsymbol{q} \to \boldsymbol{0})$ and $\chi_{ij}^{T}(\boldsymbol{q} \to \boldsymbol{0})$.

Despite these complications, it is still possible to use the response function to quantify the superfluidity in the system by calculating whether there is a difference between the longitudinal and transverse responses. Modifying Eq. (2.53) for an anisotropic system in which the f-sum rule does not hold, we define the superfluid response in the long-range limit as

$$\lim_{\boldsymbol{q} \to \boldsymbol{0}} \left(\chi_{ij}^{S}(\boldsymbol{q}) \right) = \lim_{\boldsymbol{q} \to \boldsymbol{0}} \left(\chi_{ij}^{L}(\boldsymbol{q}) - \chi_{ij}^{T}(\boldsymbol{q}) \right). \tag{7.13}$$

7.2 Longitudinal and transverse response

The longitudinal and transverse responses of the system to perturbations are found by taking the long-range limit of the response function, i.e. $\boldsymbol{q} \to \boldsymbol{0}$, where taking the momentum perpendicular to the perturbation to zero first, and that parallel to it second, yields the longitudinal response function, and taking the opposite order gives the transverse response function (see Section 2.6). For these responses to differ, there must be singular behaviour as the limit is taken. For example, for a two-dimensional, isotropic system where the perturbation is in the x-direction, Eq. (2.45) gives

$$\chi_{xx}(\boldsymbol{q}) = \frac{q_x^2}{q_x^2 + q_y^2} \chi^{L}(\boldsymbol{q}) + \left(1 - \frac{q_x^2}{q_x^2 + q_y^2} \right) \chi^{T}(\boldsymbol{q}). \tag{7.14}$$

Here, the order in which q_x and q_y are taken to zero distinguishes two separate parts of the system on account of the singular behaviour when q_x is taken to zero last. By contrast, if we artificially remove the singular behaviour by adding a constant C to the denominators,

$$\chi_{xx}'(\boldsymbol{q}) = \frac{q_x^2}{q_x^2 + q_y^2 + C} \chi_1(\boldsymbol{q}) + \left(1 - \frac{q_x^2}{q_x^2 + q_y^2 + C} \right) \chi_2(\boldsymbol{q}), \tag{7.15}$$

what we have now called χ_1 and χ_2 cannot be connected to specifically longitudinal or transverse responses as the long-range limit always picks out χ_2. This contrived case is equivalent to Eq. (7.14) when $\chi^{L}(\boldsymbol{q} \to \boldsymbol{0}) = \chi^{T}(\boldsymbol{q} \to \boldsymbol{0}) = \chi_2(\boldsymbol{q} \to \boldsymbol{0})$. That is, by removing the singular behaviour we have prevented the possibility of superfluidity.

In the case of the response function for coherently pumped polaritons, Eq. (6.90), we can see that all the terms (Eqs. (6.54), (A.40), (A.41), and (6.76)) take the form of a multiple

of

$$\frac{h(\boldsymbol{q})}{\det[(D^R)^{-1}(\omega = 0, \boldsymbol{q})]}, \tag{7.16}$$

where $h(\boldsymbol{q})$ is some polynomial in $\boldsymbol{q}$. Indeed, we can see this from the fact that every term is proportional to two factors of the momentum vertex (Eq. (6.5)) and at least one factor of $K(\boldsymbol{q})$ (Eq. (6.53)). Therefore, for singular behaviour and consequently superfluid behaviour, the static inverse retarded Green's function must vanish as $\boldsymbol{q} \to \mathbf{0}$. In fact, this is directly related to the gaplessness of the excitation spectrum. The spectrum, $\omega^{\pm}(\boldsymbol{k})$, in Eq. (5.4) is defined by

$$\det[(D^R)^{-1}(\omega^{\pm}(\boldsymbol{k}), \boldsymbol{k})] = 0. \tag{7.17}$$

That is, only if the spectrum is gapless, i.e. if $\omega^{\pm}(\boldsymbol{k} \to \mathbf{0}) = 0$, will the static inverse retarded Green's function vanish in the long-range limit and there can be superfluidity. However, because the phase of the macroscopic state is externally fixed, the excitation spectrum of coherently pumped polaritons is gapped (Fig. 5.1) and the static inverse retarded Green's function is finite as $\boldsymbol{q} \to \mathbf{0}$. As there are no singular terms, the longitudinal and transverse response functions for coherently driven microcavity-polaritons, that are homogeneously and continuously pumped below the OPO threshold, are identical, and Eq. (7.13) shows that no part of the system responds to perturbations like a superfluid.

7.3 Rigid state

All terms in the response function are proportional to two factors of the momentum vertex. Indeed, we may note that the response function can be divided into a contribution involving the response of the condensate, appearing through the coupling $\boldsymbol{\gamma}(\boldsymbol{q}) = (2\boldsymbol{k}_p + \boldsymbol{q})/2m$, and a contribution involving coupling to excitations through $\boldsymbol{\gamma}(\boldsymbol{k} + \boldsymbol{q}, \boldsymbol{k}) = (2\boldsymbol{k}_p + 2\boldsymbol{k} + \boldsymbol{q})/2m$. Numerically performing the frequency integral over the latter contribution shows these to be zero. Therefore, as the pump wavevector is $\boldsymbol{k}_p = (k_p, 0)$, in the long-range limit every finite term in the response function is proportional to two factors of $\boldsymbol{\gamma}(\boldsymbol{q} \to \mathbf{0}) = (\gamma_0, 0) = (k_p/m, 0)$. This means that only the χ_{xx} component in Eq. (7.12) can be finite. Furthermore, seeing as there are no singular terms in the response function, when the pump momentum is equal to zero the current response of the system to perturbations vanishes in all directions. Unlike superfluids, which despite not responding transversely still have a finite longitudinal response, coherently pumped polaritons at $k_p = 0$ form a rigid state that, like a solid, has a finite density but does not respond to any perturbations. This suggests that the external fixing of the phase, which causes the gapped spectrum, has a highly restrictive effect on the system. Indeed, it is already known that vortices and solitons cannot form within the

pumping region of a coherently driven system (although this changes outside the pump, where the phase is free to evolve[90,89,91]), and the lack of response to perturbations shown here indicates these restrictions are even more profound.

However, when k_p is finite there is a normal response in the long-range limit associated with χ_{xx}. Here, by 'normal' we mean simply that the longitudinal and transverse response functions are equal. We may examine the nature of this effect explicitly by taking the long-range limit of the mean-field response function (Eq. (6.52)), giving

$$\chi_{ij}^{mf}(\boldsymbol{q} \to \boldsymbol{0}) = -\delta_{xi}\delta_{xj} \frac{\gamma_0^2 \bar{\psi}_0 \psi_0}{J(\boldsymbol{0})J^*(\boldsymbol{0}) - V^2\bar{\psi}_0^2\psi_0^2} \left[J(\boldsymbol{0}) + J^*(\boldsymbol{0}) + 2V\bar{\psi}_0\psi_0 \right], \qquad (7.18)$$

Considering the zeroth order saddle point equations (Eqs. (5.6) and (5.7)), Eq. (7.18) becomes

$$\chi_{ij}^{mf}(\boldsymbol{q} \to \boldsymbol{0}) = -\delta_{xi}\delta_{xj} \frac{k_p^2 |\psi_0|^2 (\bar{\psi}_0 + \psi_0)}{m^2(F_p - V |\psi_0|^2 (\bar{\psi}_0 + \psi_0))}. \qquad (7.19)$$

This response has a very specific interpretation as a change in the occupation of the pump state. If this state has finite momentum k_p, then adding or removing particles to it will cause the current flowing in the system to change, i.e. there will be a current response. This effect is possible because particle number is not conserved and it shows that the pump state is still rigid even at finite k_p: that is, the momentum of the state is not disrupted by the perturbation, only the number of particles in it.

To see this, we consider the time-independent Gross-Pitaevskii equation (GPE) for a bosonic field ψ coupled to the current through a perturbation $\boldsymbol{f}(\boldsymbol{x})$:

$$\left(-\frac{\nabla^2}{2m} - \omega_p - i\kappa + V |\psi(\boldsymbol{x})|^2 \right)\psi(\boldsymbol{x}) = -F_p e^{i\boldsymbol{k}_p.\boldsymbol{x}} - \frac{i}{2m} \left[\boldsymbol{f}(\boldsymbol{x}).\nabla\psi(\boldsymbol{x}) + \nabla.(\boldsymbol{f}(\boldsymbol{x})\psi(\boldsymbol{x})) \right]. \qquad (7.20)$$

The origin of the perturbation term can be seen from the perturbative action, which is given by the dot product of $\boldsymbol{f}$ with the current:

$$\delta S = \int dt \iint d^2\boldsymbol{x} \left(\frac{-i}{2m} \left[(\boldsymbol{f}(\boldsymbol{x})\psi^*(\boldsymbol{x})).(\nabla\psi(\boldsymbol{x})) - (\boldsymbol{f}(\boldsymbol{x})\psi(\boldsymbol{x})).(\nabla\psi^*(\boldsymbol{x})) \right] \right). \qquad (7.21)$$

Integrating the second term by parts we have that

$$\delta S = \int dt \iint d^2\boldsymbol{x} \left(\frac{-i}{2m} \left[(\boldsymbol{f}(\boldsymbol{x})\psi^*(\boldsymbol{x})).(\nabla\psi(\boldsymbol{x})) + \psi^*(\boldsymbol{x})\nabla.(\boldsymbol{f}(\boldsymbol{x})\psi(\boldsymbol{x})) \right] \right), \qquad (7.22)$$

which leads to the GPE by differentiating with respect to $\psi^*(\boldsymbol{x})$. Fourier transforming the

perturbative action into momentum space, we get

$$\delta S = \int dt \sum_{\boldsymbol{k},\boldsymbol{q}} \boldsymbol{f}(\boldsymbol{q}).\frac{2\boldsymbol{k}+\boldsymbol{q}}{2m}\psi^*(\boldsymbol{k})\psi(\boldsymbol{k}+\boldsymbol{q}), \tag{7.23}$$

which in the long-range limit, $\boldsymbol{q} \to \boldsymbol{0}$, becomes

$$\delta S = \int dt \sum_{\boldsymbol{k}} \boldsymbol{f}(\boldsymbol{0}).\frac{\boldsymbol{k}}{m}\psi^*(\boldsymbol{k})\psi(\boldsymbol{k}), \tag{7.24}$$

and so moving back in to real space we may choose $\boldsymbol{f}$ to be independent of position,

$$\delta S = \int dt \iint d^2\boldsymbol{x}\,\psi^*(\boldsymbol{x})\boldsymbol{f}.\frac{-i\nabla}{m}\psi(\boldsymbol{x}). \tag{7.25}$$

Accordingly, the GPE reduces to

$$\left(-\frac{\nabla^2}{2m} - \omega_p - i\kappa + V\,|\psi(\boldsymbol{x})|^2\right)\psi(\boldsymbol{x}) = -F_p\mathrm{e}^{i\boldsymbol{k}_p.\boldsymbol{x}} - \boldsymbol{f}.\frac{i\nabla}{m}\psi(\boldsymbol{x}). \tag{7.26}$$

Considering a mean-field at the pump wavevector that satisfies the unperturbed GPE, $\psi_0\mathrm{e}^{i\boldsymbol{k}_p.\boldsymbol{x}}$, as well as the change in the field due to the perturbation, $\delta\psi(\boldsymbol{x}) = \phi(\boldsymbol{x})\mathrm{e}^{i\boldsymbol{k}_p.\boldsymbol{x}}$, and removing any terms higher than first order in $\phi(\boldsymbol{x})$ and $\boldsymbol{f}$, we get an equation with constant coefficients:

$$-\frac{\nabla^2}{2m}\phi(\boldsymbol{x}) - i\boldsymbol{k}_p.\frac{\nabla}{m}\phi(\boldsymbol{x}) + V\psi_0^2\phi^*(\boldsymbol{x}) + \left(\frac{k_p^2}{2m} - \omega_p - i\kappa + 2V\,|\psi_0|^2\right)\phi(\boldsymbol{x}) = \frac{\boldsymbol{f}.\boldsymbol{k}_p}{m}\psi_0. \tag{7.27}$$

Fourier transforming this equation gives,

$$\left(\frac{q^2}{2m} + \frac{\boldsymbol{k}_p}{m}.\boldsymbol{q} + \frac{k_p^2}{2m} - \omega_p - i\kappa + 2V\,|\psi_0|^2\right)\phi(\boldsymbol{q}) + \psi_0^2\phi^*(-\boldsymbol{q}) = \frac{\boldsymbol{f}.\boldsymbol{k}_p}{m}\psi_0\delta_{\boldsymbol{q},\boldsymbol{0}}, \tag{7.28}$$

and we may take the complex conjugate, leading to a matrix equation:

$$\begin{pmatrix} a(\boldsymbol{q}) & b(\boldsymbol{q}) \\ b^*(-\boldsymbol{q}) & a^*(-\boldsymbol{q}) \end{pmatrix}\begin{pmatrix} \phi(\boldsymbol{q}) \\ \phi^*(-\boldsymbol{q}) \end{pmatrix} = \frac{\boldsymbol{f}.\boldsymbol{k}_p}{m}\begin{pmatrix} \psi_0 \\ \psi_0^* \end{pmatrix}\delta_{\boldsymbol{q},\boldsymbol{0}}, \tag{7.29}$$

where

$$\begin{aligned} a(\boldsymbol{q}) &= \frac{q^2}{2m} + \frac{\boldsymbol{k}_p}{m}.\boldsymbol{q} + \frac{k_p^2}{2m} - \omega_p + 2V\,|\psi_0|^2 - i\kappa && (7.30) \\ &= \frac{q^2}{2m} + \frac{\boldsymbol{k}_p}{m}.\boldsymbol{q} + \alpha - i\kappa, \\ b(\boldsymbol{q}) &= V\psi_0^2, && (7.31) \end{aligned}$$

and we have defined $\alpha \equiv k_p^2/2m - \omega_p + 2V|\psi_0|^2 = -\delta_p + 2V|\psi_0|^2$. If $\boldsymbol{q} \neq \boldsymbol{0}$, the right-hand side is zero, which yields finite $\phi(\boldsymbol{q})$ only if the matrix on the left-hand side has zero determinant. Setting the determinant to zero gives an equation for the momentum for which the above matrix is singular:

$$\frac{q^4}{4m^2} + 2\alpha \frac{q^2}{2m} - \frac{(\boldsymbol{k_p}.\boldsymbol{q})^2}{m^2} + 2i\kappa \frac{\boldsymbol{k_p}}{m}.\boldsymbol{q} + \alpha^2 + \kappa^2 - V^2|\psi_0|^4 = 0. \qquad (7.32)$$

Noting that $\boldsymbol{k_p} = (k_p, 0)$, we may write this as

$$\frac{(q_x^2 + q_y^2)^2}{4m^2} + 2\alpha \frac{q_x^2 + q_y^2}{2m} - \frac{k_p^2}{m^2}q_x^2 + 2i\kappa \frac{k_p}{m}q_x + \alpha^2 + \kappa^2 - V^2|\psi_0|^4 = 0. \qquad (7.33)$$

Given that only the $2i\kappa(k_p/m)q_x$ term has an imaginary component, this equation can only be satisfied by real $\boldsymbol{q}$ if either q_x or $k_p = 0$. Taking the former case, we have that

$$\frac{q_y^4}{4m^2} + 2\alpha \frac{q_y^2}{2m} + \alpha^2 + \kappa^2 - V^2|\psi_0|^4 = 0, \qquad (7.34)$$

where in the $k_p = 0$ case we would have the same except that $q_y \to q$. To solve this, we write $\epsilon_y = q_y^2/2m$ to give a quadratic equation:

$$\epsilon_y^2 + 2\alpha\epsilon_y + \alpha^2 + \kappa^2 - V^2|\psi_0|^4 = 0, \qquad (7.35)$$

which in turn is solved by

$$\epsilon_y = -\alpha \pm \sqrt{V^2|\psi_0|^4 - \kappa^2}, \qquad (7.36)$$

giving for the y-momentum:

$$q_y = \pm\sqrt{2m}\sqrt{\delta_p - 2V|\psi_0|^2 \pm \sqrt{V^2|\psi_0|^4 - \kappa^2}}. \qquad (7.37)$$

Consequently, the matrix on the left-hand side of Eq. (7.29) will be singular for real values of $\boldsymbol{q}$ when $q_x = 0$ and both inequalities,

$$V|\psi_0|^2 > \kappa, \qquad\qquad \delta_p + \sqrt{V^2|\psi_0|^4 - \kappa^2} > 2V|\psi_0|^2, \qquad (7.38)$$

are true.

In Fig. 7.1, the real (blue) and imaginary (dashed red) components of q_y are plotted as the mean-field density is changed, where $\delta_p = \kappa$, $m = 5 \times 10^{-5}m_e$, $V = 0.0025\,\mathrm{meV\,\mu m}^2$, and $\kappa = 0.05\,\mathrm{meV}$ (the same parameters as in Fig. 5.1). It is clear from the finite imaginary part of q_y at all values of $|\psi_0|^2$ that for these parameters the above inequalities are not satisfied. Consequently, there are no physical solutions for which the matrix on the LHS of Eq. (7.29)

is singular and the only physically relevant solution of Eq. (7.27) is the position-independent function $\phi(\boldsymbol{x}) = \phi$. At the bistability threshold, i.e. detuning $\delta_p \geq \sqrt{3}\kappa$, solutions for which $\Im(q_y) = 0$ exist. However, these correspond approximately to the densities for which the system is unstable (the dashed green part of Fig. 5.2(a)) and a full investigation of this is beyond the scope of this thesis.
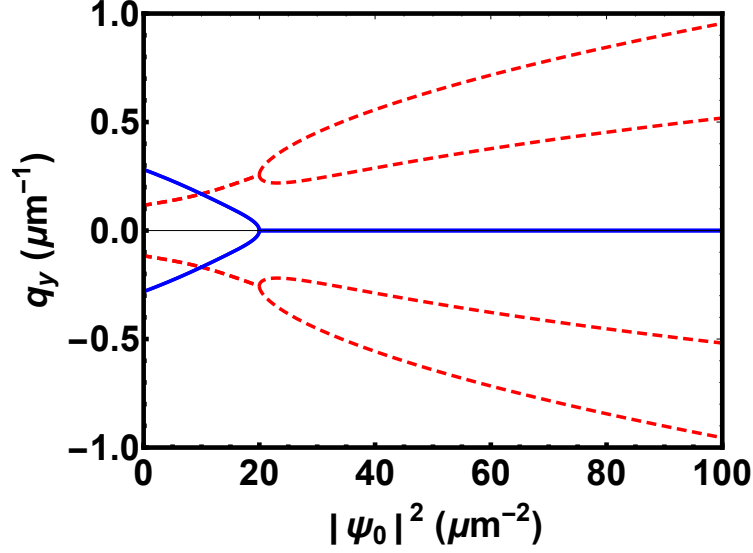
Figure 7.1: Real (blue) and imaginary (dashed red) momenta of solutions to Eq. (7.26) (given by Eq. (7.37)) at different mean-field densities, for the parameters $\delta_p = \kappa$, $m = 5 \times 10^{-5} m_e$, $V = 0.0025$meVμm^2, and $\kappa = 0.05$meV. As there is always a finite imaginary component, none of these solutions are physical.

Given that the solution to Eq. (7.27) is position-independent, $\phi(\boldsymbol{x}) = \phi$, the overall solution to the GPE (Eq. (7.26)) is the particular solution,

$$\psi(\boldsymbol{x}) = (\psi_0 + \phi)\mathrm{e}^{i\boldsymbol{k}_p \cdot \boldsymbol{x}}. \tag{7.39}$$

That is, the effect of the perturbation is simply to change the amplitude of the pump state.

Substituting Eq. (7.39) into the expression for the probability current (Eq. (2.6)), we see that to the mean-field level the current that flows in response to the perturbation is

$$\boldsymbol{j} = \frac{\boldsymbol{k}_p}{m}(\psi_0\phi^* + \phi\psi_0^*). \tag{7.40}$$

If the mean-field response given by Eq. (7.19) is indeed due entirely to this change in the amplitude of the pump state, this expression for the current should reproduce the response function through

$$j_i = \chi_{ij}^{mf}(\boldsymbol{q} \to \boldsymbol{0})f_j. \tag{7.41}$$

If we abbreviate the mean-field equation (Eq. 5.6) as $C\psi_0 = -F_p$, then Eq. (7.27) becomes

$$(C + V\,|\psi_0|^2)\phi + V\psi_0^2\phi^* = \frac{\boldsymbol{f}.\boldsymbol{k_p}}{m}\psi_0. \tag{7.42}$$

Taking this in combination with its complex conjugate leads to a matrix equation

$$\begin{pmatrix} C + V\,|\psi_0|^2 & V\psi_0^2 \\ V\psi_0^{*2} & C^* + V\,|\psi_0|^2 \end{pmatrix}\begin{pmatrix} \phi \\ \phi^* \end{pmatrix} = \frac{\boldsymbol{f}.\boldsymbol{k_p}}{m}\begin{pmatrix} \psi_0 \\ \psi_0^* \end{pmatrix}, \tag{7.43}$$

and solving for ϕ we get

$$\phi = \frac{C^*\psi_0}{|C|^2 + (C + C^*)V\,|\psi_0|^2}\left(\frac{\boldsymbol{f}.\boldsymbol{k_p}}{m}\right), \tag{7.44}$$

which through Eqs. (7.40) and (7.41) exactly reproduces the mean-field response function in Eq. (7.19).

While the above analysis was restricted to the mean-field level, the only part of the fluctuations response function that survives the long-range limit is, like in the mean-field case, the part that couples to the condensate through $\boldsymbol{\gamma}(\mathbf{0})$. Consequently, we expect the same behaviour – i.e. that the finite response at finite k_p corresponds to the perturbation coupling to the amplitude of the rigid state and causing an increase or decrease of the number of particles in that state.
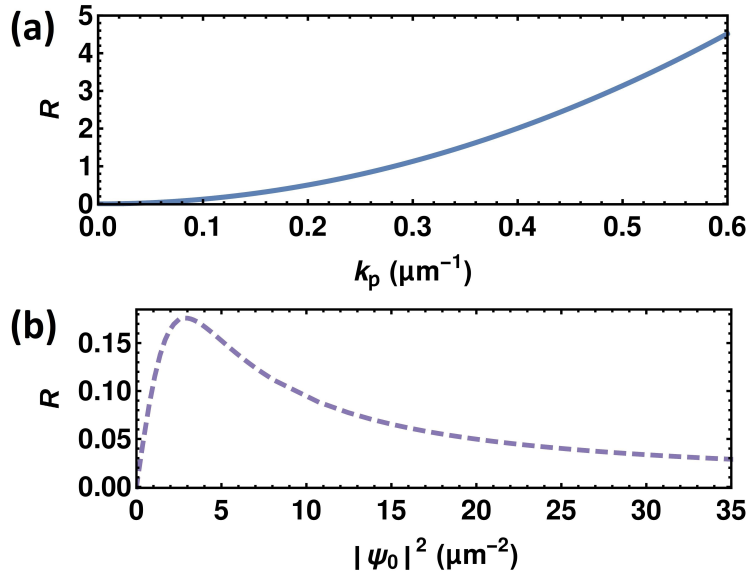
Figure 7.2: Total response in the long-range limit normalised to the mean-field density, Eq. (7.45), as a function **(a)** of pump momentum k_p at $|\psi_0|^2 = 6.9\mu\mathrm{m}^{-2}$, and **(b)** the mean-field density $|\psi_0|^2$ at $k_p = 0.1\mu\mathrm{m}^{-1}$. In both cases there is no blue-detuning away from the bare lower polariton dispersion, i.e. $\delta_p = 0$.

Numerically performing the integrals in Eq. (6.90) in the long-range limit (see Appendix C for details), we analyse how the response of the system changes with k_p and pump strength, where the latter is expressed through the mean-field polariton density $|\psi_0|^2$. Figure 7.2 shows a quantity R, which we define as the total long-range response normalised by the mean-field density,

$$R = \frac{m\chi_{xx}(\boldsymbol{q} \to \boldsymbol{0})}{|\psi_0|^2}, \tag{7.45}$$

with the system parameters: $m = 5 \times 10^{-5}m_e$, $V = 0.01\text{meV}\mu\text{m}^2$, and $\kappa = 0.05\text{meV}$. The ratio R increases quadratically with pump momentum, which is explained by the fact that if the rigid state has a larger current to begin with, changes in its amplitude will affect the overall current to a greater degree. Additionally, after an initial peak, there is an asymptotic decrease of R as intensity increases. We must conclude from this that a large pump intensity reduces the response to a weak perturbation. Furthermore, by performing these calculations we find that the mean-field term is orders of magnitude larger than the fluctuations at all momenta and densities.

7.4 Detuning

Blue-detuning can lead to the real part of the excitation spectrum fulfilling the Landau criterion (see Fig. 5.1(c)), which was the regime in which nearly-dissipationless flow was experimentally observed for coherently pumped polaritons[17]. Modifying the density for a set detuning, $\delta_p = 0.05\text{meV}$, we may examine the current response of the system in all the regimes given in Fig. 5.1. Fig. 7.3 shows how the total long-range response normalised by the mean-field density, Eq. (7.45), changes as we change the density, where $m = 5 \times 10^{-5}m_e$, $V = 0.0025\text{meV}\mu\text{m}^2$, and $\kappa = 0.05\text{meV}$. The point at which the real part of the spectrum becomes linear is the shifted resonance point, $\Delta_p = \omega_p - \epsilon(\boldsymbol{0}) - V|\psi_0|^2 = 0$. Notably, at this point the response of the system goes to zero. This is because the mean-field response (Eq. (7.19)), which is orders of magnitude larger than the fluctuations at all other points, is proportional to $\Re(\psi_0)$ and at the shifted resonance point ψ_0 is entirely imaginary. The fluctuation parts, while always finite, are very small compared to the mean-field suggesting that, even if we were to take higher orders in fluctuations, there would always be a pump strength at which the response goes from negative to positive and is thus strictly zero, and this point will be in the vicinity of $\Delta_p = 0$ where the mean-field component is zero. At higher densities the excitation spectrum is gapped in the real part and consequently still fulfils the Landau criterion. However, in contrast to the experimentally investigated regime in Fig. 5.1(c), the response in finite. Indeed, it is positive and shows an asymptotic decrease with density similar to the zero-detuning case (Fig. 7.2).

Because particle number is not conserved and the system is not Galilean invariant,
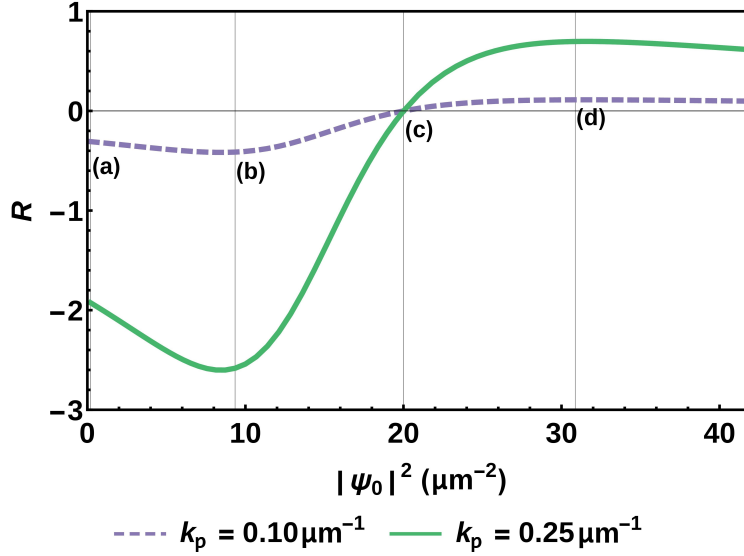
Figure 7.3: Total response in the long-range limit for $k_p = 0.1\mu m^{-1}$ (dashed purple) and $k_p = 0.25\mu m^{-1}$ (solid green) normalised with respect to the mean-field density, Eq. (7.45). Vertical lines marked **(a-d)** correspond to the excitation spectra in Fig. 5.1. For **(a)** and **(b)** the response is negative, and goes to zero close to **(c)** where the excitation spectrum is of the linear Bogoliubov form (the mean-field component, Eq. (7.19), is exactly zero at **(c)** on account of an imaginary mean-field, but the fluctuations are small and finite), before becoming positive, peaking around **(d)**, and tailing off similarly to the resonant case in Fig. 7.2. Larger k_p leads to a larger response to perturbations.

the f-sum rule does not hold and there is no physical correspondence that can be drawn between the density of the system and the current-current response function. This means that the negative responses seen at low density do not present a physical problem. We may draw parallels here to a previous study of incoherently pumped polaritons at the mean-field level[25] in which external potentials were present. The conclusion was drawn that steady state currents due to these potentials can alter the physical picture, rendering the interpretation of the superfluid and normal fractions in terms of the response of the system to a vector potential unphysical. While in that study the phase of the condensate was free to evolve, and while in the present work there are no external potentials, in both studies there exist steady state currents.

7.5   Bistability

As shown in Section 5.4, for a coherently pumped system below the OPO threshold, the only time the spectrum is gapless is at the onset of an instability (see Figs. 5.3(c) and 5.4(a)) when the imaginary part of the excitation spectrum crosses over from negative to positive, the condition for which is given in Eq. (5.16). To investigate how this change in the spectrum affects the response to perturbations of coherently pumped polaritons, we calculate the long-range behaviour of the mean-field response function (Eq. (6.52)) in this

regime. To do this, we separate the response function into its numerator and denominator,

$$\chi_{ij}^{mf}(\boldsymbol{q}) = \frac{n_{ij}(q_x, q_y)}{d(q_x, q_y)}, \tag{7.46}$$

where the latter is given by

$$d(q_x, q_y) = J(\boldsymbol{q})J^*(-\boldsymbol{q}) - V^2 |\psi_0|^4. \tag{7.47}$$

Rewriting $J(\boldsymbol{q})$ (Eq. (6.32)) in terms of the detuning and pump wavevector,

$$J(\boldsymbol{q}) = \delta_p - \frac{q_x^2 + q_y^2}{2m} - \frac{k_p q_x}{m} + i\kappa - 2V |\psi_0|^2, \tag{7.48}$$

$$J^*(-\boldsymbol{q}) = \delta_p - \frac{q_x^2 + q_y^2}{2m} + \frac{k_p q_x}{m} - i\kappa - 2V |\psi_0|^2, \tag{7.49}$$

we have that the denominator is

$$d(q_x, q_y) = \left(\frac{q_x^2 + q_y^2}{2m}\right)^2 - (2\delta_p - 4V |\psi_0|^2)\frac{q_x^2 + q_y^2}{2m} - \frac{k_p^2 q_x^2}{m^2} + \frac{2i\kappa k_p q_x}{m} \tag{7.50}$$

$$+ 3V^2 |\psi_0|^4 - 4\delta_p V |\psi_0|^2 + \delta_p^2 + \kappa^2.$$

For the gapless spectrum we are investigating, the terms on the last line equal zero through Eq. (5.16). Consequently, in the long-range limit, d will go to zero and the response function will exhibit singular behaviour. To discover whether this may be superfluid behaviour, we must look at the limiting behaviour of the numerator.

From Eqs. (6.5) and (6.52), the numerator of the χ_{xx} component is given by

$$n_{xx}(q_x, q_y) = -\frac{|\psi_0|^2}{4m^2}\Big[J(\boldsymbol{q})(4k_p^2 - 4k_p q_x + q_x^2) \tag{7.51}$$

$$+ J^*(-\boldsymbol{q})(4k_p^2 + 4k_p q_x + q_x^2) + 2V |\psi_0|^2 (4k_p^2 - q_x^2)\Big],$$

$$= \frac{|\psi_0|^2}{2m^2}\Big[\frac{q_x^4}{2m} + \frac{q_x^2 q_y^2}{2m} - \left(\frac{2k_p^2}{m} + \delta_p - 3V |\psi_0|^2\right)q_x^2 \tag{7.52}$$

$$+ \frac{2k_p^2}{m}q_y^2 + 4ik_p\kappa q_x - 4k_p^2(\delta_p - V |\psi_0|^2)\Big].$$

We see that this expression is constant in the long-range limit, except when $\delta_p = V |\psi_0|^2$ – i.e., at the shifted resonance point when the spectrum becomes linear. However, at this point the spectrum is gapped and there can be no superfluid behaviour. When the spectrum is gapless, $\delta_p \neq V |\psi_0|^2$ and so, as long as k_p is finite, the response function diverges in the

long-range limit. The longitudinal response function diverges as

$$\chi_{xx}^{mf,L}(\boldsymbol{q} \to \boldsymbol{0}) = i\frac{|\psi_0|^2 k_p}{m\kappa}(\delta_p - V|\psi_0|^2)\frac{1}{q_x \to 0}, \tag{7.53}$$

and the transverse response function as

$$\chi_{xx}^{mf,T}(\boldsymbol{q} \to \boldsymbol{0}) = \frac{2|\psi_0|^2 k_p^2}{m}\frac{\delta_p - V|\psi_0|^2}{\delta_p - 2V|\psi_0|^2}\frac{1}{(q_y \to 0)^2}. \tag{7.54}$$

While it is notable that the longitudinal and transverse response functions are different in the long-range limit, given that they both diverge at different rates and that the longitudinal response function is imaginary, it is not clear what conclusions of physical interest can be drawn from this.

The response for different solutions of the mean-field, where $\chi_{xx}^{mf,L} = \chi_{xx}^{mf,T}$ except at the divergent points, is shown in Fig. 7.4, where the mean-field transverse response function normalised with respect to the mean-field density, $R_0 = m\chi_{xx}^{mf,T}(\boldsymbol{q} \to \boldsymbol{0})/|\psi_0|^2$, is plotted against the intensity, which is tuned from below to above the bistable region. Here, $\delta_p = 3\kappa$, $m = 5 \times 10^{-5}m_e$, $V = 0.0025\text{meV}\mu\text{m}^2$, and $\kappa = 0.05\text{meV}$. The response in the two stable states (solid red and blue) diverges at the gapless points where the stable and unstable states meet (see the turning points in Fig. 5.2). The longitudinal response diverges differently, to a degree that is imperceptible at this scale.

If $k_p = 0$, the numerator and denominator become:

$$n_{xx,0}(q_x, q_y) = \frac{|\psi_0|^2}{2m^2}\left[\frac{q_x^4}{2m} + \frac{q_x^2 q_y^2}{2m} - \left(\delta_p - 3V|\psi_0|^2\right)q_x^2\right], \tag{7.55}$$

$$d_0(q_x, q_y) = \left(\frac{q_x^2 + q_y^2}{2m}\right)^2 - (2\delta_p - 4V|\psi_0|^2)\frac{q_x^2 + q_y^2}{2m}. \tag{7.56}$$

Taking the long-range limit, the transverse response function is zero and the longitudinal response function is:

$$\chi_{xx}^{mf,L}(\boldsymbol{q} \to \boldsymbol{0}) = \frac{|\psi_0|^2}{m}\left[\frac{(\delta_p - 3V|\psi_0|^2)(q_x \to 0)^2}{(2\delta_p - 4V|\psi_0|^2)(q_x \to 0)^2}\right]. \tag{7.57}$$

That is, the system is a superfluid at these precise parameters. Seeing as $\boldsymbol{k}_p = (k_p, 0)$, the χ_{yy}^{mf} response is given by Eq. (7.57), where q_x and q_y are swapped, regardless of the value of the pump momentum. This situation corresponds to the diffusive spectra in Fig. 5.5, similar to the cases of incoherent pumping and the signal state in the OPO regime.

The off-diagonal terms χ_{xy}^{mf} and χ_{yx}^{mf} are equal and share the same denominator as the
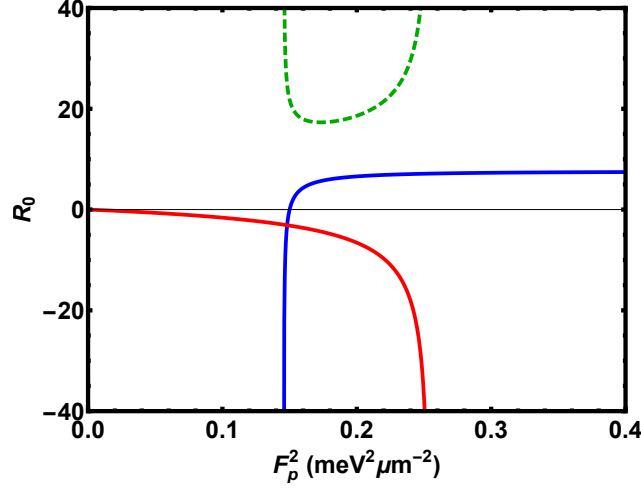
Figure 7.4: Mean-field transverse response in the long-range limit, normalised to the mean-field density, $R_0 = m\chi_{xx}^{mf,T}(\boldsymbol{q} \to \boldsymbol{0})/|\psi_0|^2$, in the bistable regime where $\delta_p = 3\kappa = 0.15$meV and $k_p = 0.1\mu$m^{-1} in the x-direction. The pump intensity is tuned from below to above the bistable region. There are three different states, the stable, lower branch of the bistability curve (solid red) (see Fig. 5.2), the stable upper branch (solid blue) and an unstable, unphysical branch (dashed green). The response function diverges at the turning points in the bistability curve where the spectrum becomes gapless and is equal to zero at the shifted resonance point when the real part of the spectrum is linear. The longitudinal response only differs at the divergent points, but to a degree that is imperceptible at this scale.

diagonal terms. The numerator is given by

$$
\begin{aligned}
n_{xy}(q_x, q_y) &= -\frac{|\psi_0|^2}{4m^2}\Big[-J(\boldsymbol{q})(2k_p - q_x)q_y + J^*(-\boldsymbol{q})(2k_p + q_x)q_y \\
&\quad + V|\psi_0|^2(2k_p - q_x)q_y - V|\psi_0|^2(2k_p + q_x)q_y\Big], \\
&= \frac{|\psi_0|^2}{2m^2}\left[\frac{q_x^3 q_y}{2m} + \frac{q_x q_y^3}{2m} - \left(\frac{2k_p^2}{m} + \delta_p - 3V|\psi_0|^2\right)q_x q_y + 2i\kappa k_p q_y\right].
\end{aligned}
$$
(7.58)

(7.59)

For $k_p = 0$, the response function is zero when the limits are taken sequentially. However, for finite k_p, while the longitudinal response function is zero, the transverse response function diverges as

$$
\chi_{xy}^{mf,T}(\boldsymbol{q} \to \boldsymbol{0}) = -i\frac{|\psi_0|^2}{m}\frac{\kappa k_p}{\delta_p - 2V|\psi_0|^2}\frac{1}{q_y \to 0}.
$$
(7.60)

Similarly to the χ_{xx} case when $k_p \neq 0$, it is not clear what the physical meaning of this divergence is.

This analysis has not included fluctuation terms and, while they were small in the optical limiter case investigated in Sections 7.3 and 7.4, they may be significant as the system approaches instability. An investigation of this and whether it helps explain the divergences seen above is left as further work.

7.6   Measuring the response experimentally

From the definition of the current-current response function in Eq. (2.43), we see that investigating the longitudinal and transverse responses of coherently driven polaritons involves two stages: the application of a perturbation and the measurement of any subsequent change in the current. Here, we outline how these might be achieved, and thus how to probe experimentally the existence of the rigid state and the trends shown in Figs. 7.2 and 7.3.

7.6.1   Applying longitudinal and transverse perturbations

Longitudinal forces take the form $F_L \sim \nabla V$, for some potential V. Therefore, applying a longitudinal perturbation requires simply the application of a potential gradient. In polaritonic systems there are a number of ways to achieve this, including using wedge-shaped cavities, etching, or applying mechanical stress[14,15].

Creating a transverse perturbation is however more difficult. One approach is to adopt a methodology used in the context of cold atoms where experiments have exploited the concept of Berry phase[102] to create artificial gauge fields which act on neutral particles[103,104]. In these experiments, a spatial profile is introduced to the Zeeman splitting in the atomic ground state by applying an inhomogeneous magnetic field. If an atom in one sublevel moves adiabatically – i.e. too slowly to change level – then the Hamiltonian becomes

$$H = \frac{(\boldsymbol{p} - \boldsymbol{A}(\boldsymbol{x}))^2}{2m} + V(\boldsymbol{x}), \tag{7.61}$$

where $\boldsymbol{A}(\boldsymbol{x})$ is an artificial gauge field given by

$$\boldsymbol{A}(\boldsymbol{x}) = i\hbar\langle\psi(\boldsymbol{x})|\nabla\psi(\boldsymbol{x})\rangle, \tag{7.62}$$

and $|\psi(\boldsymbol{x})\rangle$ is the ground state. The neutral particles feel a rotation as if they were charged particles in a magnetic field, i.e. this corresponds to the application of a transverse force. It has been suggested that this approach could be used to measure the superfluid fraction of a system of cold atoms[105].

To adapt the above technique and apply a transverse perturbation to microcavity-polaritons, a proposal[23] has suggested utilising the polariton polarisation degree of freedom rather than the Zeeman splitting. It recommended that the required inhomogeneous magnetic field could be generated using imbalanced anti-Helmholtz coils.

7.6.2 Measuring the current

Once a perturbation has been applied, to measure the current (Eq. (6.2)) which flows in response we need to find the momentum space correlation function $\langle \hat{a}_{\boldsymbol{k}}^{\dagger} \hat{a}_{\boldsymbol{k}+\boldsymbol{q}} \rangle$. If we know this at all values of $\boldsymbol{k}$ then we may calculate the current for a given $\boldsymbol{q}$. To do this, one could interfere two momentum space images of the condensate: $\hat{a}_{\boldsymbol{k}}$, which is simply the field at a momentum $\boldsymbol{k}$, and $\mathrm{e}^{i\phi} \hat{a}_{\boldsymbol{k}+\boldsymbol{q}}$, which is the field measured at $\boldsymbol{k} + \boldsymbol{q}$ and delayed by a phase factor ϕ[27]. The measured intensity from interfering these two fields is given by:

$$I_{\boldsymbol{k},\boldsymbol{q}}(\phi) = \langle (\hat{a}_{\boldsymbol{k}}^{\dagger} + \mathrm{e}^{-i\phi} \hat{a}_{\boldsymbol{k}+\boldsymbol{q}}^{\dagger})(\hat{a}_{\boldsymbol{k}} + \mathrm{e}^{i\phi} \hat{a}_{\boldsymbol{k}+\boldsymbol{q}}) \rangle. \tag{7.63}$$

This expression can be related to the current via the phase dependence. Specifically, by multiplying it out and measuring the intensity at three different phase values, we can calculate the desired correlation function:

$$\langle \hat{a}_{\boldsymbol{k}}^{\dagger} \hat{a}_{\boldsymbol{k}+\boldsymbol{q}} \rangle = \frac{[I_{\boldsymbol{k},\boldsymbol{q}}(\phi_1) - I_{\boldsymbol{k},\boldsymbol{q}}(\phi_2)](\mathrm{e}^{-i\phi_1} - \mathrm{e}^{-i\phi_3}) - [I_{\boldsymbol{k},\boldsymbol{q}}(\phi_1) - I_{\boldsymbol{k},\boldsymbol{q}}(\phi_3)](\mathrm{e}^{-i\phi_1} - \mathrm{e}^{-i\phi_2})}{(\mathrm{e}^{i\phi_1} - \mathrm{e}^{i\phi_2})(\mathrm{e}^{-i\phi_1} - \mathrm{e}^{-i\phi_3}) - (\mathrm{e}^{i\phi_1} - \mathrm{e}^{i\phi_3})(\mathrm{e}^{-i\phi_1} - \mathrm{e}^{-i\phi_2})}. \tag{7.64}$$

Thus, an experimental measurement of the response function can be found through

$$\chi_{xx}(\boldsymbol{q}) = \frac{j_x(\boldsymbol{q})}{f_x(\boldsymbol{q})} = \sum_{\boldsymbol{k}} \frac{2k_x + 2k_p + q_x}{2m} \frac{\langle \hat{a}_{\boldsymbol{k}}^{\dagger} \hat{a}_{\boldsymbol{k}+\boldsymbol{q}} \rangle}{f_x(\boldsymbol{q})}. \tag{7.65}$$

Part III

General Conclusions

Chapter 8

Conclusions

Here, we summarise the conclusions drawn in this thesis and provide brief suggestions of further work.

8.1 Superfluid response of coherently driven polaritons

Superfluidity is one of the most significant examples of quantum mechanics on a macroscopic scale and is well understood in the context of systems in thermal equilibrium, such as liquid helium[6]. Microcavity-polaritons however, which are two-dimensional quasiparticles resulting from the strong coupling of cavity photons to quantum well excitons, present a different challenge as they do not usually reach equilibrium due to photons leaking from the cavity, and must be pumped with a laser to maintain a steady state. Much theoretical and experimental work has concentrated on the question of whether polaritons may form superfluids, and notably observations were made of nearly-dissipationless flow for coherently driven polaritons moving past a defect[17], which was claimed to be evidence of superfluidity. However, unlike closed systems, polaritons have a complex excitation spectrum and, when they are coherently driven, phase fixing by the pump causes it to be gapped, raising questions as to whether these observations are of a superfluid or some other kind of very low-viscosity fluid.

The defining property of superfluids is that they respond to longitudinal but not transverse perturbations, and so by calculating the current-current response function, which is the susceptibility for a current to flow in response to a perturbing force, it is possible to quantify the superfluid fraction, i.e. the part of the system that flows like a superfluid. Such a calculation, utilising a nonequilibrium path integral method from Keldysh field theory, was carried out for incoherently pumped polaritons and found a finite superfluid density[23]. For the relationship between the superfluid fraction and the response function to be well defined, the system being studied must be isotropic and Galilean invariant, and unfortunately neither of these are true of coherently pumped polaritons. Nevertheless, it is still possible to deduce whether any part of these systems responds to perturbations like a superfluid, and

therefore whether they can form superfluids at all.

In this thesis, we use a Keldysh path integral technique to calculate the static current-current response function of a system of coherently driven microcavity-polaritons, where the pump is continuous, homogeneous, and below the optical parametric oscillation (OPO) threshold. Our calculation discovers that they respond equally to both longitudinal and transverse perturbations and therefore cannot form superfluids. The reason for this is that the phase of the macroscopic state is fixed by the coherent pump leading to a gapped excitation spectrum. In general, this gap is in the imaginary part and it prevents singular behaviour in the response function in the long-range limit, $q \rightarrow 0$, where such behaviour is required for a difference between the two types of response.

Remarkably, we find that at zero pump momentum the system does not respond to either type of perturbation at all. That is, it forms a macroscopic quantum state that is completely rigid. When the pump momentum is finite, there exists a coupling between the perturbation and the rigid state that alters its amplitude – i.e. it increases or decreases the number of particles in the state (particle number is not conserved). This produces a 'normal' response in the mathematical sense that the longitudinal and transverse responses are finite and equal. However, this does not correspond to a change in momentum, which is fixed to the pump. Simply, the rigid state has a finite current and so changing the number of particles in it changes the total current flowing in the system. This response grows smoothly and quadratically with k_p due to the coupling $\boldsymbol{\gamma}(\mathbf{0}) = k_p/m$, where each term in the response function contains two factors of $\boldsymbol{\gamma}$. After an initial peak at low density, the total response normalised to the mean-field density reduces asymptotically as the density is increased, suggesting that the perturbation has a weaker effect at larger pump powers.

A notable effect of blue-detuning is to modify the excitation spectrum such that the real component is linear as $q \rightarrow 0$, which is the regime in which nearly-dissipationless flow was observed experimentally. The current-current response function is zero very close to this point, which may be related to this observation. Significantly, though, dissipationless flow is the only property of superfluids that is exhibited by the rigid state as, further to the superfluid response being zero, vortices cannot form unless injected by the pump, and the concept of persistent currents is poorly defined when the phase of the macroscopic state is externally fixed. If the detuning is increased sufficiently the system becomes bistable, and it is possible for the spectrum to become gapless at the very precise points between the stable and unstable states, although it does not fulfil the Landau criterion. To the mean-field level, the superfluid response at these points is finite when $k_p = 0$ and divergent when $k_p \neq 0$, where the physical significance of this result requires further investigation.

Coherently driven polaritons present a complex picture when studying their macroscopic quantum behaviour, in particular because they are out-of-equilibrium, do not conserve parti-

cle number, are anisotropic, are not Galilean invariant, and have gapped, complex excitation spectra. In this work we have shown that this rich collection of attributes leads to a vibrant set of macroscopic flow properties, exemplified by the formation of a new rigid state that does not respond to either longitudinal or transverse perturbations. The existence of this state, which flows without viscosity but lacks other superfluid behaviours, serves to highlight the subtleties inherent in the set of properties known together as superfluidity.

8.2 Further work

Further investigations into the macroscopic quantum states formed by coherently driven polaritons could involve a number of approaches, notably those described in Section 7.6. We expand on additional approaches here.

- Simulations of this system could be carried out by representing the quantum fields as Wigner quasiprobability distributions and using the Fokker-Planck equation, truncated to the second order derivative term, to derive a stochastic differential equation that can be computed numerically (for examples of this method in polaritonic systems, see [79,106]). To address superfluidity, the polariton fields can be simulated in the presence of a gauge field $\boldsymbol{f}$, from which the resulting current flow can be calculated. As the current-current response function is the susceptibility for a current to flow in response to this gauge field, the longitudinal and transverse response functions are given by

$$\chi_{L/T} = \lim_{\boldsymbol{f} \to \boldsymbol{0}} \frac{|\boldsymbol{j}|}{|\boldsymbol{f}_{L/T}|}, \tag{8.1}$$

  where the different responses are distinguished by whether the perturbing field is transverse or longitudinal. By performing these simulations for coherently pumped polaritons, it would be possible to corroborate the absence of superfluidity and the existence of the rigid state, as well as potentially shed more light on the properties of the latter.

- The Keldysh path integral method that has been used in this thesis has now been applied to both incoherently pumped polaritons [23], for which superfluidity was found to survive, and coherently pumped polaritons below the OPO threshold. A natural next step would be to apply it to the signal state of coherently pumped polaritons above the OPO threshold which, like the incoherently pumped case, have a gapless spectrum. Experiments in this regime have observed metastable superflows [20] as well as nearly-dissipationless flow [18,19], and so the expected result of this calculation is that it would confirm that they are superfluids. However, we note that as there are three macroscopic states above the OPO threshold, the scale of the calculation would be substantially larger than that in this thesis.

- The finite superfluid response of coherently pumped polaritons at the mean-field level in the bistable regime could be investigated further by extending the calculation to fluctuations. Furthermore, experimental analyses could probe the behaviour of the system as the pump power is tuned through this regime, concentrating on the boundaries between the stable and unstable states at the turning points of the S-shape in Fig. 5.2 to examine whether the divergences seen in the mean-field response function in the long-range limit have a physical signature.

Appendix A

Response function coefficients

Here we present some of the steps in the calculation of the static current-current response function outlined in Chapter 6. In Section A.1, we show the matrix of second derivatives of the action, S'', evaluated at the mean-field; in Section A.2, we show the first order matrix, $A^{(1)}$, used in Section 6.4.1; in Section A.3, we give the matrices a_i and b_i used in Eq. (6.65) for the first order response function, and the coefficients $\mathcal{C}_\sigma^{a/b}$ they contain; in Section A.4, we show the second order mean-fields, $X^{(2)}$ and $Y^{(2)}$, resulting from the equations in Section 6.4.3; in Section A.5, we show the second order matrix, $A^{(2)}$, used in Section 6.4.3 as well as its derivatives with respect to the source fields; and in Section A.6, we give the coefficients, $\mathcal{C}_{\sigma,\sigma'}^{(2)}$, in Eq. (6.76) for the second order response function. For definitions of some of these terms, see Section 6.2.1.

A.1 Elements of the second derivative matrix

As shown in Eq. (6.58), the first and second order matrices, $A^{(1)}$ and $A^{(2)}$, can be calculated from the matrix of second derivatives of the action (Eq. (6.12)) with respect to the Nambu vector $\Psi(k) = (\psi^c(k), \bar{\psi}^c(-k), \psi^q(k), \bar{\psi}^q(-k))$, evaluated at the source-dependent mean-field (Eq. (6.28)). This can be written as

$$
S''|_{\Psi=\Psi_0} \equiv
\begin{pmatrix}
d/d\bar{\psi}^c(k) \\
d/d\psi^c(-k) \\
d/d\bar{\psi}^q(k) \\
d/d\psi^q(-k)
\end{pmatrix}
\begin{pmatrix}
d/d\psi^c(k') \\
d/d\bar{\psi}^c(-k') \\
d/d\psi^q(k') \\
d/d\bar{\psi}^q(-k')
\end{pmatrix}^T
S|_{\Psi=\Psi_0} \equiv
\begin{pmatrix}
S_{\bar{c}c} & S_{\bar{c}\bar{c}} & S_{\bar{c}q} & S_{\bar{c}\bar{q}} \\
S_{cc} & S_{c\bar{c}} & S_{cq} & S_{c\bar{q}} \\
S_{\bar{q}c} & S_{\bar{q}\bar{c}} & S_{\bar{q}q} & S_{\bar{q}\bar{q}} \\
S_{qc} & S_{q\bar{c}} & S_{qq} & S_{q\bar{q}}
\end{pmatrix}
\delta_{\omega,\omega'},
$$

(A.1)

where the elements are:

$$S_{\bar{c}c} = \gamma_i(\boldsymbol{k}, \boldsymbol{k}')\theta_i(\boldsymbol{k} - \boldsymbol{k}') \tag{A.2}$$

$$- V\left[\sqrt{2}\bar{\psi}_0(Y^{(1)}_{\boldsymbol{k}-\boldsymbol{k}'} + Y^{(2)}_{\boldsymbol{k}-\boldsymbol{k}'}) + \sqrt{2}\psi_0(\bar{Y}^{(1)}_{-\boldsymbol{k}+\boldsymbol{k}'} + \bar{Y}^{(2)}_{-\boldsymbol{k}+\boldsymbol{k}'})\right.$$

$$\left. + \sum_{\boldsymbol{q}}(\bar{X}^{(1)}_{\boldsymbol{k}'+\boldsymbol{q}}Y^{(1)}_{\boldsymbol{k}+\boldsymbol{q}} + \bar{Y}^{(1)}_{\boldsymbol{k}'+\boldsymbol{q}}X^{(1)}_{\boldsymbol{k}+\boldsymbol{q}})\right]$$

$$S_{\bar{c}\bar{c}} = -V\left[\sqrt{2}\psi_0(Y^{(1)}_{\boldsymbol{k}-\boldsymbol{k}'} + Y^{(2)}_{\boldsymbol{k}-\boldsymbol{k}'}) + \sum_{\boldsymbol{q}} X^{(1)}_{\boldsymbol{k}+\boldsymbol{q}}Y^{(1)}_{-\boldsymbol{k}'-\boldsymbol{q}}\right] \tag{A.3}$$

$$S_{\bar{c}q} = J^*(\boldsymbol{k})\delta_{\boldsymbol{k},\boldsymbol{k}'} + \gamma_i(\boldsymbol{k}, \boldsymbol{k}')[f_i(\boldsymbol{k} - \boldsymbol{k}') + \theta_i(\boldsymbol{k} - \boldsymbol{k}')] \tag{A.4}$$

$$- V\left[\sqrt{2}\bar{\psi}_0(X^{(1)}_{\boldsymbol{k}-\boldsymbol{k}'} + X^{(2)}_{\boldsymbol{k}-\boldsymbol{k}'}) + \sqrt{2}\psi_0(\bar{X}^{(1)}_{-\boldsymbol{k}+\boldsymbol{k}'} + \bar{X}^{(2)}_{-\boldsymbol{k}+\boldsymbol{k}'})\right.$$

$$\left. + \sum_{\boldsymbol{q}}(\bar{X}^{(1)}_{\boldsymbol{k}'+\boldsymbol{q}}X^{(1)}_{\boldsymbol{k}+\boldsymbol{q}} + \bar{Y}^{(1)}_{\boldsymbol{k}'+\boldsymbol{q}}Y^{(1)}_{\boldsymbol{k}+\boldsymbol{q}})\right]$$

$$S_{\bar{c}\bar{q}} = -V\psi_0^2\delta_{\boldsymbol{k},\boldsymbol{k}'} - V\left[\sqrt{2}\psi_0(X^{(1)}_{\boldsymbol{k}-\boldsymbol{k}'} + X^{(2)}_{\boldsymbol{k}-\boldsymbol{k}'})\right. \tag{A.5}$$

$$\left. + \frac{1}{2}\sum_{\boldsymbol{q}}(X^{(1)}_{-\boldsymbol{k}'-\boldsymbol{q}}X^{(1)}_{\boldsymbol{k}+\boldsymbol{q}} + Y^{(1)}_{-\boldsymbol{k}'-\boldsymbol{q}}Y^{(1)}_{\boldsymbol{k}+\boldsymbol{q}})\right]$$

$$S_{cc} = -V\left[\sqrt{2}\bar{\psi}_0(\bar{Y}^{(1)}_{-\boldsymbol{k}+\boldsymbol{k}'} + \bar{Y}^{(2)}_{-\boldsymbol{k}+\boldsymbol{k}'}) + \sum_{\boldsymbol{q}} \bar{X}^{(1)}_{-\boldsymbol{k}-\boldsymbol{q}}\bar{Y}^{(1)}_{\boldsymbol{k}'+\boldsymbol{q}}\right] \tag{A.6}$$

$$S_{c\bar{c}} = \gamma_i(-\boldsymbol{k}', -\boldsymbol{k})\theta_i(\boldsymbol{k} - \boldsymbol{k}') \tag{A.7}$$

$$- V\left[\sqrt{2}\bar{\psi}_0(Y^{(1)}_{\boldsymbol{k}-\boldsymbol{k}'} + Y^{(2)}_{\boldsymbol{k}-\boldsymbol{k}'}) + \sqrt{2}\psi_0(\bar{Y}^{(1)}_{-\boldsymbol{k}+\boldsymbol{k}'} + \bar{Y}^{(2)}_{-\boldsymbol{k}+\boldsymbol{k}'})\right.$$

$$\left. + \sum_{\boldsymbol{q}}(\bar{X}^{(1)}_{\boldsymbol{k}'+\boldsymbol{q}}Y^{(1)}_{\boldsymbol{k}+\boldsymbol{q}} + \bar{Y}^{(1)}_{\boldsymbol{k}'+\boldsymbol{q}}X^{(1)}_{\boldsymbol{k}+\boldsymbol{q}})\right]$$

$$S_{cq} = -V\bar{\psi}_0^2\delta_{\boldsymbol{k},\boldsymbol{k}'} - V\left[\sqrt{2}\bar{\psi}_0(\bar{X}^{(1)}_{-\boldsymbol{k}+\boldsymbol{k}'} + \bar{X}^{(2)}_{-\boldsymbol{k}+\boldsymbol{k}'})\right. \tag{A.8}$$

$$\left. + \frac{1}{2}\sum_{\boldsymbol{q}}(\bar{X}^{(1)}_{\boldsymbol{k}'+\boldsymbol{q}}\bar{X}^{(1)}_{-\boldsymbol{k}-\boldsymbol{q}} + \bar{Y}^{(1)}_{\boldsymbol{k}'+\boldsymbol{q}}\bar{Y}^{(1)}_{-\boldsymbol{k}-\boldsymbol{q}})\right]$$

$$S_{c\bar{q}} = J(-\boldsymbol{k})\delta_{\boldsymbol{k},\boldsymbol{k}'} + \gamma_i(-\boldsymbol{k}',-\boldsymbol{k})[f_i(\boldsymbol{k}-\boldsymbol{k}') - \theta_i(\boldsymbol{k}-\boldsymbol{k}')] \tag{A.9}$$

$$- V\left[\sqrt{2}\bar{\psi}_0(X^{(1)}_{\boldsymbol{k}-\boldsymbol{k}'} + X^{(2)}_{\boldsymbol{k}-\boldsymbol{k}'}) + \sqrt{2}\psi_0(\bar{X}^{(1)}_{-\boldsymbol{k}+\boldsymbol{k}'} + \bar{X}^{(2)}_{-\boldsymbol{k}+\boldsymbol{k}'}) \right.$$

$$\left. + \sum_{\boldsymbol{q}}(\bar{X}^{(1)}_{\boldsymbol{k}'+\boldsymbol{q}}X^{(1)}_{\boldsymbol{k}+\boldsymbol{q}} + \bar{Y}^{(1)}_{\boldsymbol{k}'+\boldsymbol{q}}Y^{(1)}_{\boldsymbol{k}+\boldsymbol{q}}) \right]$$

$$S_{\bar{q}c} = J(\boldsymbol{k})\delta_{\boldsymbol{k},\boldsymbol{k}'} + \gamma_i(\boldsymbol{k},\boldsymbol{k}')[f_i(\boldsymbol{k}-\boldsymbol{k}') - \theta_i(\boldsymbol{k}-\boldsymbol{k}')] \tag{A.10}$$

$$- V\left[\sqrt{2}\bar{\psi}_0(X^{(1)}_{\boldsymbol{k}-\boldsymbol{k}'} + X^{(2)}_{\boldsymbol{k}-\boldsymbol{k}'}) + \sqrt{2}\psi_0(\bar{X}^{(1)}_{-\boldsymbol{k}+\boldsymbol{k}'} + \bar{X}^{(2)}_{-\boldsymbol{k}+\boldsymbol{k}'}) \right.$$

$$\left. + \sum_{\boldsymbol{q}}(\bar{X}^{(1)}_{\boldsymbol{k}'+\boldsymbol{q}}X^{(1)}_{\boldsymbol{k}+\boldsymbol{q}} + \bar{Y}^{(1)}_{\boldsymbol{k}'+\boldsymbol{q}}Y^{(1)}_{\boldsymbol{k}+\boldsymbol{q}}) \right]$$

$$S_{\bar{q}\bar{c}} = -V\psi_0^2\delta_{\boldsymbol{k},\boldsymbol{k}'} - V\left[\sqrt{2}\psi_0(X^{(1)}_{\boldsymbol{k}-\boldsymbol{k}'} + X^{(2)}_{\boldsymbol{k}-\boldsymbol{k}'}) \right. \tag{A.11}$$

$$\left. + \frac{1}{2}\sum_{\boldsymbol{q}}(X^{(1)}_{-\boldsymbol{k}'-\boldsymbol{q}}X^{(1)}_{\boldsymbol{k}+\boldsymbol{q}} + Y^{(1)}_{-\boldsymbol{k}'-\boldsymbol{q}}Y^{(1)}_{\boldsymbol{k}+\boldsymbol{q}}) \right]$$

$$S_{\bar{q}q} = 2i\kappa\delta_{\boldsymbol{k},\boldsymbol{k}'} - \gamma_i(\boldsymbol{k},\boldsymbol{k}')\theta_i(\boldsymbol{k}-\boldsymbol{k}') \tag{A.12}$$

$$- V\left[\sqrt{2}\bar{\psi}_0(Y^{(1)}_{\boldsymbol{k}-\boldsymbol{k}'} + Y^{(2)}_{\boldsymbol{k}-\boldsymbol{k}'}) + \sqrt{2}\psi_0(\bar{Y}^{(1)}_{-\boldsymbol{k}+\boldsymbol{k}'} + \bar{Y}^{(2)}_{-\boldsymbol{k}+\boldsymbol{k}'}) \right.$$

$$\left. + \sum_{\boldsymbol{q}}(\bar{X}^{(1)}_{\boldsymbol{k}'+\boldsymbol{q}}Y^{(1)}_{\boldsymbol{k}+\boldsymbol{q}} + \bar{Y}^{(1)}_{\boldsymbol{k}'+\boldsymbol{q}}X^{(1)}_{\boldsymbol{k}+\boldsymbol{q}}) \right]$$

$$S_{\bar{q}\bar{q}} = -V\left[\sqrt{2}\psi_0(Y^{(1)}_{\boldsymbol{k}-\boldsymbol{k}'} + Y^{(2)}_{\boldsymbol{k}-\boldsymbol{k}'}) + \sum_{\boldsymbol{q}}X^{(1)}_{\boldsymbol{k}+\boldsymbol{q}}Y^{(1)}_{-\boldsymbol{k}'-\boldsymbol{q}} \right] \tag{A.13}$$

$$S_{qc} = -V\bar{\psi}_0^2\delta_{\boldsymbol{k},\boldsymbol{k}'} - V\left[\sqrt{2}\bar{\psi}_0(\bar{X}^{(1)}_{-\boldsymbol{k}+\boldsymbol{k}'} + \bar{X}^{(2)}_{-\boldsymbol{k}+\boldsymbol{k}'}) \right. \tag{A.14}$$

$$\left. + \frac{1}{2}\sum_{\boldsymbol{q}}(\bar{X}^{(1)}_{\boldsymbol{k}'+\boldsymbol{q}}\bar{X}^{(1)}_{-\boldsymbol{k}-\boldsymbol{q}} + \bar{Y}^{(1)}_{\boldsymbol{k}'+\boldsymbol{q}}\bar{Y}^{(1)}_{-\boldsymbol{k}-\boldsymbol{q}}) \right]$$

$$S_{q\bar{c}} = J^*(-\boldsymbol{k})\delta_{\boldsymbol{k},\boldsymbol{k}'} + \gamma_i(-\boldsymbol{k}',-\boldsymbol{k})[f_i(\boldsymbol{k}-\boldsymbol{k}') + \theta_i(\boldsymbol{k}-\boldsymbol{k}')] \tag{A.15}$$

$$- V\left[\sqrt{2}\bar{\psi}_0(X^{(1)}_{\boldsymbol{k}-\boldsymbol{k}'} + X^{(2)}_{\boldsymbol{k}-\boldsymbol{k}'}) + \sqrt{2}\psi_0(\bar{X}^{(1)}_{-\boldsymbol{k}+\boldsymbol{k}'} + \bar{X}^{(2)}_{-\boldsymbol{k}+\boldsymbol{k}'}) \right.$$

$$\left. + \sum_{\boldsymbol{q}}(\bar{X}^{(1)}_{\boldsymbol{k}'+\boldsymbol{q}}X^{(1)}_{\boldsymbol{k}+\boldsymbol{q}} + \bar{Y}^{(1)}_{\boldsymbol{k}'+\boldsymbol{q}}Y^{(1)}_{\boldsymbol{k}+\boldsymbol{q}}) \right]$$

$$S_{qq} = -V\left[\sqrt{2}\bar{\psi}_0(\bar{Y}^{(1)}_{-\boldsymbol{k}+\boldsymbol{k}'} + \bar{Y}^{(2)}_{-\boldsymbol{k}+\boldsymbol{k}'}) + \sum_{\boldsymbol{q}} \bar{X}^{(1)}_{-\boldsymbol{k}-\boldsymbol{q}}\bar{Y}^{(1)}_{\boldsymbol{k}'+\boldsymbol{q}}\right] \tag{A.16}$$

$$S_{q\bar{q}} = 2i\kappa\delta_{\boldsymbol{k},\boldsymbol{k}'} - \gamma_i(-\boldsymbol{k}',-\boldsymbol{k})\theta_i(\boldsymbol{k}-\boldsymbol{k}') \tag{A.17}$$

$$-V\left[\sqrt{2}\bar{\psi}_0(Y^{(1)}_{\boldsymbol{k}-\boldsymbol{k}'} + Y^{(2)}_{\boldsymbol{k}-\boldsymbol{k}'}) + \sqrt{2}\psi_0(\bar{Y}^{(1)}_{-\boldsymbol{k}+\boldsymbol{k}'} + \bar{Y}^{(2)}_{-\boldsymbol{k}+\boldsymbol{k}'})\right.$$

$$\left.+ \sum_{\boldsymbol{q}}(\bar{X}^{(1)}_{\boldsymbol{k}'+\boldsymbol{q}}Y^{(1)}_{\boldsymbol{k}+\boldsymbol{q}} + \bar{Y}^{(1)}_{\boldsymbol{k}'+\boldsymbol{q}}X^{(1)}_{\boldsymbol{k}+\boldsymbol{q}})\right]$$

A.2   Elements of the first order matrix

The first order matrix $A^{(1)}$, which we write as

$$A^{(1)} = \begin{pmatrix} A^{(1)}_{11} & A^{(1)}_{12} & A^{(1)}_{13} & A^{(1)}_{14} \\ A^{(1)}_{21} & A^{(1)}_{22} & A^{(1)}_{23} & A^{(1)}_{24} \\ A^{(1)}_{31} & A^{(1)}_{32} & A^{(1)}_{33} & A^{(1)}_{34} \\ A^{(1)}_{41} & A^{(1)}_{42} & A^{(1)}_{43} & A^{(1)}_{44} \end{pmatrix} \delta_{\omega,\omega'}, \tag{A.18}$$

is given by the terms in $S''|_{\Psi=\Psi_0}$ that are first order in the source fields. Substituting in Eqs. (6.38) and (6.39) for the first order mean-fields, $X^{(1)}$ and $Y^{(1)}$, and using the shorthands $K(\boldsymbol{q})$, defined in Eq. (6.53), and $\boldsymbol{p} = \boldsymbol{k} - \boldsymbol{k}'$, the elements of this are given by

$$A^{(1)}_{11} = \left[\gamma_i(\boldsymbol{k},\boldsymbol{k}') - K^*(\boldsymbol{p})V\bar{\psi}_0\psi_0\Big(J(-\boldsymbol{p})\gamma_i(\boldsymbol{p}) + J^*(\boldsymbol{p})\gamma_i(-\boldsymbol{p})\right. \tag{A.19}$$

$$\left.+ V\bar{\psi}_0\psi_0[\gamma_i(-\boldsymbol{p}) + \gamma_i(\boldsymbol{p})]\Big)\right]\theta_i(\boldsymbol{p})$$

$$A^{(1)}_{12} = -K^*(\boldsymbol{p})V\psi_0^2\Big[J(-\boldsymbol{p})\gamma_i(\boldsymbol{p}) + V\bar{\psi}_0\psi_0\gamma_i(-\boldsymbol{p})\Big]\theta_i(\boldsymbol{p}) \tag{A.20}$$

$$A^{(1)}_{13} = \left[\gamma_i(\boldsymbol{k},\boldsymbol{k}') - K(\boldsymbol{p})V\bar{\psi}_0\psi_0\Big(J^*(-\boldsymbol{p})\gamma_i(\boldsymbol{p}) + J(\boldsymbol{p})\gamma_i(-\boldsymbol{p})\right. \tag{A.21}$$

$$\left.+ V\bar{\psi}_0\psi_0(\gamma_i(-\boldsymbol{p}) + \gamma_i(\boldsymbol{p}))\Big)\right]f_i(\boldsymbol{p}) + \left\{\gamma_i(\boldsymbol{k},\boldsymbol{k}')\right.$$

$$+ K(\boldsymbol{p})V\bar{\psi}_0\psi_0\Big(J^*(-\boldsymbol{p})\gamma_i(\boldsymbol{p}) - J(\boldsymbol{p})\gamma_i(-\boldsymbol{p}) - V\bar{\psi}_0\psi_0[\gamma_i(-\boldsymbol{p}) - \gamma_i(\boldsymbol{p})]\Big)$$

$$- i\kappa K(\boldsymbol{p})K^*(\boldsymbol{p})V\bar{\psi}_0\psi_0\Big[J(-\boldsymbol{p})J^*(-\boldsymbol{p})\gamma_i(\boldsymbol{p}) + J(\boldsymbol{p})J^*(\boldsymbol{p})\gamma_i(-\boldsymbol{p})$$

$$+ J^*(-\boldsymbol{p})V\bar{\psi}_0\psi_0\gamma_i(-\boldsymbol{p}) + J^*(\boldsymbol{p})V\bar{\psi}_0\psi_0\gamma_i(-\boldsymbol{p}) + J(\boldsymbol{p})V\bar{\psi}_0\psi_0\gamma_i(\boldsymbol{p})$$

$$\left.+ J(-\boldsymbol{p})V\bar{\psi}_0\psi_0\gamma_i(\boldsymbol{p}) + V^2\bar{\psi}_0^2\psi_0^2[\gamma_i(\boldsymbol{p}) + \gamma_i(-\boldsymbol{p})]\Big]\right\}\theta_i(\boldsymbol{p})$$

$$A_{14}^{(1)} = -K(\boldsymbol{p})V\psi_0^2\Big[J^*(-\boldsymbol{p})\gamma_i(\boldsymbol{p}) + V\bar{\psi}_0\psi_0\gamma_i(-\boldsymbol{p})\Big]f_i(\boldsymbol{p}) \tag{A.22}$$

$$+ \Big\{K(\boldsymbol{p})V\psi_0^2\Big[J^*(-\boldsymbol{p})\gamma_i(\boldsymbol{p}) - V\bar{\psi}_0\psi_0\gamma_i(-\boldsymbol{p})\Big]$$

$$- i\kappa K(\boldsymbol{p})K^*(\boldsymbol{p})V\psi_0^2\Big[J(-\boldsymbol{p})J^*(-\boldsymbol{p})\gamma_i(\boldsymbol{p}) + J^*(-\boldsymbol{p})V\bar{\psi}_0\psi_0\gamma_i(-\boldsymbol{p})$$

$$+ J^*(\boldsymbol{p})V\bar{\psi}_0\psi_0\gamma_i(-\boldsymbol{p}) + V^2\bar{\psi}_0^2\psi_0^2\gamma_i(\boldsymbol{p})\Big]\Big\}\theta_i(\boldsymbol{p})$$

$$A_{21}^{(1)} = -K^*(\boldsymbol{p})V\bar{\psi}_0^2\Big[J^*(\boldsymbol{p})\gamma_i(-\boldsymbol{p}) + V\bar{\psi}_0\psi_0\gamma_i(\boldsymbol{p})\Big]\theta_i(\boldsymbol{p}) \tag{A.23}$$

$$A_{22}^{(1)} = \Big[\gamma_i(-\boldsymbol{k}',-\boldsymbol{k}) - K^*(\boldsymbol{p})V\bar{\psi}_0\psi_0\Big(J(-\boldsymbol{p})\gamma_i(\boldsymbol{p}) + J^*(\boldsymbol{p})\gamma_i(-\boldsymbol{p}) \tag{A.24}$$

$$+ V\bar{\psi}_0\psi_0[\gamma_i(-\boldsymbol{p}) + \gamma_i(\boldsymbol{p})]\Big)\Big]\theta_i(\boldsymbol{p})$$

$$A_{23}^{(1)} = -K(\boldsymbol{p})V\bar{\psi}_0^2\Big[J(\boldsymbol{p})\gamma_i(-\boldsymbol{p}) + V\bar{\psi}_0\psi_0\gamma_i(\boldsymbol{p})\Big]f_i(\boldsymbol{p}) \tag{A.25}$$

$$- \Big\{K(\boldsymbol{p})V\bar{\psi}_0^2\Big[J(\boldsymbol{p})\gamma_i(-\boldsymbol{p}) - V\bar{\psi}_0\psi_0\gamma_i(\boldsymbol{p})\Big]$$

$$- i\kappa K(\boldsymbol{p})K^*(\boldsymbol{p})V\bar{\psi}_0^2\Big[J(\boldsymbol{p})J^*(\boldsymbol{p})\gamma_i(-\boldsymbol{p}) + J(\boldsymbol{p})V\bar{\psi}_0\psi_0\gamma_i(\boldsymbol{p})$$

$$+ J(-\boldsymbol{p})V\bar{\psi}_0\psi_0\gamma_i(\boldsymbol{p}) + V^2\bar{\psi}_0^2\psi_0^2\gamma_i(-\boldsymbol{p})\Big]\Big\}\theta_i(\boldsymbol{p}),$$

$$A_{24}^{(1)} = \Big[\gamma_i(-\boldsymbol{k}',-\boldsymbol{k}) - K(\boldsymbol{p})V\bar{\psi}_0\psi_0\Big(J^*(-\boldsymbol{p})\gamma_i(\boldsymbol{p}) + J(\boldsymbol{p})\gamma_i(-\boldsymbol{p}) \tag{A.26}$$

$$+ V\bar{\psi}_0\psi_0[\gamma_i(-\boldsymbol{p}) + \gamma_i(\boldsymbol{p})]\Big)\Big]f_i(\boldsymbol{p}) + \Big\{-\gamma_i(-\boldsymbol{k}',-\boldsymbol{k})$$

$$+ K(\boldsymbol{p})V\bar{\psi}_0\psi_0\Big(J^*(-\boldsymbol{p})\gamma_i(\boldsymbol{p}) - J(\boldsymbol{p})\gamma_i(-\boldsymbol{p}) - V\bar{\psi}_0\psi_0(\gamma_i(-\boldsymbol{p}) - \gamma_i(\boldsymbol{p}))\Big)\Big)$$

$$- i\kappa K(\boldsymbol{p})K^*(\boldsymbol{p})V\bar{\psi}_0\psi_0\Big[J(-\boldsymbol{p})J^*(-\boldsymbol{p})\gamma_i(\boldsymbol{p}) + J(\boldsymbol{p})J^*(\boldsymbol{p})\gamma_i(-\boldsymbol{p})$$

$$+ J^*(-\boldsymbol{p})V\bar{\psi}_0\psi_0\gamma_i(-\boldsymbol{p}) + J^*(\boldsymbol{p})V\bar{\psi}_0\psi_0\gamma_i(-\boldsymbol{p}) + J(\boldsymbol{p})V\bar{\psi}_0\psi_0\gamma_i(\boldsymbol{p})$$

$$+ J(-\boldsymbol{p})V\bar{\psi}_0\psi_0\gamma_i(\boldsymbol{p}) + V^2\bar{\psi}_0^2\psi_0^2[\gamma_i(\boldsymbol{p}) + \gamma_i(-\boldsymbol{p})]\Big]\Big\}\theta_i(\boldsymbol{p})$$

$$A_{31}^{(1)} = \Big[\gamma_i(\boldsymbol{k},\boldsymbol{k}') - K(\boldsymbol{p})V\bar{\psi}_0\psi_0\Big(J^*(-\boldsymbol{p})\gamma_i(\boldsymbol{p}) + J(\boldsymbol{p})\gamma_i(-\boldsymbol{p}) \tag{A.27}$$

$$+ V\bar{\psi}_0\psi_0[\gamma_i(-\boldsymbol{p}) + \gamma_i(\boldsymbol{p})]\Big)\Big]f_i(\boldsymbol{p}) + \Big\{-\gamma_i(\boldsymbol{k},\boldsymbol{k}')$$

$$+ K(\boldsymbol{p})V\bar{\psi}_0\psi_0\Big(J^*(-\boldsymbol{p})\gamma_i(\boldsymbol{p}) - J(\boldsymbol{p})\gamma_i(-\boldsymbol{p}) - V\bar{\psi}_0\psi_0(\gamma_i(-\boldsymbol{p}) - \gamma_i(\boldsymbol{p}))\Big)$$

$$- i\kappa K(\boldsymbol{p})K^*(\boldsymbol{p})V\bar{\psi}_0\psi_0\Big[J(-\boldsymbol{p})J^*(-\boldsymbol{p})\gamma_i(\boldsymbol{p}) + J(\boldsymbol{p})J^*(\boldsymbol{p})\gamma_i(-\boldsymbol{p})$$

$$+ J^*(-\boldsymbol{p})V\bar{\psi}_0\psi_0\gamma_i(-\boldsymbol{p}) + J^*(\boldsymbol{p})V\bar{\psi}_0\psi_0\gamma_i(-\boldsymbol{p}) + J(\boldsymbol{p})V\bar{\psi}_0\psi_0\gamma_i(\boldsymbol{p})$$

$$+ J(-\boldsymbol{p})V\bar{\psi}_0\psi_0\gamma_i(\boldsymbol{p}) + V^2\bar{\psi}_0^2\psi_0^2[\gamma_i(\boldsymbol{p}) + \gamma_i(-\boldsymbol{p})]\Big]\Big\}\theta_i(\boldsymbol{p})$$

$$A_{32}^{(1)} = -K(\boldsymbol{p})V\psi_0^2\Big[J^*(-\boldsymbol{p})\gamma_i(\boldsymbol{p}) + V\bar{\psi}_0\psi_0\gamma_i(-\boldsymbol{p})\Big]f_i(\boldsymbol{p}) \tag{A.28}$$

$$+ \Big\{K(\boldsymbol{p})V\psi_0^2\Big[J^*(-\boldsymbol{p})\gamma_i(\boldsymbol{p}) - V\bar{\psi}_0\psi_0\gamma_i(-\boldsymbol{p})\Big]$$

$$- i\kappa K(\boldsymbol{p})K^*(\boldsymbol{p})V\psi_0^2\Big[J(-\boldsymbol{p})J^*(-\boldsymbol{p})\gamma_i(\boldsymbol{p}) + J^*(-\boldsymbol{p})V\bar{\psi}_0\psi_0\gamma_i(-\boldsymbol{p})$$

$$+ J^*(\boldsymbol{p})V\bar{\psi}_0\psi_0\gamma_i(-\boldsymbol{p}) + V^2\bar{\psi}_0^2\psi_0^2\gamma_i(\boldsymbol{p})\Big]\Big\}\theta_i(\boldsymbol{p})$$

$$A_{33}^{(1)} = \Big[-\gamma_i(\boldsymbol{k},\boldsymbol{k}') - K^*(\boldsymbol{p})V\bar{\psi}_0\psi_0\Big(J(-\boldsymbol{p})\gamma_i(\boldsymbol{p}) + J^*(\boldsymbol{p})\gamma_i(-\boldsymbol{p}) \tag{A.29}$$

$$+ V\bar{\psi}_0\psi_0(\gamma_i(-\boldsymbol{p}) + \gamma_i(\boldsymbol{p}))\Big)\Big]\theta_i(\boldsymbol{p})$$

$$A_{34}^{(1)} = -K^*(\boldsymbol{p})V\psi_0^2\Big[J(-\boldsymbol{p})\gamma_i(\boldsymbol{p}) + V\bar{\psi}_0\psi_0\gamma_i(-\boldsymbol{p})\Big]\theta_i(\boldsymbol{p}) \tag{A.30}$$

$$A_{41}^{(1)} = -K(\boldsymbol{p})V\bar{\psi}_0^2\Big[J(\boldsymbol{p})\gamma_i(-\boldsymbol{p}) + V\bar{\psi}_0\psi_0\gamma_i(\boldsymbol{p})\Big]f_i(\boldsymbol{p}) \tag{A.31}$$

$$- \Big\{K(\boldsymbol{p})V\bar{\psi}_0^2\Big[J(\boldsymbol{p})\gamma_i(-\boldsymbol{p}) - V\bar{\psi}_0\psi_0\gamma_i(\boldsymbol{p})\Big]$$

$$- i\kappa K(\boldsymbol{p})K^*(\boldsymbol{p})V\bar{\psi}_0^2\Big[J(\boldsymbol{p})J^*(\boldsymbol{p})\gamma_i(-\boldsymbol{p}) + J(\boldsymbol{p})V\bar{\psi}_0\psi_0\gamma_i(\boldsymbol{p})$$

$$+ J(-\boldsymbol{p})V\bar{\psi}_0\psi_0\gamma_i(\boldsymbol{p}) + V^2\bar{\psi}_0^2\psi_0^2\gamma_i(-\boldsymbol{p})\Big]\Big\}\theta_i(\boldsymbol{p})$$

$$A_{42}^{(1)} = \Big[\gamma_i(-\boldsymbol{k}',-\boldsymbol{k}) - K(\boldsymbol{p})V\bar{\psi}_0\psi_0\Big(J^*(-\boldsymbol{p})\gamma_i(\boldsymbol{p}) + J(\boldsymbol{p})\gamma_i(-\boldsymbol{p}) \tag{A.32}$$

$$+ V\bar{\psi}_0\psi_0[\gamma_i(-\boldsymbol{p}) + \gamma_i(\boldsymbol{p})]\Big)\Big]f_i(\boldsymbol{p}) + \Big\{\gamma_i(-\boldsymbol{k}',-\boldsymbol{k})$$

$$+ K(\boldsymbol{p})V\bar{\psi}_0\psi_0\Big(J^*(-\boldsymbol{p})\gamma_i(\boldsymbol{p}) - J(\boldsymbol{p})\gamma_i(-\boldsymbol{p}) - V\bar{\psi}_0\psi_0(\gamma_i(-\boldsymbol{p}) - \gamma_i(\boldsymbol{p}))\Big)$$

$$- i\kappa K(\boldsymbol{p})K^*(\boldsymbol{p})V\bar{\psi}_0\psi_0\Big[J(-\boldsymbol{p})J^*(-\boldsymbol{p})\gamma_i(\boldsymbol{p}) + J(\boldsymbol{p})J^*(\boldsymbol{p})\gamma_i(-\boldsymbol{p})$$

$$+ J^*(-\boldsymbol{p})V\bar{\psi}_0\psi_0\gamma_i(-\boldsymbol{p}) + J^*(\boldsymbol{p})V\bar{\psi}_0\psi_0\gamma_i(-\boldsymbol{p}) + J(\boldsymbol{p})V\bar{\psi}_0\psi_0\gamma_i(\boldsymbol{p})$$

$$+ J(-\boldsymbol{p})V\bar{\psi}_0\psi_0\gamma_i(\boldsymbol{p}) + V^2\bar{\psi}_0^2\psi_0^2[\gamma_i(\boldsymbol{p}) + \gamma_i(-\boldsymbol{p})]\Big]\Big\}\theta_i(\boldsymbol{p})$$

$$A_{43}^{(1)} = -K^*(\boldsymbol{p})V\bar{\psi}_0^2\Big[J^*(\boldsymbol{p})\gamma_i(-\boldsymbol{p}) + V\bar{\psi}_0\psi_0\gamma_i(\boldsymbol{p})\Big]\theta_i(\boldsymbol{p}) \tag{A.33}$$

$$A_{44}^{(1)} = \Big[-\gamma_i(-\boldsymbol{k}',-\boldsymbol{k}) - K^*(\boldsymbol{p})V\bar{\psi}_0\psi_0\Big(J(-\boldsymbol{p})\gamma_i(\boldsymbol{p}) + J^*(\boldsymbol{p})\gamma_i(-\boldsymbol{p}) \tag{A.34}$$

$$+ V\bar{\psi}_0\psi_0[\gamma_i(-\boldsymbol{p}) + \gamma_i(\boldsymbol{p})]\Big)\Big]\theta_i(\boldsymbol{p})$$

The derivative of these with respect to $\boldsymbol{f}$ gives

$$\frac{dA^{(1)}(k,k')}{df_i(\boldsymbol{q})} = \begin{pmatrix} 0 & 0 & \partial_{f_i}A_{13}^{(1)} & \partial_{f_i}A_{14}^{(1)} \\ 0 & 0 & \partial_{f_i}A_{23}^{(1)} & \partial_{f_i}A_{24}^{(1)} \\ \partial_{f_i}A_{13}^{(1)} & \partial_{f_i}A_{14}^{(1)} & 0 & 0 \\ \partial_{f_i}A_{23}^{(1)} & \partial_{f_i}A_{24}^{(1)} & 0 & 0 \end{pmatrix}\delta_{\omega,\omega'}, \tag{A.35}$$

$$= \begin{pmatrix} 0 & a_i(\boldsymbol{k},\boldsymbol{k}') \\ a_i(\boldsymbol{k},\boldsymbol{k}') & 0 \end{pmatrix}\delta_{\boldsymbol{k},\boldsymbol{k}'+\boldsymbol{q}}\delta_{\omega,\omega'},$$

where

$$a_i(\boldsymbol{k},\boldsymbol{k}') = \begin{pmatrix} \gamma_i(\boldsymbol{k},\boldsymbol{k}') & 0 \\ 0 & \gamma_i(-\boldsymbol{k}',-\boldsymbol{k}) \end{pmatrix} \tag{A.36}$$

$$- K(\boldsymbol{p})V\begin{pmatrix} \bar{\psi}_0\psi_0\left([J^*(-\boldsymbol{p}) + V\bar{\psi}_0\psi_0]\gamma_i(\boldsymbol{p})\right. & \psi_0^2\left(J^*(-\boldsymbol{p})\gamma_i(\boldsymbol{p})\right. \\ \left. + [J(\boldsymbol{p}) + V\bar{\psi}_0\psi_0]\gamma_i(-\boldsymbol{p})\right) & \left. + V\bar{\psi}_0\psi_0\gamma_i(-\boldsymbol{p})\right) \\ \\ \bar{\psi}_0^2\left(J(\boldsymbol{p})\gamma_i(-\boldsymbol{p})\right. & \bar{\psi}_0\psi_0\left([J^*(-\boldsymbol{p}) + V\bar{\psi}_0\psi_0]\gamma_i(\boldsymbol{p})\right. \\ \left. + V\bar{\psi}_0\psi_0\gamma_i(\boldsymbol{p})\right) & \left. + [J(\boldsymbol{p}) + V\bar{\psi}_0\psi_0]\gamma_i(-\boldsymbol{p})\right) \end{pmatrix}.$$

Similarly, the $\boldsymbol{\theta}$ derivative gives the matrix

$$
\frac{dA^{(1)}(k,k')}{d\theta_j(-\boldsymbol{q})} = \begin{pmatrix} \partial_{\theta_j} A^{(1)}_{11} & \partial_{\theta_j} A^{(1)}_{12} & \partial_{\theta_j} A^{(1)}_{13} & \partial_{\theta_j} A^{(1)}_{14} \\ \partial_{\theta_j} A^{(1)}_{21} & \partial_{\theta_j} A^{(1)}_{22} & \partial_{\theta_j} A^{(1)}_{23} & \partial_{\theta_j} A^{(1)}_{24} \\ \partial_{\theta_j} A^{(1)}_{31} & \partial_{\theta_j} A^{(1)}_{32} & \partial_{\theta_j} A^{(1)}_{33} & \partial_{\theta_j} A^{(1)}_{34} \\ \partial_{\theta_j} A^{(1)}_{41} & \partial_{\theta_j} A^{(1)}_{42} & \partial_{\theta_j} A^{(1)}_{43} & \partial_{\theta_j} A^{(1)}_{44} \end{pmatrix} \delta_{\omega,\omega'}, \qquad (A.37)
$$

$$
= \begin{pmatrix} b_{11j}(\boldsymbol{k},\boldsymbol{k}') & b_{12j}(\boldsymbol{k},\boldsymbol{k}') \\ b_{21j}(\boldsymbol{k},\boldsymbol{k}') & b_{22j}(\boldsymbol{k},\boldsymbol{k}') \end{pmatrix} \delta_{\boldsymbol{k}+\boldsymbol{q},\boldsymbol{k}'} \delta_{\omega,\omega'},
$$

where

$$
b_{11/22j}(\boldsymbol{k},\boldsymbol{k}') = \begin{pmatrix} \pm\gamma_j(\boldsymbol{k},\boldsymbol{k}') & 0 \\ 0 & \pm\gamma_j(-\boldsymbol{k}',-\boldsymbol{k}) \end{pmatrix} \qquad (A.38)
$$

$$
- \; K^*(\boldsymbol{p})V \begin{pmatrix} \bar{\psi}_0\psi_0\left([J(-\boldsymbol{p})+V\bar{\psi}_0\psi_0]\gamma_j(\boldsymbol{p})\right. & \psi_0^2\left(J(-\boldsymbol{p})\gamma_j(\boldsymbol{p})\right. \\ \left.+[J^*(\boldsymbol{p})+V\bar{\psi}_0\psi_0]\gamma_j(-\boldsymbol{p})\right) & \left.+V\bar{\psi}_0\psi_0\gamma_j(-\boldsymbol{p})\right) \\ \\ \bar{\psi}_0^2\left(J^*(\boldsymbol{p})\gamma_j(-\boldsymbol{p})\right. & \bar{\psi}_0\psi_0\left([J(-\boldsymbol{p})+V\bar{\psi}_0\psi_0]\gamma_j(\boldsymbol{p})\right. \\ \left.+V\bar{\psi}_0\psi_0\gamma_j(\boldsymbol{p})\right) & \left.+[J^*(\boldsymbol{p})+V\bar{\psi}_0\psi_0]\gamma_j(-\boldsymbol{p})\right) \end{pmatrix},
$$

$$
b_{21/12j}(\boldsymbol{k},\boldsymbol{k}') = \begin{pmatrix} \mp\gamma_j(\boldsymbol{k},\boldsymbol{k}') & 0 \\ 0 & \pm\gamma_j(-\boldsymbol{k}',-\boldsymbol{k}) \end{pmatrix} \qquad (A.39)
$$

$$
+ \; K(\boldsymbol{p})V \begin{pmatrix} \bar{\psi}_0\psi_0\left([J^*(-\boldsymbol{p})+V\bar{\psi}_0\psi_0]\gamma_j(\boldsymbol{p})\right. & \psi_0^2\left(J^*(-\boldsymbol{p})\gamma_j(\boldsymbol{p})\right. \\ \left.-[J(\boldsymbol{p})+V\bar{\psi}_0\psi_0]\gamma_j(-\boldsymbol{p})\right) & \left.-V\bar{\psi}_0\psi_0\gamma_j(-\boldsymbol{p})\right) \\ \\ \bar{\psi}_0^2\left(J(\boldsymbol{p})\gamma_j(-\boldsymbol{p})\right. & \bar{\psi}_0\psi_0\left([J^*(-\boldsymbol{p})+V\bar{\psi}_0\psi_0]\gamma_j(\boldsymbol{p})\right. \\ \left.-V\bar{\psi}_0\psi_0\gamma_j(\boldsymbol{p})\right) & \left.-[J(\boldsymbol{p})+V\bar{\psi}_0\psi_0]\gamma_j(-\boldsymbol{p})\right) \end{pmatrix}
$$

$$
- \; i\kappa K(\boldsymbol{p})K^*(\boldsymbol{p})V \begin{pmatrix} \beta_j(\boldsymbol{p}) & \beta'_j(\boldsymbol{p}) \\ \beta'^*_j(-\boldsymbol{p}) & \beta_j(\boldsymbol{p}) \end{pmatrix},
$$

$$\beta_j(\boldsymbol{p}) = \bar{\psi}_0\psi_0\left([J(-\boldsymbol{p})J^*(-\boldsymbol{p}) + J(\boldsymbol{p})V\bar{\psi}_0\psi_0 + J(-\boldsymbol{p})V\bar{\psi}_0\psi_0 + V^2\bar{\psi}_0^2\psi_0^2]\gamma_j(\boldsymbol{p})\right.$$

$$\left. + [J(\boldsymbol{p})J^*(\boldsymbol{p}) + J^*(-\boldsymbol{p})V\bar{\psi}_0\psi_0 + J^*(\boldsymbol{p})V\bar{\psi}_0\psi_0 + V^2\bar{\psi}_0^2\psi_0^2]\gamma_j(-\boldsymbol{p})\right),$$

$$\beta_j'(\boldsymbol{p}) = \psi_0^2\left([J(-\boldsymbol{p})J^*(-\boldsymbol{p}) + V^2\bar{\psi}_0^2\psi_0^2]\gamma_j(\boldsymbol{p}) + [J^*(-\boldsymbol{p}) + J^*(\boldsymbol{p})]V\bar{\psi}_0\psi_0\gamma_j(-\boldsymbol{p})\right).$$

A.3 Coefficients of the first order response function

The matrices $a_i(\boldsymbol{k}+\boldsymbol{q},\boldsymbol{k})$ and $b_j(\boldsymbol{k},\boldsymbol{k}+\boldsymbol{q})$ in the first order response function (Eq. (6.65)) may be written as

$$a_i(\boldsymbol{k}+\boldsymbol{q},\boldsymbol{k}) = \frac{1}{2}(\mathbb{1}+\hat{\sigma}_z)\gamma_i(\boldsymbol{k}+\boldsymbol{q},\boldsymbol{k}) + \frac{1}{2}(\mathbb{1}-\hat{\sigma}_z)\gamma_i(-\boldsymbol{k}-\boldsymbol{q},-\boldsymbol{k}) + \sum_{\sigma\in\pm}\mathcal{C}_\sigma^a(\boldsymbol{q})\gamma_i(\sigma\boldsymbol{q}), \quad \text{(A.40)}$$

$$b_j(\boldsymbol{k},\boldsymbol{k}+\boldsymbol{q}) = \frac{1}{2}(\mathbb{1}+\hat{\sigma}_z)\gamma_j(\boldsymbol{k},\boldsymbol{k}+\boldsymbol{q}) + \frac{1}{2}(\mathbb{1}-\hat{\sigma}_z)\gamma_j(-\boldsymbol{k},-\boldsymbol{k}-\boldsymbol{q}) + \sum_{\sigma\in\pm}\mathcal{C}_\sigma^b(\boldsymbol{q})\gamma_j(\sigma\boldsymbol{q}), \quad \text{(A.41)}$$

where the coefficients $\mathcal{C}_\sigma^{a/b}(\boldsymbol{q})$ are 2×2 matrices in Nambu space given by

$$\mathcal{C}_+^a(\boldsymbol{q}) = -VK(\boldsymbol{q})\begin{pmatrix} |\psi_0|^2\,[J^*(-\boldsymbol{q}) + V\,|\psi_0|^2] & \psi_0^2 J^*(-\boldsymbol{q}) \\ V\bar{\psi}_0^3\psi_0 & |\psi_0|^2\,[J^*(-\boldsymbol{q}) + V\,|\psi_0|^2] \end{pmatrix}, \quad \text{(A.42)}$$

$$\mathcal{C}_-^a(\boldsymbol{q}) = -VK(\boldsymbol{q})\begin{pmatrix} |\psi_0|^2\,[J(\boldsymbol{q}) + V\,|\psi_0|^2] & V\bar{\psi}_0\psi_0^3 \\ \bar{\psi}_0^2 J(\boldsymbol{q}) & |\psi_0|^2\,[J(\boldsymbol{q}) + V\,|\psi_0|^2] \end{pmatrix}, \quad \text{(A.43)}$$

$$\mathcal{C}_+^b(\boldsymbol{q}) = -VK(\boldsymbol{q})\begin{pmatrix} |\psi_0|^2\,[J^*(-\boldsymbol{q}) + V\,|\psi_0|^2] & V\bar{\psi}_0\psi_0^3 \\ \bar{\psi}_0^2 J^*(-\boldsymbol{q}) & |\psi_0|^2\,[J^*(-\boldsymbol{q}) + V\,|\psi_0|^2] \end{pmatrix}, \quad \text{(A.44)}$$

$$\mathcal{C}_-^b(\boldsymbol{q}) = -VK(\boldsymbol{q})\begin{pmatrix} |\psi_0|^2\,[J(\boldsymbol{q}) + V\,|\psi_0|^2] & \psi_0^2 J(\boldsymbol{q}) \\ V\bar{\psi}_0^3\psi_0 & |\psi_0|^2\,[J(\boldsymbol{q}) + V\,|\psi_0|^2] \end{pmatrix}. \quad \text{(A.45)}$$

A.4   Second order mean-field terms

The second order mean-fields, $X^{(2)}$ and $Y^{(2)}$, are found by solving Eqs. (6.74) and are given by

$$
\begin{aligned}
X_{\boldsymbol{k}}^{(2)} \;=\; & -\frac{1}{2}K(\boldsymbol{k})\Big(-2i\kappa J^*(-\boldsymbol{k})Y_{\boldsymbol{k}}^{(2)} - 2i\kappa V\psi_0^2 \bar{Y}_{-\boldsymbol{k}}^{(2)} \\
& +\sum_{\boldsymbol{q}}\Big[\sqrt{2}J^*(-\boldsymbol{k})V\Big(\psi_0 \bar{X}_{-\boldsymbol{q}}^{(1)}X_{\boldsymbol{k}-\boldsymbol{q}}^{(1)} + \frac{1}{2}\bar{\psi}_0 X_{\boldsymbol{q}}^{(1)}X_{\boldsymbol{k}-\boldsymbol{q}}^{(1)}\Big) \\
& +\sqrt{2}V^2\psi_0^2\Big(\bar{\psi}_0 \bar{X}_{-\boldsymbol{q}}^{(1)}X_{\boldsymbol{k}+\boldsymbol{q}}^{(1)} + \frac{1}{2}\psi_0 \bar{X}_{-\boldsymbol{q}}^{(1)}\bar{X}_{-\boldsymbol{k}+\boldsymbol{q}}^{(1)}\Big) \\
& -J^*(-\boldsymbol{k})\gamma_i(\boldsymbol{k},\boldsymbol{k}-\boldsymbol{q})\Big([f_i(\boldsymbol{q})-\theta_i(\boldsymbol{q})]X_{\boldsymbol{k}-\boldsymbol{q}}^{(1)} - \theta_i(\boldsymbol{q})Y_{\boldsymbol{k}-\boldsymbol{q}}^{(1)}\Big) \\
& -V\psi_0^2\gamma_i(-\boldsymbol{k}+\boldsymbol{q},-\boldsymbol{k})\Big([f_i(\boldsymbol{q})+\theta_i(\boldsymbol{q})]\bar{X}_{-\boldsymbol{k}+\boldsymbol{q}}^{(1)} - \theta_i(\boldsymbol{q})\bar{Y}_{-\boldsymbol{k}+\boldsymbol{q}}^{(1)}\Big)\Big]\Big),
\end{aligned}
\tag{A.46}
$$

$$
\begin{aligned}
\bar{X}_{-\boldsymbol{k}}^{(2)} \;=\; & -\frac{1}{2}K(\boldsymbol{k})\Big(-2i\kappa J(\boldsymbol{k})\bar{Y}_{-\boldsymbol{k}}^{(2)} - 2i\kappa V\bar{\psi}_0^2 Y_{\boldsymbol{k}}^{(2)} \\
& +\sum_{\boldsymbol{q}}\Big[\sqrt{2}J(\boldsymbol{k})V\Big(\bar{\psi}_0 \bar{X}_{-\boldsymbol{q}}^{(1)}X_{\boldsymbol{k}-\boldsymbol{q}}^{(1)} + \frac{1}{2}\psi_0 \bar{X}_{-\boldsymbol{q}}^{(1)}\bar{X}_{-\boldsymbol{k}+\boldsymbol{q}}^{(1)}\Big) \\
& +\sqrt{2}V^2\bar{\psi}_0^2\Big(\psi_0 \bar{X}_{-\boldsymbol{q}}^{(1)}X_{\boldsymbol{k}+\boldsymbol{q}}^{(1)} + \frac{1}{2}\bar{\psi}_0 X_{\boldsymbol{q}}^{(1)}X_{\boldsymbol{k}-\boldsymbol{q}}^{(1)}\Big) \\
& -J(\boldsymbol{k})\gamma_i(-\boldsymbol{k}+\boldsymbol{q},-\boldsymbol{k})\Big([f_i(\boldsymbol{q})+\theta_i(\boldsymbol{q})]\bar{X}_{-\boldsymbol{k}+\boldsymbol{q}}^{(1)} - \theta_i(\boldsymbol{q})\bar{Y}_{-\boldsymbol{k}+\boldsymbol{q}}^{(1)}\Big) \\
& -V\bar{\psi}_0^2\gamma_i(\boldsymbol{k},\boldsymbol{k}-\boldsymbol{q})\Big([f_i(\boldsymbol{q})-\theta_i(\boldsymbol{q})]X_{\boldsymbol{k}-\boldsymbol{q}}^{(1)} - \theta_i(\boldsymbol{q})Y_{\boldsymbol{k}-\boldsymbol{q}}^{(1)}\Big)\Big]\Big),
\end{aligned}
\tag{A.47}
$$

$$
\begin{aligned}
Y_{\boldsymbol{k}}^{(2)} \;=\; & -\frac{1}{2}K^*(\boldsymbol{k})\sum_{\boldsymbol{q}}\Big[\sqrt{2}J(-\boldsymbol{k})V\Big(\psi_0 \bar{Y}_{-\boldsymbol{q}}^{(1)}X_{\boldsymbol{k}-\boldsymbol{q}}^{(1)} \\
& +\psi_0 \bar{X}_{-\boldsymbol{q}}^{(1)}Y_{\boldsymbol{k}-\boldsymbol{q}}^{(1)} + \bar{\psi}_0 X_{\boldsymbol{q}}^{(1)}Y_{\boldsymbol{k}-\boldsymbol{q}}^{(1)}\Big) \\
& +\sqrt{2}V^2\psi_0^2\Big(\bar{\psi}_0 \bar{X}_{-\boldsymbol{q}}^{(1)}Y_{\boldsymbol{k}-\boldsymbol{q}}^{(1)} + \bar{\psi}_0 \bar{Y}_{-\boldsymbol{q}}^{(1)}X_{\boldsymbol{k}-\boldsymbol{q}}^{(1)} + \psi_0 \bar{X}_{-\boldsymbol{q}}^{(1)}\bar{Y}_{-\boldsymbol{k}+\boldsymbol{q}}^{(1)}\Big) \\
& -J(-\boldsymbol{k})\gamma_i(\boldsymbol{k},\boldsymbol{k}-\boldsymbol{q})\Big(\theta_i(\boldsymbol{q})X_{\boldsymbol{k}-\boldsymbol{q}}^{(1)} + [f_i(\boldsymbol{q})+\theta_i(\boldsymbol{q})]Y_{\boldsymbol{k}-\boldsymbol{q}}^{(1)}\Big) \\
& -V\psi_0^2\gamma_i(-\boldsymbol{k}+\boldsymbol{q},-\boldsymbol{k})\Big(\theta_i(\boldsymbol{q})\bar{X}_{-\boldsymbol{k}+\boldsymbol{q}}^{(1)} + [f_i(\boldsymbol{q})-\theta_i(\boldsymbol{q})]\bar{Y}_{-\boldsymbol{k}+\boldsymbol{q}}^{(1)}\Big)\Big],
\end{aligned}
\tag{A.48}
$$

$$
\begin{aligned}
\bar{Y}_{-\boldsymbol{k}}^{(2)} \;=\; & -\frac{1}{2}K^*(\boldsymbol{k})\sum_{\boldsymbol{q}}\Big[\sqrt{2}J^*(\boldsymbol{k})V\Big(\bar{\psi}_0 \bar{X}_{-\boldsymbol{q}}^{(1)}Y_{\boldsymbol{k}-\boldsymbol{q}}^{(1)} \\
& +\bar{\psi}_0 \bar{Y}_{-\boldsymbol{q}}^{(1)}X_{\boldsymbol{k}-\boldsymbol{q}}^{(1)} + \psi_0 \bar{X}_{-\boldsymbol{q}}^{(1)}\bar{Y}_{-\boldsymbol{k}+\boldsymbol{q}}^{(1)}\Big) \\
& +\sqrt{2}V^2\bar{\psi}_0^2\Big(\psi_0 \bar{Y}_{-\boldsymbol{q}}^{(1)}X_{\boldsymbol{k}-\boldsymbol{q}}^{(1)} + \psi_0 \bar{X}_{-\boldsymbol{q}}^{(1)}Y_{\boldsymbol{k}-\boldsymbol{q}}^{(1)} + \bar{\psi}_0 X_{\boldsymbol{q}}^{(1)}Y_{\boldsymbol{k}-\boldsymbol{q}}^{(1)}\Big) \\
& -J^*(\boldsymbol{k})\gamma_i(-\boldsymbol{k}+\boldsymbol{q},-\boldsymbol{k})\Big(\theta_i(\boldsymbol{q})\bar{X}_{-\boldsymbol{k}+\boldsymbol{q}}^{(1)} + [f_i(\boldsymbol{q})-\theta_i(\boldsymbol{q})]\bar{Y}_{-\boldsymbol{k}+\boldsymbol{q}}^{(1)}\Big) \\
& -V\bar{\psi}_0^2\gamma_i(\boldsymbol{k},\boldsymbol{k}-\boldsymbol{q})\Big(\theta_i(\boldsymbol{q})X_{\boldsymbol{k}-\boldsymbol{q}}^{(1)} + [f_i(\boldsymbol{q})+\theta_i(\boldsymbol{q})]Y_{\boldsymbol{k}-\boldsymbol{q}}^{(1)}\Big)\Big].
\end{aligned}
\tag{A.49}
$$

A.5 Elements of the second order matrix

Substituting the relevant second order mean-fields, Eqs. (A.48) and (A.49), into Eqs. (6.71-6.73), and dropping terms that do not contain both source fields, we get for the elements of the second order matrix:

$$
\begin{aligned}
A_A^{(2)} = -V \sum_{\boldsymbol{q'}} \Big\{ & (\bar{X}_{\boldsymbol{q'}}^{(1)} Y_{\boldsymbol{q'}}^{(1)} + \bar{Y}_{\boldsymbol{q'}}^{(1)} X_{\boldsymbol{q'}}^{(1)}) \\
& - K(\boldsymbol{0}) \Big(\big[(J(\boldsymbol{0}) + J^*(\boldsymbol{0})) V \bar{\psi}_0 \psi_0 + 2V^2 \bar{\psi}_0^2 \psi_0^2 \big] \big[\bar{Y}_{-\boldsymbol{q'}}^{(1)} X_{-\boldsymbol{q'}}^{(1)} + \bar{X}_{-\boldsymbol{q'}}^{(1)} Y_{-\boldsymbol{q'}}^{(1)} \big] \\
& + \big[J(\boldsymbol{0}) V \bar{\psi}_0^2 + V^2 \bar{\psi}_0^3 \psi_0 \big] X_{\boldsymbol{q'}}^{(1)} Y_{-\boldsymbol{q'}}^{(1)} + \big[J^*(\boldsymbol{0}) V \psi_0^2 + V^2 \bar{\psi}_0 \psi_0^3 \big] \bar{X}_{-\boldsymbol{q'}}^{(1)} \bar{Y}_{\boldsymbol{q'}}^{(1)} \\
& - \frac{1}{\sqrt{2}} \bar{\psi}_0 \big[J(\boldsymbol{0}) + V \bar{\psi}_0 \psi_0 \big] \gamma_i(-\boldsymbol{q'}) \big[\theta_i(\boldsymbol{q'}) X_{-\boldsymbol{q'}}^{(1)} + f_i(\boldsymbol{q'}) Y_{-\boldsymbol{q'}}^{(1)} \big] \\
& - \frac{1}{\sqrt{2}} \psi_0 \big[J^*(\boldsymbol{0}) + V \bar{\psi}_0 \psi_0 \big] \gamma_i(\boldsymbol{q'}) \big[\theta_i(\boldsymbol{q'}) \bar{X}_{\boldsymbol{q'}}^{(1)} + f_i(\boldsymbol{q'}) \bar{Y}_{\boldsymbol{q'}}^{(1)} \big] \Big) \Big\},
\end{aligned}
\tag{A.50}
$$

$$
\begin{aligned}
A_B^{(2)} = -V \sum_{\boldsymbol{q'}} \Big\{ & X_{\boldsymbol{q'}}^{(1)} Y_{-\boldsymbol{q'}}^{(1)} \\
& - K(\boldsymbol{0}) \Big(\big[J(\boldsymbol{0}) V \psi_0^2 + V^2 \bar{\psi}_0 \psi_0^3 \big] \big[\bar{Y}_{-\boldsymbol{q'}}^{(1)} X_{-\boldsymbol{q'}}^{(1)} + \bar{X}_{-\boldsymbol{q'}}^{(1)} Y_{-\boldsymbol{q'}}^{(1)} \big] \\
& + \big[J(\boldsymbol{0}) V \bar{\psi}_0 \psi_0 \big] X_{\boldsymbol{q'}}^{(1)} Y_{-\boldsymbol{q'}}^{(1)} + \big[V^2 \psi_0^4 \big] \bar{X}_{-\boldsymbol{q'}}^{(1)} \bar{Y}_{\boldsymbol{q'}}^{(1)} \\
& - \frac{1}{\sqrt{2}} \big[J(\boldsymbol{0}) \psi_0 \gamma_i(-\boldsymbol{q'}) \big] \big[\theta_i(\boldsymbol{q'}) X_{-\boldsymbol{q'}}^{(1)} + f_i(\boldsymbol{q'}) Y_{-\boldsymbol{q'}}^{(1)} \big] \\
& - \frac{1}{\sqrt{2}} \big[V \psi_0^3 \gamma_i(\boldsymbol{q'}) \big] \big[\theta_i(\boldsymbol{q'}) \bar{X}_{\boldsymbol{q'}}^{(1)} + f_i(\boldsymbol{q'}) \bar{Y}_{\boldsymbol{q'}}^{(1)} \big] \Big) \Big\},
\end{aligned}
\tag{A.51}
$$

$$
\begin{aligned}
A_C^{(2)} = -V \sum_{\boldsymbol{q'}} \Big\{ & \bar{X}_{-\boldsymbol{q'}}^{(1)} \bar{Y}_{\boldsymbol{q'}}^{(1)} \\
& - K(\boldsymbol{0}) \Big(\big[J^*(\boldsymbol{0}) V \bar{\psi}_0^2 + V^2 \bar{\psi}_0^3 \psi_0 \big] \big[\bar{Y}_{-\boldsymbol{q'}}^{(1)} X_{-\boldsymbol{q'}}^{(1)} + \bar{X}_{-\boldsymbol{q'}}^{(1)} Y_{-\boldsymbol{q'}}^{(1)} \big] \\
& + \big[V^2 \bar{\psi}_0^4 \big] X_{\boldsymbol{q'}}^{(1)} Y_{-\boldsymbol{q'}}^{(1)} + \big[J^*(\boldsymbol{0}) V \bar{\psi}_0 \psi_0 \big] \bar{X}_{-\boldsymbol{q'}}^{(1)} \bar{Y}_{\boldsymbol{q'}}^{(1)} \\
& - \frac{1}{\sqrt{2}} \big[V \bar{\psi}_0^3 \gamma_i(-\boldsymbol{q'}) \big] \big[\theta_i(\boldsymbol{q'}) X_{-\boldsymbol{q'}}^{(1)} + f_i(\boldsymbol{q'}) Y_{-\boldsymbol{q'}}^{(1)} \big] \\
& - \frac{1}{\sqrt{2}} \big[J^*(\boldsymbol{0}) \bar{\psi}_0 \gamma_i(\boldsymbol{q'}) \big] \big[\theta_i(\boldsymbol{q'}) \bar{X}_{\boldsymbol{q'}}^{(1)} + f_i(\boldsymbol{q'}) \bar{Y}_{\boldsymbol{q'}}^{(1)} \big] \Big) \Big\}.
\end{aligned}
\tag{A.52}
$$

A.5.1 Differentiation of the second order terms

Given the need for each term to possess a cross term in the source fields and that $Y^{(1)}$ only contains $\boldsymbol{\theta}$, only the part of $X^{(1)}$ containing $\boldsymbol{f}$ is ever relevant in the second order matrix.

Thus, we can rewrite Eqs. (6.38) and (6.39) as

$$X_{\boldsymbol{q}'}^{(1)} = \frac{1}{\sqrt{2}} K(\boldsymbol{q}')\psi_0 \Big(J^*(-\boldsymbol{q}')\gamma_i(\boldsymbol{q}') + V\bar{\psi}_0\psi_0\gamma_i(-\boldsymbol{q}') \Big) f_i(\boldsymbol{q}'), \tag{A.53}$$

$$\bar{X}_{\boldsymbol{q}'}^{(1)} = \frac{1}{\sqrt{2}} K^*(\boldsymbol{q}')\bar{\psi}_0 \Big(J(-\boldsymbol{q}')\gamma_i(\boldsymbol{q}') + V\bar{\psi}_0\psi_0\gamma_i(-\boldsymbol{q}') \Big) f_i(-\boldsymbol{q}'), \tag{A.54}$$

$$Y_{\boldsymbol{q}'}^{(1)} = \frac{1}{\sqrt{2}} K^*(\boldsymbol{q}')\psi_0 \Big(J(-\boldsymbol{q}')\gamma_i(\boldsymbol{q}') + V\bar{\psi}_0\psi_0\gamma_i(-\boldsymbol{q}') \Big) \theta_i(\boldsymbol{q}'), \tag{A.55}$$

$$\bar{Y}_{\boldsymbol{q}'}^{(1)} = \frac{1}{\sqrt{2}} K(\boldsymbol{q}')\bar{\psi}_0 \Big(J^*(-\boldsymbol{q}')\gamma_i(\boldsymbol{q}') + V\bar{\psi}_0\psi_0\gamma_i(-\boldsymbol{q}') \Big) \theta_i(-\boldsymbol{q}'). \tag{A.56}$$

Substituting these into Eqs. (A.50-A.52), we may calculate the derivatives that make up Eq. (6.75):

$$\sum_{\boldsymbol{q}'} \frac{d\bar{X}_{\boldsymbol{q}'}^{(1)}}{df_i(\boldsymbol{q})} \frac{dY_{\boldsymbol{q}'}^{(1)}}{d\theta_j(-\boldsymbol{q})} = \sum_{\boldsymbol{q}'} \frac{d\bar{X}_{-\boldsymbol{q}'}^{(1)}}{df_i(\boldsymbol{q})} \frac{dY_{-\boldsymbol{q}'}^{(1)}}{d\theta_j(-\boldsymbol{q})}$$

$$= \frac{1}{2} K(\boldsymbol{q})^2 \bar{\psi}_0\psi_0 \Big(J(\boldsymbol{q})J(\boldsymbol{q})\gamma_i(-\boldsymbol{q})\gamma_j(-\boldsymbol{q}) + J(\boldsymbol{q})V\bar{\psi}_0\psi_0\gamma_i(-\boldsymbol{q})\gamma_j(\boldsymbol{q})$$

$$+ J(\boldsymbol{q})V\bar{\psi}_0\psi_0\gamma_i(\boldsymbol{q})\gamma_j(-\boldsymbol{q}) + V^2\bar{\psi}_0^2\psi_0^2\gamma_i(\boldsymbol{q})\gamma_j(\boldsymbol{q}) \Big)$$

$$\sum_{\boldsymbol{q}'} \frac{d\bar{Y}_{\boldsymbol{q}'}^{(1)}}{d\theta_j(-\boldsymbol{q})} \frac{dX_{\boldsymbol{q}'}^{(1)}}{df_i(\boldsymbol{q})} = \sum_{\boldsymbol{q}'} \frac{d\bar{Y}_{-\boldsymbol{q}'}^{(1)}}{d\theta_j(-\boldsymbol{q})} \frac{dX_{-\boldsymbol{q}'}^{(1)}}{df_i(\boldsymbol{q})}$$

$$= \frac{1}{2} K(\boldsymbol{q})^2 \bar{\psi}_0\psi_0 \Big(J^*(-\boldsymbol{q})J^*(-\boldsymbol{q})\gamma_i(\boldsymbol{q})\gamma_j(\boldsymbol{q}) + J^*(-\boldsymbol{q})V\bar{\psi}_0\psi_0\gamma_i(-\boldsymbol{q})\gamma_j(\boldsymbol{q})$$

$$+ J^*(-\boldsymbol{q})V\bar{\psi}_0\psi_0\gamma_i(\boldsymbol{q})\gamma_j(-\boldsymbol{q}) + V^2\bar{\psi}_0^2\psi_0^2\gamma_i(-\boldsymbol{q})\gamma_j(-\boldsymbol{q}) \Big)$$

$$\sum_{\boldsymbol{q}'} \frac{dX_{\boldsymbol{q}'}^{(1)}}{df_i(\boldsymbol{q})} \frac{dY_{-\boldsymbol{q}'}^{(1)}}{d\theta_j(-\boldsymbol{q})} = \frac{1}{2} K(\boldsymbol{q})^2 \psi_0^2 \Big(J^*(-\boldsymbol{q})J(\boldsymbol{q})\gamma_i(\boldsymbol{q})\gamma_j(-\boldsymbol{q}) + J^*(-\boldsymbol{q})V\bar{\psi}_0\psi_0\gamma_i(\boldsymbol{q})\gamma_j(\boldsymbol{q})$$

$$+ J(\boldsymbol{q})V\bar{\psi}_0\psi_0\gamma_i(-\boldsymbol{q})\gamma_j(-\boldsymbol{q}) + V^2\bar{\psi}_0^2\psi_0^2\gamma_i(-\boldsymbol{q})\gamma_j(\boldsymbol{q}) \Big)$$

$$\sum_{\boldsymbol{q}'} \frac{d\bar{X}_{-\boldsymbol{q}'}^{(1)}}{df_i(\boldsymbol{q})} \frac{d\bar{Y}_{\boldsymbol{q}'}^{(1)}}{d\theta_j(-\boldsymbol{q})} = \frac{1}{2} K(\boldsymbol{q})^2 \bar{\psi}_0^2 \Big(J(\boldsymbol{q})J^*(-\boldsymbol{q})\gamma_i(-\boldsymbol{q})\gamma_j(\boldsymbol{q}) + J(\boldsymbol{q})V\bar{\psi}_0\psi_0\gamma_i(-\boldsymbol{q})\gamma_j(-\boldsymbol{q})$$

$$+ J^*(-\boldsymbol{q})V\bar{\psi}_0\psi_0\gamma_i(\boldsymbol{q})\gamma_j(\boldsymbol{q}) + V^2\bar{\psi}_0^2\psi_0^2\gamma_i(\boldsymbol{q})\gamma_j(-\boldsymbol{q}) \Big)$$

$$\sum_{\boldsymbol{q}'} \gamma_l(-\boldsymbol{q}') \frac{d\theta_l(\boldsymbol{q}')}{d\theta_j(-\boldsymbol{q})} \frac{dX^{(1)}_{-\boldsymbol{q}'}}{df_i(\boldsymbol{q})} = \frac{1}{\sqrt{2}} K(\boldsymbol{q})\psi_0 \Big(J^*(-\boldsymbol{q})\gamma_i(\boldsymbol{q})\gamma_j(\boldsymbol{q}) + V\bar{\psi}_0\psi_0\gamma_i(-\boldsymbol{q})\gamma_j(\boldsymbol{q}) \Big)$$

$$\sum_{\boldsymbol{q}'} \gamma_l(-\boldsymbol{q}') \frac{df_l(\boldsymbol{q}')}{df_i(\boldsymbol{q})} \frac{dY^{(1)}_{-\boldsymbol{q}'}}{d\theta_j(-\boldsymbol{q})} = \frac{1}{\sqrt{2}} K(\boldsymbol{q})\psi_0 \Big(J(\boldsymbol{q})\gamma_i(-\boldsymbol{q})\gamma_j(-\boldsymbol{q}) + V\bar{\psi}_0\psi_0\gamma_i(-\boldsymbol{q})\gamma_j(\boldsymbol{q}) \Big)$$

$$\sum_{\boldsymbol{q}'} \gamma_l(\boldsymbol{q}') \frac{d\theta_l(\boldsymbol{q}')}{d\theta_j(-\boldsymbol{q})} \frac{d\bar{X}^{(1)}_{\boldsymbol{q}'}}{df_i(\boldsymbol{q})} = \frac{1}{\sqrt{2}} K(\boldsymbol{q})\bar{\psi}_0 \Big(J(\boldsymbol{q})\gamma_i(-\boldsymbol{q})\gamma_j(-\boldsymbol{q}) + V\bar{\psi}_0\psi_0\gamma_i(\boldsymbol{q})\gamma_j(-\boldsymbol{q}) \Big)$$

$$\sum_{\boldsymbol{q}'} \gamma_l(\boldsymbol{q}') \frac{df_l(\boldsymbol{q}')}{df_i(\boldsymbol{q})} \frac{d\bar{Y}^{(1)}_{\boldsymbol{q}'}}{d\theta_j(-\boldsymbol{q})} = \frac{1}{\sqrt{2}} K(\boldsymbol{q})\bar{\psi}_0 \Big(J^*(-\boldsymbol{q})\gamma_i(\boldsymbol{q})\gamma_j(\boldsymbol{q}) + V\bar{\psi}_0\psi_0\gamma_i(\boldsymbol{q})\gamma_j(-\boldsymbol{q}) \Big)$$

A.6 Coefficients of the second order response function

Using the shorthands,

$$L_1 \equiv J(\boldsymbol{0}) + J^*(\boldsymbol{0}) + 2V\left|\psi_0\right|^2, \qquad\qquad L_2 \equiv J(\boldsymbol{0}) + V\left|\psi_0\right|^2, \qquad (A.57)$$

we may write the coefficients $\mathcal{C}^{(2)}_{\sigma,\sigma'}(\boldsymbol{q})$ in Eq. (6.76), which are 2×2 matrices in Nambu space, as

$$\mathcal{C}^{(2)}_{\sigma,\sigma'}(\boldsymbol{q}) = -\frac{V}{2} K(\boldsymbol{q})\mathcal{C}'^{(2)}_{\sigma,\sigma'}(\boldsymbol{q}), \qquad (A.58)$$

where

$$\mathcal{C}'^{(2)}_{+,+}(\boldsymbol{q}) = \begin{pmatrix} \begin{aligned} &|\psi_0|^2 \big(K(\boldsymbol{q}) \\ &\times[1 - K(\boldsymbol{0})V|\psi_0|^2 L_1] \\ &\times[J^*(-\boldsymbol{q})^2 + V^2|\psi_0|^4] \\ &-K(\boldsymbol{0})J^*(-\boldsymbol{q})L_1 \\ &\times[K(\boldsymbol{q})V^2|\psi_0|^4 - 1]) \end{aligned} & \begin{aligned} &\psi_0^2\big(-K(\boldsymbol{0})K(\boldsymbol{q})V|\psi_0|^2 L_2 \\ &\times[J^*(-\boldsymbol{q})^2 + V^2|\psi_0|^4] \\ &+J^*(-\boldsymbol{q})(K(\boldsymbol{q})V|\psi_0|^2 \\ &-K(\boldsymbol{0})L_2[K(\boldsymbol{q})V^2|\psi_0|^4 - 1])) \end{aligned} \\[2em] \begin{aligned} &\bar{\psi}_0^2\big(-K(\boldsymbol{0})K(\boldsymbol{q})V|\psi_0|^2 L_2^* \\ &\times[J^*(-\boldsymbol{q})^2 + V^2|\psi_0|^4] \\ &+J^*(-\boldsymbol{q})(K(\boldsymbol{q})V|\psi_0|^2 \\ &-K(\boldsymbol{0})L_2^*[K(\boldsymbol{q})V^2|\psi_0|^4 - 1])) \end{aligned} & \begin{aligned} &|\psi_0|^2 \big(K(\boldsymbol{q}) \\ &\times[1 - K(\boldsymbol{0})V|\psi_0|^2 L_1] \\ &\times[J^*(-\boldsymbol{q})^2 + V^2|\psi_0|^4] \\ &-K(\boldsymbol{0})J^*(-\boldsymbol{q})L_1 \\ &\times[K(\boldsymbol{q})V^2|\psi_0|^4 - 1]) \end{aligned} \end{pmatrix}, \qquad (A.59)$$

$$
\mathcal{C}'^{(2)}_{+,-}(\boldsymbol{q}) = \begin{pmatrix} \begin{matrix} V\left|\psi_0\right|^4\left(K(\boldsymbol{q})[1 - K(\mathbf{0})V\left|\psi_0\right|^2 L_1]\right. \\ \times[J(\boldsymbol{q}) + J^*(-\boldsymbol{q})] \\ -K(\mathbf{0})([K(\boldsymbol{q})V^2\left|\psi_0\right|^4 - 2]L_2^* \\ +K(\boldsymbol{q})J(\boldsymbol{q})J^*(-\boldsymbol{q})L_2 \end{matrix} & \begin{matrix} \psi_0^2\left(-K(\mathbf{0})V\left|\psi_0\right|^2\right. \\ \times(K(\boldsymbol{q})V\left|\psi_0\right|^2 L_2[J(\boldsymbol{q}) + J^*(-\boldsymbol{q})] \\ +K(\boldsymbol{q})J(\mathbf{0})J(\boldsymbol{q})J^*(-\boldsymbol{q}) \\ +K(\boldsymbol{q})V^3\left|\psi_0\right|^6 - 2V\left|\psi_0\right|^2) \\ +K(\boldsymbol{q})J(\boldsymbol{q})J^*(-\boldsymbol{q})) \end{matrix} \\ \\ \begin{matrix} \bar{\psi}_0^2\left(-K(\mathbf{0})V\left|\psi_0\right|^2\right. \\ \times(K(\boldsymbol{q})V\left|\psi_0\right|^2 L_2^*[J(\boldsymbol{q}) + J^*(-\boldsymbol{q})] \\ +K(\boldsymbol{q})J^*(\mathbf{0})V^2\left|\psi_0\right|^4 \\ +K(\boldsymbol{q})J(\boldsymbol{q})J^*(-\boldsymbol{q})V\left|\psi_0\right|^2 - 2J^*(\mathbf{0})) \\ +K(\boldsymbol{q})V^2\left|\psi_0\right|^4) \end{matrix} & \begin{matrix} V\left|\psi_0\right|^4\left(K(\boldsymbol{q})[1 - K(\mathbf{0})V\left|\psi_0\right|^2 L_1]\right. \\ \times[J(\boldsymbol{q}) + J^*(-\boldsymbol{q})] \\ -K(\mathbf{0})([K(\boldsymbol{q})V^2\left|\psi_0\right|^4 - 2]L_2^* \\ +K(\boldsymbol{q})J(\boldsymbol{q})J^*(-\boldsymbol{q})L_2 \end{matrix} \end{pmatrix},
$$

$$\text{(A.60)}$$

$$
\mathcal{C}'^{(2)}_{-,+}(\boldsymbol{q}) = \begin{pmatrix} \begin{matrix} V\left|\psi_0\right|^4\left(K(\boldsymbol{q})[1 - K(\mathbf{0})V\left|\psi_0\right|^2 L_1]\right. \\ \times[J(\boldsymbol{q}) + J^*(-\boldsymbol{q})] \\ -K(\mathbf{0})([K(\boldsymbol{q})V^2\left|\psi_0\right|^4 - 2]L_2 \\ +K(\boldsymbol{q})J(\boldsymbol{q})J^*(-\boldsymbol{q})L_2^* \end{matrix} & \begin{matrix} \psi_0^2\left(-K(\mathbf{0})V\left|\psi_0\right|^2\right. \\ \times(K(\boldsymbol{q})V\left|\psi_0\right|^2 L_2[J(\boldsymbol{q}) + J^*(-\boldsymbol{q})] \\ +K(\boldsymbol{q})J(\mathbf{0})V^2\left|\psi_0\right|^4 \\ +K(\boldsymbol{q})J(\boldsymbol{q})J^*(-\boldsymbol{q})V\left|\psi_0\right|^2 - 2J(\mathbf{0})) \\ +K(\boldsymbol{q})V^2\left|\psi_0\right|^4) \end{matrix} \\ \\ \begin{matrix} \bar{\psi}_0^2\left(-K(\mathbf{0})V\left|\psi_0\right|^2\right. \\ \times(K(\boldsymbol{q})V\left|\psi_0\right|^2 L_2^*[J(\boldsymbol{q}) + J^*(-\boldsymbol{q})] \\ +K(\boldsymbol{q})J^*(\mathbf{0})J(\boldsymbol{q})J^*(-\boldsymbol{q}) \\ +K(\boldsymbol{q})V^3\left|\psi_0\right|^6 - 2V\left|\psi_0\right|^2) \\ +K(\boldsymbol{q})J(\boldsymbol{q})J^*(-\boldsymbol{q})) \end{matrix} & \begin{matrix} V\left|\psi_0\right|^4\left(K(\boldsymbol{q})[1 - K(\mathbf{0})V\left|\psi_0\right|^2 L_1]\right. \\ \times[J(\boldsymbol{q}) + J^*(-\boldsymbol{q})] \\ -K(\mathbf{0})([K(\boldsymbol{q})V^2\left|\psi_0\right|^4 - 2]L_2 \\ +K(\boldsymbol{q})J(\boldsymbol{q})J^*(-\boldsymbol{q})L_2^* \end{matrix} \end{pmatrix},
$$

$$\text{(A.61)}$$

$$
\mathcal{C}'^{(2)}_{-,-}(\boldsymbol{q}) = \begin{pmatrix} \begin{matrix} \left|\psi_0\right|^2\left(K(\boldsymbol{q})\right. \\ \times[1 - K(\mathbf{0})V\left|\psi_0\right|^2 L_1] \\ \times[J(\boldsymbol{q})^2 + V^2\left|\psi_0\right|^4] \\ -K(\mathbf{0})J(\boldsymbol{q})L_1 \\ \times[K(\boldsymbol{q})V^2\left|\psi_0\right|^4 - 1]) \end{matrix} & \begin{matrix} \psi_0^2\left(-K(\mathbf{0})K(\boldsymbol{q})V\left|\psi_0\right|^2 L_2\right. \\ \times[J(\boldsymbol{q})^2 + V^2\left|\psi_0\right|^4] \\ +J(\boldsymbol{q})(K(\boldsymbol{q})V\left|\psi_0\right|^2 \\ -K(\mathbf{0})L_2[K(\boldsymbol{q})V^2\left|\psi_0\right|^4 - 1])) \end{matrix} \\ \\ \begin{matrix} \bar{\psi}_0^2\left(-K(\mathbf{0})K(\boldsymbol{q})V\left|\psi_0\right|^2 L_2^*\right. \\ \times[J(\boldsymbol{q})^2 + V^2\left|\psi_0\right|^4] \\ +J(\boldsymbol{q})(K(\boldsymbol{q})V\left|\psi_0\right|^2 \\ -K(\mathbf{0})L_2^*[K(\boldsymbol{q})V^2\left|\psi_0\right|^4 - 1])) \end{matrix} & \begin{matrix} \left|\psi_0\right|^2\left(K(\boldsymbol{q})\right. \\ \times[1 - K(\mathbf{0})V\left|\psi_0\right|^2 L_1] \\ \times[J(\boldsymbol{q})^2 + V^2\left|\psi_0\right|^4] \\ -K(\mathbf{0})J(\boldsymbol{q})L_1 \\ \times[K(\boldsymbol{q})V^2\left|\psi_0\right|^4 - 1]) \end{matrix} \end{pmatrix}.
$$

$$\text{(A.62)}$$

Appendix B

A note on dimensional factors

Dimensional factors of finite length and time introduced by the use of discrete sums have been omitted during the calculation of the static current-current response function in Chapter 6. This Appendix explains how we account for these so that the response function remains finite when we take the continuum limit in Sections 6.4.1 and 6.4.4.

Starting in real space, we write the simplest version of the action which generalises to the full problem:

$$
S = \int dt d^2 \boldsymbol{x} \left[\bar{\psi}(x)\epsilon(-i\nabla)\psi(x) + \frac{V}{2}\bar{\psi}(x)\bar{\psi}(x)\psi(x)\psi(x) \right. \tag{B.1}
$$

$$
\left. + \left(F_p(x)\bar{\psi}(x) + F_p^*(x)\psi(x) \right) - \frac{i}{2m}\left(\bar{\psi}(x)\nabla\psi(x) - [\nabla\bar{\psi}(x)]\psi(x) \right).\boldsymbol{f}(x) \right],
$$

where $x = (t, \boldsymbol{x})$, $F_p(x) = F_p \mathrm{e}^{-i\omega_p t + i\boldsymbol{k}_p.\boldsymbol{x}}$, and we have used the standard quantum mechanical current for $\boldsymbol{j}(x)$. With $\hbar = 1$, and considering that the dimensions of the integral are $\int dt \iint d^2\boldsymbol{x} \sim [T][L]^2$, we have that $\epsilon \sim [T]^{-1}$, $V \sim [T]^{-1}[L]^2$, and $\psi(x) \sim [L]^{-1}$. Fourier transforming into momentum space, where the two-dimensional transformations are defined by,

$$
A(\boldsymbol{x}) = \frac{1}{L}\sum_{\boldsymbol{k}} A_{\boldsymbol{k}}\mathrm{e}^{i\boldsymbol{k}.\boldsymbol{x}}, \qquad\qquad A_{\boldsymbol{k}} = \frac{1}{L}\int d^2\boldsymbol{x}\, A(\boldsymbol{x})\mathrm{e}^{-i\boldsymbol{k}.\boldsymbol{x}}, \tag{B.2}
$$

we get (writing $\psi_{\boldsymbol{k}}(t) = \psi_{\boldsymbol{k}}$),

$$
S = \int dt d^2\boldsymbol{x} \left[\frac{1}{L^2}\sum_{\boldsymbol{k}} \epsilon_{\boldsymbol{k}}\bar{\psi}_{\boldsymbol{k}}\psi_{\boldsymbol{k}'}\mathrm{e}^{-i(\boldsymbol{k}-\boldsymbol{k}').\boldsymbol{x}} + \frac{V}{2}\frac{1}{L^4}\sum_{\boldsymbol{k},\boldsymbol{k}',\boldsymbol{q},\boldsymbol{q}'} \bar{\psi}_{\boldsymbol{k}}\bar{\psi}_{\boldsymbol{q}}\psi_{\boldsymbol{k}'}\psi_{\boldsymbol{q}'}\mathrm{e}^{-i(\boldsymbol{k}+\boldsymbol{q}-\boldsymbol{k}'-\boldsymbol{q}').\boldsymbol{x}} \right.
$$

$$
\left. + \frac{1}{L}\left(F_p\mathrm{e}^{-i\omega_p t}\sum_{\boldsymbol{k}} \bar{\psi}_{\boldsymbol{k}}\mathrm{e}^{-i(\boldsymbol{k}-\boldsymbol{k}_p).\boldsymbol{x}} + \mathrm{c.c.} \right) + \frac{1}{L^3}\sum_{\boldsymbol{k},\boldsymbol{k}',\boldsymbol{q}} \left(\frac{\boldsymbol{k}+\boldsymbol{k}'}{2m}\bar{\psi}_{\boldsymbol{k}'}\psi_{\boldsymbol{k}}\mathrm{e}^{i(\boldsymbol{k}+\boldsymbol{q}-\boldsymbol{k}').\boldsymbol{x}} \right).\boldsymbol{f}_{\boldsymbol{q}} \right]
$$

Given that $\iint d^2x \, e^{-i(k-k').x} = L^2 \delta_{k,k'}$, this is equal to

$$S \;=\; \int dt \Bigg[\sum_k \epsilon_k \bar{\psi}_k \psi_k + \frac{V}{2} \frac{1}{L^2} \sum_{k,k',q} \bar{\psi}_{k-q} \bar{\psi}_{k'+q} \psi_k \psi_{k'} \tag{B.3}$$

$$+ L \Big(F_p e^{-i\omega_p t} \bar{\psi}_{k_p} + \text{c.c.} \Big) + \frac{1}{L} \sum_{k,q} \left(\frac{2k+q}{2m} \bar{\psi}_{k+q} \psi_k \right) . f_q \Bigg],$$

where the momentum arguments have been resummed in the second term and the fields are now dimensionless, $\psi_k \sim [1]$. Applying the Fourier transform between frequency and time,

$$A(t) = \frac{1}{\sqrt{T}} \sum_\omega A_\omega e^{-i\omega t}, \qquad\qquad A_\omega = \frac{1}{\sqrt{T}} \int dt \, A(t) e^{i\omega t}, \tag{B.4}$$

we see the same behaviour as with the spatial case, giving

$$S \;=\; \sum_\omega \sum_k \epsilon_k \bar{\psi}_{\omega,k} \psi_{\omega,k} + \frac{V}{2} \frac{1}{L^2} \frac{1}{T} \sum_{\omega,\omega',\nu} \sum_{k,k',q} \bar{\psi}_{\omega-\nu,k-q} \bar{\psi}_{\omega'+\nu,k'+q} \psi_{\omega,k} \psi_{\omega',k'} \tag{B.5}$$

$$+ L\sqrt{T} F_p \Big(\bar{\psi}_{\omega_p,k_p} + \psi_{\omega_p,k_p} \Big) + \frac{1}{L} \frac{1}{\sqrt{T}} \sum_{\omega,\nu} \sum_{k,q} \left(\frac{2k+q}{2m} \bar{\psi}_{\omega+\nu,k+q} \psi_{\omega,k} \right) . f_{\nu,q},$$

where now $\psi_{\omega,k} \sim [T]^{1/2}$. We should note that the response function we calculate in Chapter 6 is the *static* current-current response function – i.e., it is the time-independent current response due to a time-independent perturbing force. Clearly, the above action has been calculated assuming a time dependence for both j and f. That is, we have used

$$\delta S = \sum_{\nu,q} j_{\nu,q}.f_{\nu,q}. \tag{B.6}$$

To remove the time-dependence we may set the frequency argument ν to zero, formally by replacing $f_{\nu,q} \to \sqrt{T} \delta_{\nu,0} f_q$, giving

$$\delta S = \frac{1}{L} \sum_\omega \sum_{k,q} \left(\frac{2k+q}{2m} \bar{\psi}_{\omega,k+q} \psi_{\omega,k} \right) . f_{0,q}, \tag{B.7}$$

which is the form used in the action in Chapter 6 (Eq. (6.12)). However, to do this we must be careful that the response function is finite when we take the continuum limit, $T \to \infty$. Consider the Hamiltonian for a time-independent current coupled to a time-independent perturbing force,

$$\delta \hat{H} = \sum_q \hat{j}_q.f_q. \tag{B.8}$$

The current, when the fields are time-independent, has units of inverse time,

$$\boldsymbol{j_q} = \frac{1}{L}\sum_{\boldsymbol{k}}\frac{2\boldsymbol{k}+\boldsymbol{q}}{2m}\bar{\psi}_{\boldsymbol{k}+\boldsymbol{q}}\psi_{\boldsymbol{k}} \sim \frac{([L]^{-1})}{([L])([T][L]^{-2})} \sim [T]^{-1}, \tag{B.9}$$

which means that the perturbing force is dimensionless, $\boldsymbol{f_q} \sim [1]$. Consequently, the static response function also has units of inverse time,

$$\chi_{\boldsymbol{q}} = \frac{|\boldsymbol{j_q}|}{|\boldsymbol{f_q}|} \sim [T]^{-1}. \tag{B.10}$$

We note however that if $\boldsymbol{f}$ is dimensionless then differentiating the partition function twice with respect to it gives a response function with the wrong units. This is rectified by dividing through by a factor of time,

$$\chi_{ij}(\boldsymbol{q}) \sim \frac{1}{T}\frac{d^2\mathcal{Z}[\boldsymbol{f}]}{df_{i,\boldsymbol{q}}df_{j,-\boldsymbol{q}}}\bigg|_{\boldsymbol{f}=\boldsymbol{0}} \sim [T]^{-1}. \tag{B.11}$$

In fact, this expression is mathematically equivalent to starting with the frequency-dependent action in Eq. (B.5) and performing the differentiation with respect to the zero-frequency component of the force, $\boldsymbol{f}_{0,\boldsymbol{q}}$, because a factor of $1/\sqrt{T}$ is produced by each differentiation. Ultimately, as we see below, the factor of $1/T$ is required to integrate out the frequency, ω.

Returning to the question of the continuum limit in Sections 6.4.1 and 6.4.4, and of what happens to the factors of L and T in Eq. (B.5) more generally, we first note that in the mean-field approximation we have that

$$\psi_{\omega,\boldsymbol{k}} \to \sqrt{T}\psi_{0,\boldsymbol{k}}\delta_{\omega,0} = \sqrt{T}(\psi_0\delta_{\boldsymbol{k},\boldsymbol{0}} + X_{\boldsymbol{k}})\delta_{\omega,0}, \tag{B.12}$$

where ψ_0 and $X_{\boldsymbol{k}}$ are both dimensionless, and we add that, recalling Eqs. (6.38), (6.39) and (A.46-A.49), $X_{\boldsymbol{k}}$ is a function of the source fields and is proportional to a factor of ψ_0. In the semiclassical approximation to the action, we retain only those terms that are zeroth or second order in fluctuations (the first order term is zero by definition). Dealing with the latter first, we can substitute the above expression for the mean-field into the interaction term in Eq. (B.5) to reduce it to quadratic order in the (now fluctuations) fields:

$$
\begin{aligned}
S^{(2)} &= \sum_{\omega}\sum_{\boldsymbol{k}}\epsilon_{\boldsymbol{k}}\delta\bar{\psi}_{\omega,\boldsymbol{k}}\delta\psi_{\omega,\boldsymbol{k}} + \frac{1}{L}\frac{1}{\sqrt{T}}\sum_{\omega,\nu}\sum_{\boldsymbol{k},\boldsymbol{q}}\left(\frac{2\boldsymbol{k}+\boldsymbol{q}}{2m}\delta\bar{\psi}_{\omega+\nu,\boldsymbol{k}+\boldsymbol{q}}\delta\psi_{\omega,\boldsymbol{k}}\right)\cdot\boldsymbol{f}_{\nu,\boldsymbol{q}} \quad (\text{B.13})\\
&+ \frac{V}{2L^2}\sum_{\omega}\sum_{\boldsymbol{k},\boldsymbol{k}',\boldsymbol{q}}(\bar{\psi}_0\delta_{\boldsymbol{k}-\boldsymbol{q},\boldsymbol{0}} + \bar{X}_{\boldsymbol{k}-\boldsymbol{q}})(\bar{\psi}_0\delta_{\boldsymbol{k}'+\boldsymbol{q},\boldsymbol{0}} + \bar{X}_{\boldsymbol{k}'+\boldsymbol{q}})\delta\psi_{\omega,\boldsymbol{k}}\delta\psi_{-\omega,\boldsymbol{k}'} + ...,
\end{aligned}
$$

where further terms are given by different combinations of the mean-field and the fluctuations

fields in the interaction term. There are three important things to note about this action. First, the factor of time in front of the interaction term has been cancelled out. Secondly, the factors of (V/L^2) will always be multiplied by two factors of ψ_0 or its conjugate (because $X_{\boldsymbol{k}} \sim \psi_0$). And thirdly, differentiating the action by the source field $\boldsymbol{f}$ will bring down a factor of $(1/L^2T)$. Bearing these in mind, if we rescale $\psi_0 \to L\psi_0$, where now $\psi_0 \sim [L]^{-1}$, so that $(V/L^2)\psi_0^2 \to V\psi_0^2 \sim [T]^{-1}$, then when in Sections 6.4.1 and 6.4.4 the traces are taken over the fluctuation terms, we will be able to take the continuum limit ($L, T \to \infty$):

$$\frac{1}{T} \sum_{\omega} \frac{1}{L^2} \sum_{\boldsymbol{k}} \to \int \frac{d\omega}{2\pi} \int \frac{d^2\boldsymbol{k}}{4\pi^2}. \tag{B.14}$$

As the source fields are each multiplied by a factor of $(1/L\sqrt{T})$, the mean-field response function, Eq. (6.22), will acquire a factor of $(1/L^2T)$. However, each source field in the mean-field action, which is given by the expansion in Eq. (6.31), is also multiplied by a single factor of the source-free mean-field ψ_0 (from either inside $X_{\boldsymbol{k}}$ or separately) (see Eqs. (6.46) and (6.50)). These factors of ψ_0 come from the perturbation term in the action and are therefore not paired to a factor of V/L^2 as for the fluctuations terms above. Consequently, while each source field carries a factor of $1/L\sqrt{T}$, they are also multiplied by $L\sqrt{T}$ ($\sqrt{T}$ from the definition of the mean-field and the L that results when we rescale the mean-field, $\psi_0 \to L\psi_0$). These cancel leaving us with no stray factors of length or time that would cause problems in the continuum limit.

Appendix C

Integration of the response function

In this thesis, we approximate the interactions between polaritons as contact interactions (see Eq. (3.9)). These are unphysical as they have no length scale associated with them and, as a result, in order to numerically integrate Eq. (6.90) we must impose a cut-off in k_x and k_y. For polaritons, the physical range of interactions is given by the exciton Bohr radius[15,107], which is roughly 100Å, so our required cut-off in momentum is $100\,\mu\mathrm{m}^{-1}$ (which is the inverse of this).

By calculating the response function with momentum-dependent interactions, $V \rightarrow V(\boldsymbol{k})$, one may verify that the source of the divergence in Eq. (6.90) is indeed the contact interactions (and thus that imposing a cut-off is a valid approach to calculating the integral). This analysis shows that so long as these interactions have a maximum range the integral is convergent. More specifically, it involves modifying the interactions term in the Keldysh action to read

$$
\begin{aligned}
S_{int} \;=\; & -\frac{1}{2} \sum_{\omega,\omega',\nu} \sum_{\boldsymbol{k},\boldsymbol{k}',\boldsymbol{q}} V(\boldsymbol{q}) \left(\bar{\psi}_c(\omega-\nu,\boldsymbol{k}-\boldsymbol{q}) \bar{\psi}_q(\omega'+\nu,\boldsymbol{k}'+\boldsymbol{q}) \right. \\
& \times \left[\psi_c(\omega,\boldsymbol{k})\psi_c(\omega',\boldsymbol{k}') + \psi_q(\omega,\boldsymbol{k})\psi_q(\omega',\boldsymbol{k}') \right] + \mathrm{c.c.})
\end{aligned}
\tag{C.1}
$$

where we have a choice of appropriate forms for $V(\boldsymbol{q})$. For example, we may use a Gaussian,

$$
V(\boldsymbol{q}) = V_0 \exp\left(-\frac{q_x^2 + q_y^2}{2\sigma^2} \right),
\tag{C.2}
$$

for some σ, which sets the range of the interactions.

This momentum dependence leads to the following changes to the response function in the long-range limit (compared to Eq. (6.90)). The shorthand beneath Eq. (4.72) becomes

$$
J(\pm\omega,\pm\boldsymbol{k}) \equiv \pm\omega + \omega_p - \epsilon(\pm\boldsymbol{k}) + i\kappa - [V(\boldsymbol{0}) + V(\boldsymbol{k})]\,|\psi_0|^2,
\tag{C.3}
$$

and the inverse matrix of Green's functions is modified to be (where $k = (\omega, \boldsymbol{k})$):

$$
\mathcal{D}^{-1}(k, k') = \begin{pmatrix} 0 & 0 & J^*(\omega, \boldsymbol{k}) & -V(\boldsymbol{k})\psi_0^2 \\ 0 & 0 & -V(\boldsymbol{k})\bar{\psi}_0^2 & J(-\omega, -\boldsymbol{k}) \\ J(\omega, \boldsymbol{k}) & -V(\boldsymbol{k})\psi_0^2 & 2i\kappa & 0 \\ -V(\boldsymbol{k})\bar{\psi}_0^2 & J^*(-\omega, -\boldsymbol{k}) & 0 & 2i\kappa \end{pmatrix} \delta_{k,k'}. \qquad \text{(C.4)}
$$

In both the first order response function, which is given by the coefficients in Eqs. (A.42-A.45), and the second order response function, given by the coefficients in Eq. (A.58), most factors of V become $V(\boldsymbol{0}) = V_0$. The only exception in both cases is the factor premultiplying each term, where diagonal terms change like $V \to (1/2)[V(\boldsymbol{0}) + V(\boldsymbol{k})]$ and off-diagonal terms like $V \to V(\boldsymbol{k})$.

Bibliography

1. Juggins, R., Keeling, J., and Szymańska, M. *Nat. Commun.* **9**, 4062 (2018).

2. Crane, L. *New Scientist* **3202**, 6 (2018).

3. Anderson, P. W. *Science* **177**, 393–396 (1972).

4. Laughlin, R. B. *Rev. Mod. Phys.* **71**, 863 (1999).

5. Leggett, A. J. *Rev. Mod. Phys.* **71**, S318 (1999).

6. Leggett, A. J. *Quantum Liquids: Bose Condensation and Cooper Pairing in Condensed-Matter Systems.* Oxford University Press, Oxford, (2006).

7. Annett, J. F. *Superconductivity, Superfluids and Condensates*, volume 5. Oxford University Press, Oxford, (2004).

8. Klaers, J., Schmitt, J., Vewinger, F., and Weitz, M. *Nature* **468**, 545–548 (2010).

9. Marelic, J. and Nyman, R. A. *Phys. Rev. A* **91**, 033813 (2015).

10. Ritsch, H., Domokos, P., Brennecke, F., and Esslinger, T. *Rev. Mod. Phys.* **85**, 553 (2013).

11. Hartmann, M. J., Brandao, F. G. S. L., and Plenio, M. B. *Laser Photonics Rev.* **2**, 527–556 (2008).

12. Carusotto, I., Gerace, D., Tureci, H. E., De Liberato, S., Ciuti, C., and Imamolu, A. *Phys. Rev. Lett.* **103**, 033601 (2009).

13. Noh, C. and Angelakis, D. G. *Rep. Prog. Phys.* **80**, 016401 (2016).

14. Carusotto, I. and Ciuti, C. *Rev. Mod. Phys.* **85**, 299 (2013).

15. Deng, H., Haug, H., and Yamamoto, Y. *Rev. Mod. Phys.* **82**, 1489 (2010).

16. Keeling, J. and Berloff, N. G. *Contemp. Phys.* **52**, 131 (2011).

17. Amo, A., Lefrère, J., Pigeon, S., Adrados, C., Ciuti, C., Carusotto, I., Houdré, R., Giacobino, E., and Bramati, A. *Nat. Phys.* **5**, 805 (2009).

18. Amo, A., Sanvitto, D., Laussy, F. P., Ballarini, D., Del Valle, E., Martin, M. D., Lemaitre, A., Bloch, J., Krizhanovskii, D. N., Skolnick, M. S., Tejedor, C., and Viña, L. *Nature* **457**, 291–295 (2009).

19. Berceanu, A. C., Dominici, L., Carusotto, I., Ballarini, D., Cancellieri, E., Gigli, G., Szymańska, M. H., Sanvitto, D., and Marchetti, F. M. *Phys. Rev. B* **92**, 035307 (2015).

20. Sanvitto, D., Marchetti, F. M., Szymańska, M. H., Tosi, G., Baudisch, M., Laussy, F. P., Krizhanovskii, D. N., Skolnick, M. S., Marrucci, L., Lemaitre, A., et al. *Nat. Phys.* **6**, 527–533 (2010).

21. Lagoudakis, K. G., Wouters, M., Richard, M., Baas, A., Carusotto, I., André, R., Dang, L. S., and Deveaud-Plédran, B. *Nat. Phys.* **4**, 706–710 (2008).

22. Wouters, M. and Carusotto, I. *Phys. Rev. Lett.* **105**, 020602 (2010).

23. Keeling, J. *Phys. Rev. Lett.* **107**, 080402 (2011).

24. Janot, A., Hyart, T., Eastham, P. R., and Rosenow, B. *Phys. Rev. Lett.* **111**, 230403 (2013).

25. Gladilin, V. N. and Wouters, M. *Phys. Rev. B* **93**, 134511 (2016).

26. Wachtel, G., Sieberer, L. M., Diehl, S., and Altman, E. *Phys. Rev. B* **94**, 104520 (2016).

27. Keeling, J., Sieberer, L. M., Altman, E., Chen, L., Diehl, S., and Toner, J. In *Universal Themes of Bose-Einstein Condensation,* Proukakis, N. P., Snoke, D. W., and Littlewood, P. B., editors, 205. Cambridge University Press, Cambridge (2017).

28. Keeling, J. and Berloff, N. G. *Nature* **457**, 273–274 (2009).

29. Cancellieri, E., Marchetti, F. M., Szymańska, M. H., and Tejedor, C. *Phys. Rev. B* **82**, 224512 (2010).

30. Pitaevskii, L. and Stringari, S. *Bose-Einstein Condensation.* Oxford University Press, Oxford, (2003).

31. Baym, G. In *Mathematical Methods in Solid State and Superfluid Theory,* Clark, R. C. and Derrick, G. H., editors, 121–156. Oliver & Boyd, Edinburgh (1969).

32. Nozières, P. and Pines, D. *The Theory of Quantum Liquids.* Perseus, Cambridge, MA, (1999).

33. Griffin, A. *Excitations in a Bose-Condensed Liquid.* Cambridge University Press, Cambridge, (1993).

34. Leggett, A. J. *J. Stat. Phys.* **93**, 927–941 (1998).

35. Rousseau, V. G. *Phys. Rev. B* **90**, 134503 (2014).

36. Kasprzak, J., Richard, M., Kundermann, S., Baas, A., Jeambrun, P., Keeling, J., Marchetti, F. M., Szymańska, M. H., Andre, R., Staehli, J. L., V., S., Littlewood, P. B., Deveaud, B., and Dang, L. S. *Nature* **443**, 409–414 (2006).

37. Szymańska, M., Keeling, J., and Littlewood, P. *Phys. Rev. B* **75**, 195331 (2007).

38. Wouters, M. and Carusotto, I. *Phys. Rev. Lett.* **99**, 140402 (2007).

39. Baas, A., Karr, J.-P., Romanelli, M., Bramati, A., and Giacobino, E. *Phys. Rev. Lett.* **96**, 176401 (2006).

40. Tartakovskii, A., Krizhanovskii, D., Kurysh, D., Kulakovskii, V., Skolnick, M., and Roberts, J. *Phys. Rev. B* **65**, 081308 (2002).

41. Wouters, M. and Carusotto, I. *Phys. Rev. B* **75**, 075332 (2007).

42. Griffin, A. *J. Phys. Conden. Matter* **21**, 164220 (2009).

43. Landau, L. *Phys. Rev.* **60**, 356 (1941).

44. Donnelly, R. J. *Phys. Today* **62**, 34–39 (2009).

45. Bogoliubov, N. *J. Phys* **11**, 23 (1947).

46. Beliaev, S. *Sov. Phys., JETP* **34**, 299 (1958).

47. Feynman, R. P. *Rev. Mod. Phys.* **29**, 205 (1957).

48. Sokol, P. In *Bose-Einstein Condensation,* Griffin, A., Snoke, D. W., and Stringari, S., editors, 51–85. Cambridge University Press, Cambridge (1995).

49. Anderson, M. H., Ensher, J. R., Matthews, M. R., Wieman, C. E., and Cornell, E. A. *Science* **269**, 198–201 (1995).

50. Davis, K. B., Mewes, M.-O., Andrews, M. R., Van Druten, N., Durfee, D., Kurn, D., and Ketterle, W. *Phys. Rev. Lett.* **75**, 3969 (1995).

51. Raman, C., Köhl, M., Onofrio, R., Durfee, D., Kuklewicz, C., Hadzibabic, Z., and Ketterle, W. *Phys. Rev. Lett.* **83**, 2502 (1999).

52. Bishop, D. and Reppy, J. *Phys. Rev. Lett.* **40**, 1727 (1978).

53. Desbuquois, R., Chomaz, L., Yefsah, T., Léonard, J., Beugnon, J., Weitenberg, C., and Dalibard, J. *Nat. Phys.* **8**, 645 (2012).

54. Kosterlitz, J. M. and Thouless, D. J. *J. Phys. C* **5**, L124 (1972).

55. Kosterlitz, J. M. and Thouless, D. J. *J. Phys. C* **6**, 1181 (1973).

56. Raman, C., Abo-Shaeer, J., Vogels, J., Xu, K., and Ketterle, W. *Phys. Rev. Lett.* **87**, 210402 (2001).

57. Huang, K. In *Bose-Einstein Condensation,* Griffin, A., Snoke, D. W., and Stringari, S., editors, 15–30. Cambridge University Press, Cambridge (1995).

58. Andronikashvili, E. and Mamaladze, Y. G. *Rev. Mod. Phys.* **38**, 567 (1966).

59. Altland, A. and Simons, B. *Condensed Matter Field Theory.* Cambridge University Press, Cambridge, (2010).

60. Mermin, N. D. and Wagner, H. *Phys. Rev. Lett.* **17**, 1133 (1966).

61. Kosterlitz, J. *J. Phys. C* **7**, 1046 (1974).

62. Keeling, J. *Phys. Rev. B* **74**, 155325 (2006).

63. Mahan, G. D. *Many-Particle Physics.* Kluwer Academic/Plenum Publishers, New York, (2000).

64. Keeling, J. *Thermodynamics and signatures of Bose-condensation of excitons and polaritons.* PhD thesis, University of Cambridge, (2005).

65. Weisbuch, C., Nishioka, M., Ishikawa, A., and Arakawa, Y. *Phys. Rev. Lett.* **69**, 3314 (1992).

66. Dang, L. S., Heger, D., André, R., Boeuf, F., and Romestain, R. *Phys. Rev. Lett.* **81**, 3920 (1998).

67. Ciuti, C., Schwendimann, P., and Quattropani, A. *Semicond. Sci. Technol.* **18**, S279 (2003).

68. Dunnett, K. and Szymańska, M. H. *Phys. Rev. B* **93**, 195306 (2016).

69. Keeling, J., Szymańska, M. H., and Littlewood, P. B. In *Optical generation and control of quantum coherence in semiconductor nanostructures*, 293–329. Springer, Berlin, Heidelberg (2010).

70. Haken, H. *Light: Waves, Photons, and Atoms, Vol. 1.* North-Holland, Amsterdam, (1981).

71. Tassone, F., Piermarocchi, C., Savona, V., Quattropani, A., and Schwendimann, P. *Phys. Rev. B* **56**, 7554 (1997).

72. Balili, R., Hartwell, V., Snoke, D., Pfeiffer, L., and West, K. *Science* **316**, 1007–1010 (2007).

73. Roumpos, G., Lohse, M., Nitsche, W. H., Keeling, J., Szymańska, M. H., Littlewood, P. B., Löffler, A., Höfling, S., Worschech, L., Forchel, A., et al. *Proc. Natl. Acad. Sci.* **109**, 6467–6472 (2012).

74. Altman, E., Sieberer, L. M., Chen, L., Diehl, S., and Toner, J. *Phys. Rev. X* **5**, 011017 (2015).

75. Sieberer, L. M., Wachtel, G., Altman, E., and Diehl, S. *Phys. Rev. B* **94**, 104521 (2016).

76. Daskalakis, K. S., Maier, S. A., Murray, R., and Kéna-Cohen, S. *Nat. Mater.* **13**, 271–278 (2014).

77. Savvidis, P., Ciuti, C., Baumberg, J., Whittaker, D., Skolnick, M., and Roberts, J. *Phys. Rev. B* **64**, 075311 (2001).

78. Stevenson, R. M., Astratov, V. N., Skolnick, M. S., Whittaker, D. M., Emam-Ismail, M., Tartakovskii, A. I., Savvidis, P. G., Baumberg, J. J., and Roberts, J. S. *Phys. Rev. Lett.* **85**, 3680 (2000).

79. Dagvadorj, G., Fellows, J., Matyjaśkiewicz, S., Marchetti, F., Carusotto, I., and Szymańska, M. *Phys. Rev. X* **5**, 041028 (2015).

80. Zamora, A., Sieberer, L., Dunnett, K., Diehl, S., and Szymańska, M. *Phys. Rev. X* **7**, 041006 (2017).

81. Szymańska, M. H., Keeling, J., and Littlewood, P. B. *Phys. Rev. Lett.* **96**, 230602 (2006).

82. Wouters, M. and Carusotto, I. *Phys. Rev. A* **76**, 043807 (2007).

83. Ciuti, C. and Carusotto, I. *Phys. Status Solidi (b)* **242**, 2224–2245 (2005).

84. Carusotto, I. and Ciuti, C. *Phys. Rev. Lett.* **93**, 166401 (2004).

85. Sieberer, L. *Universality in Driven-Dissipative Quantum Many-Body Systems*. PhD thesis, University of Innsbruck, (2015).

86. Wouters, M. and Savona, V. *Phys. Rev. B* **81**, 054508 (2010).

87. Krizhanovskii, D., Whittaker, D., Bradley, R., Guda, K., Sarkar, D., Sanvitto, D., Vina, L., Cerda, E., Santos, P., Biermann, K., et al. *Phys. Rev. Lett.* **104**, 126402 (2010).

88. Marchetti, F., Szymańska, M., Tejedor, C., and Whittaker, D. *Phys. Rev. Lett.* **105**, 063902 (2010).

89. Amo, A., Pigeon, S., Sanvitto, D., Sala, V., Hivet, R., Carusotto, I., Pisanello, F., Leménager, G., Houdré, R., Giacobino, E., et al. *Science* **332**, 1167–1170 (2011).

90. Pigeon, S., Carusotto, I., and Ciuti, C. *Phys. Rev. B* **83**, 144513 (2011).

91. Nardin, G., Grosso, G., Léger, Y., Pitka, B., Morier-Genoud, F., and Deveaud-Plédran, B. *Nat. Phys.* **7**, 635–641 (2011).

92. Pigeon, S. and Bramati, A. *New J. Phys.* **19**, 095004 (2017).

93. Lerario, G., Fieramosca, A., Barachati, F., Ballarini, D., Daskalakis, K. S., Dominici, L., De Giorgi, M., Maier, S. A., Gigli, G., Kéna-Cohen, S., et al. *Nat. Phys.* **13**, 837 (2017).

94. Berceanu, A., Cancellieri, E., and Marchetti, F. *J. Phys. Conden. Matter* **24**, 235802 (2012).

95. Riley, K. F., Hobson, M. P., and Bence, S. J. *Mathematical Methods for Physics and Engineering.* Cambridge University Press, Cambridge, (2006).

96. Abrikosov, A. A., Gorkov, L. P., and Dzyaloshinski, I. E. *Methods of Quantum Field Theory in Statistical Physics.* Dover Publications, New York, (1963).

97. Kamenev, A. *Field Theory of Non-Equilibrium Systems.* Cambridge University Press, Cambridge, (2011).

98. Dalla Torre, E. G., Diehl, S., Lukin, M. D., Sachdev, S., and Strack, P. *Phys. Rev. A* **87**, 023831 (2013).

99. Kohnle, V., Léger, Y., Wouters, M., Richard, M., Portella-Oberli, M. T., and Deveaud-Plédran, B. *Phys. Rev. Lett.* **106**, 255302 (2011).

100. Baas, A., Karr, J. P., Eleuch, H., and Giacobino, E. *Phys. Rev. A* **69**, 023809 (2004).

101. Keeling, J. *Private communication.*

102. Berry, M. V. *Proc. R. Soc. Lond. A* **392**, 45–57 (1984).

103. Dalibard, J., Gerbier, F., Juzeliūnas, G., and Öhberg, P. *Rev. Mod. Phys.* **83**, 1523 (2011).

104. Galitski, V., Juzeliūnas, G., and Spielman, I. B. *Physics Today* **72**, 38 (2019).

105. Cooper, N. R. and Hadzibabic, Z. *Phys. Rev. Lett.* **104**, 030401 (2010).

106. Carusotto, I. and Ciuti, C. *Phys. Rev. B* **72**, 125335 (2005).

107. Ciuti, C., Savona, V., Piermarocchi, C., Quattropani, A., and Schwendimann, P. *Phys. Rev. B* **58**(12), 7926 (1998).